Author:
Mordant, Francesca

Title:
Investigation into the effects of a mutation in the dengue virus NS4B protein that confers a persistently-infecting phenotype

Investigation into the effects of a mutation in the dengue virus NS4B protein that confers a persistently-infecting phenotype

Francesca Lea Mordant

A dissertation submitted to the University of Bristol in accordance with the requirements for award of the degree of Master of Science by Research (MScR) in the Faculty of Life Sciences.

School of Cellular and Molecular Medicine

September 2018

Abstract

Dengue virus (DENV) of the *Flaviviridae* family is the most significant cause of human arboviral disease worldwide. While other members of the *Flaviviridae* family can cause persistent infections, there are few reports of persistent DENV infections in mammalian cells. A DENV-2 mutant that can establish persistent infection in a range of cultured cells was previously discovered, and the phenotype was attributed to a single amino acid substitution in the DENV-2 NS4B protein, T66A. However, prior studies failed to reveal the mechanism conferring the persistent phenotype. To further address this question, a comparative RNAseq transcriptomic analysis using RNA from HEK293T cells that were infected with DENV-2, persistently-infected, or stably expressing a wild-type (RepDV-GP2A) or $NS4B_{T66A}$ mutant replicon (RepDV-GP2A-$NS4B_{T66A}$) was performed. Bioinformatic analysis of the transcriptomic dataset revealed that the expression of a range of interferon-stimulated genes was increased in the persistently-infected cells compared to control and DENV-2 infected cells. Immunomicroscopy revealed that the distribution of STAT1 was altered between persistently-infected and DENV-2 infected cells, indicating an effect of the $NS4B_{T66A}$ mutation on DENV-induced modulation of the host interferon response. Interestingly, genes involved in cholesterol biosynthesis (*HMGCR, HMGCS1, IDI1, INSIG1, MSMO1, SQLE*) were downregulated in the persistently-infected cells compared to the control cells, but upregulated during DENV-2 infection. Downregulation of target genes was validated by quantitative real-time PCR. The distribution of intracellular cholesterol was also examined and found to be altered upon persistent and wild-type DENV-2 infection. Attempts to pharmacologically clear persistently-infected cells of virus were unsuccessful; thus, the persistently-infecting virus genome was sequenced to identify mutations that arose and potentially conferred resistance to the anti-DENV drugs. This study provides further insight into the mechanism by which persistent infection with the mutated DENV-2 strain, v601-$4B_{T66A}$, is maintained *in vitro*.

Dedication and Acknowledgements

My utmost thanks must be expressed to Dr Andrew Davidson for taking me on as his student, for providing continuous support and excellent guidance throughout the course of this project, and for his encouragement to continue to pursue a career in virology research. I am also highly grateful to Dr David Matthews and Dr Yohei Yamauchi for sharing their knowledge and providing valuable comments and insights at various stages of the project.

Thank you to all members of the Davidson group and E50 lab for making my time in Bristol so fun and giving the lab such an encouraging and enjoyable atmosphere: Ali Antonopoulos, I'ah Donovan-Banfield, Jack Hales, Viravarn Luvira, Sam Saunders, Edsel Ayes, Cait Simpson, Josh Lee, Dr Lisa Stevens, Dr Phil Lewis and Alina Rudnicka. Special thanks to Ali Antonopoulos for performing the required experiments after my departure.

Finally, thank you to all the staff in the Faculty of Biomedical Sciences that have helped at various stages of my time at the University of Bristol, particularly the technicians that kept our lab running smoothly. Additionally, staff at the Woldson Bioimaging Facility for giving access to their facilities, particularly Alan Leard and Dr Katy Jepson for microscopy training and Dr Dominic Alibhai for compiling a personalised software program that was used for image analysis.

This work is dedicated to my late father, Lionel Mordant, who I am sure would be very proud if he were here to witness its completion. Also of course to the rest of my family, especially my mother, Linda Mordant, who I know is extremely proud of my academic career thus far and has given unconditional love and support throughout.

Author’s Declaration

I declare that the work in this dissertation was carried out in accordance with the requirements of the University's *Regulations and Code of Practice for Research Degree Programmes* and that it has not been submitted for any other academic award. Except where indicated by specific reference in the text, the work is the candidate's own work. Work done in collaboration with, or with the assistance of, others, is indicated as such. Any views expressed in the dissertation are those of the author.

SIGNED:  DATE: 10/9/18

Table of Contents

Table of Tables

Table of Figures

Chapter 1. Introduction

1.1. Dengue virus: a global burden on public health

Dengue virus (DENV) is globally considered the most prevalent human arboviral disease, with approximately 3.9 billion people at risk of infection worldwide (Brady *et al.,* 2012). Dengue is endemic in over 100 countries, and approximately 50-100 million people present with symptomatic infections annually (Bhatt *et al.,* 2013; World Health Organisation, 2017).

1.1.1. Dengue virus epidemiology and transmission

Dengue is endemic in over 100 countries, including throughout the Americas, Africa, Eastern Mediterranean, South-East Asia and Western Pacific (World Health Organisation, 2017), and is regarded as ubiquitous throughout the tropics and subtropics. It was estimated that there were 96 million dengue infections worldwide that manifested some level of clinical disease in 2010, with 67 million occurring in Asia, 16 million in Africa, and 13 million in the Americas (Bhatt *et al.,* 2013). However, due to issues such as misdiagnoses, incomplete understanding of the full spectrum of disease caused by DENV, and lack of infrastructure to maintain robust surveillance programmes, it has been suggested that under-reporting of dengue cases in certain countries is between 8- and 28-fold (Sharp *et al.,* 2017).

DENV is an arthropod-borne virus (arbovirus); its primary vector is the *Aedes aegypti* mosquito which has a vast geographic range, spanning tropical and subtropical areas worldwide (Kraemer *et al.,* 2015). *Ae. aegypti* lives in close proximity to both rural and urban human habitats, preferentially feeds on humans, and has a high multiple-feeding rate (Harrington *et al.,* 2014; Ndenga *et al.,* 2017; Ponlawat and Harrington, 2005). *Ae. albopictus* is the secondary vector of DENV which has also been shown to preferentially feed on humans (Ponlawat and Harrington, 2005). The native range of *Ae. albopictus* is Eastern Asia and India, however this species' range has expanded rapidly in the last thirty years and this mosquito is now an invasive species that is present on all continents (Kraemer *et al.,* 2015; Paupy *et al.,* 2009). Expansion of the geographic range of both of these vector species is attributed to several factors, including urbanisation and population growth, trade and travel, and climate change, among many others. These various vector factors – expanding worldwide distribution, climate change, and anthropophilic mosquito feeding behaviours – as well as increasing human travel, population growth, and urbanisation all contribute to the efficient transmission and increasingly extensive global spread of DENV and its associated disease burden.

1.1.2. Flaviviridae family

DENV is a member of the *Flaviviridae* family of viruses, of the genus *Flavivirus*. Typically, flaviviruses are small and enveloped, with positive-stranded, non-segmented RNA genomes of approximately 10.6-10.9 kb (Simmonds *et al.,* 2017). There are around 15 other human disease-causing flaviviruses, including Zika (ZIKV), West Nile (WNV), Japanese encephalitis (JEV), and yellow fever (YFV) viruses (Burrell *et al.,* 2017).

Flaviviruses constitute a great number of emerging and resurging diseases worldwide. Many flaviviruses are arboviruses (Mackenzie *et al.,* 2004), and as such, their ability to spread and become established in new areas where suitable vectors exist is significant. WNV is transmitted primarily by *Culex* spp. mosquitoes, and caused a large outbreak in New York in 1999 which rapidly spread throughout North America in the following years, and also spread to Central and South America *via* migratory birds and their flyways (Gubler, 2007). JEV is endemic and causes epidemic outbreaks throughout temperate and tropical areas of East and southern Asia and some northern areas of Oceania, and is also transmitted by mosquitoes in the *Culex* genus (van den Hurk *et al.,* 2009). There are several other flaviviruses, such as ZIKV and YFV, that, similarly to DENV, are transmitted by *Ae. aegypti* and other *Aedes* mosquito species; thus, there is much overlap in geographic range of these diseases, particularly between DENV and ZIKV, and another arbovirus, chikungunya virus (CHIKV) from the *Togaviridae* family. These viruses are all distributed and have caused major epidemics throughout the tropics and subtropics, particularly in South America, Africa, and Asia (Messina *et al.,* 2016; Staples *et al.,* 2009). DENV, ZIKV and CHIKV are known to co-circulate in many areas, and as anticipated, co-infections with either two or all three of the viruses have been discovered in Central and South America (Pessoa *et al.,* 2016; Waggoner *et al.,* 2016).

1.1.3. DENV serotypes

There are four serotypes of dengue, DENV-1-4; these originated approximately 1000 years ago, evolved from a common ancestral strain in non-human primates and seemed to transmit to humans between 320 and 125 years ago (Holmes and Twiddy, 2003).

DENV serotypes share between 60-75% amino acid sequence homology, and are antigenically distinct (Holmes, 1998). Phylogenetic analysis of DENV serotypes is often based on sequencing the envelope (E) gene which encodes the viral envelope protein and is the major antigenic determinant of DENV. Phylogenetic analysis has enabled distinction of the four DENV serotypes, as well as further characterisation of distinct genotypes within each serotype (Chen and Vasilakis, 2011). Viruses within the same serotype share approximately 6% sequence homology at the nucleotide level, and 3% at the amino acid level (Harris *et al.,* 2015). Genetic diversity among the various DENV serotypes is increasing; this is attributed to

factors such as genetic recombination, high mutation rates during viral replication, natural selection and genetic bottlenecks. Increasing viral genetic diversity has many implications for potential changes in phenotypic effects, such as increased virulence, epidemic potential, transmissibility, or changing host and vector ranges (Harris *et al.,* 2015; Holmes and Burch, 2000; Holmes and Twiddy, 2003).

All four DENV serotypes can be found throughout the tropics and subtropics, typically in urban and peri-urban environments. Due to the ubiquitous spread of all four DENV serotypes throughout the tropics, co-circulation and incidences of co-infection with multiple serotypes is increasing in many areas (Shrivastava *et al.,* 2018).

Recently, there has been debate over the discovery of a putative fifth DENV serotype in samples collected during an outbreak in Malaysia in 2007. Genetic sequencing revealed a strain that most closely resembled DENV-4 but was phylogenetically distinct from all four DENV serotypes and infection of rhesus macaques with the new strain following pre-infection with the other four serotypes revealed a distinct antibody response. The putative DENV-5 strain follows the sylvatic cycle between non-human primates and *Aedes* spp. mosquitoes; as such, it is possible that this human case in Malaysia was a chance event and the infected human was an incidental host (Mustafa *et al.,* 2015). However, little follow-up has been carried out since the initial report, therefore more data is required to fully characterise this strain and determine whether it is truly the first novel DENV serotype to be discovered in over 50 years, or whether it is a variant of an existing DENV serotype (Taylor-Robinson, 2016).

1.2. Dengue pathogenesis

Previous estimates suggest that approximately 96 million cases of dengue infection manifest clinically per year (Bhatt *et al.,* 2013), with approximately 500,000 cases of severe dengue that require hospitalisation, and a mortality rate of 2.5% (World Health Organisation, 2017).

1.2.1. Dengue disease

While most infections with DENV are asymptomatic or subclinical, infection can produce a wide spectrum of disease. In 2009, the WHO recommended a revised case classification system, classifying clinical dengue infections into dengue fever, dengue with warning signs, and severe dengue with the intention of improving dengue clinical treatments and surveillance (Barniol *et al.,* 2011). Most commonly, patients suffer from dengue fever, a relatively severe but self-limiting flu-like illness characterised by rapid onset of fever, rash, myalgia, arthralgia,

and retro-orbital pain. Dengue with warning signs progresses to include abdominal pain, vomiting, clinical fluid accumulation and liver enlargement, which are used as indicators of a patient's potential progression to severe dengue. Severe dengue is characterised by severe plasma leakage which can lead to shock, called Dengue Shock Syndrome (DSS), haemorrhaging, called Dengue Haemorrhagic Fever (DHF), and organ impairment, including effects on the liver, heart, and central nervous system, which can lead to death. Other atypical manifestations of dengue disease are also being more frequently reported, such as encephalitis and acute respiratory distress syndrome (Barniol *et al.,* 2011; Harris *et al.,* 2015; Martina *et al.,* 2009; Whitehorn and Simmons, 2011).

1.2.2. Immunopathology and risk factors in severe dengue disease

All four DENV serotypes can cause the full spectrum of dengue disease, however severe dengue most commonly occurs upon secondary infection with a different serotype when pre-existing immunity to the first serotype is already present. Additionally, the peak in symptoms is often associated with a rapid reduction in viral load and a cytokine storm, which suggests a key role for the host immune response in dengue pathogenesis (Screaton *et al.,* 2015).

Primary infection with one DENV serotype generates virus-neutralising antibodies that provide long-lasting serotype-specific immunity, and E-protein-specific antibodies that are cross-reactive to different serotypes (Reich *et al.,* 2013). Antibody-mediated protection is transient, and over time when antibody levels decline the individual is no longer protected from infection with a heterologous serotype. Following primary infection, subsequent infection with the same serotype is neutralised and no clinical disease is usually apparent (Whitehorn and Simmons, 2011). However, upon secondary infection with a heterologous serotype, non-neutralising cross-reactive antibodies bind the virus and, rather than offering a protective effect, the antibodies bind to Fc receptor-bearing cells and facilitate viral entry (Vaughn *et al.,* 2000). This phenomenon is termed antibody-dependent enhancement (ADE). ADE can be readily demonstrated *in vitro* and in animal studies, however, there is still ongoing debate surrounding the role of ADE during human infection with DENV and its potential implications for the development of a successful dengue vaccine.

In addition to the B cell-mediated response, cross-reactive DENV-specific T lymphocytes are also thought to play a role in immunopathology during both primary and secondary infection, with the magnitude of the T cell response correlating with disease severity (Screaton *et al.,* 2015). $CD8^+$ T cells produce greater levels of proinflammatory cytokines such as tumour necrosis factor (TNF) and interferon gamma (IFNγ) during severe dengue disease than during mild dengue fever, causing a cytokine storm (Rothman, 2011). This inflammatory response

contributes to vascular permeability and plasma leakage, which are important clinical manifestations of severe dengue (Whitehorn and Simmons, 2011). Additionally, during secondary infection it is thought that the T cell response does not clear infection as effectively as during primary infection, and this is partially attributed to the phenomenon of original antigenic sin. While some T cells that expand during secondary infection are cross-reactive for peptides derived from viruses of both primary and secondary infections, some of the expanded T cell population are also cross-reactive but preferentially respond to the primary infecting serotype and have lower avidity for the secondary infecting serotype. This may be detrimental to the overall response to infection, resulting in delayed and/or weaker viral clearance and increased pathogenesis (Mongkolsapaya *et al.,* 2003; Rothman, 2011; Screaton *et al.,* 2015). Furthermore, during severe disease caused by secondary DENV infection, cross-reactive $CD8^+$ T cells do not degranulate to as high a level as T cells with single specificity for the current infecting virus, which potentially also reduces their ability to control virus infection (Mongkolsapaya *et al.,* 2006; Rothman, 2011). However, the impact of original antigenic sin on dengue disease pathogenesis remains controversial because it has yet to be well demonstrated in human DENV infections (Rothman, 2011; Screaton *et al.,* 2015).

Sequential infection with a heterologous serotype and the associated immunopathology is considered the largest risk factor for severe dengue (Burke *et al.,* 1988; Katzelnick *et al.,* 2017), however there are many other factors that come together to lead to severe dengue disease. Host risk factors for severe dengue disease include host genetic determinants of disease susceptibility and pre-existing comorbidities, as well as certain ages, genders and nutrition status which are more susceptible to severe disease (Anders *et al.,* 2011; Coffey *et al.,* 2009). Viral determinants of disease severity include viral genotype and viremia titre at early stages of infection (Vaughn *et al.,* 2000). Viral epidemiology also plays a role; oscillations in the prevalence of each serotype in DENV-endemic areas due to the development of herd immunity puts more people at risk of sequential infection with a heterologous serotype (Adams *et al.,* 2006). DENV serotypes are phylogenetically distinct and therefore each has distinct characteristics of infection and different likelihoods of causing DHF in different areas; for example, it was suggested that DENV-2 and DENV-3 are twice as likely to result in severe dengue disease as DENV-4 during secondary infection in hospitalised children in Thailand (Fried *et al.,* 2010), but in Singapore, infection with DENV-1 was more highly associated with DHF than DENV-2 and DENV-3 (Yung *et al.,* 2015).

Overall, the outcome of dengue infection is influenced by complex interactions between various viral, host, and immunopathologic factors.

1.3. Dengue virus genome organisation and virion particle

1.3.1. DENV virion structure

The DENV virion particle is icosahedral, approximately 50 nm in diameter (Kuhn *et al.,* 2002). Three structural proteins, C, prM/M and E are the components of the virion particles. The outer surface of the DENV particle is comprised of the E glycoprotein and M protein which function in host-viral interactions for fusion and entry, antigenic determination and aid viral assembly and budding (Zhang *et al.,* 2004). Below the outer shell is an internal lipid bilayer derived from the host endoplasmic reticulum (ER), in which the E and M proteins are both anchored *via* their C-terminal domains. This membrane surrounds the virion's nucleocapsid core which is comprised of multiple copies of the C protein and the viral genomic RNA (Zhang *et al.,* 2003). The external surface structure and protein composition is distinct between the immature and mature particles. While the mature virion has a smooth surface, comprised of 90 E protein homodimers arranged in a herringbone pattern (Kuhn *et al.,* 2002), the external surface of the immature virion is composed of 60 trimers of prM-E heterodimers which form protruding spikes (Perera and Kuhn, 2008; Zhang *et al.,* 2003).

1.3.2. DENV genome organisation

The viral genome contains a single positive-strand, non-segmented, ~10.7 kb RNA genome. This genome encodes a single long open reading frame (ORF) that is flanked by 5′ and 3′ untranslated regions (UTRs) (Figure 1.1). Translation of the single ORF generates a large polyprotein that is co- and post-translationally cleaved into 10 proteins: 3 structural proteins, C, prM/M and E, and 7 non-structural (NS) proteins, NS1, NS2A, NS2B, NS3, NS4A, NS4B, and NS5 (Gebhard *et al.,* 2011) (Figure 1.1).

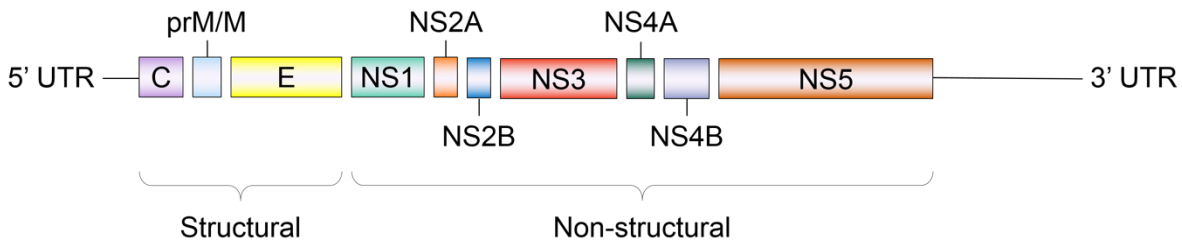

Figure 1.1: Diagram of the DENV genome. Diagram of the 10.7 kb DENV genome showing the single ORF that encodes 10 viral proteins (C, prM/M, E, NS1, NS2A, NS2B, NS3, NS4A, NS4B, and NS5), and the flanking 5' and 3' UTRs.

1.3.3. C protein

The DENV C protein is a small dimeric protein of approximately 12 kDa, with an alpha-helical structure. Multiple C copies form the nucleocapsid core that surrounds a single copy of the viral genome (Jones *et al.,* 2003). Within infected cells, DENV C localises to both the cytoplasm and the nucleus and has a range of functions, both as a structural component of infectious virions, and in the viral replication cycle. DENV C accumulates around ER-derived lipid droplets (LDs), and this localisation is necessary for DENV replication. Association with LD structures possibly provides a mechanism by which the C protein encapsidates the genome, by forming a scaffold to allow encapsidation during nucleocapsid assembly (Samsa *et al.,* 2009). DENV C has also been shown to be involved in pathogenesis; when localised to the nucleus, the C protein physically interacts with the human death domain-associated protein, Daxx. This interaction was previously shown to be involved in apoptosis of infected liver cells *in vitro*, and may play a role in clinical manifestations during severe dengue disease that lead to hepatic failure (Limjindaporn *et al.,* 2007; Netsawang *et al.,* 2010).

1.3.4. prM and M proteins

The prM pre-membrane protein is a 26 kDa precursor to the mature M protein. The primary function of prM is as a chaperone to mediate proper folding and secretion of E protein. During virion maturation, prM associated with E on the outer surface of immature virions undergoes furin cleavage, and the pr pre-peptide is retained in association with E and is thought to prevent premature fusion of virions with host intracellular membranes. pH-dependent dissociation of pr enables E to become fusogenic and virions to become infectious (Yu *et al.,* 2008; Zybert *et al.,* 2008). However, it has been shown that the cleavage of prM to M is not very efficient, and cell lines release high numbers of virion particles that still contain uncleaved prM (Zybert *et al.,* 2008). During infection, antibodies to prM can be detected, however these are non-neutralising and possibly actually promote antibody-dependent enhancement of the host

immune response (Dejnirattisai *et al.,* 2010). Non-structural functions of prM/M are largely unknown; however, one study has shown that prM interacts with host vacuolar-ATPases (V-ATPases) which acidify intracellular organelles. V-ATPase mediates the low pH-dependent endosomal pathway entry of DENV, suggesting that the prM-V-ATPase interaction may play a role in mediating low pH-dependent processes such as viral entry, secretion, and exocytosis. It was also suggested that this interaction is important for viral replication, which was significantly reduced upon treatment with a V-ATPase inhibitor (Duan *et al.,* 2008).

1.3.5. E protein

The E protein is a glycoprotein of approximately 53 kDa, consisting of 495 amino acid residues (Kuhn *et al.,* 2002; Zhang *et al.,* 2003). As a class II fusion protein, it is composed of three domains: Domain I, the central domain; Domain II, an elongated domain that bears the fusion loop which is directly involved in the fusion of viral and cellular membranes; Domain III, an Ig-like structure with a stem that connects the structure to the transmembrane anchor, and is responsible for recognising host cell receptors (Harrison, 2015; Kielian, 2006).

The DENV E protein functions in viral-host cell receptor interactions that subsequently allow viral fusion and entry into host cells (Modis *et al.,* 2003), however DENV binds to a wide range of host receptors, thus specific binding sites on the E protein for cellular receptors remain unclear (Cruz-Oliveira *et al.,* 2015). As the surface protein of infectious DENV particles, it is the major antigenic determinant of dengue infection that elicits a neutralising antibody response within the host (de Alwis *et al.,* 2012; Crill *et al.,* 2009). While the majority of antibodies raised against DENV during infection recognise various epitopes on the E protein, antibodies against the prM and NS1 proteins can also be expressed during infection, but to a lesser extent or with a poorer neutralising effect (Beltramello *et al.,* 2010).

1.3.6. NS1 protein

The DENV NS1 protein is a 46-50 kDa glycoprotein that is found in various cellular locations and displays a wide range of distinct functions during infection. During infection, DENV modifies host cellular membranes to form convoluted membranes (CM), vesicle packets (VP), and establish sites of replication, termed replication complexes (RC). An ER membrane-bound form of NS1 localises to VPs and cytoplasmic vacuoles that facilitate viral RNA replication and it is widely known that NS1 plays a central role during early stages of viral RNA replication (Mackenzie *et al.,* 1996; Muller and Young, 2013; Watterson *et al.,* 2016). While the exact mechanism remains elusive, it is thought that NS1 may play a structural role by anchoring the replication complex to the membrane through interactions with NS4A and NS4B at the ER

membrane (Lindenbach and Rice, 1999; Muller and Young, 2013). A critical function of NS1 in the assembly of infectious DENV particles has also been described, with multiple NS1 mutants found to release up to 100-fold fewer infectious particles than wild-type, with negligible or minor defects in viral RNA replication or NS1 protein stability (Scaturro *et al.,* 2015). The authors also describe NS1 interactions with DENV structural proteins, E and prM, which they suggested could mediate its function during viral assembly. Additionally, NS1 can be found on the surface of the plasma membrane, and can also be secreted from infected cells during infection (Young *et al.,* 2000); both of these forms of NS1 are highly immunogenic and play a paradoxical role by eliciting both a protective host immune response and inducing inflammatory cytokine release that contributes to immune-modulated pathogenicity (Beatty *et al.,* 2015; Modhiran *et al.,* 2015; Modhiran *et al.,* 2017). Secreted NS1 also aids in subversion of the host immune response through inhibition of complement activation (Avirutnan *et al.,* 2011; Avirutnan *et al.,* 2010).

1.3.7. NS2A protein

NS2A is a 22 kDa hydrophobic protein found on the ER membrane of infected cells (Xie *et al.,* 2013) that has been shown to play an important role in viral RNA replication by co-localising with dsRNA, NS4A, and other non-structural proteins NS1, NS3 and NS5 within the viral RC in VPs (Mackenzie *et al.,* 1998). It also plays an important role in viral assembly by contributing to the remodelling of membranes and formation of virus-induced membrane structures that contain the sites of viral RNA replication and of viral assembly (Nemésio and Villalaín, 2014). It has also been suggested that NS2A may function as a transporter of the partially-assembled replicase complex *via* hydrophobic interactions with NS4A, consisting of viral RNA, NS2A, NS3 and NS5, from the replication complex to the site of virion assembly (Leung *et al.,* 2008; Liu *et al.,* 2003; Xie *et al.,* 2015). Interestingly, it has been proposed that two distinct sets of NS2A molecules function in either DENV RNA replication or DENV particle assembly, and these are either located in viral replication complexes in the rough ER, or at viral assembly sites in rough ER lumen and Golgi vesicles, respectively (Xie *et al.,* 2015). Additionally, NS2A has also been implicated in evasion of the host immune response through inhibition of the type I interferon (IFN) signalling pathway (Muñoz-Jordan *et al.,* 2003, 2005).

1.3.8. NS2B protein

NS2B is a 14 kDa integral ER membrane protein that is comprised of three domains: a central region of 47 amino acids that acts as an essential cofactor to facilitate proper folding and catalytic function of the viral NS3 protease, which is flanked by two hydrophobic transmembrane regions that anchor the NS2B-NS3 complex in the ER membrane (Clum *et*

al., 1997; Falgout *et al.,* 1991, 1993). The NS2B-NS3 serine protease functions in proteolytic processing of the viral polyprotein encoded by the single ORF in the DENV genome; NS2B-NS3 is responsible for cleavages at the NS2A/NS2B, NS2B/NS3, NS3/NS4A, NS4A/2K, and NS4B/NS5 junctions (Lindenbach *et al.,* 2007). NS2B-NS3 is also implicated in evasion of the host immune response during infection by targeting the human adaptor protein, stimulator of the interferon gene (STING), for proteolytic degradation (Aguirre *et al.,* 2012). Recently, it was shown that cyclic GMP-AMP synthase (cGAS) is also degraded during DENV infection; cGAS is a cytosolic DNA sensor that binds to viral nucleic acids and specifically activates STING as part of the type I IFN induction pathway. Interestingly, degradation of cGAS was mediated by the NS2B cofactor alone, was not dependent on the formation of the NS2B-NS3 protease complex or on NS3 alone, and this was the first report of an IFN antagonist function for NS2B by itself (Aguirre *et al.,* 2017). By targeting STING and cGAS for degradation, DENV is able to disrupt the type I IFN signalling pathway and evade these branches of the innate immune response (Aguirre *et al.,* 2012). While its role as a cofactor for the NS3 protease is its most well-studied function, NS2B has also been tentatively suggested to function as a viroporin that forms pore-like structures in lipid environments (Dionicio *et al.,* 2018; León-Juárez *et al.,* 2016); however, further investigation is required to assess this viroporin effect and its potential functional relevance during DENV infection.

1.3.9. NS3 protein

NS3 is a large, 70 kDa, multifunctional protein, that localises to CMs and RCs on the ER membrane (Welsch *et al.,* 2009), and possesses several domains that play distinct and essential roles in the viral life cycle. As mentioned previously, NS3 possesses an N-terminal serine protease domain that requires NS2B as a cofactor to become catalytically-active, and functions in viral polyprotein processing (Falgout *et al.,* 1991, 1993). At its C-terminus, NS3 encodes a region with RNA triphosphatase (RTPase), RNA-stimulated nucleoside triphosphatase (NTPase), and, interestingly, both RNA helicase and strand annealing activities (Gebhard *et al.,* 2012; Li *et al.,* 1999; Wang *et al.,* 2009a), all of which are essential functions for viral genome replication. NS3 has been shown to localise to convoluted membranes (CM) on the ER (Welsch *et al.,* 2009), which, together with its known functions in viral genome replication, suggest that NS3 is an integral part of the viral replication complex. In addition to its well-characterised interaction with NS2B to form the NS2B-NS3 serine protease complex, NS3 also interacts with other viral and host proteins to carry out various roles during infection. During DENV infection, host fatty acid biosynthesis pathways are altered and it is thought that this plays a role in the establishment of viral RCs. NS3 has been shown to interact strongly with and recruit the host fatty acid synthase (FASN) enzyme to sites of

replication, and also increase fatty acid synthesis in a dose-dependent manner (Heaton *et al.,* 2010), however the exact mechanism by which NS3 stimulates fatty acid biosynthesis is yet to be elucidated. Overall, this suggests that NS3 plays a role in enhancing viral replication not only through its function as a protease together with NS2B, but also by modulating host fatty acid biosynthesis pathways. DENV-mediated modulation of fatty acid biosynthesis is discussed in more detail in Section 1.6. NS2B-NS3 also plays a role in pathogenesis by inducing host cell apoptosis (Lin *et al.,* 2014). The viral protease interacts with members of the IκB family of inhibitory proteins that, upon degradation, activate translocation of the nuclear factor kappa-light-chain-enhancer of activated B cells (NF-κB) transcription factor to the nucleus, which activates target genes that encode cytokines, chemokines and proteins involved in apoptosis. NS2B-NS3 cleaves both IκBα and IκBβ, leading to infected cell death and haemorrhage development in mice (Lin *et al.,* 2014).

1.3.10. NS4A protein

NS4A is a small, 16 kDa hydrophobic protein that is still relatively poorly characterised compared to other DENV proteins. During polyprotein processing, the N-terminus of NS4A is generated by NS2B-NS3-mediated cleavage (Miller *et al.,* 2007). NS4A co-localises with DENV E protein and dsRNA to sites of viral replication and induces intracellular membrane alterations that are thought to form the basis of RC generation (Miller *et al.,* 2007; Welsch *et al.,* 2009). NS4A also directly interacts and co-localises with vimentin, a host protein that undergoes reorganisation during DENV infection, and through its interaction with NS4A is thought to form a structural scaffold to anchor DENV RCs in the ER membrane (Teo and Chu, 2014). Furthermore, NS4A also interacts with NS4B in the RC, and mutants containing mutations that disrupted this interaction are defective in viral replication (Zou *et al.,* 2015b). Together, these factors suggest that NS4A is an important component of the viral replication complex.

NS4A has been shown to play a key role in the regulation of host cell autophagy during infection in a cell type-specific manner. DENV induces autophagy in epithelial cells which enhances viral replication and protects from cell death, while in macrophages apoptosis was induced. In one study, each DENV gene was expressed individually in Madin-Darby Canine Kidney (MDCK) cells and protection against cell death induced by camptothecin (CPT), a DNA-damaging agent, was measured. NS4A was shown to be the only protein that protected the cells from cell death, decreasing CPT toxicity by 35%, almost to a similar extent as infection with whole virus which decreased CPT toxicity by 40%. The authors also showed that NS4A-expressing cells induced autophagy to a similar extent as infection with live DENV virus (McLean *et al.,* 2011).

1.3.11. NS4B protein

NS4B is a small hydrophobic, integral membrane protein of 27 kDa that resides in ER membranes. During viral polyprotein processing, the 2K fragment facilitates translocation of NS4B from the cytoplasm to the ER lumen and is then removed from the NS4B N-terminus by host signalase. Mutational analyses have shown that functional NS4B is essential for viral replication, and NS4B co-localisation with NS3, NS4A and dsRNA in the perinuclear region, as well as ER protein markers, but not Golgi markers or lipid droplets, suggests that NS4B plays an integral role in viral replication and not a later stage of infection (Miller *et al.,* 2006; Zou *et al.,* 2015b; a). NS4B dissociates NS3 from ssRNA, thus enabling it to bind to a new duplex and enhancing the function of NS3 as an RNA helicase (Umareddy *et al.,* 2006), and this direct NS3-NS4B interaction is critical for successful viral replication (Chatel-Chaix *et al.,* 2015). DENV NS4B has also been shown to be a key viral modulator of the host immune response, allowing immune evasion to enhance viral infection. During infection NS4B inhibits the phosphorylation and activation of signal transducer and activator of transcription 1 (STAT1) (Muñoz-Jordan *et al.,* 2003); STAT1 is an important component of the type I IFN pathway which functions as the first line of defence against viral infections and therefore is a key determinant of infection progression (Morrison *et al.,* 2012; Shresta *et al.,* 2004). The function of NS4B as an antagonist of host immune responses is a focus of this project and is discussed in more detail in Section 1.5. Elucidating the specific roles of NS4B in viral replication and as an antagonist of the host innate immune response has been of great focus, and these key functions have led to the development of antiviral compounds that specifically target the flavivirus NS4B (van Cleef *et al.,* 2013; Xie *et al.,* 2011, 2015b), however none of these have yet reached the clinical trial stage.

1.3.12. NS5 protein

NS5 is the largest of the DENV proteins (~102 kDa) and is found in the cytoplasm and nucleus of infected cells. At its N-terminus there is a methyltransferase domain (MTase) with putative guanylyltransferase activity that is responsible for capping viral RNA in a two-step reaction, such that the cap resembles the 5′ capped eukaryotic mRNA which prevents its degradation and enhances interaction with the ribosome for translation (Issur *et al.,* 2009; Zhao *et al.,* 2015a). Capping the viral RNA also enables the virus to avoid detection by pathogen recognition receptors (PRR) that detect dsRNA or uncapped 5′ triphosphate RNA, such as retinoic acid inducible gene I (RIG-I) or melanoma differentiation-associated protein 5 (MDA5) (Chang *et al.,* 2016). At its C-terminus, NS5 possesses an RNA-dependent RNA polymerase (RdRp) domain that replicates viral RNA. During infection, the positive sense viral RNA is released into the cytoplasm where the NS5 RdRp transcribes it as a negative sense strand,

and then uses the negative strand from the dsRNA intermediate to synthesise viral positive strand RNA which is then used for translation or packaged into new virion particles (Sahili and Lescar, 2017). A linker sequence connects the two domains which determines their relative positions and provides distinct molecular conformations that may be required for its functions; mutation studies of linker residues suggest that the flexible linker domain is important for NS5 RdRp activity and viral replication (Lim *et al.,* 2013; Zhao *et al.,* 2015b).

NS5 functions as an antagonist of the type I IFN response by directly interacting with STAT2 and ubiquitin ligase E3 recognin 4 (UBR4) to promote the proteosomal degradation of STAT2, thus blocking the signalling pathway leading to the production of type I IFN (Ashour *et al.,* 2009). The NS5 protein has also been implicated in induction of interleukin-8 (IL-8) expression and secretion. IL-8 is a chemokine that is found in elevated levels in patients with DHF and is thought to be a key determinant of DENV pathogenesis (Clyde *et al.,* 2006; Li *et al.,* 2010). NS5 expression increased transcription of three transcription factors involved in IL-8 mRNA induction: CAAT/enhancer binding protein (c/EBP), and to a lesser extent, NF-κB and activating protein 1 (AP-1) (Medin *et al.,* 2005). Thus, DENV NS5 is an important determinant for establishment of infection, subversion of host immunity, and DENV pathogenesis.

1.4. Overview of DENV replication cycle in human hosts

Upon infection following a blood meal taken by an infected mosquito vector, DENV infects a wide range of human host cell types. The primary targets for DENV infection are phagocytes of the mononuclear lineage, including monocytes, macrophages, dendritic cells (DC) and Langerhans cells. As the infected leukocytes travel through the lymphatic system, DENV is able to spread and viral antigens can be found in the liver, spleen, lymph nodes, kidney and thymus of infected hosts (Jessie *et al.,* 2004; Rodenhuis-Zybert *et al.,* 2010).

1.4.1. Binding and entry

DENV entry into target cells is mediated by the E protein which facilitates binding to cellular receptors, and enable fusion of viral and cellular membranes (Crill and Roehrig, 2001; Harrison, 2015; Heinz *et al.,* 2004).

DENV enters target cells *via* receptor-mediated clathrin-dependent endocytosis (Van Der Schaar *et al.,* 2008). Since DENV infects a wide range of target cells, it is able to exploit multiple different cell surface receptors to enable viral entry including, but not limited to, dendritic cell-specific intercellular adhesion molecular-3-grabbing non-integrin (DC-SIGN) on

DCs, mannose receptor (MR) on macrophages and heparan sulfate (Chen *et al.,* 1997; Cruz-Oliveira *et al.,* 2015; Miller *et al.,* 2008; Tassaneetrithep *et al.,* 2003). Upon internalisation, virus-receptor complexes are delivered to Rab5-positive early endosomes, which mature into Rab7-positive late endosomes. Low pH in the late endosomes triggers a conformational change in the E protein to allow fusion of viral and cellular membranes. The nucleocapsid escapes the endosomes and then uncoats to release the viral RNA into the cytosol (Krishnan *et al.,* 2007; Van Der Schaar *et al.,* 2008).

1.4.2. DENV genome replication and the replication complex

Once in the cytosol, the viral RNA is translated into a single polyprotein in association with ER-derived membranes. The polyprotein is then co- and post-translationally cleaved by both cellular proteases and the viral NS2B-NS3 protease to generate the 10 viral proteins. Translation and processing of the polyprotein is a fundamental process that must occur before viral genome replication can proceed; once the proteins are generated, the virus can then switch to genome replication (Clyde *et al.,* 2006; Fischl and Bartenschlager, 2011). Viral non-structural proteins are involved in replication, as described in more detail from Section 1.3.6.

DENV induces invaginations of the ER membrane, primarily *via* the NS4A protein, which forms structures with different morphologies, including VP and CM structures (Miller *et al.,* 2007; Welsch *et al.,* 2009). These structures serve as a scaffold for the viral RC that contains viral proteins, RNA, and likely also host cell factors being exploited for viral replication. The lumen of these structures are connected to the cytosol *via* a pore, which allows entry of nucleotides and other factors required for replication and exit of newly-synthesised copies of the viral genome to be packaged into progeny virions (Welsch *et al.,* 2009).

The non-structural proteins primarily coordinate replication of the viral genome and assembly of virus particles. NS3 and NS5 play enzymatic roles; NS3 has helicase, RTPase, NTPase and, together with NS2B, serine protease activities, while NS5 functions as a MTase and RdRp (Lindenbach and Rice, 2007). NS2A, NS4A and NS4B are all non-enzymatic; NS2A is thought to function in both viral replication and assembly (Xie *et al.,* 2015a), NS4A is thought to induce ER membrane invaginations (Miller *et al.,* 2007), and NS4B is essential for replication but while the primary mechanism is still unknown, it has been shown that NS4B dissociates ssRNA from NS3 to enhance replication (Miller *et al.,* 2006; Umareddy *et al.,* 2006). NS1 is known to be essential for both viral replication and assembly, but its exact function also remains elusive (Muller and Young, 2013).

In the replication complex, the positive-sense genomic RNA template is copied asymmetrically to favour generation of excess positive-sense RNA, as this serves as both viral genome and mRNA, however the mechanism by which asymmetric RNA replication occurs has not yet been described (Clyde *et al.,* 2006; Lindenbach *et al.,* 2007).

1.4.3. Virion assembly and maturation

Once all proteins are translated and RNA is replicated, the RNA interacts with the C protein to form the nucleocapsid; the flavivirus nucleocapsid has no regular geometry and appears highly unstructured, unlike in the virions of other groups such as alphaviruses of the *Togaviridae* family (Freire *et al.,* 2013). The nucleocapsid buds into the ER lumen, and the host-derived lipid membrane is acquired surrounding the nucleocapsid. This membrane also contains prM-E heterodimers that become incorporated to form immature DENV virions *via* interaction with the nucleocapsid (Apte-Sengupta *et al.,* 2014).

Immature DENV particles undergo maturation as they are transported along the secretory pathway through the trans-Golgi network (TGN), which is an acidic environment and induces a pH-dependent, reversible, conformational change in the E proteins. This conformational change in the E protein enables access and subsequent cleavage of the prM proteins by furin, a cellular protease found in the TGN. Following cleavage of prM into its' components, the M protein exists as a transmembrane protein beneath the E protein outer layer, while the pre-peptide (pr) remains associated with the E protein (Yu *et al.,* 2008).

It has been previously shown that processing of prM to M using host furin or a furin-like protease, during maturation is required for infectivity of the virion particles. One study compared the infectivity of fully immature DENV-2 particles cultured in cell lines that lack functional furin with DENV-2 cultured in cell lines that possessed the furin protease. The authors determined, through calculation of the ratio of genome-containing particles (GCP) to infectious units (IU), that immature particles were at least 10,000-fold less infectious due to the absence of functional furin (Zybert *et al.,* 2008). Another study showed that furin cleavage occurs only under acidic conditions at pH 5.0 to 6.0 and while uncleaved virions at pH 8.0 and pH 6.0 are mildly infectious, there is a 1000-fold increase in infectivity following low pH-dependent furin cleavage (Yu *et al.,* 2008).

The mature virions are released into the cytoplasm from the TGN and are transported to the outer cell membrane where they are released by exocytosis. When the virion reaches the pH-neutral extracellular environment, the pr peptide dissociates and exposes the E protein in the mature particle to allow E protein-mediated viral-host fusion to infect new cells. Neutral pH-

dependent dissociation of pr peptides from E proteins is thought to be a mechanism that prevents premature fusion of the mature virion with host membranes prior to release (Perera and Kuhn, 2008; Yu *et al.,* 2008).

1.5. Dengue virus evasion of the host innate immune response

1.5.1. Activation of the innate immune response during DENV infection

The innate immune response is the host's first line of defence against viral infection and is responsible for limiting viral spread during the early stages of infection. Several host PRRs have been reported to recognise DENV antigens as pathogen-associated molecular patterns (PAMPs) which then go on to activate various branches of the innate immune response (Sprokholt *et al.,* 2018). Viral dsRNA and ssRNA produced as replication intermediates are recognised by the cytoplasmic helicases RIG-I and MDA5 that detect intracellular viral nucleic acids (Loo *et al.,* 2008; Loo and Gale, 2011; Nasirudeen *et al.,* 2011), and Toll-like receptors (TLRs) that patrol extracellular and endosomal compartments. TLRs that are activated upon DENV infection include TLR3, TLR7, TLR8 and TLR9 (Barton, 2007; Xagorari and Chlichlia, 2008), and differential expression of these TLRs was reported in DCs of patients with dengue fever compared to DHF which may play an important role in disease progression (Torres *et al.,* 2013).

Triggering of PRRs by DENV leads to the activation of various intracellular signalling pathways that contribute to defence against infection, such as the protective IFN response and the inflammatory response. Activation of the transcription factor NF-κB results in the transcriptional activation and expression of proinflammatory cytokines and chemokines. While this is protective in many cases, overexpression of these inflammatory molecules can contribute to the pathogenesis associated with dengue disease. DC-SIGN, MR and C-type lectin domain family 5, member A (CLEC5A) are receptors found on the surface of innate immune cells, such as DCs, macrophages, monocytes and neutrophils that interact with the DENV E protein. DC-SIGN and MR primarily function in enabling DENV entry into target cells, however CLEC5A activation results in expression of high levels of IL-1β, IL-6, IL-8, IL-18 and tumour necrosis factor (TNF), all of which are pro-inflammatory cytokines (Chen *et al.,* 2008; Sprokholt *et al.,* 2018). Additionally, TLR4 can recognise the DENV NS1 protein which also results in the release of proinflammatory cytokines and chemokines and may be associated with DENV pathogenicity (Modhiran *et al.,* 2015, 2017).

1.5.2. The type I interferon signalling pathway

Upon virus recognition by PRRs infected immune cells such as DCs and macrophages produce high levels of type I IFNs, IFNα and IFNβ, within hours of infection and thus IFN production is often considered to be a critical first line of defence (Shresta *et al.,* 2004). Type I IFNs have three major functions: i) to induce an antiviral response that serves to limit viral infection; ii) to modulate the innate immune response to promote optimal antigen presentation, modulate NK cell functions, and regulate the inflammatory response; iii) to activate the adaptive immune system and enhance the antiviral immune response and induce antigen-specific B and T cell responses and immunological memory (Ivashkiv and Donlin, 2015).

Upon antigen recognition, RIG-I and MDA5 interact with an adaptor protein called mitochondrial antiviral signalling protein (MAVS) which interacts with STING to recruit and phosphorylate the kinases IκB kinase (IKK) and TANK-binding kinase 1 (TBK1). IKK and TBK1 activate the transcription factors IFN regulatory factor 3 (IRF3) and NF-κB, which transcriptionally induce the expression of IFNα/β. IFNα/β is then secreted out of infected cells (Castillo Ramirez and Urcuqui-Inchima, 2015; Liu *et al.,* 2015). On the surface of neighbouring cells, secreted IFNα/β binds to the transmembrane IFNα receptor (IFNAR) which activates the receptor-associated Janus kinase 1 (JAK1) and tyrosine kinase 2 (TYK2) kinases. JAK1 and TYK2 phosphorylate the cytoplasmic transcription factors STAT1 and STAT2, which causes pSTAT1 and pSTAT2 to dimerise and form a heterotrimeric complex with IRF9 called IFN-stimulated gene factor 3 (ISGF3). ISGF3 translocates to the nucleus and binds a specific genetic element called the interferon-stimulated response element (ISRE), found in the promoter region of IFN-stimulated genes (ISGs) (Ivashkiv and Donlin, 2015).

ISGs encode proteins with a plethora of antiviral functions, including the inhibition of viral genome replication and translation of viral proteins, degradation of nucleic acids and proteins, regulation of the inflammatory and adaptive immune responses, and modulation of host cellular pathways that are utilised by the virus, such as lipid metabolism (Ivashkiv and Donlin, 2015; Schneider *et al.,* 2014). IFN-inducible transmembrane proteins (IFITM) are ISG-encoded proteins with a wide range of antiviral functions at any stage of viral entry, and IFITM2 and IFITM3 have been shown to inhibit DENV infection, and siRNA knockdown of IFITM3 leads to an increase in DENV replication (Brass *et al.,* 2009; Jiang *et al.,* 2010). ISG20 has been identified as an inhibitor of DENV infection (Jiang *et al.,* 2010) and is thought to degrade viral RNA and potentially indirectly act on cellular factors that are necessary for viral replication or transcription (Zheng *et al.,* 2017). Viperin is another IFN-encoded protein that is upregulated during DENV infection and inhibits DENV genome replication and infectious particle release that limits infection progression (Helbig *et al.,* 2013; Jiang *et al.,* 2010).

1.5.3. DENV as an antagonist of the type I IFN immune response

The type I IFN response is a critical determinant of pathogenicity and as such, many viruses have evolved to express proteins that can actively function in evasion of the type I IFN response to enhance their own replication. During DENV infection, subversion of the immune response is primarily mediated by the viral non-structural proteins.

NS2A, NS4A and NS4B can disrupt signalling through RIG-I and MAVS by inhibiting TBK1 and IRF3 phosphorylation (Dalrymple *et al.,* 2015; He *et al.,* 2016), and the NS2B/NS3 protease cleaves STING and targets cGAS for degradation which, upon DNA binding, activates STING (Aguirre *et al.,* 2012, 2017; Yu *et al.,* 2012). Through these mechanisms DENV is able to disrupt the initial induction of IFNα/β and reduce its production in infected cells. Following IFNα/β production the NS2A, NS4A and NS4B proteins can block STAT1 phosphorylation and nuclear translocation and inhibit activation of the ISRE promoter, with NS4B having the strongest inhibitory effect (Muñoz-Jordan *et al.,* 2003, 2005). Additionally, NS5 binds to STAT2 and targets it for ubiquitination and proteasomal degradation, leading to reduced levels of STAT2 in infected cells (Ashour *et al.,* 2009), and also inhibits STAT2 phosphorylation and activation (Mazzon *et al.,* 2009). Together, inhibition of the function of STAT1 and STAT2 interferes with the IFNα/β signalling pathway and inhibits downstream activation of expression of key antiviral ISGs. Additionally, it has been suggested that induction of the formation of intracellular vesicles to function as sites for viral replication could be a mechanism by which DENV passively evades the immune response through avoiding intracellular recognition (Castillo Ramirez and Urcuqui-Inchima, 2015; Welsch *et al.,* 2009).

Altogether, mechanisms by which DENV evades the innate immune response are critical determinants of infection progression and pathogenicity. Due to their important functions in immune evasion, mutations in the non-structural proteins, particularly NS4B, that would diminish these function have been proposed as a strategy for the development of dengue live attenuated vaccines and DENV protein-targeted antivirals (Xie *et al.,* 2011; Xie *et al.,* 2015).

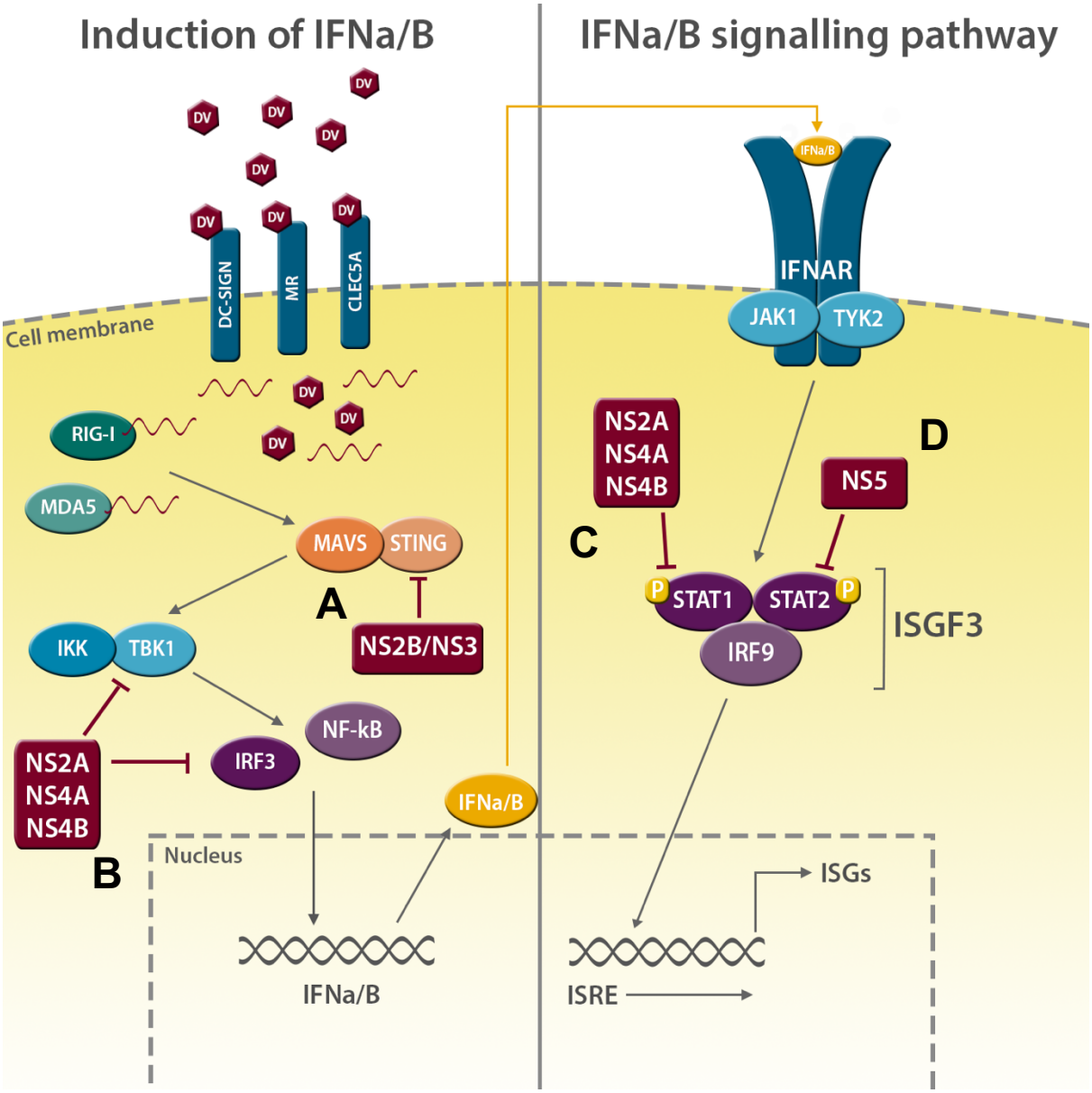

Figure 1.2: DENV antagonism of the type I IFN response. DENV particles enter target cells using receptors such as DC-SIGN, MR and CLEC5A and uncoat to release viral RNA genomes into the cytoplasm which are recognised by RIG-I and MDA5. RIG-I and MDA5 interact with MAVS which interacts with STING to phosphorylate IKK and TBK1. The DENV NS2B/NS3 protease cleaves STING **(A)**. IKK and TBK1 activate IRF3 and NF-κB transcription factors which induce the expression of IFNα/β; the DENV NS2A, NS4A and NS4B proteins inhibit the activation of TBK1 and IRF3 **(B)**. IFNα/β is secreted from infected cells and binds to IFNAR on the surface of neighbouring cells. This activates the JAK1 and TYK2 kinases, which phosphorylate STAT1 and STAT2 cytoplasmic transcription factors. The DENV NS2A, NS4A and NS4B proteins block STAT1 phosphorylation and nuclear translocation (C), while NS5 protein targets STAT2 for ubiquitination and proteasomal degradation (D). STAT1, STAT2 and IRF9 form a heterotrimer which translocates to the nucleus and binds the ISRE which initiates transcription and expression of antiviral ISGs. Adapted from (Ivashkiv and Donlin, 2015).

1.6. Dengue virus interaction with host lipid metabolism pathways

Viruses commonly exploit various aspects of host lipid metabolism pathways and lipid stores to promote their own replication cycle and enhance infection. Interactions between viruses and lipids have been shown to facilitate cell attachment and entry, to form replication complexes that allow viral genome replication, and to allow viral assembly and secretion (Heaton and Randall, 2011). Sterol biosynthesis pathways are downregulated upon viral infection and activation of the IFN response, which suggests that lipid metabolism constitutes a target for regulation mediated by the host immune response (Blanc *et al.,* 2011). Additionally, LDs are intracellular organelles that function as cellular stores of triglycerides and cholesterol esters and are closely linked to energy and lipid homeostasis, and they have increasingly been shown to play a role in modulating the host immune response. LDs play a role in antigen cross presentation, autophagy and production of inflammatory mediators and ISGs such as viperin localise to LDs in response to viral infection (Saka and Valdivia, 2012).

1.6.1. DENV modulation of cellular lipids and lipid metabolism pathways

Cellular lipids play important roles at various stages throughout the DENV replication cycle. Soon after DENV infection, total intracellular cholesterol levels increase which is mediated by enhanced activation of 3-hydroxy-3-methyl-glutaryl-CoA reductase (HMGCR), a key rate-limiting enzyme in cholesterol biosynthesis pathways, and an increase in low density lipoprotein receptor (LDLR) on the surface of infected cells to increase cholesterol synthesis and uptake, respectively (Soto-Acosta *et al.,* 2013). An increase in fatty acid synthesis is also stimulated, mediated by the DENV NS3 protein which recruits the FASN enzyme to sites of viral replication and allows establishment of RC structures (Heaton *et al.,* 2010). Early DENV infection is also associated with an increase in lipid raft formation (Soto-Acosta *et al.,* 2013) and host receptors required for DENV entry into cells, such as DC-SIGN, are have been found to co-localise with lipid rafts; it was suggested that this association enhances interaction of virus particles with DC-SIGN to facilitate entry into DCs, a major target cell for DENV infection (Cambi *et al.,* 2004). Upon DENV infection, the number of LDs per cell is also increased and LDs are thought to be exploited by DENV for multiple functions. Mature DENV C protein localises to the surface of LDs and proper localisation was found to be essential for the formation of infectious particles (Samsa *et al.,* 2009). However, co-localisation of LDs and viral replication complexes has not been observed (Welsch *et al.,* 2009) so LDs may play a more indirect role in the viral replication cycle (Fischl and Bartenschlager, 2011). Interestingly, an alternative function for LDs has also been reported; DENV-induced autophagy regulates lipid metabolism, and in cells with high numbers of autophagosomes it was observed that there is an associated decrease in lipid droplet area, reduced levels of triglycerides, and increased β-

oxidation. Autophagy is known to be required for DENV replication, and a model was proposed whereby autophagy-dependent depletion of cellular lipid stores results in the release of free fatty acids which undergo β-oxidation in mitochondria to generate ATP that is used to facilitate viral RNA replication (Heaton and Randall, 2010). Altogether, this suggests that DENV infection induces both anabolic and catabolic alterations to lipid metabolism. While depleting LDs and increasing intracellular ATP levels through β-oxidation provides energy that may facilitate viral replication, simultaneously increasing lipid biosynthesis may enable the formation of membrane-bound replication complexes through membrane remodelling (Heaton *et al.,* 2010; Heaton and Randall, 2010; Miller *et al.,* 2007; Soto-Acosta *et al.,* 2013; Welsch *et al.,* 2009).

During viral uptake and transport through the endosomal pathway, DENV utilises late endosome membrane-specific lipids, bis(monoacylglycerol)phosphate and phosphatidylserine, to mediate entry into late endosomes *via* fusion with the viral E protein (Zaitseva *et al.,* 2010).

Loss of cholesterol in the viral envelope through pre-treatment with a cholesterol-depleting drug, methyl-beta-cyclodextrin (MCD) results in inhibition of fusion between the virion envelope and the late endosomal membrane such that virion uncoating and release of the nucleocapsid into the cytosol is prevented (Carro and Damonte, 2013). DENV replication can also be inhibited by pharmacological inhibition of cholesterol biosynthesis or LD metabolism (Carro and Damonte, 2013; Rothwell *et al.,* 2009; Samsa *et al.,* 2009). Thus, interference with host lipid metabolism pathways could be an attractive target for antiviral drug development.

1.7. Dengue virus and flavivirus persistence

There is evidence that several members of the *Flaviviridae* family, such as Zika virus (ZIKV), hepatitis C virus (HCV), Murray Valley encephalitis virus (MVE), JEV, West Nile virus WNV and tick-borne encephalitis virus (TBEV) are capable of causing persistent infection (Barzon *et al.,* 2016; Gritsun *et al.,* 2003; Large *et al.,* 1999; Murray *et al.,* 2010; Poidinger *et al.,* 1991; Ravi *et al.,* 1993). Isolation of viable viral particles, antigens, or RNA from patient samples long after the initial acute illness can indicate persistent infection, and this can also be evident in blood donation samples and cell culture studies (Mlera *et al.,* 2014; Murray *et al.,* 2010; Poidinger *et al.,* 1991).

There have been several observed mechanisms that contribute to persistence in flaviviruses, the most important being subversion of host immune responses and regulation of apoptosis

and autophagy. During infection, the IFN response is activated within hours but flaviviruses commonly induce intracellular membrane rearrangements that are capable of hiding viral antigens, thus delaying activation of the IFN pathway and expression of antiviral ISGs (Overby *et al.,* 2010; Welsch *et al.,* 2009). Chronic infections and HCV persistence are well documented and associated with immune evasion strategies such as blocking RIG-I and MAVS signalling during the IFN response and persistent presence of viral antigen that chronically activates T cells leading to exhaustion and loss of T cell function (Baril *et al.,* 2009; Breiman *et al.,* 2005; Rehermann, 2009).

Immune evasion is primarily a temporary mechanism by which the virus establishes infection, however to establish persistent infection a common mechanism is virus-mediated regulation of autophagy and prevention of apoptosis. It has been observed that establishment of persistent infection by flaviviruses *in vitro* is characterised by an acute phase in which most of the cells are killed but a small population of cells survive and, while still infected, proliferate, suggesting that apoptotic host factors must be modulated (Mlera *et al.,* 2014). Indeed, *in vitro*, the DENV NS4A protein was shown to upregulate the number of autophagosomes to promote autophagy which prevented cell death and enhanced viral replication in epithelial cells and fibroblasts. However, this is cell type-specific as apoptosis was enhanced in macrophages (McLean *et al.,* 2011). Prevention of cell death in cell types naturally infected by DENV, yet increased apoptosis in immune cells such as macrophages, could be potential mechanisms by which DENV could theoretically establish persistent infection.

However, despite observations of modulation of autophagy and apoptosis by DENV, a major question still remains regarding whether or not DENV can cause persistent infections similarly to other flaviviruses. Mosquitoes and mosquito cell lines become persistently-infected with DENV (Chen *et al.,* 1994; Igarashi, 1979; Juárez-Martínez *et al.,* 2013; Salas-Benito and De Nova-Ocampo, 2015), however only few studies have shown that DENV can establish persistent human infections *in vitro* in which DENV infection persisted in human monocyte cell lines for several months (Kurane *et al.,* 1990; Nakao *et al.,* 1989). It was suggested that differences in host immune responses influence the difference in infection outcomes, with the *Ae. aegypti* RNA interference (RNAi) innate immune response being a critical factor for allowing maintenance of persistent infection in the mosquito (Sánchez-Vargas *et al.,* 2009).

Overall, previous evidence for persistent DENV infection and any clinical correlates in humans is sparse.

1.7.1. Discovery of a persistently-infecting dengue virus mutant

Preceding this project, Dr. Andrew Davidson and colleagues at the University of Bristol discovered a cell line persistently-infected with DENV-2. Baby hamster kidney (BHK)-21 cells were found to be infected with DENV-2, as confirmed by agarose gel electrophoresis analysis of RT-PCR products produced from extracellular RNA and immunofluorescence assay (IFA) analysis of the BHK-21 cells using an antibody against the DENV E protein (Figure 1.3A and B). This infection was non-cytopathic and found to be persistent as the infection was maintained during cell passaging.

Supernatant from the cultures of persistently-infected BHK-21 cells was transferred to cultures containing either uninfected C6/36 (mosquito) or Vero (mammalian) cells and was sufficient to infect the naïve cells (Figure 1.3C), which demonstrated that the cell lines were infected and producing viable, infectious particles. Once infection of C6/36 and Vero cells was established, it was also found to be persistent. DENV-2 RNA and protein levels were measured by qRT-PCR and western blot (Figure 1.3D and E); these showed that the persistently-infected cells were expressing lower levels of wild-type DENV-2 RNA at all time-points, and lower levels of NS5 protein than wild-type infected cells 30 hours post-infection. The viral genome from supernatants collected from BHK, C6/36 and Vero cells was sequenced, and mutations that were found are summarised in Table 1.1. The only mutation that was present in the genome of viruses isolated from supernatant collected from all cell types was at nucleotide 7021 (ACA → GCA), encoding a non-silent mutation that changed threonine (Thr) to alanine (Ala). This residue is located at position 66 encoded by the NS4B gene ($NS4B_{T66A}$). Another mutation present in the genome of all viruses except for those isolated from Vero cells was at nucleotide 7020 (CTA → CTG) which encoded a silent mutation next to the T66A amino acid mutation.

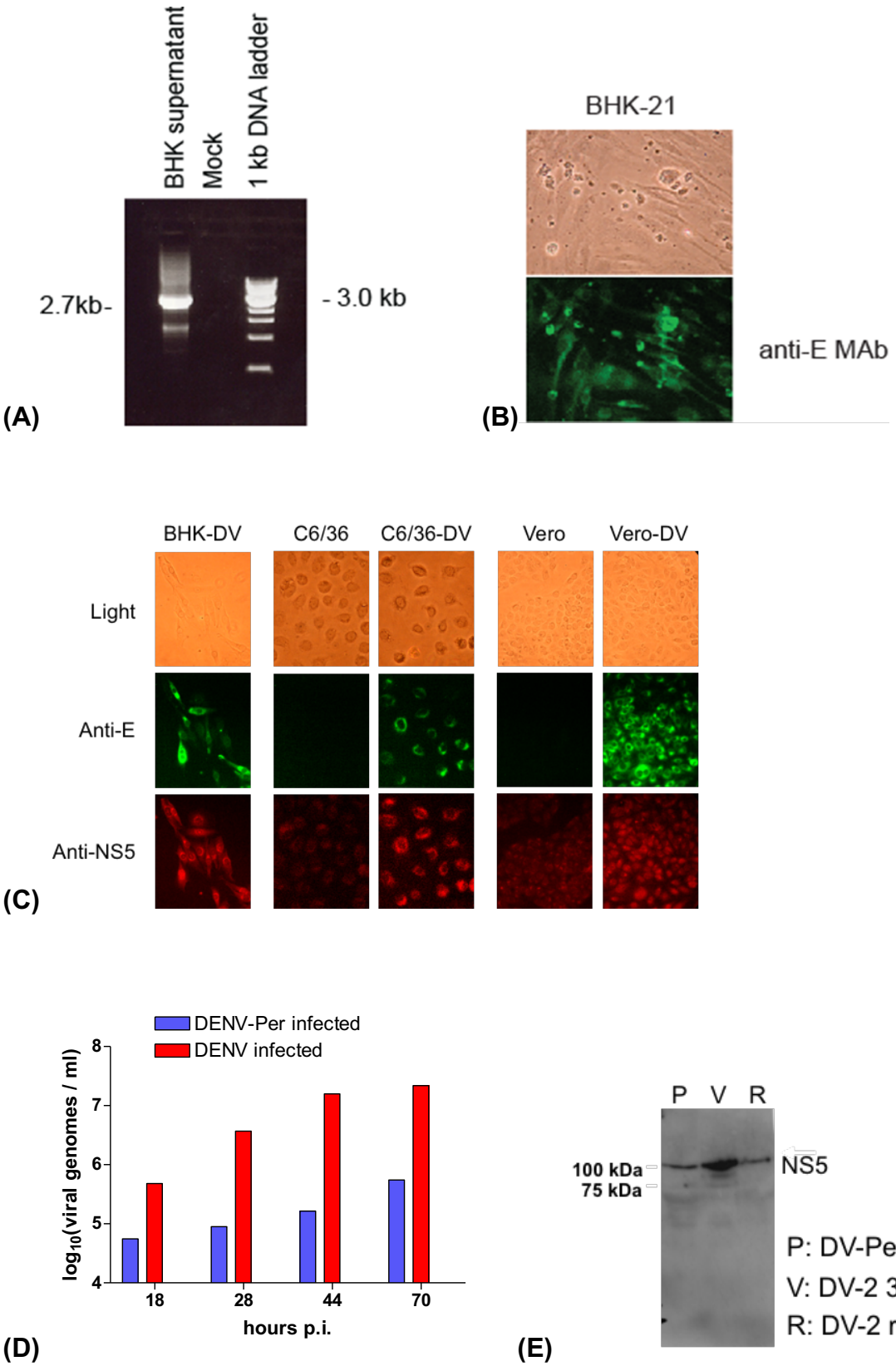

Figure 1.3: Discovery of BHK-21 cell line persistently-infected with DENV-2. Presence of DENV-2 RNA in supernatant of persistently-infected BHK-21 cells was confirmed by agarose gel electrophoresis on RT-PCR cDNA products (A). Intracellular presence of DENV E protein was confirmed by immunofluorescent staining using an anti-E mAb (B). Supernatant containing infectious particles collected from persistently-infected BHK-21 cell cultures was transferred to C6/36 and Vero cell cultures; infection in C6/36 and Vero cells was confirmed by immunofluorescent staining for the DENV

E and NS5 proteins (C). qRT-PCR was performed to measure the levels of DENV-2 RNA from the persistently-infected and wild-type-infected BHK-21 cells (D). Western blot for NS5 shows DENV-2 protein levels in persistently-infected, wild-type-infected, and replicon-containing BHK-21 cells (E). The figure was provided by Dr Andrew Davidson.

Table 1.1: Summary of mutations in the genome of a persistently-infecting virus aligned to the wild-type DENV-2 genome. Viral RNA was extracted from the supernatant of BHK, C6/36 and Vero cell lines persistently-infected with DENV-2 and sequenced by RT-PCR and Sanger sequencing. The only mutation present in viral samples isolated from supernatant from all cell types was in the NS4B gene (*). Data provided by Dr Andrew Davidson.

Gene	NT	Nucleotide sequence change				Codon change	Amino acid change
		BHK 1	BHK 2	C6/36	Vero		
NS3	6336	-	-	-	G → A	CT**G** → CT**A**	Leu
NS4A	6461	-	C → T	C → T	-	G**C**A → G**T**A	Ala → Val
NS4A	6463	T > G	G → T	G → T	-	**G**TG → **T**TG	Val → Leu
NS4A	6494	C → T	C → T	C → T	-	G**C**G → G**T**G	Ala → Val
NS4A	6502	-	-	-	C → G	**C**AT → **G**AT	His → Asp
2K	6786	-	T → A	T → A	-	GT**T** → GT**A**	Val
NS4B	7020	A → G	A → G	A → G	-	CT**A** → CT**G/A**	Leu
NS4B*	7021	A → G	A → G	A → G	A → G	**A**CA → **G**CA	Thr → Ala

The $NS4B_{T66A}$ mutation was engineered into a reverse genetic system by Dr Rebecca Ward using the plasmid pDVWS601, and this showed that the mutation was sufficient for establishing a persistent DENV-2 infection. The resulting virus, called v601-$NS4B_{T66A}$, was used to establish a persistent infection in two human embryonic kidney (HEK293T) cell lines (Ismail, 2015), termed H-v601-Per1 and H-v601-Per2 from here onwards, which were used throughout this project. Interestingly, upon infection of the naïve cells, the majority of cells in the population died, while a small subset of the population survived and proliferated to form the persistently-infected cell population.

Cell lines expressing subgenomic reporter replicons were also previously created to study the effects of this $NS4B_{T66A}$ mutation (Ismail, 2015) and were used throughout this project. In the replicon construct, pRepDV-GP2A, the structural protein gene sequences have been deleted except for sequences encoding the first 27 amino acids of the C protein and the last 24 amino acids of the E protein. The deleted sequence was replaced with a fusion gene expressing enhanced green fluorescent protein (eGFP) for replicon detection, and puromycin N-

acetyltransferase (PAC) for selection by puromycin (Massé *et al.,* 2010). Another replicon encoding plasmid, pRepDV-GP2A-NS4B$_{T66A}$, was also engineered to be identical to the pRepDV-GP2A sequence but containing the base mutations at nucleotides 7020 and 7021 to encode the NS4B$_{T66A}$ mutation. RNA transcribed from the plasmids pRepDV-GP2A and pRepDV-GP2A-NS4B$_{T66A}$ replicons was transfected into HEK293T cells and selected for stable expression of the replicon RNA (Ismail, 2015) (termed H-Rep and H-Rep-4B$_{T66A}$, respectively from here onwards).

RNAseq was performed for high-throughput transcriptomic analysis and transcriptome data was obtained prior to the commencement of this project (provided by Dr Andrew Davidson and Dr Rosmani Ismail). Total intracellular RNA was extracted from six cell samples in duplicate: HEK293T, H-v601-Per1, H-v601-Per2, H-Rep, H-Rep-4B$_{T66A}$ and HEK293T cells infected with wild-type DENV-2 virus, (termed H-v601 from here onwards). In short, low quality reads were filtered out after sequencing, and differential gene expression analysis was carried out using Tophat and Cufflinks software tools to ultimately generate pairwise comparisons of the RNAseq reads between each dataset and significant differences in gene expression between each of the cell types were identified.

We were particularly interested in how, when v601-NS4B$_{T66A}$ was introduced to naïve cell cultures, only a small subset of the cells in the original culture survived, proliferated and became persistently-infected. It was hypothesised that, as well as potential defects in protein function conferred by the NS4B$_{T66A}$ mutation, there may be cellular defects in the surviving cell population which allowed cell proliferation and acted to create a balance between host and virus that facilitated establishment of a persistent infection.

1.8. Aims of this project

The overall aim of this Masters project was to discover mechanisms by which the NS4B$_{T66A}$ mutation facilitated establishment of a persistent DENV-2 infection in human cells, and determine whether there is a defect in the persistently-infected cells that allowed establishment of a persistent infection.

The specific aims of the project were to:

1. determine whether the NS4B$_{T66A}$ mutation has an effect on the ability of the virus to subvert the type I IFN response in host cells.
2. bioinformatically analyse the transcriptomics dataset to:

a. identify any cellular pathways that are differentially modulated by persistently-infecting virus, relative to DENV-2 wild-type and
b. determine if there are any defects in cellular pathways that facilitated the establishment of persistent virus infection.

3. cure H-v601-Per1 and H-v601-Per2 cell lines of virus using antiviral drugs and analyse the cells to identify any potential defects in cellular pathways that have allowed establishment of persistent infection.

Chapter 2. Materials and Methods.

2.1. Cell culture methods.

2.1.1. Cell culture maintenance.

Human embryonic kidney 293 T (HEK293T) cells were maintained by successive passage in Dulbecco's Modified Eagle's Medium (DMEM; Lonza, Belgium) containing L-glutamine and 4.5 g/l glucose and supplemented with 10% foetal bovine serum (FBS; Invitrogen, ThermoFisher, USA), 100 µg/ml streptomycin and 100 units (U)/ml penicillin (Sigma-Aldrich, USA), and 0.1 mM non-essential amino acids (Invitrogen, ThermoFisher). Cells were grown in culture vessels in a humidified incubator at 37 °C with 5% carbon dioxide (CO_2) unless otherwise specified. When passaging, cell monolayers were detached with 1X trypsin (Invitrogen, ThermoFisher) in phosphate-buffered saline (PBS; Lonza).

2.1.2. Maintenance of replicon-containing cell lines.

Replicon-containing cell lines were previously established as detailed in (Ismail, 2015). In short, linearised plasmids were transcribed *in vitro*, the RNA was extracted and transfected into HEK293T cells. Replicon-positive cells were selected using 3.5 µg/ml puromycin (SantaCruz Biotechnology, USA) and confirmed by detection of GFP expression. Replicon-containing cells used in this study were established using the DENV-2 replicon plasmid pRepDV-GP2A, and the plasmid pRepDV-GP2A-NS4B$_{T66A}$ which encodes a DENV-2 replicon containing a T66A mutation in the NS4B gene (as described in (Ismail, 2015)). These cells were maintained similarly to the control HEK293T cells as described in Section 2.1.1, but with the addition of 3.5 µg/ml puromycin with each passage.

2.1.3. Maintenance of persistently-infected cells.

Two cell lines persistently-infected with v601-NS4B$_{T66A}$, H-v601-Per1 and H-v601-Per2, were previously established by Dr Rosmani Ismail (as described in (Ismail, 2015)), as detailed in Section 1.7.1. These cells were maintained similarly to HEK293T cells, as detailed in Section 2.1.1, in the biological safety level 3 (BSL3) laboratory.

2.1.4. Infection of HEK293T cells with DENV-2 virus.

HEK293T cells were infected with DENV-2 New Guinea C strain (NGC), produced from the DENV-2 infectious clone, pDVWS601 (Gualano *et al.,* 1998; Pryor *et al.,* 2001). The stock virus titre was 3.7 x 10^7 plaque-forming units (PFU)/ml, and cells were infected at a multiplicity of infection (MOI) > 5.

1.5 x 10^5 HEK293T cells in cell culture media as described in Section 2.1.1 were seeded into 24 well plates and incubated at 37 °C for 24 hours (h). Media was removed and each cell monolayer was washed twice with PBS. 0.2 ml of virus stock in culture supernatant was added to each well, and plates were incubated for 1.5 h at 37 °C, and gently rocked every 15 min. Virus-containing supernatant was removed, 1 ml of Eagle's minimum essential media (EMEM; (Lonza) supplemented with 10% FBS and non-essential amino acids) was added to each cell, and plates were incubated for at least 24 h before cells were used for further experiments.

2.1.5. Cryopreservation and restoration of cell stocks.

Cells were grown to ~80% confluency, to ensure healthy cells were cryopreserved, before being detached with trypsin and resuspended in DMEM media. The cells were centrifuged at 150 x *g* for 5 minutes, and the supernatant removed. The cell pellet was resuspended in freezing medium (70% FBS, 20% DMEM containing 10% FBS, 10% dimethyl sulfoxide (DMSO; Sigma-Aldrich)). 3-5 x 10^6 cells/ml were transferred in 1 ml aliquots into cryotubes in a homogenous cell suspension. The cryotubes were kept in an isopropanol chamber and stored at -70 °C overnight before being transferred to liquid nitrogen and stored in the gas phase above the liquid.

To thaw cells, cryotubes were placed in a 37 °C water bath to thaw the cells rapidly. The cell suspensions were transferred to DMEM media, centrifuged at 150 x *g* for 7 min and the supernatant containing DMSO was removed. The cell pellet was resuspended in DMEM media and transferred into an appropriate culture vessel which was then incubated at 37 °C.

2.1.6. Long-term treatment of virus-infected cells with drugs.

Cells persistently-infected with virus or containing replicons were treated with drugs to cure the cells of virus/replicons in order to analyse various cellular pathways and characteristics.

Drugs used were: 4-hydroxyphenylretinamide (4-HPR; Enzo, UK), mycophenolic acid (MPA; SantaCruz Biotechnology), 2'-C-methylcytidine (2CMC; Sigma-Aldrich), and ribavirin (RBV; Sigma-Aldrich). 5 mg 4-HPR was dissolved in 1.28 ml DMSO to make a working stock of 10 mM. 100 mg MPA was dissolved in 2 ml DMSO to make a stock of 50 mg/ml. 10 mg RBV was dissolved in 818 µl DMSO to make a 50 mM working stock. A 20 mM working stock of 2CMC was made by dissolving 5 mg of 2CMC in 970 µl nuclease-free water.

HEK293T, H-v601-Per1 or H-v601-Per2 cells were seeded into T25 flasks and incubated for 24 h until approximately 10-20% confluent. Media was removed and replaced with media containing appropriate concentrations of drug. Any cells that reached 80-100% confluency

were passaged as detailed in Section 2.1.1, and the drug was replaced at the appropriate concentration.

2.1.7. Cell viability assay.

96 well plates were seeded with 3 x 10^4 cells per well and incubated for 16 h. Media was replaced with DMEM media containing appropriate concentrations of drugs to be tested. 2 days and 4 days post-drug addition, the Vybrant® MTT Cell Proliferation Assay Kit (ThermoFisher Scientific, USA) was used according to the manufacturer's instructions to determine cell proliferation and viability in the presence or absence of drugs. Cell culture media was removed and replaced with 110 µl of 1.2 mM 3-(4,5-dimethylthiazol-2-yl)-2,5-diphenultetrazolium bromide) (MTT) in phenol red-free FluoroBrite™ DMEM media (Invitrogen, ThermoFisher) supplemented with 10% FBS, non-essential amino acids, and 2 mM L-glutamine (Invitrogen, ThermoFisher). Plates were incubated at 37 °C for 4 h. 1 g SDS was dissolved in 10 ml of 0.01 M hydrochloric acid (HCl), and 100 µl of the SDS-HCl mixture was added to each well and mixed thoroughly. The plates were incubated at 37 °C for 4 h. Plates were read using a spectrophotometer (SpectraMax 190 Microplate Reader) at 570 nm.

2.2. DNA/RNA analysis.

2.2.1. Intracellular RNA isolation by TRIzol™ or RiboZol™.

Cells to be used for intracellular RNA isolation were grown to 80% confluency in a T75 flask. Media was removed and 1 ml TRIzol™ Reagent (Invitrogen, ThermoFisher) or RiboZol™ RNA extraction reagent (AMRESCO) was added per flask and pipetted up and down several times to lyse cells and homogenise. Each cell lysate was incubated for 5 min, before 0.2 ml of chloroform (Fisher Chemical, USA) was added. Samples were incubated for 3 min and centrifuged for 15 min at 12,000 x *g* at 4 °C. The upper aqueous phase containing RNA was carefully transferred to a new microfuge tube such that no interphase or organic layer was also transferred. To precipitate the RNA, 0.5 ml of isopropanol (Sigma-Aldrich) was added to the aqueous phase. Samples were incubated for 10 min, centrifuged for 10 min at 12,000 x *g* at 4 °C, and the supernatant removed. RNA samples were washed by re-suspending the pellet in 1 ml of 75% ethanol (Sigma-Aldrich) diluted in nuclease-free water (Invitrogen, ThermoFisher), mixed by vortexing, and centrifuged for 5 min at 7500 x *g* at 4 °C. Supernatant was discarded, and the RNA pellet air-dried for 10 min. To solubilise the RNA, the pellet was resuspended in 30 µl of nuclease-free water and incubated at 60 °C for 10 min. Final RNA samples were stored at -70 °C before use in further downstream applications.

2.2.2. Intracellular RNA isolation.

This method was used when inclusion of a DNase I incubation step was desired.

To prepare cells for intracellular RNA isolation, cells were detached using trypsin, resuspended in DMEM media, and counted using a disposable haemocytometer (Kova International, USA). 2 x 10^6 cells were collected, suspended in a total volume of 10 ml DMEM media, and centrifuged at 300 x *g* for 5 min after which the supernatant was removed. The cell pellet was resuspended in 25 ml PBS, centrifuged at 300 x *g* for 5 min, and the supernatant was removed again.

RNA extraction was performed using an SV Total RNA Isolation Kit (Promega, USA) according to the manufacturer's instructions for the spin protocol, and once completed the RNA samples were stored at -70 °C before further processing.

2.2.3. Extracellular RNA isolation.

140 µl cell culture supernatant was sampled from cell cultures and used for extracellular RNA extraction using the QIAamp Viral RNA Mini Kit (Qiagen, Germany) following the manufacturer's instructions for the spin protocol. Samples were stored at -70 °C until required for further use.

2.2.4. Determination of nucleic acid concentration.

Nucleic acids were analysed by spectrophotometry using a Nanodrop ND-1000 Spectrophotometer to determine the concentration (ng/µl) and ratios of absorbance values (260/230 and 260/280).

2.2.5. One-step reverse-transcription polymerase chain reaction (RT-PCR).

RNA samples were converted to RT-PCR products using a One Taq One-Step RT-PCR Kit (New England Biolabs, USA). 25 µl RT-PCR reaction mix, 2 µl 10 pmol/µl forward primer, 2 µl 10 pmol/µl reverse primer, and 2 µl reverse transcriptase enzyme mix were mixed into a mastermix. Primers used for specific detection of viral RNA are shown in Table 2.1, or total cellular RNA was detected using a random hexamer primer (ThermoFisher Scientific). A volume containing an appropriate concentration of RNA was added, and the mix was adjusted to 50 µl with nuclease-free water. A GS1 thermocycler machine (G-Storm, UK) was used, and set to program 1 (

Table 2.2) to generate RT-PCR products with lengths of < 1 kb, or program 2 for RT-PCR products with lengths of > 1 kb.

2.2.6. Two-step RT-PCR.

For the reverse-transcription step of the two-step RT-PCR reaction, a volume containing 200 ng of the RNA sample was mixed with 1 µl 10 pmol/µl primer and made up to a total of 10 µl with nuclease-free water. The RNA-primer mixture was heated to 70 °C for 5 min, and then immediately chilled on ice. A mastermix containing 1.6 µl nuclease-free water, 4 µl ImProm-II™ 5X reaction buffer (Promega), 2.4 µl 25 mM $MgCl_2$ to a final concentration of 3 mM (Promega), 1 µl 10 mM deoxynucleotide (dNTP) mix for a final concentration of 0.5 mM (Promega), and 1 µl ImProm-II™ reverse transcriptase (Promega), per sample, was created and added to the RNA-primer mixture. Program 3 (

Table 2.2) was used for the first step of this reaction to generate RT-PCR products. Primers used for specific detection of viral RNA are shown in Table 2.1, or total cellular RNA was detected using a random hexamer primer (ThermoFisher Scientific).

For the PCR step, a mastermix was created containing 14.35 µl nuclease-free water, 2.5 µl 10X Maxima Hot Start Taq buffer (ThermoFisher Scientific), 2.5 µl 2 mM dNTP mix, 1.25 µl 10 pmol/µl forward primer, 1.25 µl 10 pmol/µl reverse primer, 2 µl 25 mM $MgCl_2$, and 0.15 µl Taq DNA polymerase (ThermoFisher Scientific), per reaction. 1 µl template RT-PCR product was added to 24 µl mastermix for a 25 µl reaction, and Program 4 (

Table 2.2) was used to amplify the RT-PCR product.

Table 2.1: DENV-specific primers. Names and sequences of DENV-2-specific primers used for either RT-PCR or viral genome sequencing during this project.

Primer*	Primer sequence (5' → 3')
DV2_1-24	AGTTGTTAGTCTACGTGGACCGAC
DV2_665	CTTATGGGACGTGTACCACCACAGG
DV2_1399	ACAGGAAAACATGGCAAGG
DV2_1800	ATGGACAAACTACAGCTCAAAGG
DV2_1925r	CCGTCCCCTTCATATTGTACTCTG
DV2_2205	ATCCCTGGGAGGAGTGTTTACATC
DV2_2950	GTATTCTGCGACTCAAAACTC
DV2_3151	CCAAAGAATTTCGCTGGACCAGTG
DV2_3186r	GCGACCTGGTCACAGTGTTGTGTTG

DV2_3611	CAGGGAACATGTCCTTTAGAGACC
DV2_3700r	GATAAGTCACGCCCATACCTATGTC
DV2_4133	AGCTGGCCACTAAATGAGGCTATC
DV2_4804	GTCCAGGTCTTGGCATTGG
DV2_5428	CGAGTAGAGATGGGTGAGG
DV2_6167	GAGTGGCAGCTGAAGGCATCAAC
DV2_6776	TACGTTGTCATAGCCATCC
DV2_6823	CAGTGGTGGCCGCAACCATGG
DV2_7200	CCAAGCAAAAGCAACCAGGGAAGC
DV2_7230	AAGAGCAGCAGCGGGCATC
DV2_7295r	CCTTATTGTCACTAACTGGATCTAGG
DV2_8085	GAACAACAACACCCAATTTTGC
DV2_8865	GGAGCTGGTTGACAAGGAAAGG
DV2_9045	GAATGAAGATCACTGGTTCTCC
DV2_9682	CAAGTGCCCTTCTGTTCACACC

* “r” indicates a reverse primer.

Table 2.2: RT-PCR settings. RT-PCR cycle settings showing the time spent at that temperature, and for how many cycles.

Program	Temperature	Time	Number of cycles
1 (RT-PCR < 1 kb)	48 °C	15 min	1
	94 °C	1 min	1
	94 °C	15 sec	40
	55 °C	30 sec	
	68 °C	30 sec	
	68 °C	5 min	1
	4 °C	Stored infinitely	
2 (RT-PCR > 1 kb)	48 °C	30 min	1
	94 °C	1 min	1
	94 °C	15 sec	40
	55 °C	30 sec	

	68 °C	4 min	
	68 °C	5 min	1
	4 °C	Stored infinitely	
3 (RT)	25 °C	5 min	1
	42 °C	1 h	1
	70 °C	15 min	1
	4 °C	Stored infinitely	
4 (PCR)	95 °C	10 min	1
	95 °C	15 sec	30-40
	60 °C	60 sec	
	4 °C	Stored infinitely	

2.2.7. Agarose gel electrophoresis.

Gels consisted of 1% agarose (Bioline, USA) in 1X TBE buffer (89 mM Tris base, 89 mM boric acid, 2 mM ethylenediaminetetraacetic acid (EDTA)) and 0.5 µg/ml ethidium bromide (Sigma-Aldrich). GeneRuler 1 kb Plus DNA Ladder (ThermoFisher Scientific) was used to allow estimation of the size and concentration of the products. 5 µl RT-PCR product was mixed with 1 µl 6X DNA Loading Dye (ThermoFisher Scientific, USA), and the gels were run at 100 V for approximately 1 h. The gel bands were then visualised, and photos were recorded using a UVP Biodoc-It™ Imaging System (Analytik Jena, Germany).

For analysis of smaller RT-PCR products, 4% agarose in 1X TBE buffer and 0.5 µg/ml ethidium bromide gels were used, and an O'RangeRuler 20 bp low molecular weight DNA ladder (ThermoFisher Scientific) was used to estimate the product size and concentration. 10 µl of RT-PCR product samples were combined with 2 µl 6X DNA Loading Dye (ThermoFisher Scientific), gels were run at 100 V for approximately 1 h, and visualised using the UVP Biodoc-It™ Imaging System.

2.2.8. Purification of PCR products.

For the purification of RT-PCR products, the GeneJET PCR Purification Kit (ThermoFisher Scientific) was used and the protocol was performed according to the manufacturer's instructions. Samples were stored at -20 °C.

2.2.9. DNA sequencing and analysis.

Samples were sent with an accompanying primer (Table 2.1) to Eurofins Genomics (Germany) for sequencing. Sequencing alignments were performed using the Nucleotide Basic Local Alignment Search Tool (BLASTn) online resource.

2.2.10. Quantitative real-time PCR (qPCR).

200 ng of each RNA sample was converted to a cDNA in a reverse transcription reaction as per Section 2.2.6 using a random hexamer primer (Promega). Each cDNA sample was either retained at 10 ng/µl or diluted with nuclease-free water to a final concentration of 5 ng/µl.

Validation of gene-specific qPCR primers (Table 2.3) was performed using PCR (Section 2.2.6) on cDNA samples and agarose gel electrophoresis (Section 2.2.7).

qPCR mastermixes were created for primer sets listed in Table 2.3, containing 4 µl nuclease-free water, 6.25 µl Maxima SYBR Green qPCR Master Mix (2X) containing ROX (ThermoFisher Scientific), and 1.25 µl primer, per well. For DENV-specific primers listed in Table 2.4, the mastermixes contained 4.5 µl nuclease-free water, 6.25 µl Maxima SYBR Green qPCR Master Mix (2X) containing ROX, 0.375 µl forward primer and 0.375 µl reverse primer, per well. 11.5 µl of this mastermix was added to each well, and 1 µl of template RT-PCR product was added per well.

For generation of standard curves to determine primer efficiency, cDNA samples were serially diluted 1:10, with a starting concentration of either 10 ng/µl or 5 ng/µl, to generate 4 template concentrations, and were added to wells containing mastermix in triplicate. For experimental qPCR reactions, a template cDNA sample was added to wells in either duplicate or triplicate. No template controls (NTC) were included with each run for all primers being tested. A Stratagene Mx3000P qPCR machine was used with the thermal profile cycle shown in Table 2.5.

2.2.11. Double-delta Ct (ΔΔCt) analysis.

Relative fold change in gene expression between cell types was expressed using the double-delta Ct (ΔΔCt) analysis. The ΔΔCt value was calculated for each gene in each cell type, as detailed in (Livak and Schmittgen, 2001), using Microsoft Excel. Gene expression values obtained from control HEK293T cells were used as calibrators. Expression of target genes in each sample was normalised to expression of GAPDH as a reference gene from the same sample.

Table 2.3: Gene-specific primers used for qPCR.

Gene	Source	Catalogue no.	Amplicon length (bp)
ACTB	Qiagen	QT01680476	146
GAPDH	Qiagen	QT00079247	95
HMGCS1	Qiagen	QT00055531	123
HMGCR	Qiagen	QT00004081	87
IDI1	Qiagen	QT00030912	133
INSIG1	Qiagen	QT00090314	81
MSMO1	Qiagen	QT00017871	97

Table 2.4: DENV-specific primers used for qPCR and their sequences.

Primer	DENV-2 target	Primer sequence (5' → 3')
C14A	C gene	AATATGCTGAAACGCGAGAGAAACCGCG
DV2-C69Br	C gene	CCCATCTCTTCAGTATCCCTGCTGTTGG
DV_3'UTR_f	3' UTR	TTAGAGGAGACCCCTCCC
DV_3'UTR_r	3' UTR	TCTCCTCTAACCTCTAGTCC

Table 2.5: Thermal profile for qPCR reactions.

Temperature	Time	Number of cycles
95 °C	10 min	1
95 °C	15 sec	40
60 °C	1 min	
95 °C	30 sec	1
55 °C	30 sec	1
95 °C	30 sec	1

2.3. Cell imaging.

2.3.1. Immunofluorescence assays (IFA).

Coverslips were incubated in 0.1 mg/ml poly-D-lysine (Sigma-Aldrich) for 5 min, before being washed twice with PBS. Cells were detached using trypsin and resuspended in DMEM media, before centrifuging at 150 x *g* for 8 min and resuspension in DMEM media. Cells were seeded at an appropriate density onto coverslips in 24 well trays and the culture volume adjusted to 1 ml with DMEM media, followed by incubation at 37 °C for 24 h.

If required for the experiment, cells were first treated with interferon-α (IFN-α; Sigma-Aldrich) as detailed in Section 2.3.2 prior to fixation.

Cells were fixed by treatment with 4% (w/v) paraformaldehyde (PFA) for 5 min at room temperature, before washing with PBS 3 times and then permeabilised with 1% (v/v) Triton-X-100 (Sigma-Aldrich) before washing with PBS 3 times. Alternatively, cells were fixed and simultaneously permeabilised with methanol for 5 min at -20 °C. Coverslips were then transferred to 6-well trays and blocked using 10% FBS in PBS for at least 1 h at room temperature while shaking.

Coverslips were stained with 100 µl of 1% FBS in PBS containing an appropriate dilution of the primary antibody (for a summary of antibodies used in this project, please see Table 2.6) for 1 h, before washing with PBS 4 times for 5 min per wash. Coverslips were then drained and covered with 100 µl 1% FBS in PBS containing an appropriate dilution of secondary antibody for 1 h, before washing 4 times with PBS for 5 min each time.

After antibody binding, the coverslips were mounted onto microscope slides with VectaShield mounting medium (Vector Laboratories, Inc., USA) containing DAPI for fluorescent nuclear staining. The edges of the coverslips were sealed with nail polish, and they were stored in a box to block out light at 4 °C until ready for imaging under a fluorescent microscope (Section 2.3.4).

2.3.2. IFN treatment.

Prior to cell fixation, cells were treated with 500 µl DMEM media containing IFNα at a concentration of 1000 U per ml. IFNα-treated cells (IFNα+) were incubated at 37 °C for 1 h. IFNα-containing media was removed, and cells were washed twice with PBS before the subsequent fixation steps. Control cells were left untreated with IFNα (IFNα-).

Table 2.6: Summary of the antibodies used during this project for IFA. Primary and secondary antibodies used for IFA in this project, their targets, type of antibody, antibody dilution, and their source and catalogue number.

Primary antibody target	Primary antibody type	Dilution	Source	Catalogue no.
STAT1	Rabbit mAb	1:400	Cell Signalling Technologies (USA)	14994
pSTAT1	Rabbit mAb	1:100	Cell Signalling Technologies	7649
STAT2	Rabbit mAb	1:200	BD Transduction Laboratories™ (USA)	610187
DENV NS1 protein	Rabbit pAb	1:200	GeneTex (USA)	GTX103346
DENV-2 E protein	Mouse mAb	1:500	Absolute Antibody (UK)	Ab0023-2.0
dsRNA	Mouse mAb	1:200	English and Scientific Consulting Kft (SCICONS; Hungary)	SCICONS J2
Secondary antibodies		**Dilution**	**Source**	**Catalogue no.**
Alexa Fluor® 568 goat anti-mouse IgG (H+L)		1:1000	Invitrogen	A11004
Alexa Fluor® 568 goat anti-rabbit IgG (H+L)		1:500-1:1000	Invitrogen	A11036

2.3.3. Cholesterol staining with Filipin III.

Coverslips were treated with poly-D-lysine as detailed in Section 2.3.1. Cells were prepared as detailed previously, and approximately 7 x 10^4 cells were seeded onto coverslips in a 24 well plate, and made up to 1 ml volume with DMEM media. Cells were incubated at 37 °C for 48 h. After 24 h, the cells could be infected with DENV-2 if necessary for the experiment, as detailed in Section 2.1.4.

After incubation, media from the cells was removed and cells were washed once with PBS. Cells were then fixed with 4% (w/v) PFA for 10 min, quenched with 50 mM ammonium chloride for 10 min, and permeabilised in 1 ml 1% Triton-X-100 for 5 min, with 3 PBS washes following

each step. Cells were transferred to 6 well plates and blocked in 10% FBS in PBS for 1 h at room temperature while shaking.

Cells were then covered with 100 µl diluted primary antibody for 1 h, and washed with PBS 4 times for 5 min per wash. Cells were then treated with 100 µl of diluted Alexa Fluor® 568 secondary antibody for 1 h, and washed twice with PBS for 5 min per wash.

Nuclei were stained with TO-PRO-3 nuclear stain (ThermoFisher Scientific). Cells were covered with 100 µl of TO-PRO-3 at a 1:1000 dilution in PBS for 15-20 min, protected from light, and then washed twice with PBS for 5 min per wash.

Intracellular cholesterol was stained using filipin III (Sigma-Aldrich). 1 mg filipin III was dissolved in 200 µl DMSO to make a 5 mg/ml stock, which was further diluted in PBS to make a working stock of 100 µg/ml. Cells were covered with 100 µl of 100 µg/ml filipin III for 25 min, protected from light, before washing with PBS 3 times for 5 min per wash. Coverslips were mounted onto microscope slides using Vectashield without DAPI.

An SP5-II tandem scanner confocal with 'hybrid' GaAsP detectors was used for imaging to reduce photobleaching of filipin III. Filipin III exhibits fluorescence at a UV excitation of 360 nm and emission of 480 nm (Maxfield and Wüstner, 2012), and TO-PRO-3 exhibits far-red fluorescence with excitation at 642 nm and emission at 661 nm.

2.3.4. Fluorescence imaging.

Samples were imaged at the Wolfson Bioimaging Facility, University of Bristol. The widefield microscope used was a Leica DMI6000 inverted epifluorescence microscope fitted with a Leica DFC365FX monochrome CCD camera. Confocal microscopes used were a Leica SP5-AOBS confocal laser scanning microscope attached to a Leica DMI6000 inverted epifluorescence microscope, and a 'hybrid' SP5-II tandem scanner confocal with GaAsP detectors that boost low signal and therefore reduces photobleaching.

2.3.5. Image analysis.

Images were captured using LAS X software (Leica Microsystems, UK) and post-processing was carried out on LAS X, FIJI-Image J (FIJI, USA), and Serif PhotoPlus X6 (Serif, UK).

Quantitation of fluorescence was performed using CellProfiler software (CellProfiler, USA) and a program assembled by Dr Dominic Alibhai at the Wolfson Bioimaging Facility. The program identified fluorescence in the nuclei and fluorescence in the cytoplasm of cells imaged on the confocal microscope and quantified fluorescence. It then calculated the ratio of nuclear

fluorescence to cytoplasmic fluorescence to determine localisation of the target protein in the cells.

2.4. Statistical analysis.

One-way or two-way analysis of variance (ANOVA) tests and Tukey's multiple comparisons post-hoc tests were carried out using GraphPad Prism version 7 software.

2.5. Transcriptomics analysis.

RNAseq analysis was previously carried out by Dr Andrew Davidson, University of Bristol, on six cell lines: HEK293T (Mock), H-Rep, H-Rep-4B$_{T66A}$, H-v601-Per1, H-v601-Per2, and DENV-2 virus-infected cells (H-v601). In short, total intracellular RNA was isolated from the cells which was analysed at the Beijing Genomics Institute (BGI) using an Illumina HiSeq 2000 sequencer. High-quality reads were filtered out, and Tophat and Cufflinks software suite tools in the Galaxy Platform (https://usegalaxy.org/) (Trapnell *et al.,* 2012) were used for differential gene expression analysis. The reads were aligned to the human genome (Human (*Homo sapiens*) (B38):hg38) using Tophat2, assembled and merged using Cufflinks and Cuffmerge. Cuffdiff (in the Cufflinks suite of software) generated an output file that contained pairwise comparisons from each of the six datasets and identified significant differences in levels of gene expression in each pairwise comparison. More details can be found in (Ismail, 2015).

This data was then analysed as part of this project using the Search Tool for the Retrieval of Interacting Genes/Proteins (STRING) version 10.0 to identify gene/protein interaction networks, and the Database for Annotation, Visualisation and Integrated Discovery (DAVID) version 6.8 for analysis of functionally-related gene clusters that were enriched in each dataset.

Chapter 3. Characterisation and transcriptomic analysis of cell lines

Following identification of the $NS4B_{T66A}$ mutation, Dr Rosmani Ismail performed experiments to investigate whether the mutation altered any properties of the NS4B protein that potentially allowed establishment of persistent infection. NS4B is a hydrophobic membrane protein which often presents challenges when utilising techniques to allow protein expression, purification, and characterisation. As such, several techniques were used to express and study the NS4B protein, including transient gene expression followed by cellular localisation (by IFA) and ISG expression antagonism assays. However the $NS4B_{T66A}$ mutation did not affect the localisation of NS4B, nor its ability to antagonise JAK/STAT signalling using the assays employed (Ismail, 2015). Flp-In™T-Rex™ 293 (Flp) cell lines expressing either the NS4B or $NS4B_{T66A}$ proteins were also generated and used for high-throughput mass spectrometry (MS) based immunoprecipitation analysis to identify any altered interactions between NS4B and $NS4B_{T66A}$ amongst cellular proteins; however, this analysis did not yield conclusive results. Results from these studies suggested that the T66A amino acid mutation potentially only operates in the context of the viral polyprotein, and that alterations in host pathways could also be involved in allowing persistent infection. Previously, high-throughput RNA sequencing (RNAseq) and comparative transcriptomic analysis of mock and DENV-infected cells and has been utilised to study changes to the host cell transcriptome that occur in response to viral infection and replication (Fink *et al.,* 2007; Liew and Chow, 2006; Sessions *et al.,* 2013; Ubol *et al.,* 2008). In addition to utilising this technique for studying the effect of viral infection on the host cell transcriptome, we aimed to also study effects that are potentially altered between wild-type infection and persistent infection.

3.1. Introduction to cell lines and transcriptomics data.

A virus encoding the NS4B codon change T66A (v601-$4B_{T66A}$) was generated by reverse genetics from the plasmid pDVWS601, containing a full length cDNA clone corresponding to the genome of the DENV-2 strain New Guinea C (Gualano *et al.,* 1998; Pryor *et al.,* 2001). HEK293T cells were infected with v601-$4B_{T66A}$ at an MOI of 2.0 in duplicate. Over 90% of the cells displayed clear cytopathic effect (CPE) and died, however the remaining cells continued to grow to confluency. The duplicate cell population were passaged further and were found to be 100% infected at passage 2 (P2) by IFA analysis. The two cell lines were thereafter persistently-infected with v601-$4B_{T66A}$ and were termed H-v601-Per1 and H-v601-Per2.

Replicons are viral sub-genomes that contain the viral non-structural genes, but lack the structural genes; therefore, they are capable of viral replication but do not produce infectious virions and as such are relatively bio-safe and permissible for use in a lower containment level

laboratory. HEK293T cell lines expressing replicons were generated prior to the commencement of this project by Dr. Rosmani Ismail (Ismail, 2015). The replicon plasmid pRepDV-GP2A was engineered to contain a fusion gene encoding enhanced GFP which allows visualisation by immunofluorescence microscopy, and puromycin N-acetyltransferase which allows puromycin selection, in place of the viral structural genes (Massé *et al.,* 2010). The replicon plasmid pRepDV-GP2A-NS4B$_{T66A}$, was constructed from pRepDV-GP2A and is identical except that it contains nucleotide sequence changes encoding the NS4B$_{T66A}$ mutation. The pRepDV-GP2A and pRepDV-GP2A-NS4B$_{T66A}$ replicon plasmids were linearised and transcribed *in vitro* to produce replicon RNA transcripts, which were transfected into HEK293T cells. Replicon-containing cell lines were selected for by the addition of 3.5 µg/ml puromycin to generate the H-Rep and H-Rep-4B$_{T66A}$ cell lines, respectively (Figure 3.1).

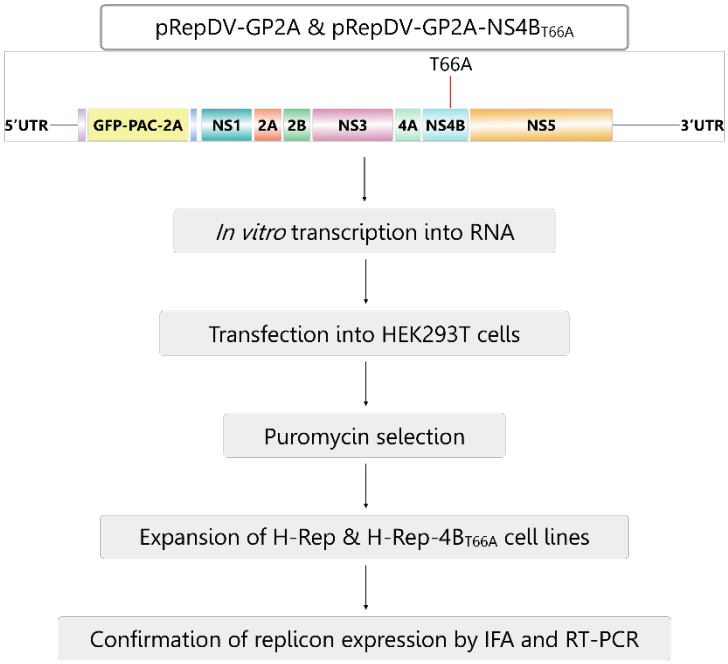

Figure 3.1: Generation of replicon-containing cell lines. The replicon plasmid pRepDV-GP2A and pRepDV-GP2A-NS4B$_{T66A}$ are identical except for presence of the NS4B$_{T66A}$ mutation. These plasmids were linearised and transcribed *in vitro* to produce RNA transcripts which were transfected into HEK293T cells. 3.5 µg/ml was used to select for cells containing either replicon plasmid. Replicon expression was confirmed by RT-PCR and IFA.

Prior to the commencement of this project, RNAseq analysis was performed by Dr. Andrew Davidson and Dr Rosmani Ismail. RNAseq is used for high-throughput transcriptomics analysis using deep-sequencing technologies to analyse the whole cell transcriptome (Wang *et al.,* 2009b). Cell lines included in the analysis were as follows: uninfected control HEK293T cells, "Mock"; persistently-infected cells, "H-v601-Per1" and "H-v601-Per2"; cells infected for

24 h with wild-type DENV-2 v601 virus, “H-v601”; cells containing replicons encoding the wild-type NS4B gene, “H-Rep”; cells expressing the replicons containing the $NS4B_{T66A}$ mutation, “H-Rep-$4B_{T66A}$”. Pairwise comparisons between the transcriptome of each cell line provided differential fold changes in gene expression, which were then analysed using bioinformatic methods. This enabled identification of genes and pathways of interest that constituted targets for further investigation during this project.

3.2. Characterisation of all cell lines.

The identity of the cell lines and the stability of the $NS4B_{T66A}$ mutation in v601-$4B_{T66A}$ or pRepDV-GP2A-$NS4B_{T66A}$ during passaging were confirmed prior to use in further experiments. At several passage numbers, RT-PCR products spanning the NS4B genes of the RepDV-GP2A and RepDV-GP2A-$NS4B_{T66A}$ replicons were produced using RNA isolated from H-Rep and H-Rep-$4B_{T66A}$ cells, respectively, and sequenced to confirm the presence or absence of the $NS4B_{T66A}$ mutation and its stability. Replicon expression in the H-Rep and H-Rep-$4B_{T66A}$ cell lines was further confirmed by detection of NS1 protein by IFA, as genes encoding the DENV structural proteins are absent in the replicon sequences. Similarly, RNA from H-v601-Per1 and H-v601-Per2 cells was isolated and the NS4B gene of the v601-$4B_{T66A}$ virus was amplified by RT-PCR and sequenced. The presence of a persistently-infecting virus in these cells was further confirmed by detection of the DENV E protein by IFA.

3.2.1. Agarose gel electrophoresis on RT-PCR products from H-Rep and H-Rep-$4B_{T66A}$ cells.

H-Rep and H-Rep-$4B_{T66A}$ cells (at passage 4) were cultured and intracellular RNA was extracted from cells at passage 9 (P9), 15 (P15), and 19 (P19). RT-PCR was performed to generate RT-PCR products corresponding to the NS4B gene with an expected size of 493 bp. Agarose gel electrophoresis was performed to confirm production of the NS4B gene RT-PCR products from each cell type. A typical result is shown in Figure 3.2. No NS4B RT-PCR product was produced using RNA extracted from the control HEK293T cells, while clear bands were displayed using RNA from the H-Rep and H-Rep-$4B_{T66A}$ cells for RT-PCR. The bands detected were approximately 500 base pairs (bp) in length.

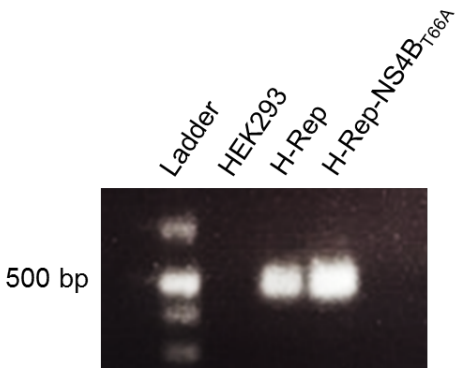

Figure 3.2: Confirmation of the DENV genome in H-Rep and H-Rep-4B$_{T66A}$ cells. Intracellular RNA was extracted from HEK293T, H-Rep, and H-Rep-4B$_{T66A}$ cells at passage 15 using the SV Total RNA Isolation Kit. RT-PCR using primers DV2_6823 and DV2_7295r generated RT-PCR products corresponding to the NS4B gene. RT-PCR products were purified using a GeneJet PCR Purification Kit, and agarose gel electrophoresis was performed on the purified products to detect the RT-PCR product (~500 bp) in each sample, and the product size estimated using a GeneRuler 1 kb Plus DNA Ladder.

3.2.2. DNA sequencing of pRepDV-GP2A and pRepDV-GP2A-NS4B$_{T66A}$ NS4B genes.

The presence and stability of the NS4B$_{T66A}$ mutation in the RepDV-GP2A-NS4B$_{T66A}$ replicon NS4B gene was confirmed by sequencing. RT-PCR products derived from RNA extracted from H-Rep and H-Rep-4B$_{T66A}$ cells at P9, P15, and P19 were sequenced by Eurofins Genomics using a modified version of Sanger sequencing. Table 3.1 shows a summary of all mutations compared to the wild-type DENV-2 genome sequence.

The NS4B gene in RepDV-GP2A had not mutated from the wild-type DENV-2 genome in P9 or 15 samples, however in the P19 sample there was a nonsynonymous mutation at nucleotide 7279 (G → A) which conferred an amino acid change of Val to Met at position 152 in the NS4B gene (V152M); this mutation had a mixed peak of occurrence in a 1:1 ratio, suggesting it was potentially a heterologous population for this mutation. The nucleotide 7020/7021 (AA → GG) mutation was retained in all H-Rep-4B$_{T66A}$ samples at P9, P15, and P19, conferring an amino acid change of Thr to Ala at position 66 in the NS4B gene (T66A). In addition to the expected NS4B$_{T66A}$ mutations, a nonsynonymous mutation at nucleotide 6905 (T → C) conferred an amino acid change of Ile to Thr at position 27 in the NS4B gene (I27T). This mutation was present in all H-Rep-4B$_{T66A}$ samples and in each, displayed a mixed peak of occurrence suggesting a heterologous population for this mutation. Another mutation at nucleotide 7099 (C → T) encoding a Pro to Ser amino acid change at position 92 in the NS4B gene (P92S) was found in H-Rep-4B$_{T66A}$ samples from P9 and P15, however these mutations showed mixed peaks of occurrences, and the mutation was lost in the P19 sample, suggesting this was an unstable transient mutation in the population.

Table 3.1: Mutations in the NS4B genes of the RepDV-GP2A and RepDV-GP2A-NS4B$_{T66A}$ replicons. RNA was extracted from H-Rep and H-Rep-4B$_{T66A}$ cells at passage 9, 15, and 19 and RT-PCR products spanning the NS4B gene from RepDV-GP2A and RepDV-GP2A-NS4B$_{T66A}$ replicons, respectively generated. The RT-PCR products were sequenced by Sanger sequencing, and BLASTn alignment tools identified mutations in the NS4B gene that differed from the wild-type DENV-2 genome sequence (NCBI gene accession number: AF038403.1).

Passage number	Cell type	Nucleotide mutation position on DENV-2 genome	DENV-2 genome sequence	Mutated nucleotide sequence	Amino acid mutation position in NS4B gene	DENV-2 genome amino acids	Mutated amino acids	Occurrence (Top: H-Rep Bottom: H-Rep-4B$_{T66A}$)
9	H-Rep-4B$_{T66A}$	6905	A**T**C	A**C/T**C	27	I	T	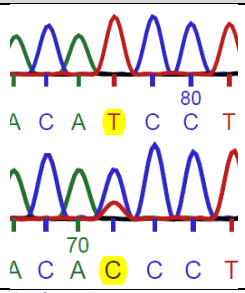
	H-Rep-4B$_{T66A}$	7020 & 7021	CT**A** **A**CA	CT**G** **G**CA	65 & 66	L T	L A	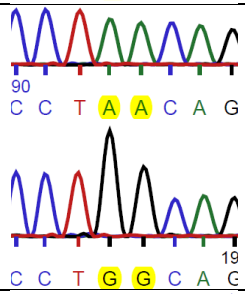
	H-Rep-4B$_{T66A}$	7099	**C**CC	**T/C**CC	92	P	S	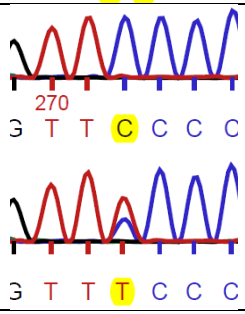

15	H-Rep-4B$_{T66A}$	6905	A**T**C	A**C/T**C	27	I	T	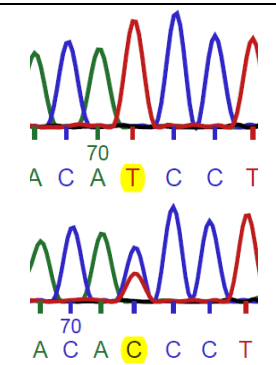
	H-Rep-4B$_{T66A}$	7020 & 7021	CT**A** **A**CA	CT**G** **G**CA	65 & 66	L T	L A	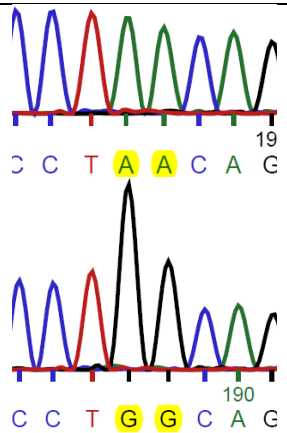
	H-Rep-4B$_{T66A}$	7099	**C**CC	**T/C**CC	92	P	S	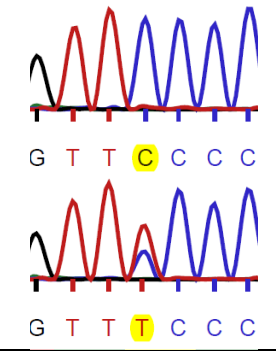

19	H-Rep	7279	**G**TG	**A/G**TG	152	V	M	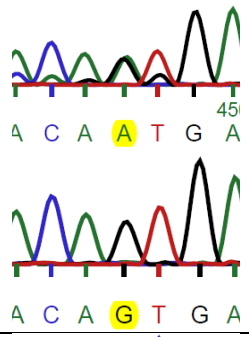
	H-Rep-4B$_{T66A}$	6905	A**T**C	A**C/T**C	27	I	T	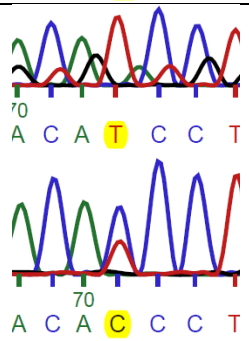
	H-Rep-4B$_{T66A}$	7020 & 7021	CT**A** **A**CA	CT**G** **G**CA	65 & 66	L T	L A	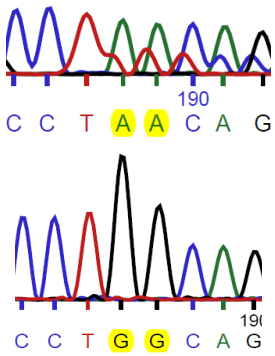

3.2.3. Agarose gel electrophoresis on RT-PCR products from H-v601-Per1 and H-v601-Per2 cells.

H-v601-Per1 and H-v601-Per2 cells were cultured (from passage 4) and analysed for the presence of persistently-infecting virus. Extracellular RNA was extracted from cells at passage 8 (P8) and intracellular RNA was extracted from cells at P10. RT-PCR generated products corresponding to the size of the DENV NS4B gene. Agarose gel electrophoresis showed that the NS4B gene RT-PCR product was produced using RNA isolated from both H-v601-Per1 and H-v601-Per2 intracellular and extracellular samples, but absent using RNA isolated from control HEK293T cell samples (Figure 3.3). The PCR product was approximately 500 bp in length, as expected.

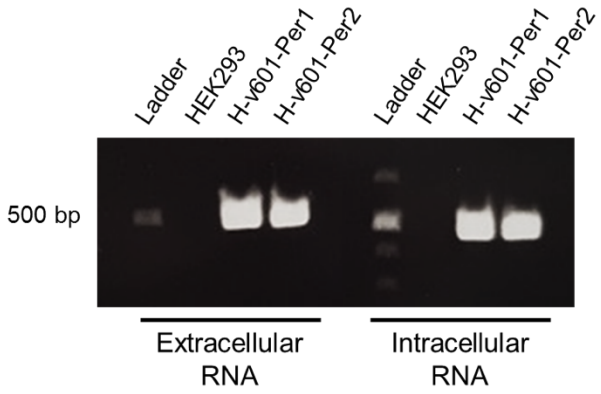

Figure 3.3: Confirmation of the DENV genome in H-v601-Per1 and H-v601-Per2 cells. H-v601-Per1 and H-v601-Per2 cells were cultured, extracellular RNA was extracted from P8 cells, and intracellular RNA was extracted from P10 cells. RT-PCR was performed on the RNA using the DENV NS4B gene-specific primers, DV2_6823 and DV2_7295r, to generate an RT-PCR product corresponding to the NS4B gene. Agarose gel electrophoresis was performed to detect the RT-PCR product (~500 bp) in each sample, and the product size estimated using a GeneRuler 1 kb Plus DNA Ladder.

3.2.4. Sequencing the v601-4B$_{T66A}$ virus from H-v601-Per1 and H-v601-Per2 cells.

The NS4B gene of persistently-infecting virus were amplified from extracellular and intracellular RNA from H-v601-Per1 and H-v601-Per2 cells by RT-PCR and sequenced to confirm the presence of the NS4B$_{T66A}$ mutation. All mutations discovered in the NS4B gene of these samples when aligned to the wild-type DENV-2 NS4B gene sequence are summarised in Table 3.2.

The same mutations were discovered in both H-v601-Per1 and H-v601-Per2 cells from both the extracellular and intracellular RNA. In both H-v601-Per1 and H-v601-Per2 cells, the

expected $NS4B_{T66A}$ mutation was retained. However, there was a mixed peak in occurrence of the A → G nucleotide change at position 7021 in H-v601-Per1 extracellular samples and H-v601-Per1 and H-v601-Per2 intracellular RNA samples, with a minor population of virus containing "A" suggesting a partial reversion of the mutation in a minority of the population. In addition, there was a non-silent mutation at nucleotide 6915 (A → G) that conferred an amino acid change from Ile → Met at position 30 in the NS4B gene (I30Met). This mutation often had a mixed peak of occurrence between G and A nucleotides, and thus is potentially not stable in the whole population.

3.2.5. IFA to confirm replicon presence in H-Rep and H-Rep-$4B_{T66A}$ cells.

The DENV NS1 protein was detected by IFA to confirm the presence of the RepDV-GP2A and RepDV-GP2A-$NS4B_{T66A}$ replicons in the H-Rep and H-Rep-$4B_{T66A}$ cells, respectively (Figure 3.4). Red fluorescence indicates the presence of NS1 in both the H-Rep and H-Rep-$4B_{T66A}$ cells, which is absent in the control HEK293T cells. Further confirmation was provided by the examination of GFP fluorescence as both replicons contain a gene encoding GFP in place of the structural genes. GFP fluorescence was detected in both H-Rep and H-Rep-$4B_{T66A}$ cells, and not in the control cells.

3.2.6. IFA to detect DENV E protein in H-v601-Per1 and H-v601-Per2 cells.

The presence of persistently-infecting virus in the H-v601-Per1 and H-v601-Per2 cells was further confirmed by detection of the structural DENV E protein by IFA (Figure 3.5). The DENV E protein was only present in the H-v601-Per1 and H-v601-Per2 samples and was absent in the control uninfected HEK293T cells.

Table 3.2: Mutations in the NS4B gene of the virus isolated from cultures of H-v601-Per1 and H-v601-Per2 cells. Extracellular and intracellular RNA was extracted from samples of H-v601-Per1 and H-v601-Per2 cell samples at P8 and P10, respectively. RT-PCR generated RT-PCR products corresponding to the DENV NS4B gene, which were then sequenced. NS4B gene sequences were aligned to the wildtype DENV-2 genome using BLASTn.

RNA source & passage number	Cell type	Nucleotide mutation position on DENV-2 genome	DENV-2 genome sequence	Mutated nucleotide sequence	Amino acid mutation position in NS4B gene	DENV-2 genome amino acids	Mutated amino acids	Occurrence of mutation
Extracellular RNA P8	H-v601-Per1	6915	AT**A**	AT**G/A**	30	I	Met	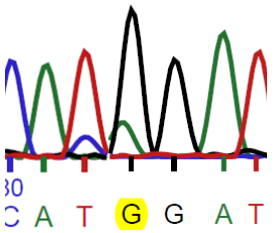
	H-v601-Per1	7020 & 7021	CT**A** **A**CA	CT**G** **G/A**CA	65 & 66	L T	L A	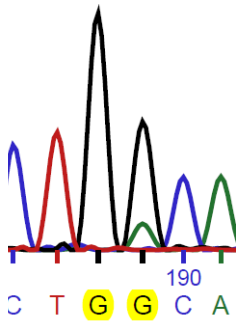
	H-v601-Per2	6915	AT**A**	AT**G/A**	30	I	Met	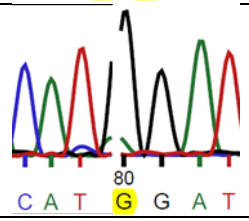

	H-v601-Per2	7020 & 7021	CT**A** **A**CA	CT**G** **G**CA	65 & 66	L T	L A	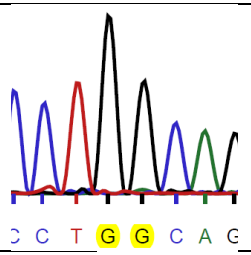
Intracellular RNA P10	H-v601-Per1	6915	AT**A**	AT**G/A**	30	I	Met	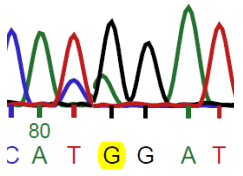
	H-v601-Per1	7020 & 7021	CT**A** **A**CA	CT**G** **G**CA	65 & 66	L T	L A	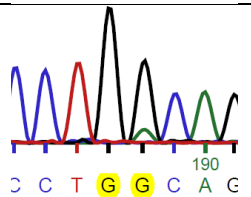
	H-v601-Per2	6915	AT**A**	AT**G**	30	I	Met	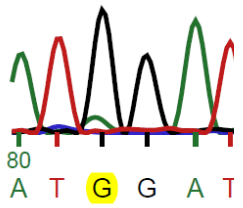
	H-v601-Per2	7020 & 7021	CT**A** **A**CA	CT**G** **G**CA	65 & 66	L T	L A	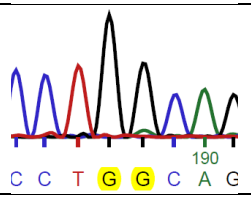

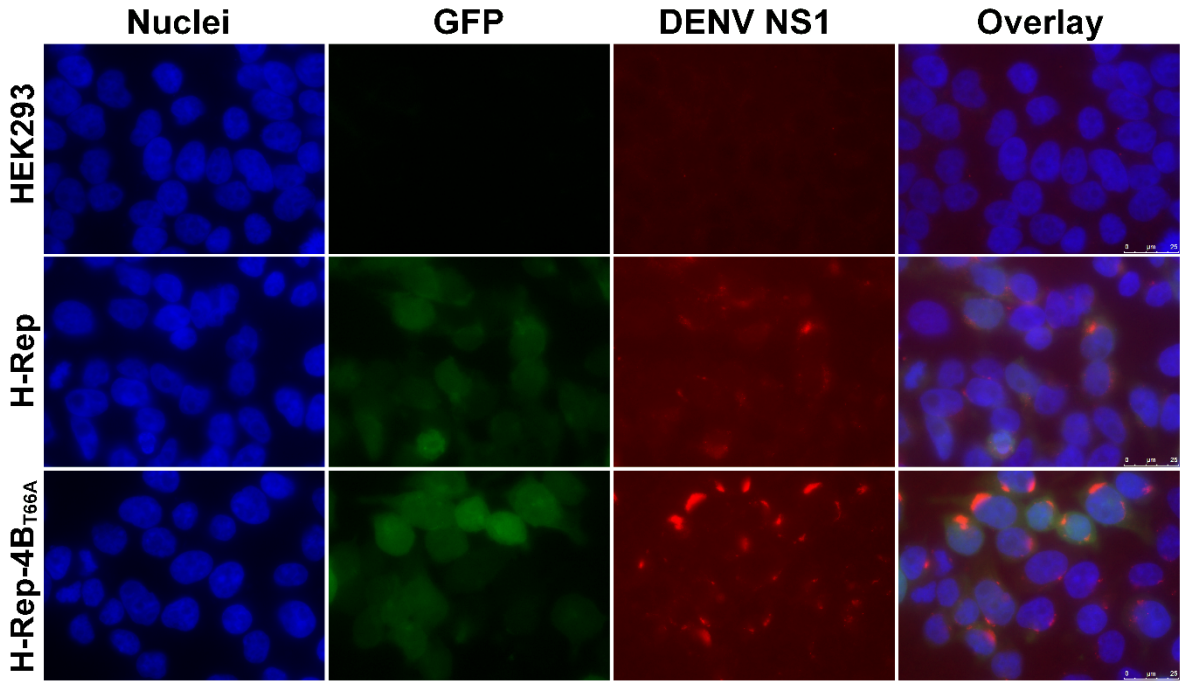

Figure 3.4: Detection of DENV NS1 in H-Rep and H-Rep-4B$_{T66A}$ cells. HEK293T, H-Rep and H-Rep-4B$_{T66A}$ cells were grown on coverslips. 24 h post-seeding, the cells were fixed with 4% paraformaldehyde, permeabilised with 1% Triton-X-100, and blocked with 10% FBS in PBS. Coverslips were then treated with a 1:200 dilution of mouse anti-NS1 primary antibody, and 1:1000 dilution of goat anti-mouse IgG secondary antibody conjugated with a 568 Alexa Fluor® (red) to detect the presence of DENV-2 NS1 protein expression, before mounting using VectaShield with DAPI to stain the nuclei (blue). Replicons contain a GFP-expressing gene (green). Fluorescence was detected using a widefield microscope (Leica DMI6000 inverted epifluorescence microscope fitted with a Leica DFC365FX monochrome CCD camera) with a 40x objective.

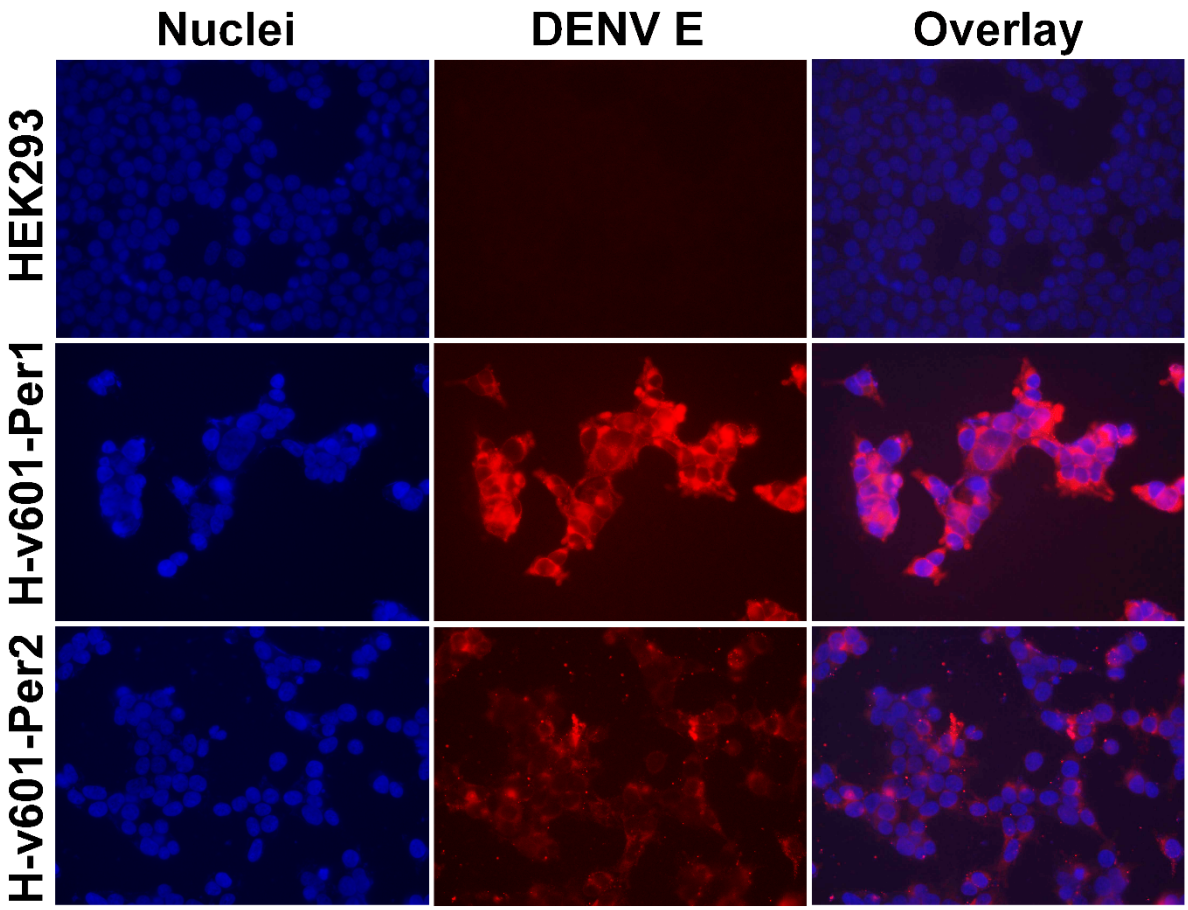

Figure 3.5: IFA detection of DENV E protein in H-v601-Per1 and H-v601-Per2 cells. H-v601-Per1 and H-v601-Per2 cells were seeded on to coverslips and after 24 h, were fixed with 4% paraformaldehyde and permeabilised in 1% Triton-X-100. The samples were blocked in 10% FBS in PBS, then stained with primary mouse anti-DENV E antibody at a 1:500 dilution, followed by anti-mouse secondary antibody conjugated with a 568 Alexa Fluor® (red) at a 1:1000 dilution. Cover slips were mounted using VectaShield with DAPI to stain the nuclei (blue), and imaged on a widefield microscope (Leica DMI6000 inverted epifluorescence microscope fitted with a Leica DFC365FX monochrome CCD camera) with a 40x objective.

3.2.7. Quantification of DENV RNA expression in each sample by qPCR.

To quantify the levels of DENV-2 viral RNA present in each of the sample sets, two DENV-specific primer sets were tested, corresponding to the DENV-2 3′UTR and capsid (C) gene. The expected product size of the 3′UTR primer set was 97 bp, and of the C gene primer set was 169 bp. Both of these observed bands displayed the expected approximate product sizes, however the 3′UTR primer band was relatively faint (Figure 3.14B).

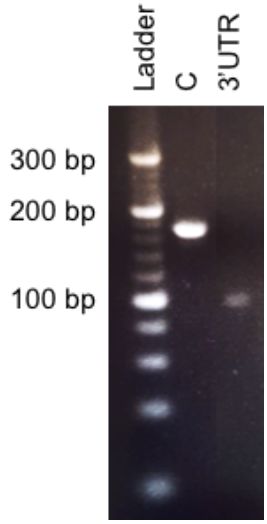

Figure 3.6: Agarose gel electrophoresis to confirm target gene-specific binding of qPCR primer sets. Total intracellular RNA from HEK293T and H-v601-Per1 cells was extracted and converted to RT-PCR product by reverse transcription. PCR was performed using each primer set on H-v601-Per1 RT-PCR product to test DENV-specific primers. 5 µl RT-PCR product and 1 µl 6 X loading dye was loaded in to each well of a 1% agarose gel and run at 100 V for approximately 1 h. O'RangeRuler 20 bp DNA ladder was used to estimate product sizes.

Primers specific for the DENV 3′UTR were used for qRT-PCR because, despite generating a weaker band than the C-specific primers, they could be used for detection of both v601-4B$_{T66A}$ virus and the RepDV-GP2A and RepDV-GP2A-NS4B$_{T66A}$ replicons which do not contain the full sequence of the C gene. HEK293T cells were infected with v601 for 24 h at an MOI of > 5, to generate H-v601 cells, which were used as a calibrator when calculating the relative expression of DENV viral RNA in all other cell lines. In other words, viral RNA expression in H-v601 cells was set at 1, and relative expression of viral RNA in all other cell lines was calculated relative to this.

H-v601-Per1 and H-v601-Per2 had significantly less viral RNA present than the H-v601 cells ($p < 0.0001$ for both), with H-v601-Per2 expressing more than H-v601-Per1 (Figure 3.7). Both persistently-infected cell lines were expressing greater levels of viral RNA than both replicon-containing cells; H-v601-Per2 was significantly greater than H-Rep and H-Rep-4B$_{T66A}$ (p = 0.019 and 0.047, respectively). There were no detectable levels of viral RNA in the control HEK293T cell line.

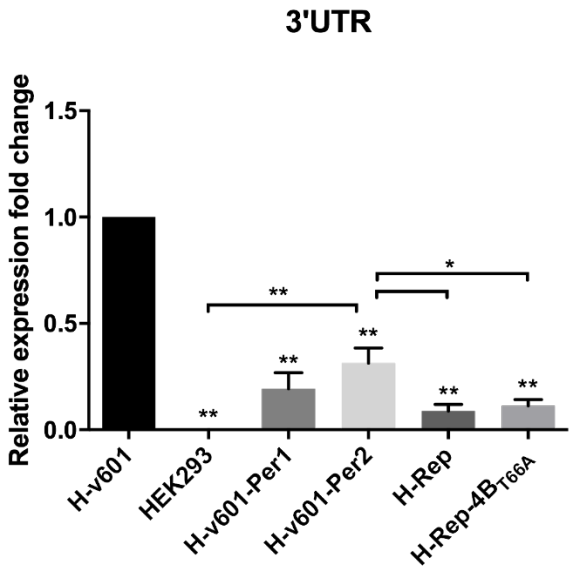

Figure 3.7: Quantification of DENV RNA in each cell line by qPCR. Cell lines at passage 6 (P6) were seeded and incubated for 48 h; HEK293T cells were seeded, after 24 h were infected with v601 virus at an MOI of > 5, and incubated at 37 °C for 24 h. Total intracellular RNA was extracted from all cell lines at the same time, and 200 ng RNA was converted to RT-PCR product by reverse transcription. This was repeated for cells at passage 8 (P8). The DENV-2 3'UTR primer was used for the qPCR reaction; each sample set was analysed 3 times by qPCR, and each sample was analysed in triplicate on each plate and results were combined. GAPDH was used as a reference gene for all reactions. Relative gene expression fold change was determined using the double-delta Ct (ΔΔCt) method with gene expression in H-v601 cells used as the calibrator; error bars show standard deviation. * = $p > 0.05$; ** = $p > 0.001$.

3.3. Bioinformatic analysis of RNAseq transcriptomics data.

RNAseq was performed prior to the commencement of this project in order to analyse the transcriptome of the different cell lines with the aim of studying differences in specific gene or pathway expression between different cell lines. Cell lines analysed by RNAseq were: HEK293T (Mock), H-v601-Per1, H-v601-Per2, H-Rep, H-Rep-4B$_{T66A}$, and wild-type DENV-2-infected HEK293T cells (H-v601). Persistently-infected cells and replicon-containing cells were generated at the same time using the same parental HEK293T cells. RNAseq analysis was performed when cells were at P4 following several passages performed for initial propagation.

In short, cells were seeded into T25 flasks and grown under identical conditions in duplicate until ready for harvest at 60% confluency. Total intracellular RNA was isolated using the TRIzol method, and equal amounts of RNA samples were sent to the Beijing Genomics Institute (BGI) for RNAseq analysis using an Illumina HiSeq 2000 sequencer. Differential gene expression

analyses was performed on the RNAseq data using the Tophat and Cufflinks software tools in the Galaxy Platform (https://usegalaxy.org/) (Trapnell *et al.,* 2012). The reads were first aligned to the human genome (Human (*Homo sapiens*) (B38): hg38) using Tophat2, then the transcripts were assembled and merged using Cufflinks and Cuffmerge. Cuffdiff was then used to detect differentially expressed genes and transcripts in each pairwise comparison between datasets for each of the 6 samples corresponding to each cell line analysed. A summary of this process is provided in Figure 3.8. The resulting data file provided values that corresponded to the levels of expression for each gene in each of the different cell lines, and pairwise comparisons of these values between cell lines gave Log_2 fold change values in gene expression and highlighted significant differences in gene expression between each cell line. Analysis of this transcriptomics data was carried out as part of this project to direct further experiments.

In total, 27893 genes were identified. Of these, 726 genes were significantly differentially regulated, while 3862 genes were upregulated or downregulated by at least two-fold in at least one of the pairwise comparisons. The genes that were differentially expressed significantly and by at least two-fold in pairwise comparisons of interest, i.e. between Mock and all other samples, and between samples infected with virus/expressing replicons that either possess or do not possess the $NS4B_{T66A}$ mutation, were identified. These gene sets were then analysed by DAVID to identify clusters of genes with related functions that may be enriched in the datasets (Table 3.3).

Host immunity pathways were upregulated during persistent infection relative to mock and wild-type infection. Genes that were upregulated in H-v601-Per1 and H-v601-Per2 relative to Mock were enriched in the “Antiviral response” function; while “Immunity/type I IFN pathway” was enriched in genes that were upregulated during persistent infection in H-v601-Per1 and H-v601-Per2 cells relative to wild-type infection in H-v601 cells. “Antiviral Response” genes were also enriched in genes that were upregulated during wild-type infection relative to Mock, but to a lesser extent than the persistently-infected cells. Unfolded protein response and ER-functionally related genes were upregulated in H-v601 relative to Mock, and also relative to persistent infection. Genes that were upregulated in H-v601 relative to H-v601-Per1 and H-v601-Per2 were also enriched for “Lipid metabolism” functionally-related genes, while “Lipid/sterol metabolism” was downregulated in H-v601-Per1 relative to Mock.

Genes of particular interest that constituted potential targets for further validation experiments were those that were specifically downregulated during persistent infection while also upregulated during wild-type infection, and vice versa.

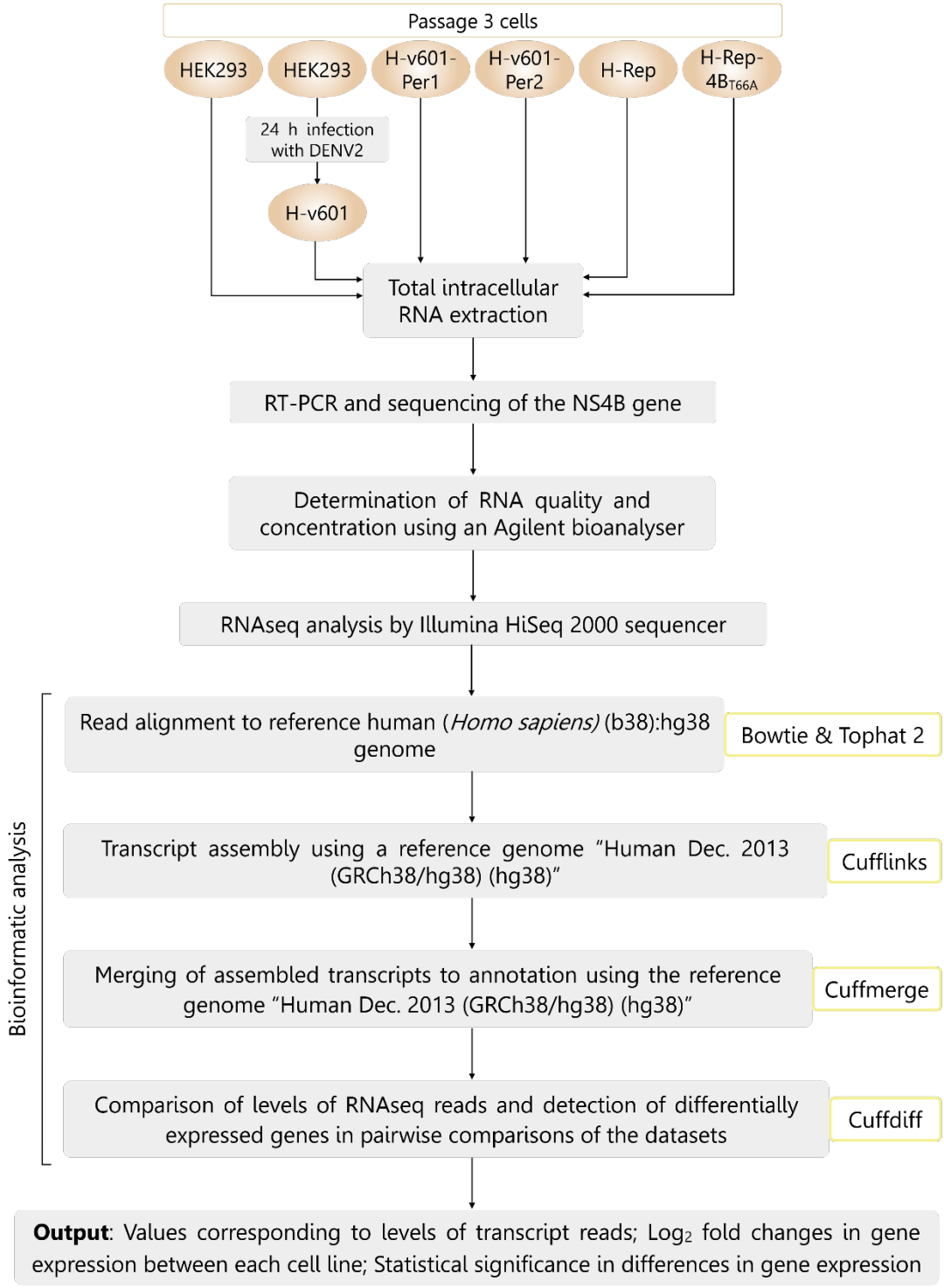

Figure 3.8: Overview of RNAseq analysis and generation of the transcriptomics dataset analysed for this project. Total intracellular RNA was extracted from HEK293T, H-v601-Per1, H-v601-Per2, H-Rep and H-Rep-4B$_{T66A}$ cells, and H-v601 cells 24 hours post-infection with wild-type DENV-2. Samples were generated in duplicate, and RNAseq analysis was performed at the BGI. Bioinformatic analysis was performed to ultimately generate a data file showing values corresponding to gene expression levels in each cell line. Pairwise comparisons of these values provided Log_2 fold change values in gene expression between different cell lines.

Table 3.3: Results summary of DAVID analysis on genes differentially expressed by at least two-fold or significantly. Genes that were differentially expressed in each pairwise comparison of interest were identified and analysed by DAVID to identify enriched clusters of genes in the datasets that were functionally related. Two-fold up- or downregulated in Sample X vs. Sample Y indicates that the genes were up- or downregulated by at least two-fold in Sample Y, relative to Sample X.
* = Clusters of genes that are involved in the same host pathways were identified and assigned a functional annotation using analysis by DAVID). The top three most enriched functional annotations for each pairwise comparison with an EASE score ≥ 1.3 (which corresponds to a p value < 0.05) are listed, with the corresponding EASE score. If there were fewer than three functional annotations with an EASE score ≥ 1.3 for any pairwise comparison, no other functional annotations with an EASE score < 1.3 are shown.

Pairwise comparison	Number of genes	Functional annotation (EASE score)*
Two-fold upregulated		
Mock vs. H-v601	241	Endoplasmic reticulum (4.54); IRE1-mediated unfolded protein response (UPR) (3.41); antiviral response (2.12)
Mock vs. H-v601-Per1	436	Antiviral response (8.18); glycoprotein/extracellular region (2.85)
Mock vs. H-v601-Per2	305	Antiviral response (7.96); growth factor activity (2.7); glycoprotein/extracellular region (1.93)
Mock vs. H-Rep	519	Nucleus/transcription (4.84); glycoprotein/signal peptide (2.29); apoptosis (1.74)
Mock vs. H-Rep-4B$_{T66A}$	565	Nucleus/transcription (8.18); zinc finger region (3.59); antiviral response (2.66)
H-Rep vs. H-Rep-4B$_{T66A}$	296	Nucleus/DNA-binding (3.36); metal ion-binding site (2.52); antiviral response (1.99)
H-v601-Per1 vs. H-v601	308	Unfolded protein binding (4.10); protein processing in ER (3.86); lipid metabolism (3.1)
H-v601-Per2 vs. H-v601	248	Endoplasmic reticulum (7.56); protein processing in the ER (4.3); lipid metabolism (1.78)
Two-fold downregulated		
Mock vs. H-v601	409	Nucleus/DNA-binding (3.12); nucleosome (1.99)
Mock vs. H-v601-Per1	214	Nucleus (2.18); lipid/sterol metabolism (1.82)
Mock vs. H-v601-Per2	188	Nucleus (2.24)
Mock vs. H-Rep	965	Cell junction (4.96); Ubl conjugation (3.95); glycoprotein (3.41)
Mock vs. H-Rep-4B$_{T66A}$	916	Homeodomain-like (3.65); cell junction (2.36)

H-v601-Per1 vs. H-v601	766	Immunity/type I IFN pathway (7.19); cell junction (5.85); chromosome (5.84)
H-v601-Per2 vs. H-v601	588	Immunity/type I IFN pathway (7.46); glycoprotein (3.37); cell junction (3.32)
Significantly upregulated		
Mock vs. H-v601	28	No functional annotations with EASE score ≥ 1.3 found
Mock vs. H-v601-Per1	51	Antiviral defence (7.26); NF-κB signalling pathway (2.5); type I IFN signalling pathway (1.76)
Mock vs. H-v601-Per2	25	Antiviral defence (3.05); protein binding (1.3)
Mock vs. H-Rep	80	Transcription regulation (4.11); glycoprotein (1.3)
Mock vs. H-Rep-4B$_{T66A}$	98	Transcription regulation (5.7); TNF-mediated signalling pathway (1.6); innate immunity (1.35)
H-Rep vs. H-Rep-4B$_{T66A}$	17	Type I IFN signalling pathway (3.63)
H-v601-Per1 vs. H-v601	33	No functional annotations with EASE score ≥ 1.3 found
H-v601-Per2 vs. H-v601	22	No functional annotations with EASE score ≥ 1.3 found
Significantly downregulated		
Mock vs. H-v601	13	No functional annotations with EASE score ≥ 1.3 found
Mock vs. H-v601-Per1	3	No functional annotations with EASE score ≥ 1.3 found
Mock vs. H-v601-Per2	5	No functional annotations with EASE score ≥ 1.3 found
Mock vs. H-Rep	141	Intermediate filament protein (2.3); negative regulation of transcription from RNA polymerase II promoter (1.97); DNA-binding (1.95)
Mock vs. H-Rep-4B$_{T66A}$	134	Intermediate filament protein (1.86); glycoprotein (1.53); leucine-rich repeat (1.35)
H-Rep vs. H-Rep-4B$_{T66A}$	10	No functional annotations with EASE score ≥ 1.3 found
H-v601-Per1 vs. H-v601	76	Antiviral defence (8.62); immunity (3.83); negative regulation of type I IFN production (3.23)

3.3.1. Bioinformatic analysis of genes specifically downregulated during persistent infection.

164 genes were identified that were both downregulated in H-v601-Per1 and H-v601-Per2 cells relative to Mock, and upregulated in H-v601 cells relative to Mock (Supplementary Table 1). DAVID analysis of these 164 genes identified a functional annotation cluster, "Cholesterol Biosynthetic Process", with the greatest enrichment score of 3.29. The following cluster was "Chromosome" with an EASE score of 1.3, and all other clusters had EASE scores < 1.3. The "Cholesterol Biosynthetic Process" cluster contained 6 genes: *HMGCR, HMGCS1, INSIG1, IDI1, MSMO1,* and *SQLE*. STRING functional protein association analysis on the same 164 genes was performed to identify any protein-protein interactions within the gene set (Figure 3.9). The top three Biological Process (GO) pathways based on ascending *p* value were highlighted using coloured nodes which indicate proteins involved in each pathway. The top three pathways identified using STRING were "Cholesterol Biosynthetic Process", "Alcohol Biosynthetic Process" and "Organic Hydroxy Compound Biosynthetic Process". The cluster of proteins highlighted in red in Figure 3.9 correspond to the cholesterol biosynthetic process, and were the same proteins identified by the DAVID analysis. Due to the importance of lipids during flavivirus infections (for more details see Section 1.6), genes involved in cholesterol biosynthesis constituted an attractive target for further validation experiments and this pathway subsequently became a focus for experiments in this project.

Table 3.4: Summary of top three enriched pathways identified using DAVID and STRING from genes specifically downregulated during persistent infection and upregulated during wild-type DENV-2 infection. Genes that were downregulated in H-v601-Per1 and H-v601-Per2 cells relative to Mock, and upregulated in H-v601 cells relative to Mock were identified and analysed by DAVID and STRING. The top three functional annotation clusters, corresponding EASE score (only showing clusters with EASE score ≥ 1.3) and number of genes in each cluster identified by DAVID analysis is shown. The top three biological process (GO) pathways identified by STRING, corresponding *p* values and the number of proteins in each pathway is also shown.

DAVID			STRING		
Functional annotation cluster	**EASE score (≥ 1.3)**	**Number of genes**	**Biological Process (GO) pathway**	***p* value**	**Number of genes**
Cholesterol biosynthetic process	3.29	6	Cholesterol biosynthetic process	0.000361	6
Chromosome	1.3	7	Alcohol biosynthetic process	0.000361	8

-	-	-	Organic hydroxy compound biosynthetic process	0.0007	9

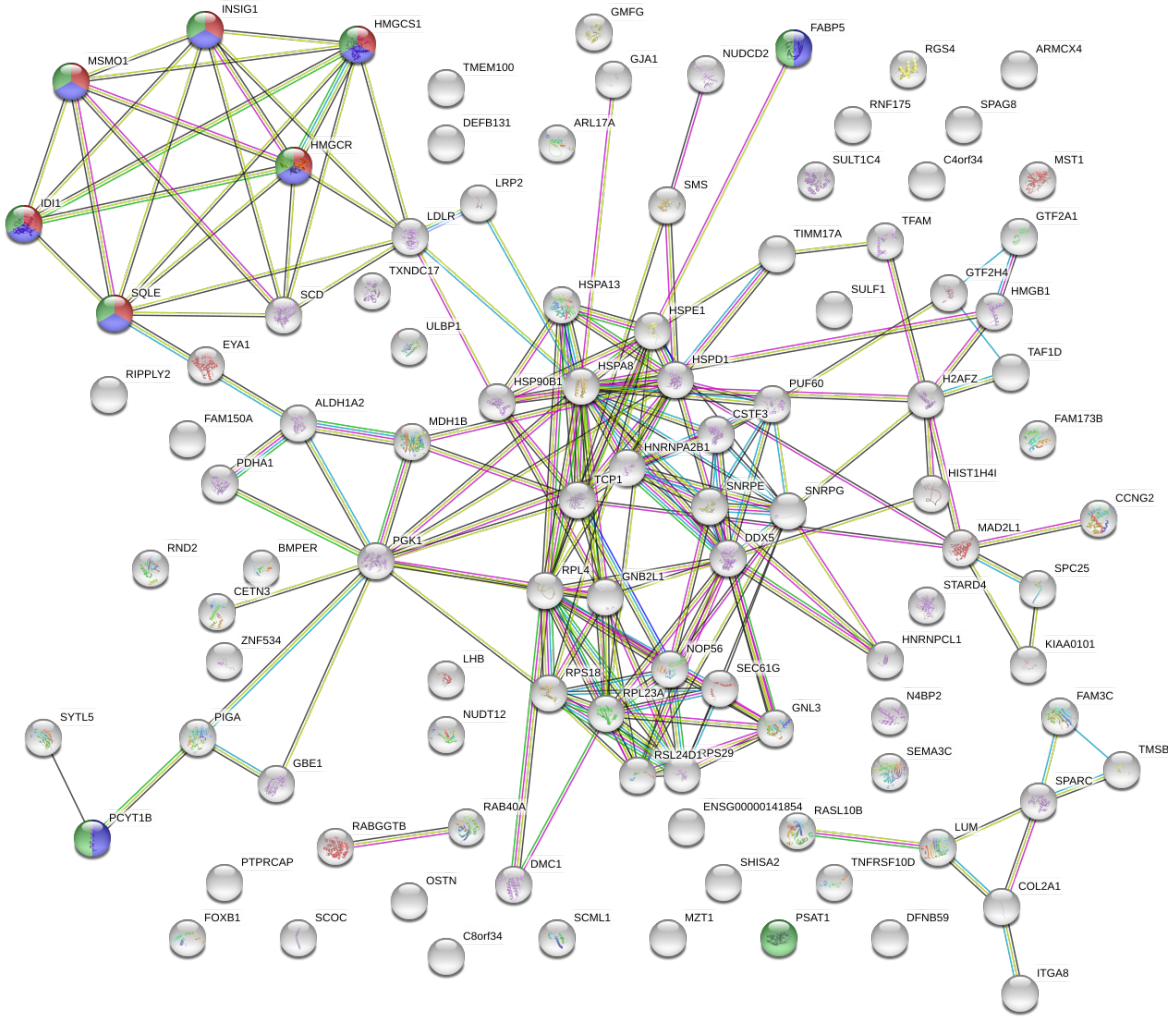

Figure 3.9: STRING analysis on genes that were downregulated in H-v601-Per1 and H-v601-Per2 cells, and upregulated in H-v601 cells, relative to mock. Pairwise comparisons between the transcriptome of HEK293T (Mock), H-v601-Per1, H-v601-Per2, and H-v601 cells was performed. All genes that were differentially expressed by at least two-fold in at least one pairwise comparison were identified, and from these, 164 genes that were downregulated in H-v601-Per1 and H-v601-Per2 relative to mock, and upregulated in H-v601 relative to mock were further identified. STRING analysis was performed on these 164 genes to identify clusters of associated proteins or protein-protein interactions. Highlighted nodes in colour indicate proteins in the top three Biological Process (GO) pathways identified by the STRING software according to ascending *p* value. Red indicates the pathway "Cholesterol Biosynthetic Process" ($p = 0.000361$); blue indicates "Alcohol Biosynthetic Process" ($p = 0.000361$); green indicates "Organic Hydroxy Compound Biosynthetic Process" ($p = 0.0007$).

3.3.2. Bioinformatic analysis of genes specifically upregulated during persistent infection.

673 genes were identified that were upregulated in H-v601-Per1 or H-v601-Per2 relative to Mock and H-v601 cells (Supplementary Table 2). STRING analysis was performed on these 673 genes (Figure 3.10) to visualise clusters of interactions between proteins encoded by these genes. These genes were then further analysed by DAVID to identify functionally-related clusters of genes that are upregulated during persistent infection. The top annotation cluster with an enrichment score of 6.73 was "Response to virus", with the next two being "Growth factor activity" and "Post-synaptic cell membrane" with enrichment scores of 4.9 and 4.72, respectively (Table 3.5). In the "Response to virus" functional annotation cluster, there were 35 genes identified. Additionally, STRING analysis identified enriched pathways and the top three pathways are shown in Table 3.5, with the top pathway "Response to virus", followed by "Cell-cell signalling" and "Response to external stimulus" (p = 1.87 x 10^{-8}, 1.87 x 10^{-8}, and 1.87 x 10^{-8}, respectively). STRING analysis was then performed on the smaller group of 35 genes (Figure 3.11) to further characterise and filter them to identify potential targets for further validation experiments. This revealed 24 genes enriched in the "Response to virus" pathway (p = 8.21 x 10^{-36}), 27 genes in the "Response to other organism" pathway (p = 6.74 x 10^{-31}), and 26 genes in the "Response to biotic stimulus" pathway (p = 1.51 x 10^{-28}). *C19orf66, CD70, CLU, CYP1A1* and *GDF15* were the only genes encoding proteins that did not have a known interaction with any other proteins encoded by genes in the list, however *C19orf66, CD70, CLU* and *CYP1A1* are known ISGs or have known roles in the innate immune response (Echebli *et al.,* 2017; Lulli *et al.,* 2016; Sonn *et al.,* 2010; Suzuki *et al.,* 2016). Similarly, *CCL27* was not highlighted by STRING as being involved in any of the top three enriched pathways, yet is a known ISG (Moerman-Herzog and Nakagawa, 2015). Overall, 32 genes were identified as ISGs that were upregulated in H-v601-Per1 or H-v601-Per2 compared to Mock and wild-type DENV-2-infected cells: *ACTA2, BCL3, BST2, C19orf66, CCL20, CCL27, CD70, CLU, CXCL1, CXCL10, CXCL11, CXCL8, CYP1A1, DDX58, DDX60, DHX58, FOSL1, HSPB1, IFI44, IFIH1, IFIT1, IFIT2, IFIT3, IFITM1, IFITM2, IFITM3, IFNB1, ISG15, ISG20, NFKBIA, OASL,* and *RSAD2*.

Table 3.5: Summary of top three functional annotation clusters identified by DAVID and enriched pathways identified by STRING from genes specifically upregulated during persistent infection. Genes upregulated in H-v601-Per1 or H-v601-Per2 relative to Mock and H-v601 were analysed by DAVID or STRING software. The top three functional annotation clusters, the corresponding EASE score, and number of genes in each cluster identified by DAVID analysis is shown. The top three biological process (GO) pathways identified by STRING, corresponding *p* values and the number of proteins in each pathway is also shown.

DAVID			STRING		
Functional annotation cluster	**EASE score (≥ 1.3)**	**Number of genes**	**Biological Process (GO) pathway**	***p* value**	**Number of proteins**
Response to virus	6.73	35	Response to virus	1.87×10^{-8}	29
Growth factor activity	4.9	20	Cell-cell signaling	1.88×10^{-8}	60
Synapse	4.72	30	Response to external stimulus	1.88×10^{-8}	95

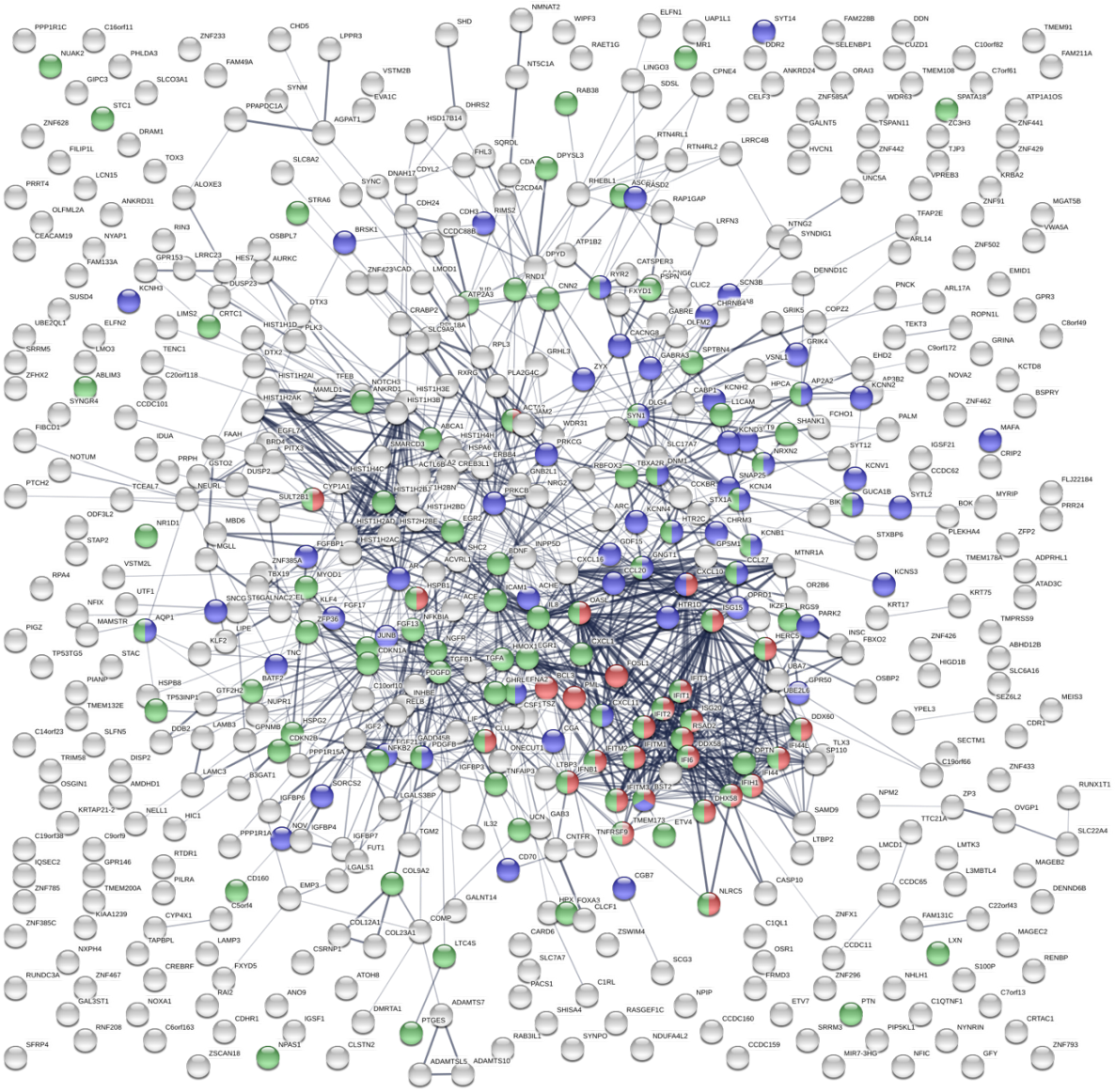

Figure 3.10: STRING analysis on genes that were upregulated in H-v601-Per1 and H-v601-Per2, relative to Mock and H-v601. 673 genes were identified that were upregulated in H-v601-Per1 and H-v601-Per2 relative to Mock and H-v601 by at least two-fold. STRING analysis was performed on these 673 genes to identify functionally-related clusters of genes within the data. Highlighted nodes in colour indicate proteins in the top three Biological Process (GO) pathways identified by the STRING software according to ascending *p* value. Red indicates the pathway "Response to virus" ($p = 1.87 \times 10^{-8}$); blue indicates "Cell-cell signalling" ($p = 1.88 \times 10^{-8}$); green indicates "Response to external stimulus" ($p = 1.88 \times 10^{-8}$).

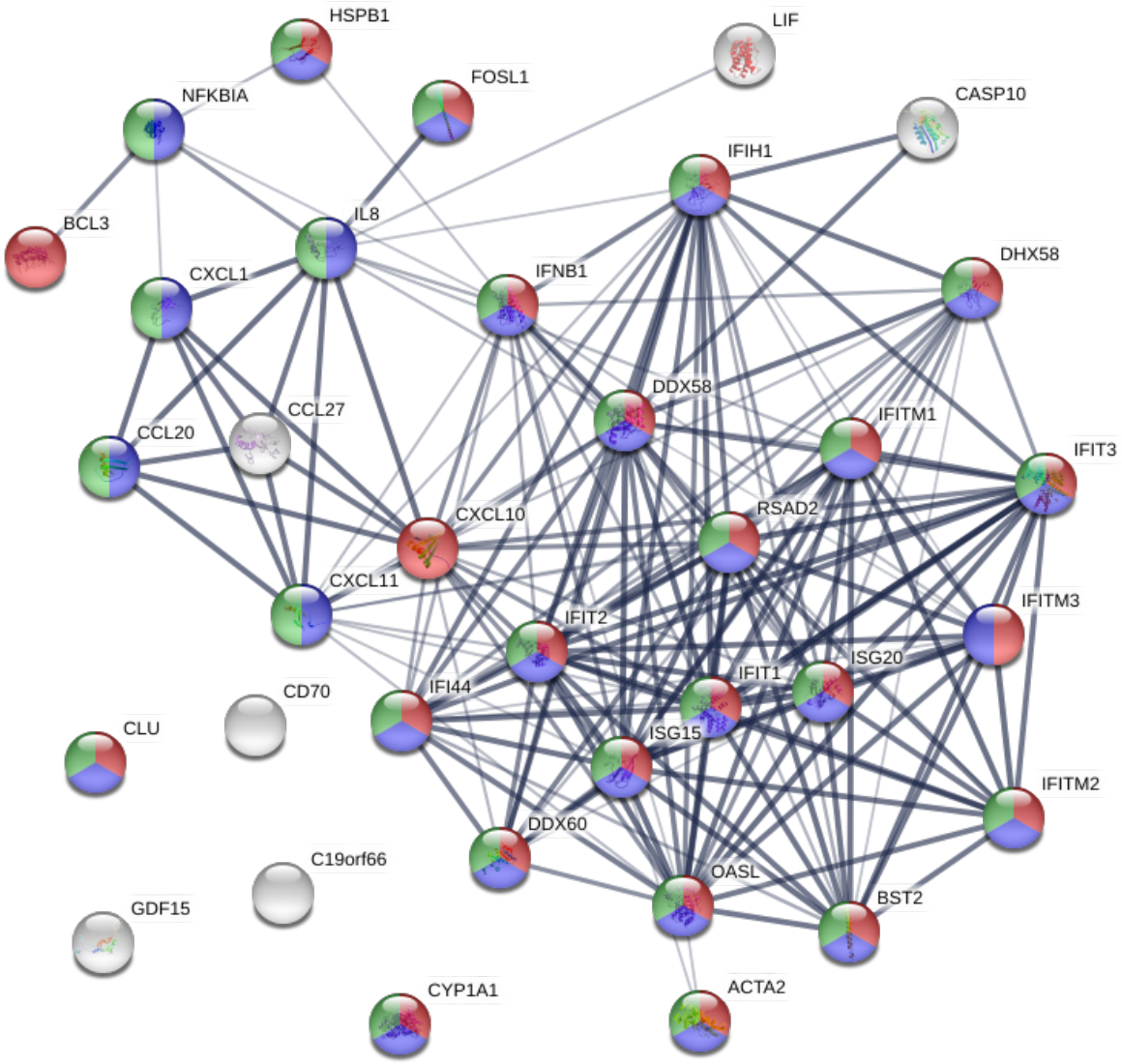

Figure 3.11: STRING analysis on 35 "Response to virus" genes. In the transcriptomics dataset, 673 genes were identified to be upregulated in H-v601-Per1 and H-v601-Per2 cells by at least two-fold, relative to Mock and H-v601 cells. DAVID analysis on these genes revealed 35 genes that were included in the "Response to virus" annotation cluster. STRING analysis was performed to determine if these 35 genes encoded proteins that had known interactions; proteins identified as part of enriched biological process (GO) pathways are highlighted by coloured nodes. 24 genes were in the enriched "Response to virus" pathway ($p = 8.21 \times 10^{-36}$) (red); 27 genes were in the "Response to other organism" pathway ($p = 6.74 \times 10^{-31}$) (blue); 26 genes in the "Response to biotic stimulus" pathway ($p = 1.51 \times 10^{-28}$) (green).

3.4. Investigation into the effects of persistent DENV infection on cholesterol biosynthesis pathways.

Cholesterol is a multi-functional lipid that plays key functions in many aspects of cellular biology and immunology, and critically for this project, cholesterol biosynthesis plays an important role during viral infection as outlined in more detail in Section 1.6. Cholesterol biosynthesis is a highly complex process that takes place in multiple subcellular locations and utilises many different enzymes to generate a number of intermediate molecules before cholesterol can be synthesised. There are several branches of the cholesterol biosynthesis pathway, including the mevalonate and sterol branches; for a comprehensive overview of the cholesterol biosynthesis pathway, please see Mazein *et al.,* 2013.

3.4.1. Introduction to target cholesterol biosynthesis genes.

Genes of interest for this project were those involved in cholesterol biosynthesis that were downregulated in H-v601-Per1 and H-v601-Per2 cells, and upregulated in H-v601 cells, relative to Mock because this would indicate differential expression of a cellular pathway that potentially supports persistent infection. Genes identified through bioinformatics analysis were: *HMGCR, HMGCS1, IDI1, INSIG1*, *MSMO1* and *SQLE*. *HMGCR, HMGCS1, IDI1, MSMO1* and *SQLE* encode enzymes that are involved in both the mevalonate and sterol branches of the cholesterol biosynthesis pathway (Goldstein and Brown, 1990), while *INSIG1* plays a key role in the regulation of cholesterol homeostasis (Yabe *et al.,* 2002; Ye and DeBose-Boyd, 2011) (Figure 3.12). Sterol regulatory element-binding proteins (SREBPs) are ER membrane-bound transcription factors that mediate the feedback system regulating cholesterol and fatty acid biosynthesis pathways. In short, when sterols are abundant in ER membranes, SREBPs bind SREBP-cleavage-activating protein (Scap), a membrane protein, which then binds INSIG proteins (Radhakrishnan *et al.,* 2004). This retains the INSIG/Scap/SREBP complex in the ER membrane and the expression of SREBP target genes is not induced. Under sterol deprivation, INSIG proteins dissociate from Scap and are rapidly deubiquitinated and degraded (Gong *et al.,* 2006). The Scap/SREBP complex enters the Golgi network where SREBPs undergo sequential proteolytic cleavage events by S1P and S2P, and the transcription factor domain of SREBP is released into the nucleus to transcriptionally activate the expression of its target genes (Ye and DeBose-Boyd, 2011). *HMGCR, HMGCS1, IDI1, INSIG1,* and *SQLE* are all directly regulated by SREBPs (Horton *et al.,* 2003; Maxwell *et al.,* 2003; Sharpe and Brown, 2013; Tabor *et al.,* 1999).

During DENV infection, it has previously been shown that expression or activity of genes involved in cholesterol biosynthesis pathways, and accordingly, intracellular cholesterol levels

are increased (Rothwell *et al.,* 2009; Soto-Acosta *et al.,* 2017). Out of the identified targets, HMGCR is the enzyme that has been most widely studied in the context of DENV infection. Previously, using immunofluorescence techniques, the intracellular HMGCR protein level was found to be unaltered during DENV infection relative to mock (Peña and Harris, 2012). However, the dephosphorylated form of HMGCR is more active and DENV infection has been shown to reduce the phosphorylation level of HMGCR by 70% relative to mock-infected cells; this suggests that the phosphorylation state of HMGCR plays a role in increasing intracellular cholesterol levels during infection (Soto-Acosta *et al.,* 2013). Here, the transcriptomics data suggested that expression of the *HMGCR* gene may be modulated during DENV infection, where *HMGCR* was upregulated during DENV-2 infection relative to mock by more than 2-fold but during persistent infection it was downregulated by more than 2-fold.

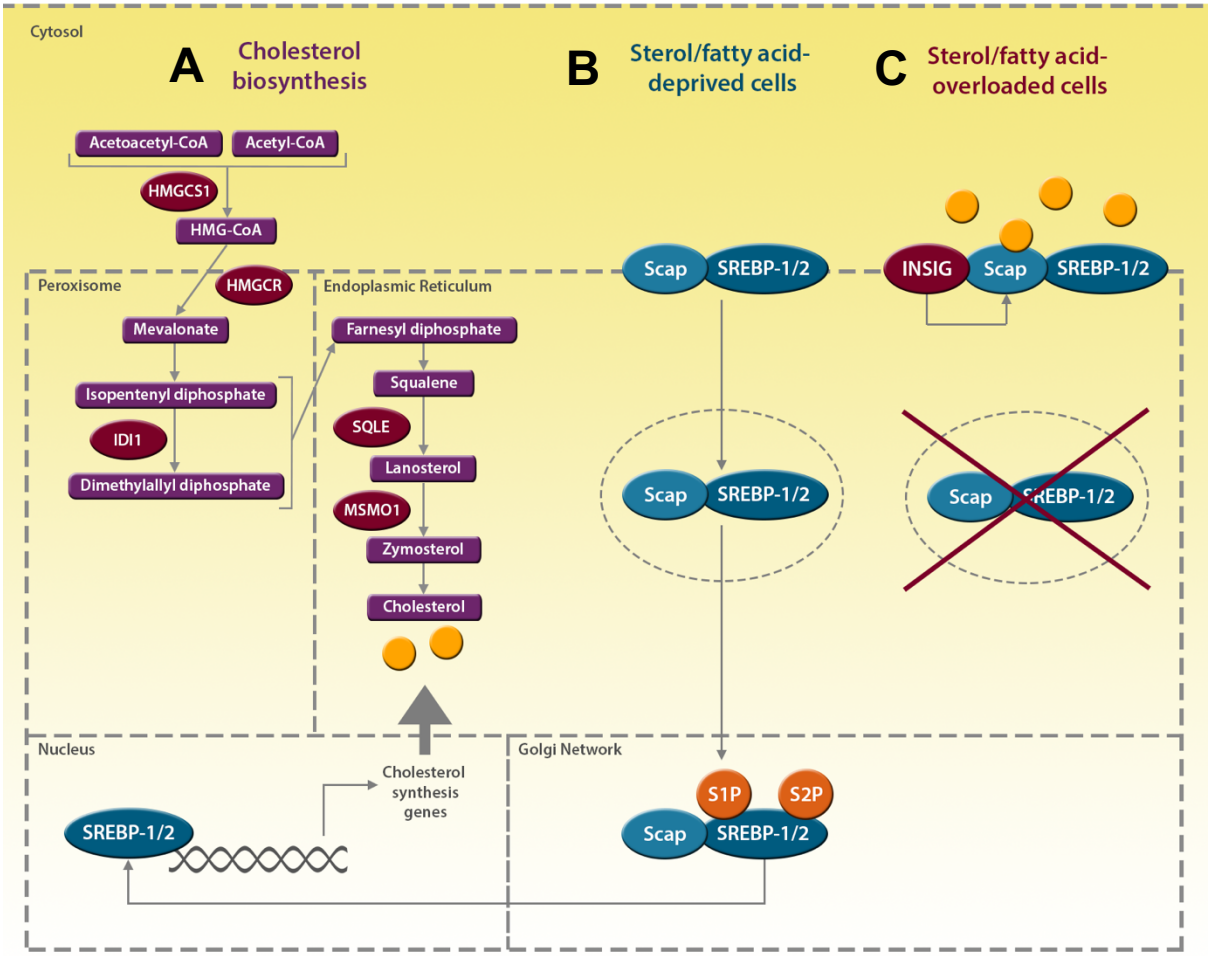

Figure 3.12: Overview of the cholesterol biosynthesis pathway and SREBP-mediated regulation of this pathway. In the cholesterol biosynthesis pathway (A), HMGCS1 converts acetyl-CoA and acetoacetyl-CoA into HMG-CoA; HMGCR converts this into mevalonate which is converted into isopentenyl-diphosphate. IDI1 isomerises isopentenyl-diphosphate into dimethylallyl diphosphate, and these two molecules are transformed into geranyl diphosphate, then farnesyl diphosphate. This is converted to squalene, and SQLE converts this into squalene epoxide. From here, lanosterol is

generated by MSMO1, which is converted to zymosterol then finally cholesterol. Under sterol and fatty acid deprivation (B), Scap and SREBPs form a complex that is transported via COP-II-containing vesicles from the ER membrane to the Golgi network, where SREBPs are cleaved by S1P and S2P proteases to release the transcription factor domain of SREBPs into the nucleus. SREBPs then transcriptionally activate the expression of target genes. When cholesterol and fatty acids are abundant (C), INSIG proteins bind Scap which retains the Scap/SREBP complex in the ER membrane, thus preventing cholesterol and fatty acid biosynthesis genes from being expressed by SREBP. Enzymes encoded by genes identified by our bioinformatics analysis are displayed in red.

3.4.2. Using qPCR to validate the transcriptomics results on cholesterol biosynthesis-related genes.

The transcriptomics results indicated that cholesterol biosynthesis-related genes, *HMGCR, HMGCS1, IDI1, INSIG1, MSMO1,* and *SQLE* were downregulated during persistent infection, and upregulated during wild-type DENV-2 infection by at least 2-fold. Genes for which primer sets were readily available were chosen for further validation using qPCR: *HMGCR, HMGCS1, IDI1, INSIG1* and *MSMO1*. Persistently-infected cells and replicon-containing cells were generated at the same time using the same parental HEK293T cells. Cells at P4 were analysed by RNAseq and frozen for storage. In this project, the same P4 cells were restored and maintained for several passages before qPCR analysis was carried out on cells at P6 and P8. Total intracellular RNA was extracted from HEK293T (Mock), H-v601-Per1, H-v601-Per2, H-Rep, H-Rep-4B$_{T66A}$ and HEK293T cells infected with v601 wild-type DENV-2 (H-v601), and converted to cDNA for qPCR analysis in order to investigate changes in target gene expression between cell lines, as shown in Figure 3.13.

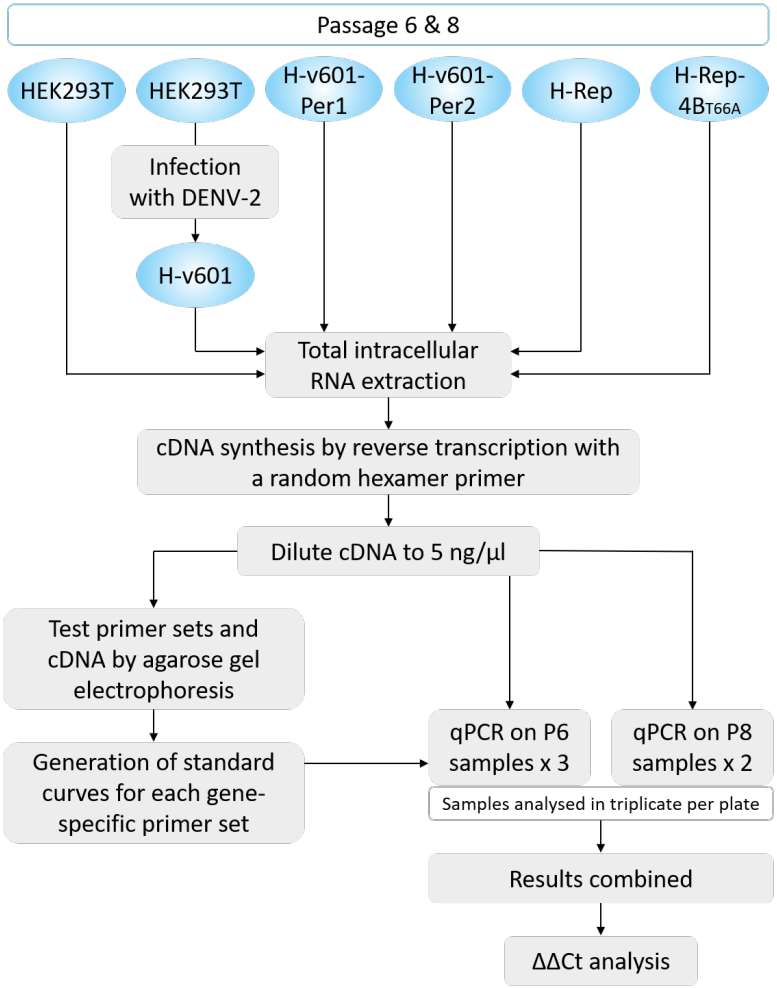

Figure 3.13: An overview of qPCR workflow. HEK293T, H-v601-Per1, H-v601-Per2, H-Rep and H-Rep-4B$_{T66A}$ cells were seeded into 24 well plates and incubated at 37 °C for 48 h. After 24 h, HEK293T cells were infected with v601 (MOI > 5), and incubated for another 24 h to generate the H-v601 cell line. Total intracellular RNA was extracted from the cells, and RNA was converted to cDNA by reverse transcription with a random hexamer primer. This was performed on cells at passage 6 (P6) and P8. Random primed cDNA was used for every subsequent step at a concentration of 5 ng/µl. Gene-specific primer sets for qPCR and successful reverse transcription reaction were tested using PCR and agarose gel electrophoresis to confirm gene-specific binding and successful generation of RT-PCR products. Dilution series of RT-PCR products were prepared and used to generate standard curves to determine primer efficiency. qPCR mastermixes containing SYBR green with ROX, gene-specific primers and nuclease-free water were created and added to a 96 well qPCR plate. Template RT-PCR product was mixed with the mastermix in each well, in triplicate per sample. qPCR reactions were repeated 3 times for P6 samples, and twice for P8 samples. These results were combined and analysed by double-delta Ct (ΔΔCt) analysis for normalisation and to indicate relative expression fold changes of target genes.

3.4.3. Optimisation of qPCR reactions.

The gene specific primers were first checked for successful binding and specific amplification of the correct target gene sequence using PCR and agarose gel electrophoresis (Figure 3.14). The expected product sizes of each primer set are as follows: *ACTB* = 147 bp; *GAPDH* = 95 bp; *HMGCR* = 87 bp; *HMGCS1* = 123 bp; *IDI1* = 133 bp; *INSIG1* = 81 bp; *MSMO1* = 97 bp.

All approximate sizes of observed bands on the gel corresponded to the expected product sizes, however the *ACTB* primer set produced a very faint band relative to other gene-specific primer sets (Figure 3.14). As the transcriptomics dataset indicated that *ACTB* expression changed between different cell lines, *ACTB* was not used as a reference gene and was not analysed further; thus, *GAPDH* was used as a reference gene for all experiments.

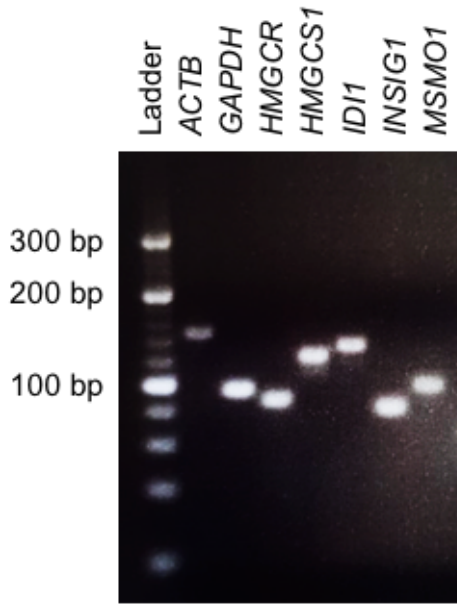

Figure 3.14: Agarose gel electrophoresis to confirm target gene-specific binding of qPCR primer sets. Total intracellular RNA from HEK293T and H-v601-Per1 cells was extracted and converted to cDNA by reverse transcription. PCR was performed using each primer set on the HEK293T RT-PCR product sample to test the cholesterol biosynthesis-related gene-specific primers. 5 ng of cDNA and 1 µl 6 X loading dye was loaded into each well of a 1% agarose gel and run at 100 V for approximately 1 h. O'RangeRuler 20 bp DNA ladder was used to estimate product sizes.

Additionally, standard curves for each primer set were generated using 10-fold serial dilutions of template RT-PCR product with a starting concentration of 10 ng/µl or 5 ng/µl to calculate the primer efficiencies (graphs not shown). Primer efficiency measures the rate at which the polymerase enzyme converts the reagents into amplicons and should ideally fall in the range of 90-110% (Taylor *et al.,* 2010). The efficiency of primer sets for *GAPDH,* and all cholesterol biosynthesis-related genes ranged from 92.3-110.5%, with the exception of the *HMGCS1* primer which demonstrated an efficiency of 134.4%. However, a common cause of high primer efficiency is the formation of primer-dimers or non-specific amplicons (Taylor *et al.,* 2010), but it was clear from the results of agarose gel electrophoresis on genes amplified using the same

primer set that no non-specific binding or primer-dimer formation had occurred (Figure 3.14). Thus, it was concluded that all primer sets were suitable for further qPCR analysis.

3.4.4. qPCR on cholesterol biosynthesis-related genes.

qPCR was used to analyse the expression of *HMGCR, HMGCS1, IDI1, INSIG1* and *MSMO1* in all cell lines, including uninfected HEK293T (Mock), wild-type DENV-2-infected HEK293T (H-v601), H-v601-Per1, H-v601-Per2, H-Rep and H-Rep-4B$_{T66A}$. As described above in Figure 3.13, total intracellular RNA was extracted from these cells at both P6 and P8, and qPCR was performed either 2 or 3 times on samples from each passage number, and results from all assays were pooled to generate the results shown in

Figure 3.15. The results show relative quantitation, meaning *GAPDH* was used as a reference gene for analysis of target gene expression, and the expression of each target gene in mock cells was used as a calibrator to calculate relative fold changes in gene expression in the other cell lines.

The expression of *HMGCR* was significantly reduced in the H-v601-Per1 and H-v601-Per2 cell types relative to Mock (p = <0.0001 and 0.0003, respectively); these results were consistent with the transcriptomics data which suggested *HMGCR* was downregulated during persistent infection. However, *HMGCR* was not upregulated during wild-type DENV-2 infection as suggested in the transcriptomics data, and in fact was also significantly reduced in H-v601 cells relative to Mock (p = 0.0085). Expression of *HMGCR* was significantly reduced in both H-Rep and H-Rep-4B$_{T66A}$ relative to Mock (p = <0.0001 for both) and H-v601 (p = 0.0224 and 0.0466, respectively). However, there was no significant difference in *HMGCR* expression between either H-v601-Per1 or H-v601-Per2 and H-v601, or between H-Rep and H-Rep-4B$_{T66A}$, i.e. with or without the presence of the NS4B$_{T66A}$ mutation (

Figure 3.15).

Expression of *HMGCS1* was significantly reduced in both H-v601-Per1 and H-v601-Per2 relative to Mock (p = <0.0001 for both), however *HMGCS1* expression was not significantly altered between Mock and H-v601 as was predicted by the transcriptomics data. *HMGCS1* was significantly downregulated in H-Rep and H-Rep-4B$_{T66A}$, relative to Mock (p = <0.0001 for both), H-v601 (p = <0.0001 for both) and H-v601-Per2 (p = 0.0475 and 0.0352, respectively), but not H-v601-Per1. Interestingly, *HMGCS1* was significantly downregulated in H-v601-Per1 and H-v601-Per2 relative to H-v601 (p = 0.0003 and 0.0074, respectively), indicating there was differential expression of *HMGCS1* between cells infected with wild-type virus and cells

persistently-infected with v601-4B$_{T66A}$, however there was no significant difference in expression between H-Rep and H-Rep-4B$_{T66A}$ (

Figure 3.15).

***IDI1* was significantly downregulated in H-v601-Per2, H-Rep and H-Rep-4B$_{T66A}$ relative to Mock (p = 0.0031, <0.0001 and <0.0001, respectively), but there was no significant difference in expression between H-v601-Per1 or H-v601 and Mock. *IDI1* was also significantly downregulated in H-Rep and H-Rep-4B$_{T66A}$ relative to all virus-infected cell lines H-v601-Per1, H-v601-Per2 and H-v601 (p = <0.0001 for all). *IDI1* expression was significantly reduced in H-v601-Per1 and H-v601-Per2 relative to H-v601 (p = 0.0067 and 0.0001, respectively), again indicating differential expression of this gene between cells infected with wild-type DENV-2 and v601-4B$_{T66A}$, however there was no significant difference in expression between H-Rep and H-Rep-4B$_{T66A}$ (**

Figure 3.15).

The expression of *INSIG1* was only significantly reduced in H-Rep and H-Rep-4B$_{T66A}$ relative to Mock (p = <0.0001 for both), but there was no significant difference in expression between H-v601-Per1, H-v601-Per2 or H-v601 and Mock, which is inconsistent with the results from the transcriptomics analysis. Again, *INSIG1* was significantly downregulated in H-Rep relative to all virus-infected cell lines, H-v601-Per1, H-v601-Per2 and H-v601 (p = 0.0001, 0.0019 and <0.0001, respectively), and in H-Rep-4B$_{T66A}$ (p = 0.0002, 0.0030 and <0.0001, respectively). There was a significant difference in expression of *IDI1* between H-v601-Per2 and H-v601 (p = 0.0077), but not between H-v601-Per1 and H-v601 or H-Rep and H-Rep-4B$_{T66A}$, suggesting a mild difference in expression of *INSIG1* between persistent infection and wild-type infection as it was only observed in one of the persistently-infected cell lines (

Figure 3.15).

***MSMO1* was significantly reduced in H-v601-Per2, H-Rep and H-Rep-4B$_{T66A}$ relative to Mock (p = 0.0405, 0.0037 and 0.0045, respectively), but not in H-v601-Per1 or H-v601. *MSMO1* in H-Rep and H-Rep-4B$_{T66A}$ was significantly reduced relative to H-v601 (p = 0.0079 and 0.0098, respectively), however not compared to H-v601-Per1 or H-v601-Per2 as was observed for other genes. Additionally, there was no significant difference in *MSMO1* expression between cell lines infected with viruses or containing replicons that either did or did not express the NS4B$_{T66A}$ mutation (**

Figure 3.15).

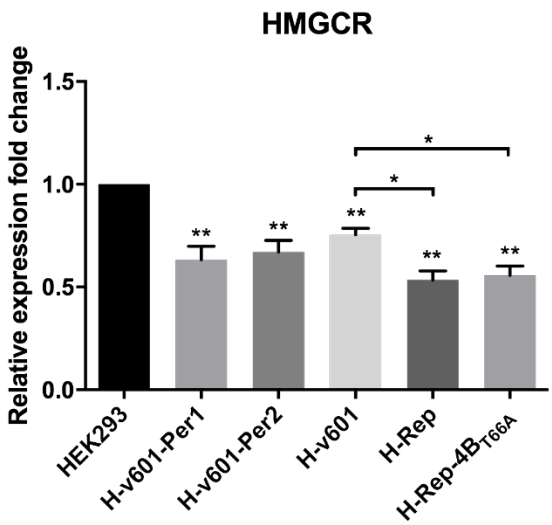
HMGCR
Relative expression fold change
1.5
1.0
0.5
0.0
HEK293
H-v601-Per1
H-v601-Per2
H-v601
H-Rep
H-Rep-4B$_{T66A}$

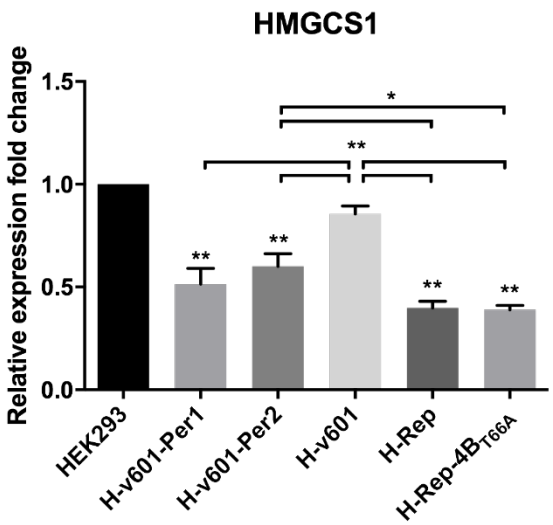
HMGCS1
Relative expression fold change
1.5
1.0
0.5
0.0
HEK293
H-v601-Per1
H-v601-Per2
H-v601
H-Rep
H-Rep-4B$_{T66A}$

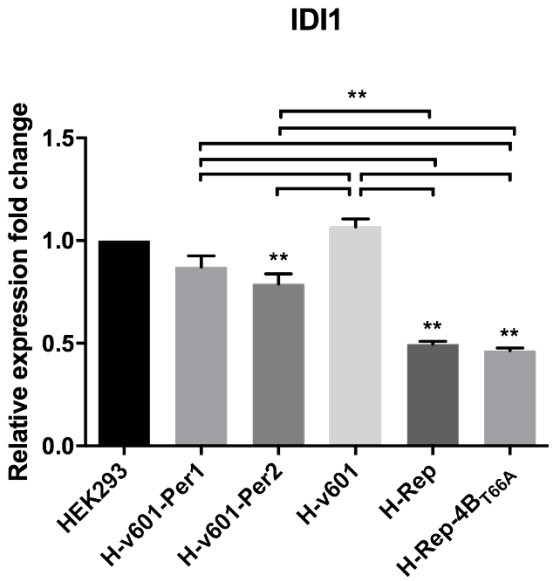
IDI1
Relative expression fold change
1.5
1.0
0.5
0.0
HEK293
H-v601-Per1
H-v601-Per2
H-v601
H-Rep
H-Rep-4B$_{T66A}$

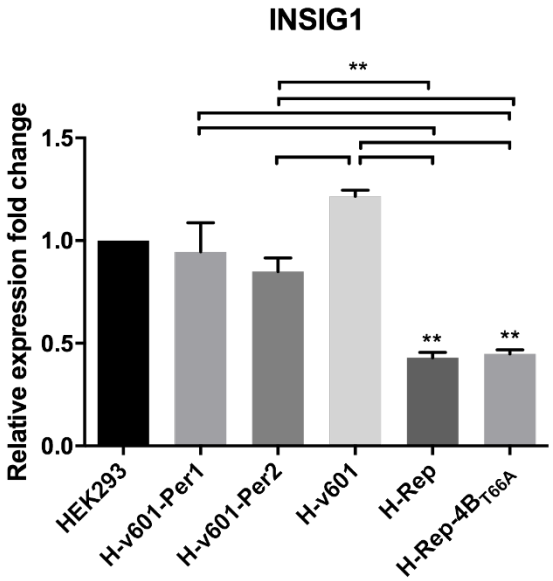
INSIG1
Relative expression fold change
1.5
1.0
0.5
0.0
HEK293
H-v601-Per1
H-v601-Per2
H-v601
H-Rep
H-Rep-4B$_{T66A}$

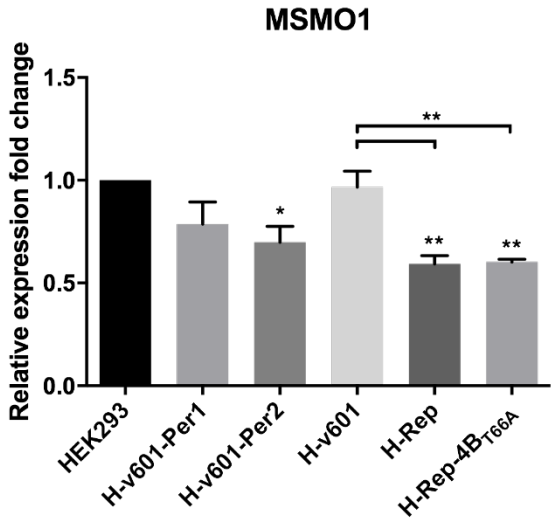
MSMO1
Relative expression fold change
1.5
1.0
0.5
0.0
HEK293
H-v601-Per1
H-v601-Per2
H-v601
H-Rep
H-Rep-4B$_{T66A}$

Figure 3.15: qPCR quantification of cholesterol biosynthesis genes. Cells were seeded into 24 well plates and incubated for 48 hours total. After 24 hours, HEK293T cells were infected with v601 (MOI > 5) and incubated for 24 hours; this was the H-v601 cell line. After the incubation period, cells were lysed and total intracellular RNA was extracted from cell lines at passage 6 (P6) and P8. 200 ng of each RNA sample was converted to RT-PCR product by a reverse transcription reaction using a random hexamer primer, and diluted to a final concentration of 5 ng/µl. 4 µl nuclease-free water, 6.25 µl Maxima SYBR Green mastermix, and 1.25 µl of each primer set, and 1 µl of template RT-PCR product was mixed in each well of a 96 well qPCR plate. Gene-specific primers for *HMGCR, HMGCS1, IDI1, INSIG1* and *MSMO1* from QIAgen were used. The qPCR reaction was performed 3 times on P6 samples, and 2 times on P8 samples, and in triplicate on each plate, and the results combined. GAPDH was used as a reference gene for all reactions. Relative gene expression fold change was determined using the double-delta Ct (ΔΔCt) method with gene expression in HEK293T cells used as the calibrator; error bars show standard deviation. * = $p > 0.05$; ** = $p > 0.001$.

3.4.5. Cellular staining for cholesterol.

To investigate the different effects of wild-type and persistent DENV infection on intracellular cholesterol levels and localisation, intracellular cholesterol was stained using filipin III. Filipin is a polyene antibiotic first isolated from *Streptomyces filipinensis* which is sterol-binding and fluorescent, and is commonly used for visualization of free cholesterol and to detect sterol-rich areas within cells using fluorescence microscopy (Boutté *et al.,* 2011; Maxfield and Wüstner, 2012). Filipin III is the predominant component of filipin and has a high affinity for binding to cholesterol (Volpon and Lancelin, 2000).

A specific Filipin III detection protocol was specifically designed for this experiment (Section 2.3.3). It was also of interest to investigate whether there was any increase in co-localisation of cholesterol with viral replication complexes; thus, fixed cells were stained for dsRNA using primary and fluorophore-conjugated secondary antibodies. Cell nuclei were stained using TO-PRO-3, before staining intracellular cholesterol with filipin III. Coverslips were mounted onto microscope slides using VectaShield without DAPI as filipin III is detected at the same wavelength. As filipin fluorescence photobleaches rapidly, a tandem scanner confocal microscope with hybrid detectors was used, and filipin solutions were protected from light at all times throughout the protocol. However, despite having these protective measures in place, photobleaching during the cell imaging process was still significant. Therefore, filipin fluorescence levels on images should not be taken as an indication of cholesterol abundance and this experiment instead focused on investigating co-localisation of dsRNA and intracellular cholesterol.

In uninfected cells, cholesterol was detected in the cell membranes with uniform distribution (Figure 3.16). There was some faint staining for dsRNA in the HEK293T cells, however compared to dsRNA staining in all virus-infected cells this was much lower in the uninfected cells and therefore could potentially be attributed to unspecific background fluorescence. In the wild-type DENV-2-infected cells, cholesterol distribution appeared disrupted, with cholesterol staining appearing more punctate and irregular when compared to cholesterol distribution in the HEK293T cells. Additionally, there appeared to be some moderate co-localisation of cholesterol and dsRNA in the H-v601 cells in the peri-nuclear areas, as indicated by white arrows in Figure 3.16. In the H-v601-Per1 cells, distribution of cholesterol was still slightly irregular when compared to uninfected control cells, with cholesterol staining in the membranes appearing thinner and with more punctate areas. dsRNA did not appear to be co-localised with cholesterol in this sample, and was localised closer to the nucleus. In H-v601-Per2 cells, cholesterol distribution in the membranes appeared much more irregular than all other samples, while dsRNA localisation seemed mutually-exclusive to cholesterol localisation. Overall, these results could indicate that while cholesterol may slightly co-localise and be recruited to viral replication complexes during wild-type infection, during persistent infection there is no such co-localisation.

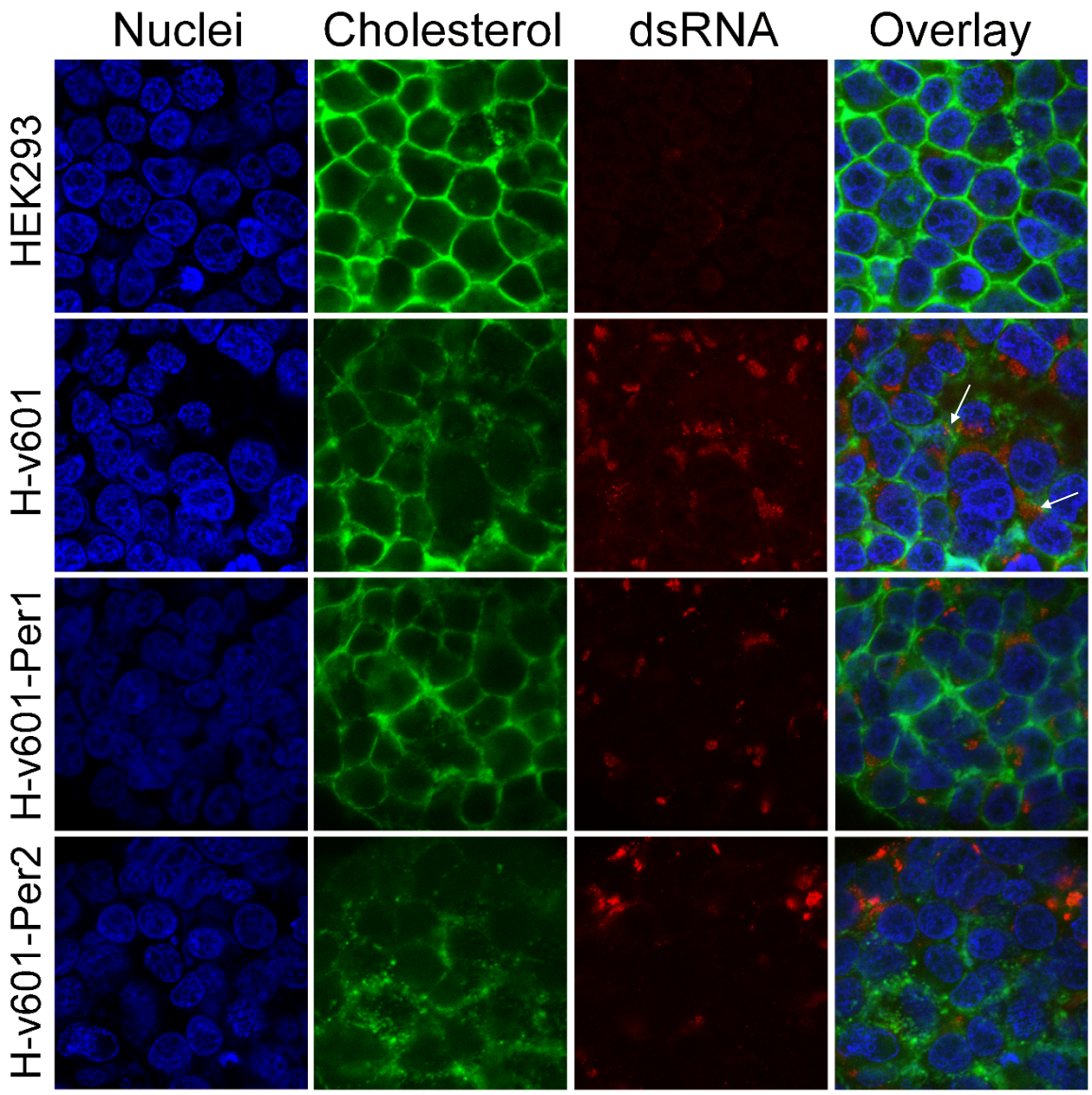

Figure 3.16: Staining intracellular cholesterol with filipin III. HEK293T, H-v601-Per1, and H-v601-Per2 cells were seeded onto coverslips in a 24 well plate. After 24 h, HEK293T cells were infected with v601 virus to generate wild-type DENV-2-infected cells. Cells were incubated at 37 °C. After 24 h, cells were fixed with 4% PFA, quenched with 50 mM ammonium chloride, permeabilised by 1% Triton-X-100, and blocked in 10% FBS in PBS. dsRNA (red) was stained with mouse anti-dsRNA primary antibody at a 1:200 dilution, followed by a goat anti-mouse secondary antibody conjugated with a 568 Alexa Fluor® at a 1:1000 dilution. Nuclei (blue) were stained with TO-PRO-3 at a 1:1000 dilution, protected from light. Intracellular cholesterol (green) was stained with filipin III at a concentration of 100 µg/ml, protected from light, before mounting onto microscope slides using VectaShield without DAPI. The mounted samples were imaged using an SP5-II tandem scanner confocal microscope with 'hybrid' GaAsP detectors.

3.5. Investigation into the type I IFN response.

The type I IFN response is known to be an important factor in a host's response to viral infection, including during DENV infection. Consequently, this is also a common pathway for viruses to target for inhibition or evasion of the host innate immune response, as discussed in more detail in Section 1.5.3.

3.5.1. Type I IFN response and persistent DENV infection.

As previously described in Section 3.3.2, bioinformatic analysis of a transcriptomics dataset was used to discover 673 genes that were specifically upregulated in the persistently-infected cells, H-v601-Per1 and H-v601-Per2, relative to Mock and wild-type DENV-2-infected cells, H-v601. Within these, through functional annotation and protein interaction analyses, 32 genes encoding ISGs that express proteins with antiviral functions were identified: *ACTA2, BCL3, BST2, C19orf66, CCL20, CCL27, CD70, CLU, CXCL1, CXCL10, CXCL11, CXCL8, CYP1A1, DDX58, DDX60, DHX58, FOSL1, HSPB1, IFI44, IFIH1, IFIT1, IFIT2, IFIT3, IFITM1, IFITM2, IFITM3, IFNB1, ISG15, ISG20, NFKBIA, OASL,* and *RSAD2*. Genes encoding proteins that have roles within the type I IFN signaling pathways, such as JAK1, JAK2, STAT1, STAT2, IRF9, were not found to be differentially expressed by at least two-fold during infection with wild-type virus or during persistent infection, relative to Mock. This may indicate that components of the signaling pathway are not targeted by the virus for subversion of the host antiviral response at a transcriptional level. As it is known that STAT1 and STAT2 proteins are targeted by DENV viral proteins to facilitate infection (Ashour *et al.,* 2009; Muñoz-Jordan *et al.,* 2003, 2005), it is likely that this modulation of STAT1 and STAT2 by the virus occurs only at a post-translational stage, rather than by modifying gene expression levels.

3.5.2. Effect of persistent infection on STAT1.

To study the effect of the $NS4B_{T66A}$ mutation on the virus's ability to inhibit the activation and nuclear localisation of STAT1 during the host immune response, STAT1 was imaged in the different cell lines (Figure 3.17). During the host immune response, IFNα/β is produced which binds to the IFNAR receptor and induces the type I IFN pathway during which STAT1, in complex with STAT2 and IRF9, is phosphorylated and translocated to the nucleus (Ivashkiv and Donlin, 2015). The ratio of nuclear/cytoplasmic fluorescence indicating localisation of STAT1 was calculated using CellProfiler software; a fluorescence ratio of > 1 indicates nuclear localisation (Figure 3.18).

IFNα treatment resulted in significant nuclear translocation of STAT1 in the HEK293T, H-v601, H-v601-Per2 and H-Rep-4B$_{T66A}$ cells compared to cells of the same cell line that were left untreated with IFNα (p = <0.0001 for all), however there was no significant difference in nuclear localisation of STAT1 upon IFNα treatment in H-v601-Per1 or H-Rep cells (Figure 3.17).

When cells were left untreated with IFNα, STAT1 in H-v601-Per1, H-v601-Per2, H-Rep and H-Rep-4B$_{T66A}$ was significantly more localised to the nucleus than in the control HEK293T cells (p = <0.0001, 0.0045, <0.0001, and <0.0001, respectively), while in the H-v601 cells, STAT1 was significantly more localised to the cytoplasm compared to untreated HEK293T cells (p = 0.0002) (Figure 3.17).

When cells were treated with IFNα, nuclear localisation of STAT1 was significantly lower in H-v601 and H-v601-Per1 cells, relative to uninfected cells (p = <0.0001 for both); however, STAT1 was significantly more localised to the nucleus in the H-v601-Per2 and H-Rep-4B$_{T66A}$ cells, relative to uninfected cells (p = 0.0027 and <0.0001, respectively). There was no significant difference in STAT1 localisation between uninfected cells and H-Rep. STAT1 was significantly more nuclear localised in H-v601-Per2 cells than in H-v601 cells (p = <0.0001), and in H-Rep-4B$_{T66A}$ cells than in H-Rep cells (p = <0.0001) (Figure 3.17).

Overall, these results suggested that the presence of the NS4B$_{T66A}$ mutation alters the effect of DENV-2 infection on the host type I IFN immune response during wild-type or persistent infection both with and without addition of exogenous IFNα.

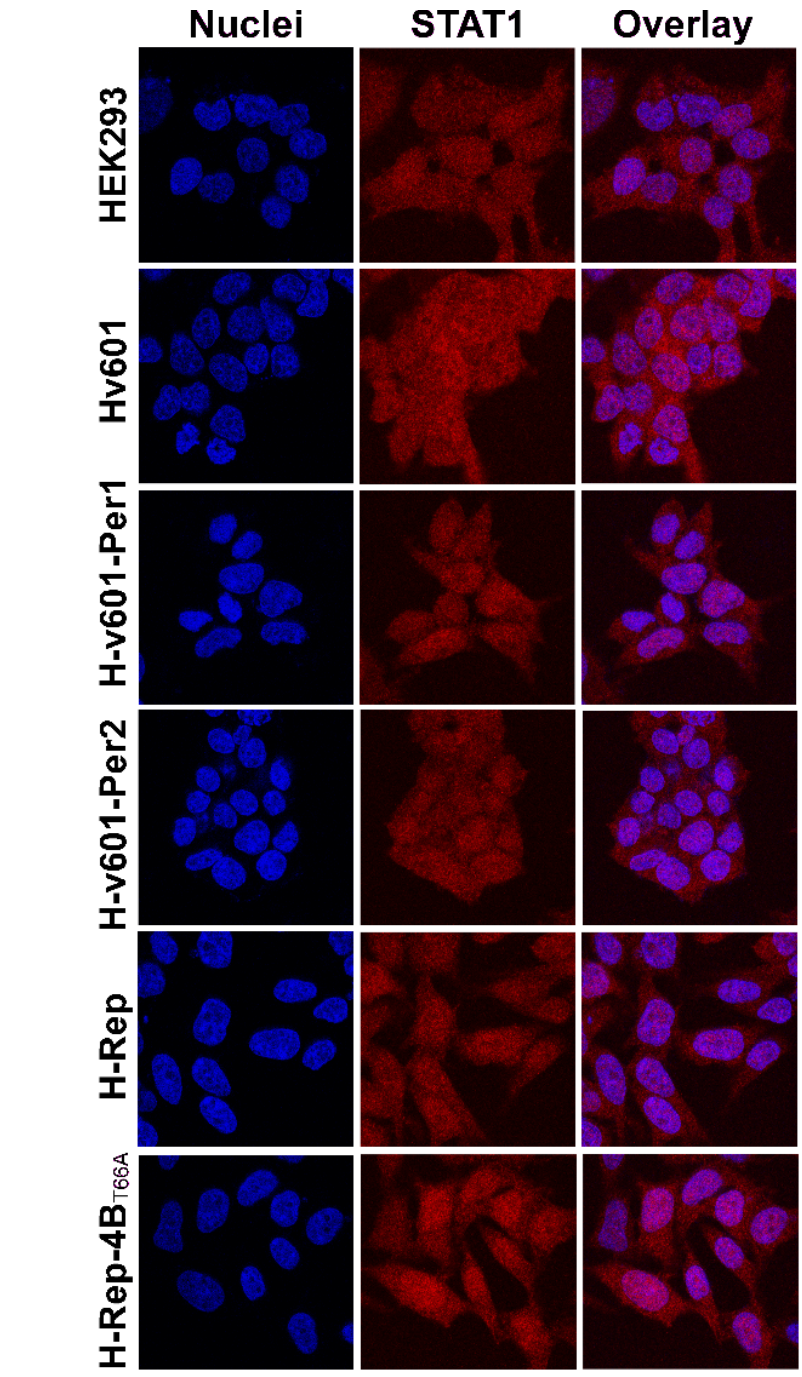
Nuclei
STAT1
Overlay
HEK293
Hv601
H-v601-Per1
H-v601-Per2
H-Rep
H-Rep-4B$_{T66A}$
IFN-

A

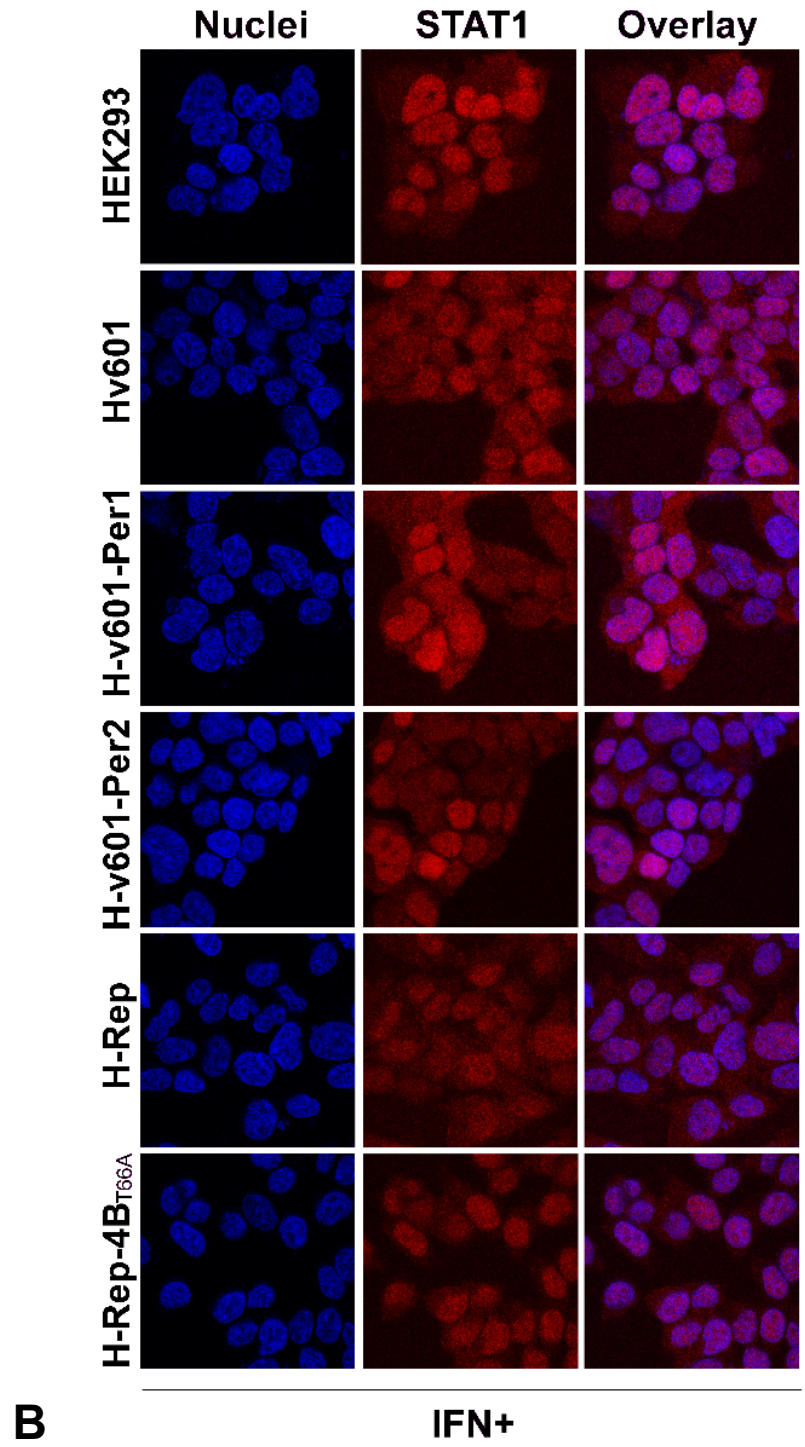

Figure 3.17: IFA to detect STAT1 in all cell lines. HEK293T, H-v601-Per1, H-v601-Per2, H-Rep, and H-Rep-4B$_{T66A}$ cells were seeded onto coverslips in 24 well plates and incubated at 37 °C for 24 h. HEK293T cells were infected with v601 for 1.5 h, the virus was removed, and all cells were incubated for a further 24 h. Cells were either left untreated; termed IFN- **(A),** or treated with 1000 U/ml IFNα for 1 h; termed IFN+ **(B).** Cells were fixed with 4% paraformaldehyde, permeabilised with 1% Triton-X-100, and blocked with 10% FBS in PBS. STAT1 proteins were stained with a rabbit anti-STAT1 antibody at a 1:400 dilution, followed by a goat anti-mouse secondary antibody conjugated with a 568 Alexa Fluor® at a 1:1000 dilution. Coverslips were mounted onto microscope slides using VectaShield with DAPI, and imaged using a Leica SP5-AOBS confocal laser scanning microscope attached to a Leica DMI6000 inverted epifluorescence microscope with 63x objective, and a 2.5x optical zoom.

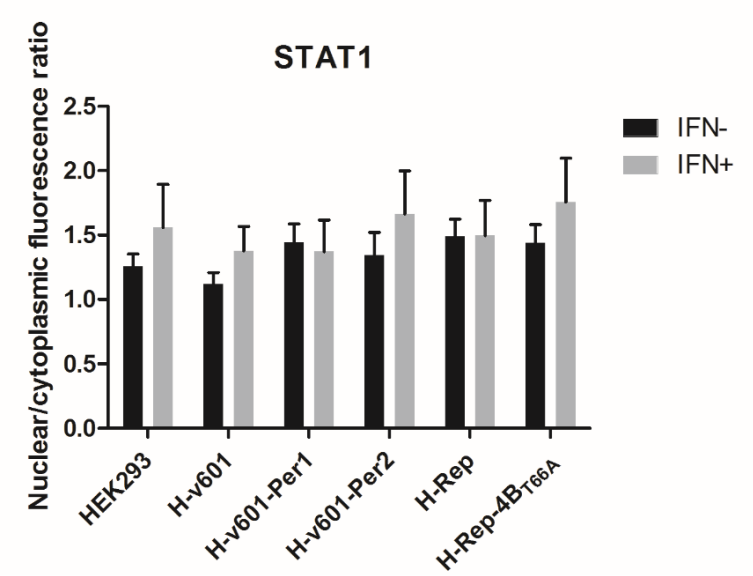

Figure 3.18: Quantification of the nuclear/cytoplasmic fluorescence ratio of STAT1 in all cell lines. STAT1 was stained in HEK293T, H-v601, H-v601-Per1, H-v601-Per2, H-Rep, and H-Rep-4B$_{T66A}$ cells that had either been left untreated or treated with IFNα prior to fixation, and images were captured using a Leica SP5-AOBS confocal laser scanning microscope attached to a Leica DMI6000 inverted epifluorescence microscope with 63x objective, and a 2.5x optical zoom. The images were analysed by CellProfiler software using a program that quantifies the fluorescence corresponding to STAT1 that is detected within the nucleus and within the cytoplasm of each cell in each image. From this, an average nuclear/cytoplasmic fluorescence ratio is calculated; for each dataset, averages were calculated from between 142 and 311 objects. Graphs were created using GraphPad Prism 7; two-way ANOVA and Tukey's multiple comparison post-hoc tests were used for statistical analysis.

3.5.3. Effect of persistent infection on STAT2.

STAT2 was stained in HEK293T, H-Rep and H-Rep-4B$_{T66A}$ cells to study the effect of the presence of the DENV non-structural proteins encoded by the replicons, and to investigate whether any effects on STAT2 were altered by the presence of the NS4B$_{T66A}$ mutation (Figure 3.19). Localisation of STAT2 proteins was quantified using CellProfiler which calculated the nuclear/cytoplasmic fluorescence ratio; a ratio of > 1 indicates nuclear localisation.

Under activation by IFNα treatment, STAT2 in the IFN+ HEK293T cell lines displayed clear translocation from the cytoplasm to the nucleus, relative to IFN- cells (p = <0.0001). With no exogenous IFNα present, STAT2 localisation to the nucleus was greater in the H-Rep and H-Rep-4B$_{T66A}$ cells than the HEK293T cells (p = 0.0183 and 0.0015, respectively) although the overall amounts of STAT2 appeared less. This could potentially be caused by the presence of replicon genomes inducing a small immune response, thus a relatively small activation of the type I IFN response causing STAT2 translocation to the nucleus, however this activation of

the type I IFN pathway may not be as great as during the presence of exogenous IFNα prior to cell fixation.

In cells that were treated with IFNα prior to fixation, nuclear localisation of STAT2 in the HEK293T cells was greater than both H-Rep and H-Rep-4B$_{T66A}$ cells (p = <0.0001 for both). However, neither H-Rep or H-Rep-4B$_{T66A}$ cells displayed significant translocation of STAT2 to the nucleus upon IFNα treatment. Once again, the amounts of STAT2 appeared to be much less in the replicon containing cells. These results were somewhat expected because it is known that the phosphorylation and activation of STAT2 is blocked and STAT2 is targeted for proteasomal degradation by NS5 (Ashour *et al.,* 2009; Mazzon *et al.,* 2009) which is encoded by both replicon constructs. This experiment was carried out on biosafe replicon-containing cells, but as the results indicated no differential effect caused by the NS4B$_{T66A}$ mutation, the experiment was not repeated using virus-infected cells.

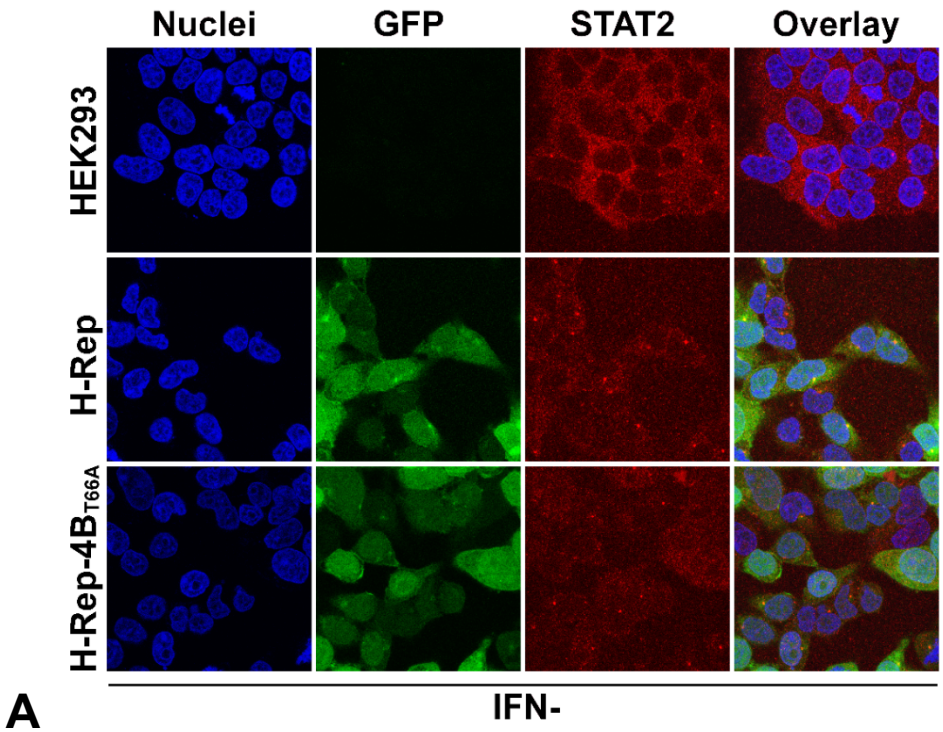

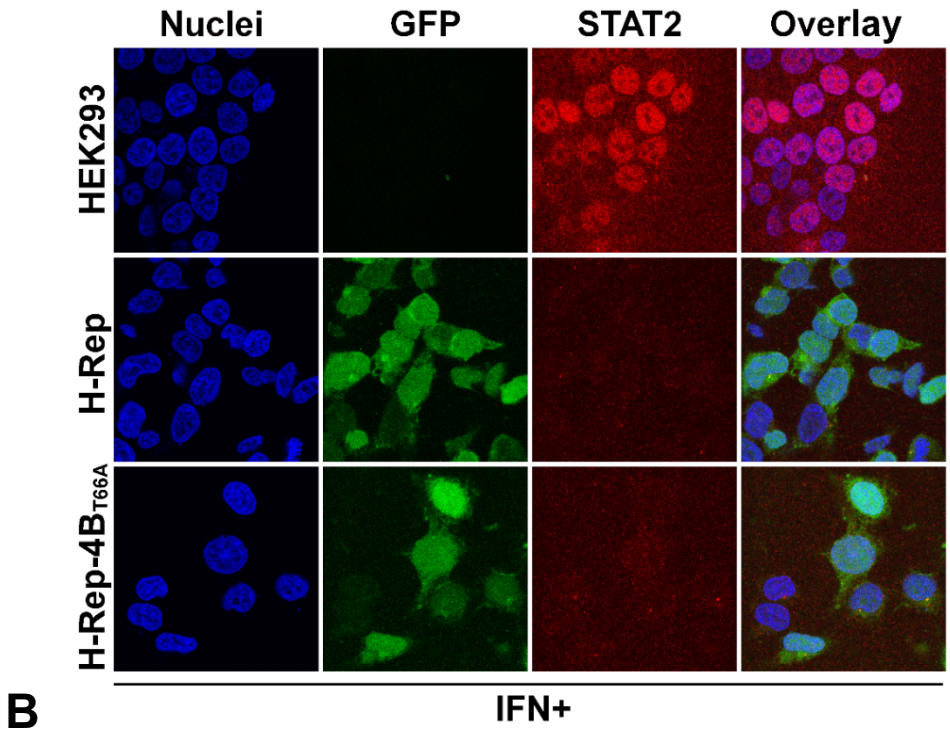

Figure 3.19: IFA to detect STAT2 in HEK293T, H-Rep and H-Rep-4B$_{T66A}$ cells. Cells from each cell line were seeded onto coverslips in 24 well plates and incubated at 37 °C for 24 h. Cells were either left untreated, termed IFN- **(A)**, or treated with 1000 U/ml IFNα for 1 h, termed IFN+ **(B)**. Cells were fixed with 4% paraformaldehyde, permeabilised with 1% Triton-X-100, and blocked with 10% FBS in PBS. Cells were treated with rabbit anti-STAT2 antibody at a 1:200 dilution, followed by a secondary goat anti-rabbit secondary antibody conjugated to a 568 Alexa Fluor® at a 1:1000 dilution. Coverslips were mounted onto glass slides using VectaShield with DAPI, and imaged with a Leica SP5-AOBS confocal laser scanning microscope attached to a Leica DMI6000 inverted epifluorescence microscope with 63x objective, and a 2.5x optical zoom.

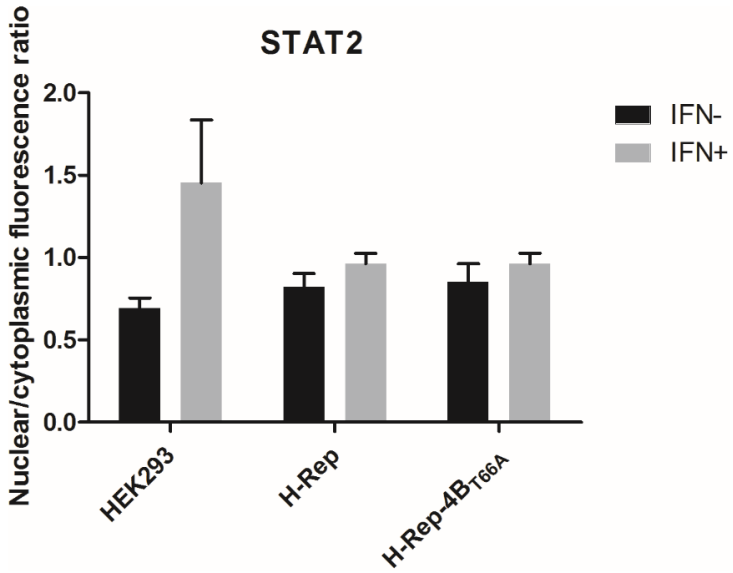

Figure 3.20 STAT2 nuclear/cytoplasmic fluorescence ratio quantification in HEK293T, H-Rep and H-Rep-4B$_{T66A}$ cells. STAT2 proteins were stained in HEK293T, H-Rep and H-Rep-4B$_{T66A}$ cells that were either untreated or treated with IFNα prior to fixation, and cells were imaged using a Leica SP5-AOBS confocal laser scanning microscope attached to a Leica DMI6000 inverted epifluorescence

microscope with 63x objective, and a 2.5x optical zoom. Fluorescence corresponding to STAT2 proteins was quantified using CellProfiler software in the cytoplasm and in the nucleus, and the nuclear/cytoplasmic fluorescence ratio was calculated to indicate intracellular localisation of the proteins. Graphs were generated using GraphPad Prism 7; statistical analysis was performed using a two-way ANOVA with Tukey's multiple comparison post-hoc tests.

3.6. Discussion

3.6.1. Initial characterisation of cell lines.

The H-Rep and H-Rep-4B$_{T66A}$ cell lines were confirmed to be stably expressing DENV-2 replicons by RT-PCR and IFA to detect the DENV NS1 protein. The NS4B genes of the RepDV-GP2A and RepDV-GP2A-NS4B$_{T66A}$ replicons were sequenced, and the NS4B$_{T66A}$ mutation was found to be present in the RepDV-GP2A-NS4B$_{T66A}$ replicon up to at least 19 passages in all cells within the population. The other mutations discovered in the RepDV-GP2A-NS4B$_{T66A}$ replicon NS4B sequence, NS4B$_{I27T}$ and NS4B$_{P92S}$, showed mixed peaks of occurrence and NS4B$_{P92S}$ was also lost in the P19 samples, suggesting these mutations were not stable in the population. The only mutation discovered in the NS4B gene of the RepDV-GP2A replicon, NS4B$_{V152M}$, was only present in P19 samples in a 1:1 ratio. This mutation could have arisen due to some selective pressure or been a random mutation that arose due to continued passaging of the cells over time; however, the cells were shut down shortly after this analysis and therefore the cause of this mutation was not investigated further.

The presence of intracellular and extracellular virus persistently-infecting the H-v601-Per1 and H-v601-Per2 cell lines was confirmed by RT-PCR and IFA for the DENV E protein. There were two nonsynonymous mutations that were discovered in intracellular and extracellular RNA isolated from H-v601-Per1 and H-v601-Per2 samples: NS4B$_{I30Met}$ and NS4B$_{T66A}$. The NS4B$_{T66A}$ mutation was present in all samples, however there was a mixed peak of occurrence in the H-v601-Per1 extracellular RNA and both H-v601-Per1 and H-v601-Per2 intracellular RNA samples, although the peak corresponding to the mutated G nucleotide was predominant (Table 3.2). This suggests that the cell population was not homogenous for this mutation, and the NS4B$_{T66A}$ mutation in the viral genome is less stable than in the replicon sequence, which was present in all replicon-containing cells up to passage 19. However, there was also not a strong selective pressure for the sequence to revert back to wild-type. There were also mixed peaks of occurrence for the NS4B$_{I30Met}$ mutation, suggesting that this was potentially an unstable mutation in the population.

The relative amount of viral RNA was analysed using qPCR, which showed that both persistently-infected and replicon-containing cell lines had significantly lower quantities of viral RNA than wild-type infected cells at 24 h post-infection with a high MOI (>5) (Figure 3.7), suggesting that replication of the v601-4B$_{T66A}$ virus in the persistently-infected cells was either not as efficient as the wild-type virus, due to a defect in RNA synthesis or inhibition by host cell processes. This was also shown previously by Dr. Andrew Davidson and colleagues, who also used qPCR to show that persistently-infected BHK-21 cells expressed 10-100-fold fewer viral genomes/ml than wild-type from 18-70 hours post-infection (Figure 1.3). However, it would be beneficial to conduct further experiments using distinct techniques to quantify the viral load and compare this between wild-type and persistently-infecting viruses.

3.6.2. Bioinformatic analysis of a transcriptomics dataset.

The aim of analysing transcriptomics data from the various cell lines was to identify cellular pathways that are differentially expressed during either wild-type or persistent infection which may indicate a mechanism facilitating persistent infection. Analysis of genes that are downregulated during persistent infection and upregulated during wild-type infection revealed enrichment of genes involved in cholesterol biosynthesis pathways. This suggests that downregulation of cholesterol biosynthesis potentially constitutes a mechanism by which the v601-4B$_{T66A}$ virus establishes a persistent phenotype during infection. Alternatively, this could be a defective pathway in the H-v601-Per1 and H-v601-Per2 host cells that enables maintenance of persistent infection. In total, 6 genes were identified as potential targets for further validation experiments: *HMGCR, HMCGS1, IDI1, INSIG1, MSMO1* and *SQLE*. Conversely, 32 genes involved in the antiviral response were identified that are upregulated during persistent infection, relative to mock and wild-type infection which suggested that the antiviral immune response to DENV infection is enhanced during persistent infection compared to wild-type.

3.6.3. The effect of persistent infection on host cholesterol biosynthesis pathways.

qPCR analysis revealed that expression of *HMGCR, HMGCS1, MSMO1 and IDI1* were reduced in H-v601-Per2 cells, and *HMGCR* and *HMGCS1* were reduced in H-v601-Per1 cells relative to mock-infected cells. These results validated the transcriptomics data which showed that these genes were downregulated in H-v601-Per1 and H-v601-Per2 compared to uninfected Mock cells. However, according to the transcriptomics results this reduction was by at least 2-fold, which was only the case for *HMGCS1* out of 5 genes tested.

It was evident that *HMGCS1, IDI1,* and to a lesser extent, *INSIG1* were differentially expressed during wild-type and persistent infection, suggesting that the presence of the $NS4B_{T66A}$ mutation may alter the effect of DENV-2 infection on cholesterol biosynthesis gene expression. However, this was not corroborated by any observable differences in the expression of any of the genes analysed between H-Rep and H-Rep-$4B_{T66A}$ which express identical replicon constructs that only differ by the presence of the $NS4B_{T66A}$ mutation. None of these genes were significantly differentially-expressed between H-Rep and H-Rep-$4B_{T66A}$ cells in the transcriptomics data, thus this result was somewhat expected. Cell lines stably expressing replicon constructs could be considered persistently-infected, which may inherently influence their effect on the host cell transcriptome. This would suggest that it may not be presence of the $NS4B_{T66A}$ mutation in the persistently-infecting virus that causes downregulation of these genes, but rather a result of the persistent infection itself.

Overall, the qPCR results confirm the transcriptomics results in that genes involved in cholesterol biosynthesis are generally downregulated during persistent infection. Interestingly, suppression of expression of genes involved in cholesterol biosynthesis pathways could indicate an increase in cholesterol abundance following viral infection because the expression of these genes is activated when cholesterol levels are low, and this has been observed with the expression of *HMGCR* and *LDLR* following DENV-2 infection (Rothwell *et al.,* 2009). However, the transcriptomics data suggested that the cholesterol biosynthesis genes investigated showed increased expression during wild-type DENV-2 infection compared to mock, but this observation was not corroborated by the qPCR results as the expression of none of these genes were significantly increased in H-v601 compared to mock-infected cells, thus, this requires further investigation going forwards.

Downregulation of cholesterol biosynthesis genes during persistent infection could potentially constitute a mechanism by which the v601-$4B_{T66A}$ virus is able to persistently-infect host cells without causing normal progression of infection as seen during wild-type DENV-2 infection. However, the effects of wild-type infection on the target genes under investigation remain unclear due to conflicting results between transcriptomic and qPCR analyses. Other studies surrounding the expression of genes involved in lipid metabolism pathways have shown that these changes in expression are highly dynamic and time-dependent; the expression and activity of an enzyme in the fatty acid biosynthesis pathway, stearoyl-CoA desaturase 1 (SCD1), was found to be crucial during early DENV-2 infection, and *SCD1* mRNA levels increased 6 hours post-infection, decreased 12 hours post-infection, and increased again 24 hours post-infection (Gullberg *et al.,* 2018). This suggests that changes in expression of target genes identified through our transcriptomics analysis may have been observed due to the time

at which samples were taken, thus, it would be beneficial to include a time-course experiment for further validation in the future.

To investigate whether patterns of intracellular cholesterol are modified during wild-type or persistent infection, cholesterol was stained using filipin III and dsRNA was stained to represent sites of viral replication in the cells. The results suggested that while there may be a degree of co-localisation between cholesterol and viral replication sites during wild-type infection, there was no co-localisation during persistent infection.

Further work is required to investigate the effect of wild-type and persistent infection on genes and proteins involved in the cholesterol biosynthesis pathway. The expression of six of these genes is already known to be regulated by SREBP transcription factors (Horton *et al.,* 2003; Maxwell *et al.,* 2003; Sharpe and Brown, 2013; Tabor *et al.,* 1999), thus, it would be interesting to investigate and compare the effect of wild-type and persistent DENV infection on SREBP transcription factor activity which has not been described previously. If infection with DENV does alter the activity of SREBP transcription factors this could explain why the expression of these genes is altered during both wild-type and persistent DENV infection. On a protein level, it has been shown that wild-type DENV infection increases activity of HMGCR through its dephosphorylation (Soto-Acosta *et al.,* 2013, 2017), thus it would be interesting to assess and compare the phosphorylation levels of HMGCR during persistent infection with v601-4B$_{T66A}$ also. Similar experiments comparing the activity of the other proteins identified through our analyses, HMGCS1, IDI1, INSIG1, MSMO1 and SQLE, during infection would also be of interest. In addition, utilizing a method of quantifying intracellular cholesterol levels to compare these between types of infection would be beneficial for this work; while staining with filipin III enables co-localisation studies between cholesterol and viral replication sites, the rapid photobleaching property of this molecule renders the images inadequate for immunofluorescence-based quantification. It has been shown using a colourimetric assay that total intracellular cholesterol levels increased by 15% and 20% at 1 and 6 hpi, respectively, during DENV infection (Soto-Acosta *et al.,* 2013), thus, it would be interesting to determine whether total intracellular cholesterol levels change during persistent infection.

Taken together, the results suggest that virus-induced modifications to intracellular cholesterol levels, localisation and gene expression differ between infection with wild-type DENV-2 and v601-4B$_{T66A}$. This suggests that the NS4B$_{T66A}$ mutation may have an effect on the ability of DENV to modify these aspects of cellular lipid metabolism to promote viral replication. Alternatively, defects in the host cholesterol biosynthesis pathways of the small population of cells that survived upon initial infection with v601-4B$_{T66A}$ may be a factor that facilitated establishment of persistent infection.

3.6.4. The effect of persistent infection on the host innate immune response.

Using bioinformatics analysis, 32 genes involved in the innate immune response were identified to be upregulated in persistently-infected cells compared to mock and DENV-2-infected cells. DENV is known to evade the host type I IFN response by inhibiting and degrading components of the type I IFN pathway such as STAT1, STAT2 and STING (Aguirre *et al.,* 2012; Ashour *et al.,* 2009; Muñoz-Jordan *et al.,* 2003, 2005), which ultimately prevents the expression of ISGs that possess antiviral functions. All of the 32 genes identified in the bioinformatics analysis are ISGs and play a role in eliminating viral infections, as such, it makes sense that their expression was not induced by wild-type infection due to the IFN-antagonistic functions of DENV; however, it is interesting that their expression was upregulated during persistent infection with v601-4B$_{T66A}$. Previously, qPCR analysis revealed that ISGs such as *ISG15* and *OASL* were significantly activated in H-v601-Per1, H-v601-Per2 and H-Rep-4B$_{T66A}$ cells compared to control HEK293T and H-Rep cells (Ismail, 2015). The author concluded that the NS4B$_{T66A}$ mutation may influence production of chemokines which may control viral replication and regulate the maintenance of persistent infection (Ismail, 2015). It is also possible that the NS4B$_{T66A}$ mutation does not fully abrogate DENV-mediated inhibition of the IFN response, but weakens it, thus allowing ISGs to be expressed and perhaps the subset of ISGs that are activated are insufficient for full clearance of the virus.

Immunofluorescence staining of STAT1 in all different cell lines showed that STAT1 became more localised to the nucleus in HEK293T, wild-type DENV-2-infected, H-v601-Per2 and H-Rep-4B$_{T66A}$ cells upon IFNα treatment compared to equivalent cells that remained untreated. This result was expected because addition of IFNα activates the type I IFN response pathway which induces translocation of the ISGF3 heterotrimer containing STAT1, STAT2 and IRF9 to the nucleus (Ivashkiv and Donlin, 2015). However, there was no significant difference in nuclear localisation of STAT1 in H-v601-Per1 or H-Rep cells upon IFNα treatment. In the H-Rep cells, blocking of nuclear translocation may be a result of the expression of a wild-type NS4B protein; NS4B is known to interfere with the type I IFN pathway (Muñoz-Jordan *et al.,* 2003, 2005), and thus this result may have been observed because of this function of the NS4B protein. However, that does not explain why nuclear translocation of STAT1 was observed in the wild-type DENV-2-infected cells which also express wild-type NS4B protein. Additionally, the pattern of STAT1 distribution observed in uninfected HEK293T cells was unexpected as STAT1 should typically only be localised to the cytoplasm in the absence of exogenous IFNα because the type I IFN pathway should be inactive. An expected result would be more similar to the pattern of STAT2 distribution in uninfected HEK293T cells observed in Figure 3.19, yet there was signal corresponding to STAT1 present in the nucleus of uninfected

HEK293T cells (Figure 3.17). This may be a result of non-specific binding by the STAT1 antibody. Ideally, an antibody that specifically detects phosphorylated-STAT1 (pSTAT1) should have been used for this experiment, such that STAT1 would only be detectable when the type I IFN pathway is active and STAT1 becomes phosphorylated. However, several attempts to perform this experiment using an anti-pSTAT1 antibody proved inconclusive due to very high background signal and likely non-specific binding detected on each attempt. Nevertheless, the anti-STAT1 antibody was still able to detect an accumulation of STAT1 upon exogenous IFNα treatment as anticipated.

Without the addition of exogenous IFNα, compared to uninfected cells, STAT1 was localised to the nucleus in H-v601-Per1, H-v601-Per2, H-Rep and H-Rep-4B$_{T66A}$ cells, but more localised to the cytoplasm in wild-type DENV-2-infected cells (Figure 3.17). Increased nuclear localisation of STAT1 in both persistently-infected cell lines and replicon-containing cells without IFNα treatment could suggest that persistent infection with v601-4B$_{T66A}$ virus and presence of replicons elicits an immune response to some degree, even without the presence of exogenous IFNα to activate the type I IFN signaling pathway. On the other hand, DENV-2 virus, though it should also have been detected by the host immune response in these cells in the absence of exogenous IFNα, may be capable of suppressing this response, thus preventing type I IFN pathway activation and inhibiting STAT1 nuclear localisation.

Following the addition of exogenous IFNα, STAT1 was more localised to the cytoplasm in wild-type DENV-2-infected and H-v601-Per1 cells, and more localised to the nucleus in H-v601-Per2 and H-Rep-4B$_{T66A}$ compared to mock uninfected cells. The results showing that wild-type DENV infection inhibited STAT1 activation and translocation to the nucleus (Figure 3.17) are consistent with a previous study which showed that phosphorylated STAT1 was undetectable in 77% of NS4B-expressing cells treated with IFNβ (Muñoz-Jordan *et al.,* 2003). Additionally, while there was no difference in localisation between uninfected and H-Rep cells, STAT1 in H-Rep-4B$_{T66A}$ cells was more localised to the nucleus than in H-Rep cells. This was also observed in H-v601-Per2 than in wild-type DENV-2-infected cells. Overall, these results suggest that presence of the NS4B$_{T66A}$ mutation may attenuate the ability of the mutated NS4B protein in either the v601-4B$_{T66A}$ virus or RepDV-GP2A-NS4B$_{T66A}$ replicon to inhibit the translocation of STAT1 proteins to the nucleus of H-v601-Per2 and H-Rep-4B$_{T66A}$ cells. However, this effect was not evident in the H-v601-Per1 cells, which suggests that this potential effect of the NS4B$_{T66A}$ mutation in the persistently-infecting virus may be relatively mild compared to that observed in the replicon-containing cells. Additionally, the Thr → Ala mutation is located at position 66 in the NS4B protein; it been shown that residues at the N-terminus are important for IFN signalling inhibition by blocking ISRE promoter activation but

residues 77 to 125 were critical (Muñoz-Jordan *et al.,* 2005), therefore perhaps T66 does not play a critical function in blocking IFN signalling and the $NS4B_{T66A}$ mutation may not fully abrogate this function of the NS4B protein.

STAT2 clearly translocated from the cytoplasm of untreated HEK293T cells to the nucleus with IFNα treatment, which was as expected following activation of the type I IFN pathway (Ivashkiv and Donlin, 2015). However, the level of STAT2 signal remained lower in the replicon-expressing cells H-Rep and H-Rep-$4B_{T66A}$ than that observed in uninfected HEK293T cells both with and without IFNα treatment. This result was not wholly unexpected because STAT2 is known to be targeted for proteasomal degradation and its phosphorylation inhibited by the DENV NS5 protein (Ashour *et al.,* 2009; Mazzon *et al.,* 2009), and a fully functional, wild-type NS5 protein is encoded by both replicon constructs. Thus, there was no observable difference in the effect on STAT2 distribution between H-Rep and H-Rep-$4B_{T66A}$ Figure 3.17.

Using the results from immunofluorescence experiments on STAT1, we hypothesised that this $NS4B_{T66A}$ mutation may attenuate the ability of the DENV NS4B protein to inhibit components of the type I IFN pathway, thus allowing antiviral ISGs to be expressed as shown by our transcriptomics data. Interestingly, ISGs can still be expressed despite the observable reduction in STAT2 during infection compared to uninfected cells, with or without the $NS4B_{T66A}$ mutation (Figure 3.19). This suggests a STAT2-independent mechanism is potentially responsible for activating the expression of ISGs in the persistently-infected cells; this could be STAT1-dependent as the $NS4B_{T66A}$ mutation potentially prevents full inhibition of STAT1 function, or possibly dependent on alternative pathways such as the type II IFN pathway which becomes activated in response to IFNγ production and, unlike IFNα, is not thought to be antagonised by DENV-2 infection (Ho *et al.,* 2005). However, while STAT1-independent mechanisms of IFN signalling activation have been described (Blaszczyk *et al.,* 2015), evidence of STAT2-independent mechanisms are relatively limited. Consequently, since STAT2 is known to be highly important for production of IFNα/β (Blaszczyk *et al.,* 2016), further experiments using distinct techniques to IFA should also be performed to determine whether STAT2 is completely lost within the cells, or whether, despite being expressed at much lower levels than in uninfected cells, it is still present at sufficient levels to activate ISG expression.

Taken together, these results raise the question of how persistent infection is maintained despite the expression of ISGs with antiviral activity. Upregulation of ISGs in H-v601-Per1 and H-v601-Per2 cells but not wild-type-infected cells suggests an enhancement of the antiviral IFN response to DENV infection during persistent infection compared to wild-type, which could represent a potential mechanism by which persistent infection is maintained. Type I IFNs have

pleiotropic effects during viral infections and the signalling pathways been shown to paradoxically regulate the antiviral response, particularly during chronic viral infections; on one hand, the antiviral functions of the type I IFN response are extensive and well-characterised, but on the other hand, IFNα/β also has regulatory functions that suppress the immune response and can promote viral persistence (Odorizzi and Wherry, 2013; Teijaro, 2016). Recently, a direct causal link was found between type I IFN signalling and activated expression of ISGs and persistence of lymphocytic choriomeningitis virus (LCMV) infections (Teijaro *et al.,* 2013), while in HCV patients an elevated IFN signature can be observed despite chronic presence of viral infection (Wieland *et al.,* 2014). It has been suggested that immunoregulatory functions of IFNα/β could have evolved during persistent infections to limit damaging immunopathology that could result from prolonged IFN pathway activation (Odorizzi and Wherry, 2013), such as cytokine storms which are known to play a role in dengue pathogenesis. It may be possible that the IFN response is altered between wild-type DENV-2 and persistent v601-4B$_{T66A}$ infection such that the immunosuppressive function is favoured during the latter, potentially to limit immunopathology which could also explain the lack of CPE observed in H-v601-Per1 and H-v601-Per2 cell culture.

Chapter 4. Anti-DENV drug treatment

The overall aim of this section of the project was to cure the persistently-infected cells of v601-4B$_{T66A}$ virus to subsequently examine host cells and any potential defects in specific pathways that may have enabled the establishment of a persistent infection.

4.1. Introduction to anti-DENV drug treatment.

When Dr. Andrew Davidson and Dr. Rosmani Ismail generated the H-v601-Per1 and H-v601-Per2 cell lines, infection of naïve cells with the reverse-engineered v601-4B$_{T66A}$ virus caused a large percentage of the cell population to display CPE and die. A small percentage of the population, however, survived and expanded to confluency but were found to be persistently-infected. By comparison, infection of the cells with the wild-type virus resulted in 100% cell death. It was hypothesised that the cells that became persistently-infected may have possessed a cellular defect that, in conjunction with the NS4B$_{T66A}$ viral mutation, enabled the establishment of a persistent infection with this strain of DENV in cell culture. As the bioinformatic analysis and qPCR validation in Section 3.4. showed, it may be plausible that defects in cholesterol biosynthesis pathways could exist which may allow persistent infection to occur.

Drugs that have previously been shown to possess anti-DENV activity were selected to attempt to clear v601-4B$_{T66A}$ from the persistently-infected cell lines to ultimately allow the study of possible existing cellular defects. 4-hydroxyphenyl retinamide (4-HPR) is a synthetic retinoid compound which inhibits steady-state accumulation of DENV genomic RNA, reduces infectious virus titre by >100-fold and reduces intracellular viral RNA by 1000-fold *in vitro* compared to untreated, DENV-infected controls (Carocci *et al.,* 2015; Fraser *et al.,* 2014). Mycophenolic acid (MPA) is a non-nucleoside inhibitor of inosine monophosphate that depletes intracellular guanosine pools by blocking the synthesis of xanthosine monophosphate. MPA is used clinically as an immunosuppressant and was found to potently inhibit replication of both positive- and negative-strand DENV RNA by between 10- to 1000-fold with an IC$_{50}$ of 0.1 μg/ml (Diamond *et al.,* 2002). Ribavirin (RBV) is a guanosine analogue that at a concentration of ≥ 200 μM reduced virus titre by nearly 1000-fold. Inhibition of viral RNA synthesis by treatment with both MPA and RBV is reversed by addition of exogenous guanosine to restore intracellular guanosine pools which suggests that nucleotide depletion is likely to be the mechanism of action for inhibition of DENV infection (Diamond *et al.,* 2002; Takhampunya *et al.,* 2006). 2'C-methylcytidine (2CMC) is another nucleoside analogue that inhibits DENV NS5 polymerase activity, and reduces viral RNA replication (Lee *et al.,* 2015).

4.2. Cell viability assays.

Using existing literature, dosages of each drug that are commonly used *in vitro* were selected and each compound was tested at a wide range of concentrations around this dose for their cellular effects using a cell viability assay. This process served to identify maximum concentration of each drug that could be used for potentially long-term treatment of the cell lines in a subsequent experiment to attempt to clear the persistent infection without causing significant CPE. 4-HPR has previously been used at concentrations between 5 and 7.5 μM, and does not affect cell viability at up to 10 μM (Carocci *et al.,* 2015; Fraser *et al.,* 2014). *In vitro* treatment with 10 μg/ml MPA reduced virus production by > 6 log, while 25 μg/ml RBV reduced virus production by 3 log, however cytostatic effects were observed under treatment with ≥10 μg/ml MPA and ≥50 μg/ml RBV which inhibited cell growth by 50% (Diamond *et al.,* 2002). Treatment of BHK-21 cells expressing a DENV replicon with RBV gave a half maximal effective concentration (EC_{50}) of 6.77 ± 1.33 μM and a cytotoxic concentration causing death in 50% of viable cells (CC_{50}) value of 75 μM (Hsu *et al.,* 2012; Ng *et al.,* 2007). 2CMC treatment at concentrations of 12.5, 25 and 50 μM reduced DENV RNA replication by 20%, 40% and 80%, respectively and had an IC_{50} value between 11 and 20 μM and did not affect cell viability at concentrations ≤ 50 μM (Lee *et al.,* 2015).

The MTT (3-(4,5-dimethylthiazolyl-2)-2,5-diphenyltetrazoliumbromide) assay is a commonly-used quantitative cell viability assay that indicates cellular metabolic activity. When added to metabolically-active cells, MTT is reduced by mitochondrial dehydrogenases to produce purple formazan crystals; this colourimetric change is measured spectrophotometrically at 570 nm (van Meerloo and Cloos, 2011).

HEK293T, H-v601-Per1 and H-v601-Per2 cells were seeded into 96 well plates and treated with a range of drug doses per row for each drug, in duplicate. After 2 and 4 days, the MTT assay was performed and cell viability was measured to determine the concentration of drugs that should be used in long-term treatment of all cell types. The % cell viability was calculated using the OD values of each cell type at each drug concentration, relative to the OD value obtained from HEK293T cells that remained untreated which for the purposes of analysis were defined as 100% viable.

Across all experiments, the viability of H-v601-Per1 cells was significantly lower than the % viability of HEK293T cells when analysed after 2 days, ranging from 38.5-45.6% viability relative to HEK293T cells, even when left untreated (p = <0.0001). However, the reduction in untreated H-v601-Per1 cell viability compared to HEK293T cells was not as great when analysed after 4 days (20-23%). This potentially suggests that it takes longer for this cell line

to start propagating following seeding into a new cell culture dish compared to the other cell lines, particularly when compared to the uninfected, untreated HEK293T cells which were used as a reference for calculating % cell viability. Alternatively, there may be greater cytotoxic effects in the cells that were analysed after 2 days of drug treatment, following which they were able to recover slightly by the 4-day timepoint. As it was planned to treat the cells with drugs for a longer time period, the 4-day timepoint was considered more representative of the intended long-term treatment of the cells in subsequent experiments, therefore the results from the 4-day experiments were used to determine which concentrations of drugs were selected for subsequent experiments.

4-HPR treatment at the lowest concentration of 0.75 μM reduced cell viability of H-v601-Per1 and H-v601-Per2 by 17-24% after 2 days and 8-15% after 4 days, relative to the viability of each cell line when left untreated. Subsequent increases in 4-HPR concentration from 0.75 μM up to 5 μM only reduced viability by 0.4-4.4% after 4 days in the H-v601-Per1 and H-v601-Per2 cells (Figure 4.1). Thus, 4-HPR was selected for use at concentrations of 5, 2.5 and 1.25 μM for long-term treatment of persistently-infected cells.

MPA treatment at the lowest concentration tested of 0.75 μg/ml reduced the viability of HEK293T, H-v601-Per1 and H-v601-Per2 by 52.7%, 20% and 41%, respectively, after 2 days, and after 4 days by 40%, 47.1% and 24.7%, respectively, compared to the same cell lines that were left untreated at each time-point. However, subsequent increases in concentration of MPA from 0.75 μg/ml up to 20 μg/ml after 4 days only further reduced the % cell viability of all cell lines by between 2.3-11.9% (Figure 4.1). The concentrations at which % cell viability was greatest after 4 days ranged between 2.5-10 μg/ml, so to avoid potentially using a concentration of MPA that was too cytostatic to cells over longer periods of time, doses of 5, 2.5 and 1.25 μg/ml were selected for subsequent experiments.

With RBV treatment, there was a large difference in % cell viability between cells analysed after 2 and 4 days. After 4 days of treatment the largest drop in cell viability compared to untreated cells was in the H-v601-Per1 cell line at the lowest RBV concentration of 12.5 μM which fell by 22.3% from 79.2% to 56.9%, and then decreased more gradually with increasing concentrations of drug down to 33.9% at 300 μM. In the HEK293T cells there was a large reduction in % cell viability from 86% at 100 μM to 62.4% at 200 μM (Figure 4.1), therefore in subsequent experiments RBV was used at 50 and 100 μM to avoid high cytotoxicity over longer periods of time.

Treatment with 2CMC also showed a large difference in overall cell viability between the two time-points. After 4 days of treatment, the viability of HEK293T and H-v601-Per1 cells remained relatively constant at increasing concentrations of 2CMC; HEK293T cells were 81.7% and 87% viable, and H-v601-Per1 cells were 68.9% and 74.3% viable at concentrations of 1.25 and 50 μM, respectively. H-v601-Per2 cells were 83.3% and 89.5% viable at 1.25 and 25 μM, respectively, but the % cell viability decreased further with 50 μM treatment to 65.3%. Therefore, concentrations of 25 and 50 μM 2CMC were selected for subsequent experiments.

4.3. Long-term treatment with 4-HPR and MPA.

HEK293T, H-v601-Per1 and H-v601-Per2 cells were seeded into T25 culture flasks, incubated overnight, and treated with 4-HPR (5, 2.5, 1.25 μM) and MPA (5, 2.5, 1.25 μg/ml) the following day. Over the course of the experiment, cells were passaged when they reached ~80% confluency which varied in frequency between the treatments and cell lines. Additionally, media was changed once a week and the drugs were replenished if the cells were not passaged within that time to ensure that the drugs in the media remained active.

Cells treated with 5 μM 4-HPR or 5 μg/ml MPA showed very strong CPE following addition of drugs and were cytostatic, thus these cell lines were terminated after 7 days of drug treatment. 2.5 and 1.25 μg/ml MPA-treated H-v601-Per1 and H-v601-Per2 cells also showed CPE and were mostly cytostatic after 8 days of drug treatment. To determine if the virus was cleared by the drug treatment, 21 days post-drug addition, supernatant samples were taken and analysed for the presence of viral RNA. Within this time, MPA-treated cells were cytostatic and thus were not passaged, however HPR-treated cells were passaged once during this time. Only the cells treated with the higher concentration of 4-HPR and both concentrations of MPA were analysed to determine whether there had been any loss of virus. All drug-treated H-v601-Per1 and H-v601-Per2 samples still had viral RNA present in the supernatant samples as determined by non-quantitative RT-PCR (Figure 4.2A). After this analysis, MPA-treated cells were terminated because of the unsuccessful clearance of virus and strong CPE observed which meant the cells were completely cytostatic. After 40 days of continued drug treatment which included 5 passages of each cell line at both concentrations of 4-HPR, intracellular RNA was extracted from untreated and 4-HPR-treated cells, and v601-4B$_{T66A}$ RNA was present in all H-v601-Per1 and H-v601-Per2 cells (Figure 4.2B). Thus, it was concluded that the doses of 4-HPR and MPA used, in combination with cell cytotoxicity effects were insufficient to clear the v601-4B$_{T66A}$ virus, and the same experiment was attempted with RBV and 2CMC.

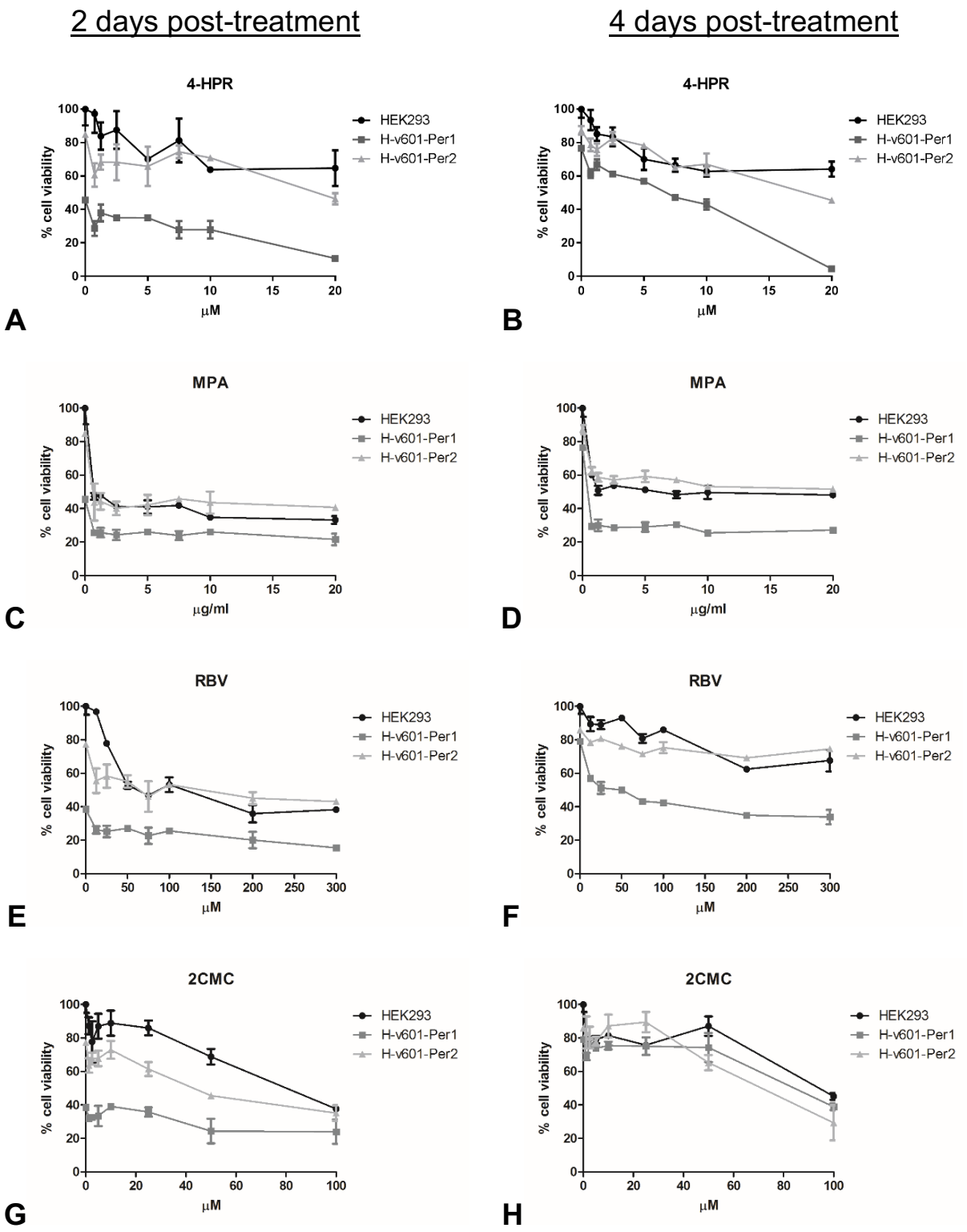

Figure 4.1: Cell viability of HEK293T, H-v601-Per1 and H-v601-Per2 cells when treated with 4-HPR, MPA, RBV and 2CMC drugs. HEK293T, H-v601-Per1 and H-v601-Per2 cells were seeded into 96 well plates at 3 x 10^4 cells per well and incubated for 16 h before appropriate concentrations of drugs were added to wells in duplicate. 2 and 4 days post-treatment, the Vybrant® MTT Cell Proliferation Assay Kit was used according to manufacturer's instructions and colourimetric change was measured with a SpectraMax 190 Microplate Reader at 570 nm. Mean % cell viability of each sample was calculated as a percentage of the OD reading from untreated HEK293T cells which was defined as 100% viable for analysis purposes.

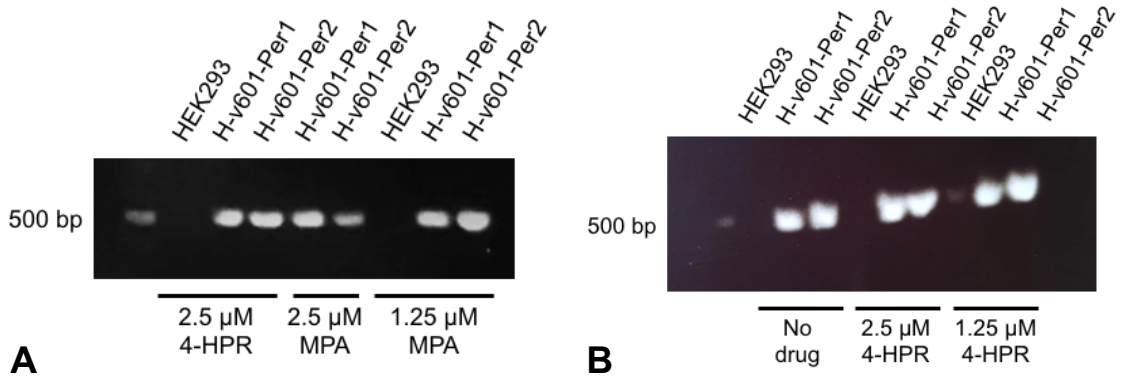

Figure 4.2: Presence of v601-NS4B$_{T66A}$ in 4-HPR- and MPA-treated cell lines after 21 and 40 days. 3 x 10^5 HEK293T, H-v601-Per1 and H-v601-Per2 cells were seeded into T25 flasks for 1 day, then 4-HPR and MPA drugs were added to the cell culture medium the following day. (A) 21 days post-drug inoculation, extracellular RNA was extracted from the supernatant of cells treated with 2.5 μM 4-HPR and 2.5 and 1.25 μg/ml MPA. (B) 40 days post-drug inoculation, intracellular RNA was extracted from the supernatant of untreated cells and cells treated with 2.5 and 1.25 4-HPR. RT-PCR was performed on RNA samples to detect presence of the v601-4B$_{T66A}$ virus using DENV NS4B gene-specific primers, DV2_6823 and DV2_7295r. Agarose gel electrophoresis was performed to detect the RT-PCR product (~500 bp) in each sample; product size was estimated using a GeneRuler 1 kb Plus DNA ladder.

4.4. Long-term treatment with RBV and 2CMC.

HEK293T, H-v601-Per1, H-v601-Per2, H-Rep and H-Rep-4B$_{T66A}$ cells were seeded into cell culture flasks, and the following day RBV (100, 50 μM) and 2CMC (50, 25 μM) were added to the medium. H-Rep and H-Rep-4B$_{T66A}$ cells were included to determine whether replicon constructs could be cleared from the cells as well as the v601-4B$_{T66A}$ virus. Cells were passaged when they reached ~80% confluency, and media changed once a week if the cells were not passaged in that time. H-Rep and H-Rep-4B$_{T66A}$ cells were also treated in separate flasks with puromycin added during each passage to select for cells that were still expressing the replicon genomes; this allowed us to investigate whether any reduction in replicon RNA detection was due to possible attrition over time or as a result of drug treatment.

The cells did not immediately show CPE, but after 3 weeks of drug treatment which included 1 round of passaging and an additional change of media to introduce fresh drugs, the cells treated with 50 μM of 2CMC were cytostatic and were terminated. Samples treated with 100 μM RBV grew as well as those treated with 50 μM, so samples treated with the higher concentration of RBV were analysed for subsequent experiments. RNA was analysed from supernatant and intracellular RNA samples at various time points over a 3-month period of ongoing drug-treatment which included a total of 14 rounds of passaging for each cell line.

After 3 months, intracellular RNA was extracted and analysed by qPCR using primers specific for the 3'UTR of the viral genome. In the H-v601-Per1 and H-v601-Per2 cell lines, neither of the drug treatments cleared the virus and viral RNA was detected in all samples. For analysis purposes, the amount of viral RNA detected in the H-Rep samples was used as a calibrator against which the other samples were compared to calculate their relative expression fold change. The relative fold change of DENV 3'UTR amounts in uninfected HEK293T cells ranged from 9.1 x 10^{-5} to 0.0025 (Figure 4.3). The H-Rep-4B$_{T66A}$ cells treated with 100 μM RBV were potentially free of the replicon RNA with a relative fold change of 0.0019, while 2CMC treatment also reduced the levels of replicon RNA in H-Rep-4B$_{T66A}$ cells to 0.38. However, in the H-Rep-4B$_{T66A}$ cells, replicon RNA was also significantly decreased in the untreated cell lines with a relative fold change of 0.049, but was still detectable in puromycin-treated cell lines with a relative fold change of 1.60. Therefore, it was difficult to determine whether the loss of replicon RNA observed in RBV- or 2CMC-treated H-Rep-4B$_{T66A}$ cells was due to the effects of the drugs or to natural attrition of the replicon RNA. The level of replicon RNA was reduced in RBV-treated H-Rep cells with a relative fold change of 0.23, yet still present in both untreated and puromycin-treated H-Rep cells, which suggests that the reduction in replicon RNA expression in these cells was possibly due to the effects of RBV.

While the replicon RNA was cleared from H-Rep and H-Rep-4B$_{T66A}$ cells treated with RBV, the primary aim of the experiment, to clear the persistently-infecting virus, was unsuccessful as the v601-4B$_{T66A}$ virus was still present in both cell lines despite the constant presence of either RBV or 2CMC. Therefore, the long-term drug treatment experiment was terminated and the viral and replicon RNA sequences determined to identify any mutations that have arisen as a result of the selection pressure conferred by the presence of antiviral drugs.

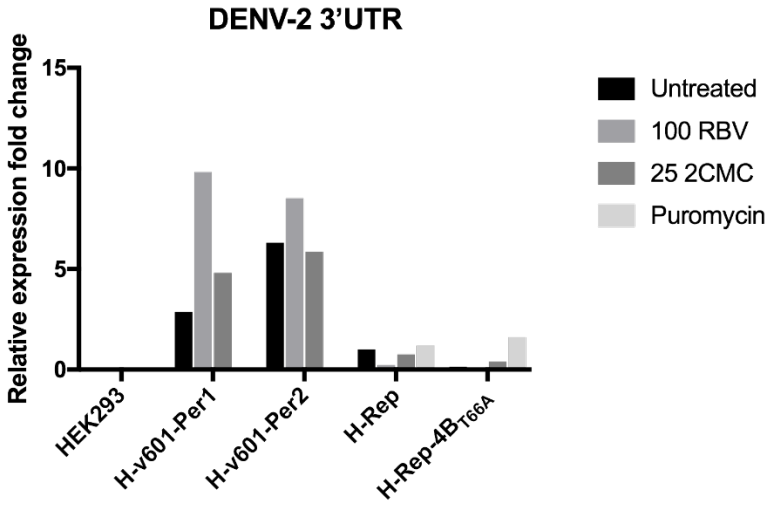

Figure 4.3: Presence of v601-NS4B$_{T66A}$, RepDV-GP2A, or RepDV-GP2A-NS4B$_{T66A}$ RNA after 3 months of treatment with RBV and 2CMC drugs. HEK293T, H-v601-Per1, H-v601-Per2, H-Rep and H-Rep-4B$_{T66A}$ cells were cultured in T25 flasks for a total period of 3 months, either remaining untreated, or in the constant presence of 100 μM RBV, 25 μM 2CMC, or 3.5 μg/ml puromycin in the culture medium. Intracellular RNA was extracted from each sample, 200 ng was converted to cDNA using random hexamer primers, and qPCR was performed using 3'UTR-specific primers, DV_3'UTR_f and DV_3'UTR_r. Samples were analysed in triplicate on each plate. GAPDH was used as a reference gene for all reactions. Relative gene expression was calculated using the ΔΔCt method using Ct values from untreated H-Rep cells as a calibrator.

4.5. Sequencing for resistance mutations in drug-treated samples.

Previous experiments were unsuccessful in clearing v601-4B$_{T66A}$ virus from H-v601-Per1 or H-v601-Per2 cell lines using RBV or 2CMC treatments over a 3-month period. Based on these results, samples were selected for viral genome sequencing that still clearly had virus or replicon RNA present at the end of the 3-month period to identify any resistance mutations: H-v601-Per1 and H-v601-Per2 untreated, treated with 100 μM RBV or 25 μM 2CMC, and H-Rep and H-Rep-4B$_{T66A}$ treated with 3.5 μg/ml puromycin or 25 μM 2CMC. Total intracellular RNA was extracted from each sample and RT-PCR performed to generate cDNA products corresponding to 6 fragments of the v601-4B$_{T66A}$ genome, or 4 fragments of the replicon RNA construct. The fragments were sequenced using 3-4 primers per fragment. An overview of the workflow for sequencing the whole viral genome is shown in Figure 4.4.

79 mutations that potentially arose as a result of drug selection pressure are shown in Table 4.1. Many of the mutations that were present in the drug-treated samples were also present in the untreated samples, indicating that these particular mutations are did not arise as a result of the selection pressure conferred by constant presence of the drug; 10 mutations that were unique to drug-treated samples are highlighted with asterisks in Table 4.1.

Interestingly, in the virus persistently-infecting the H-v601-Per1 cells that either remained untreated or were treated with 100 μM RBV, the NS4B$_{T66A}$ mutation was lost, while the v601-4B$_{T66A}$ virus treated with 25 μM in the H-v601-Per1 cells retained this mutation. However, in the H-v601-Per2 cells both of the A → G nucleotide mutations at positions 7020 (Leu → Leu) and 7021 (Thr → Ala) were still present following all treatment conditions.

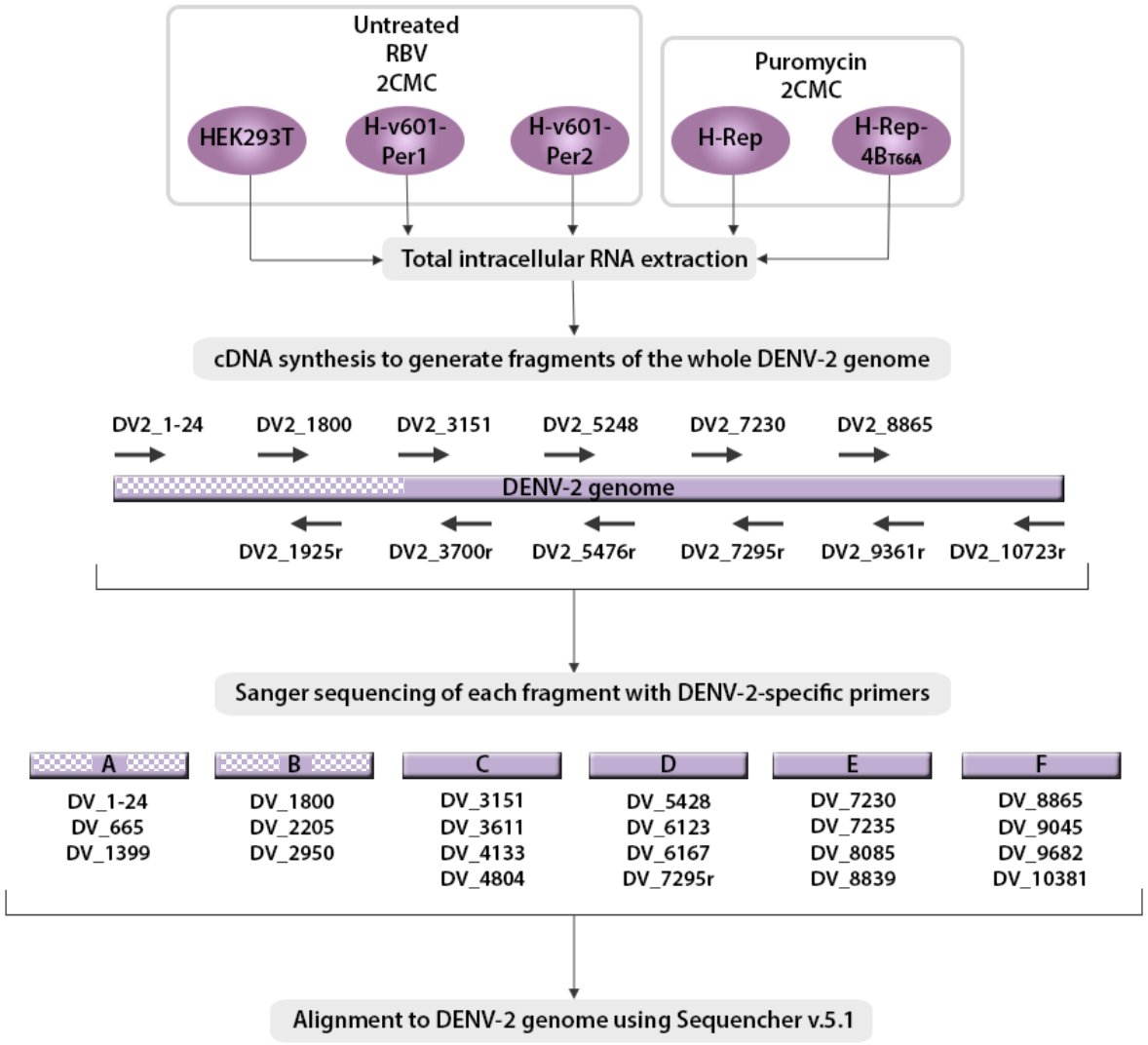

Figure 4.4: Overview of workflow for sequencing the whole viral genome of drug-treated samples. HEK293T, H-v601-Per1 and H-v601-Per2 cells were treated with 100 μM or 25 μM 2CMC, and H-Rep and H-Rep-4B$_{T66A}$ cells were treated with 25 μM 2CMC, or remained untreated, for 3 months. Total intracellular RNA was extracted from cells and cDNA was synthesised by RT-PCR using DENV-2-specific primers to generate 6 fragments of the DENV-2 genome. cDNA of replicon RNA was synthesised to generate only fragments C onwards as the eGFP-PAC fusion protein-encoding sequence that replaced the structural genes could not be sequenced. Each of the fragments was sent for Sanger sequencing at the BGI with 3-4 DENV-2-specific primers. Sequence alignment to the DENV-2 New Guinea C wild-type sequence (NCBI gene accession number: AF038403.1) was performed using Sequencher v.5.1.

Table 4.1: Mutations identified in the DENV-2 genome of all drug-treated samples. H-v601-Per1, H-v601-Per2, H-Rep and H-Rep-4B$_{T66A}$ cells were cultured for 3 months in the constant presence of either RBV or 2CMC anti-viral drugs. Intracellular RNA was extracted, and cDNA synthesis performed using DENV-2-specific primers to generate 6 fragments that were sequenced using 3-4 DENV-2-specific primers (Figure 4.4) by Sanger sequencing at Eurofins genomics. Sequence analysis was performed using Sequencher v.5.1. Sequences were compared to the DENV-2 New Guinea C wild-type sequence (NCBI gene accession number: AF038403.1).

Cell line	Drug treatment	Nucleotide position on DENV-2 genome	Nucleotide change from DENV-2 genome	Amino acid change from DENV-2 genome	Gene	Amino acid position within gene
H-v601-Per1	Untreated	168	TC**G** → TC**A/G**	Ser	C	24
		418	**C**TG → **A/C**TG	Leu → Met	C	108
		483	AG**T** → AG**A/T**	Ser → Arg	prM	15
		485	A**G**A → A**T/G**A	Arg → Ile	prM	16
		1779	GG**A** → GG**G/A**	Gly	E	281
		3964	**A**AC → **C**AC	Asn → His	NS2A	163
		6437	G**C**A → G**T**A	Ala → Val	NS4A	21
		6443	G**A**C → G**G**C	Asp → Gly	NS4A	23
		6556	**C**TG → **A/C**TG	Leu → Met	NS4A	61
		6629	A**T**G → A**C**G	Met → Thr	NS4A	85
		6730	**C**TT → **T**TT	Leu → Phe	NS4A	119
		6818	A**C**C → A**T**C	Thr → Ile	NS4A	148
		7020	CT**A** → CT**G**	Leu	NS4B	65
		7096	**G**TT → **T/G**TT	Val → Phe	NS4B	91
H-v601-Per1	100 μM RBV	168	TC**G** → TC**A/G**	Ser	C	24
		1779	GG**A** → GG**G/A**	Gly	E	281
		3964	**A**AC → **C/A**AC	Asn →His	NS2A	163
		6437	G**C**A → G**T**A	Ala → Val	NS4A	21
		6556	**C**TG → **A/C**TG	Leu → Met	NS4A	61
		6629	A**T**G → A**C**G	Met → Thr	NS4A	85

		7020	CT**A** → CT**G**	Leu	NS4B	65
		7096	**G**TT → **T**TT	Val → Phe	NS4B	91
		9846*	GC**C** → GC**T/C**	Ala	NS5	759
H-v601-Per1	25 μM 2CMC	982*	**T**CA → **G**CA	Ser → Ala	E	16
		2312*	A**T**A → A**C**A	Ile → Thr	E	459
		6437	G**C**A → G**T**A	Ala → Val	NS4A	21
		6629	A**T**G → A**C/T**G	Met → Thr	NS4A	85
		6818	A**C**C → A**T**C	Thr → Ile	NS4A	148
		7020	CT**A** → CT**G**	Leu	NS4B	65
		7021	**A**CA → **G/A**CA	Thr → Ala	NS4B	66
		7510*	**T**AC → **C**AC	Tyr → His	NS4B	229
		7562*	A**C**G → A**T**G	Thr → Met	NS4B	246
		9898*	**A**AT → **G**AT	Asn → Asp	NS5	777
H-v601-Per2	Untreated	112	**A**AA → **T/A**AA	Lys → Stop	C	6
		982	**T**CA → **G/T**CA	Ser → Ala	E	16
		5198	G**T**C → G**C/T**C	Val → Ala	NS3	226
		6437	G**C**A → G**T**A	Ala → Val	NS4A	21
		6818	A**C**C → A**T**C	Thr → Ile	NS4A	148
		6915	AT**A** → AT**G**	Ile → Met	NS4B	30
		7020	CT**A** → CT**G**	Leu	NS4B	65
		7021	**A**CA → **G**CA	Thr → Ala	NS4B	66
		7403	G**C**G → G**T/C**G	Ala → Val	NS4B	193
H-v601-Per2	100 μM RBV	894*	GC**C** → GC**T/C**	Ala	M	61
		6915	AT**A** → AT**G**	Ile → Met	NS4B	30
		7020	CT**A** → CT**G**	Leu	NS4B	65

H-v601-Per2	25 μM 2CMC	4238*	G**G**G → G**C/G**G	Gly → Ala	NS2B	36
		6437	G**C**A → G**T/C**A	Ala → Val	NS4A	21
		6818	A**C**C → A**T/C**C	Thr → Ile	NS4A	148
		7020	CT**A** → CT**G**	Leu	NS4B	65
		7021	**A**CA → **G/A**CA	Thr → Ala	NS4B	66
H-Rep	3.5 μg/ml puromycin	3665	A**C**T → A**T**T	Thr → Ile	NS2A	63
		4254	TG**C** → TG**T**	Cys	NS2B	41
		4258	**G**TG → **A**TG	Val → Met	NS2B	43
		5254	**C**CA → **T**CA	Pro → Ser	NS3	245
		6639	AT**A** → AT**G**	Ile → Met	NS4A	88
		7556	A**C**C → A**T**C	Thr → Ile	NS4B	244
		8631	GT**T** → GT**C**	Val	NS5	354
H-Rep	25 μM 2CMC	4258	**G**TG → **A**TG	Val → Met	NS2B	43
		6639	AT**A** → AT**G/A**	Ile → Met	NS4A	88
		7096	**G**TT → **T/G**TT	Val → Phe	NS4B	91
		7556	A**C**C → A**T**C	Thr → Ile	NS4B	244
H-Rep-4B$_{T66A}$	3.5 μg/ml puromycin	3791	A**C**C → A**T/C**C	Thr → Ile	NS2A	105
		4300	**G**CC → **A/G**CC	Ala → Thr	NS2B	57
		4397	G**A**A → G**C/A**A	Glu → Ala	NS2B	89
		6733	**A**TT → **G/A**TT	Ile → Val	NS4A	120
		7020	CT**A** → CT**G**	Leu	NS4B	65
		7021	**A**CA → **G**CA	Thr → Ala	NS4B	66
		7178	T**A**T → T**G/A**T	Tyr → Cys	NS4B	118
		7556	A**C**C → A**T/C**C	Thr → Ile	NS4B	244
		10121	AT**T** → AT**C/T**	Ile → Thr	NS5	851

		6733	**A**TT → **G**TT	Ile → Val	NS4A	120
		7020	CT**A** → CT**G**	Leu	NS4B	65
		7021	**A**CA → **G**CA	Thr → Ala	NS4B	66
		7178	T**A**T → T**G**T	Tyr → Cys	NS4B	118
		9893*	G**C**G → G**T**G	Ala → Val	NS5	775

4.6. Discussion of drug-treatment.

The aim of this chapter was to cure persistently-infected cells of the v601-4B$_{T66A}$ virus using drugs previously shown to have anti-DENV properties which would allow further analysis of the cells; in particular, investigation of any cellular pathways that may be defective compared to control cells which may have facilitated establishment of persistent infection when the cells were first infected with v601-4B$_{T66A}$. The drugs 4-HPR, MPA, RBV and 2CMC were chosen for long-term treatment of the persistently-infected cell lines, H-v601-Per1 and H-v601-Per2, and replicon-containing cell lines, H-Rep and H-Rep-4B$_{T66A}$ because they have been previously shown to effectively reduce DENV infection *in vitro*. Unfortunately, none of these drugs were able to clear the v601-4B$_{T66A}$ virus from H-v601-Per1 or H-v601-Per2, and the only cell line that was potentially cleared of its persistent infection was H-Rep with constant presence of 100 μM RBV. However, the result may be explained by the fact that the v601-4B$_{T66A}$ virus had already firmly established a persistent infection, while previous studies mostly tested the drugs for their ability to prophylactically inhibit DENV infection (Carocci *et al.,* 2015; Diamond *et al.,* 2002; Fraser *et al.,* 2014; Lee *et al.,* 2015). There may also be inherent differences in the characteristics of the wild-type and persistently-infecting viruses which affect the anti-viral properties of the drugs when used against v601-4B$_{T66A}$. Additionally, while the drugs were previously reported to effectively reduce DENV infection, complete clearance of DENV was not achieved; treatment with 2CMC at concentrations up to 50 μM reduced DENV RNA levels to 15-20% relative to RNA levels in untreated cells (Lee *et al.,* 2015). Thus, it is possible that there was a reduction in DENV infection upon treatment with the drugs, but the remaining virus population was sufficient to allow the development of mutations that potentially conferred resistance to the drugs and enabled proliferation.

To investigate whether the persistent-infecting virus or replicons had acquired new mutations that may have conferred resistance to the antiviral drugs, the viral or replicon RNA from cell lines in which virus or replicon RNA was still present after 3 months of constant passaging in the presence of the drugs RBV or 2CMC were sequenced.

Table 4.1 shows the mutations from wild-type DENV-2 that were present in the v601-4B$_{T66A}$ virus genome or replicon RNA from all samples. Loss of the NS4B$_{T66A}$ mutation in the H-v601-Per1 cells that remained untreated or were treated with RBV was unexpected as reversion had not been observed in previous studies. However, when sequenced, the NS4B$_{T66A}$ mutation was sometimes presented as a mixed peak of occurrence (see Table 3.2). Additionally, these particular cell lines were passaged for a total time of 4 months, whereas as a general rule the cell line would be terminated after 2.5-3 months of passaging. Thus, it is possible that the NS4B$_{T66A}$ mutation in the v601-4B$_{T66A}$ virus was present in a mixed population of cells and reverted naturally over time.

Chapter 5. General summary

This project focused on a mutated strain of DENV-2, v601-4B$_{T66A}$, that contained two mutations in the NS4B gene allowing persistent infection in a variety of cell types *in vitro*. There are limited reports of persistent infection with DENV from natural infection or *in vivo* studies (Kurane *et al.,* 1990; Nakao *et al.,* 1989), however other members of the *Flaviviridae* family are known to cause persistent infections (Gritsun *et al.,* 2003; Large *et al.,* 1999; Murray *et al.,* 2010; Poidinger *et al.,* 1991; Ravi *et al.,* 1993). Thus, the discovery of a persistently-infecting strain of DENV by members of our research group which preceded this project is of great interest. The more specific purpose of this project was to investigate the mechanisms behind how persistent infection was established, either by the NS4B$_{T66A}$ mutation or by any defects in cellular pathways in a surviving subset of cells upon infection with v601-4B$_{T66A}$ that allowed persistent infection to occur.

The first stage of this project was to confirm that the v601-4B$_{T66A}$ virus and RepDV-GP2A-NS4B$_{T66A}$ replicons contained the NS4B$_{T66A}$ mutation, and that H-v601-Per1, H-v601-Per2, H-Rep and H-Rep-4B$_{T66A}$ cell lines were persistently-infected with virus or stably expressing replicons (Chapter 3). This was carried out by sequencing the NS4B gene of the replicons or v601-4B$_{T66A}$ viruses, which showed that the NS4B$_{T66A}$ mutation was still present in all samples and other mutations found are shown in Table 3.1 and Table 3.2. To confirm the identity of the cell lines, IFAs were performed to detect the NS1 protein in H-Rep and H-Rep-4B$_{T66A}$ (Figure 3.2) and the E protein in the H-v601-Per1 and H-v601-Per2 cell lines, because the E protein is not encoded by the replicon RNA (Figure 3.3).

The next step was to utilise a transcriptomics dataset, which was previously generated and compiled by other members of the research group, to study whether any cellular pathways are

differentially expressed in the H-v601-Per1 and H-v601-Per2 cell lines when compared to Mock, uninfected HEK293T cells and to inform the design of subsequent experiments. The transcriptomics data was analysed using online bioinformatics tools such as DAVID and STRING.

Genes involved in host cholesterol biosynthesis pathways were downregulated by at least 2-fold in the persistently-infected cell lines relative to Mock, but also upregulated during wild-type DENV-2 infection. This was particularly interesting because it may represent a pathway that was defective in the cells which allowed establishment of persistent infection, however, during wild-type infection it may be targeted for modulation by the virus which suggests it is potentially important for progression of infection. qPCR analysis validated the findings of transcriptomics analysis in that *HMGCR, HMGCS1, IDI1* and *MSMO1* were significantly downregulated in at least one of the persistently-infected cell lines compared to the uninfected cells. However, the finding from the transcriptomics analysis that these genes were significantly upregulated during wild-type DENV-2 infection was not confirmed by qPCR analysis, thus, the results were inconsistent and further validation would be required. Further investigation into the effect of persistent infection on host lipid metabolism pathways would be interesting, particularly the effect of wild-type and persistent infection on the activity of SREBP transcription factors which are known to regulate the expression of at least six of the identified genes, and on total intracellular cholesterol levels.

Conversely, the transcriptomics data revealed that genes involved in the type I IFN response were upregulated by at least 2-fold during persistent infection, when compared to Mock cells or wild-type DENV-2-infected cells. IFA results of the localisation of STAT1 proteins in each cell line suggest that the $NS4B_{T66A}$ mutation may have an effect on the ability of NS4B to inhibit the translocation of STAT1 proteins to the nucleus of H-v601-Per2 and H-Rep-$4B_{T66A}$, but not H-v601-Per1 cells. Loss of this STAT1 attenuation may explain why ISGs are upregulated during persistent infection compared to Mock or wild-type DENV-2-infected cells, and this must be *via* a mechanism that is STAT2-independent or still operative with low levels of STAT2 as this was degraded in cells expressing replicons that both encoded and did not encode the $NS4B_{T66A}$ mutation. It would be interesting to investigate further the mechanism by which ISGs specifically become upregulated during persistent infection, or the functional activity of STAT1 and whether this is altered between mock, wild-type, and persistent infection.

Long-term drug treatment to clear the persistently-infected cells of virus or replicon RNA was largely inconclusive, and while there was some reduction in replicon RNA observed in the RBV-treated cell lines, the experiment was particularly unsuccessful in clearing the persistently-infecting virus from H-v601-Per1 and H-v601-Per2 cells. However, this allowed

sequencing analysis to be performed on viruses or replicon constructs that had been treated for up to 3 months with RBV or 2CMC to identify potential mutations conferring resistance to the drugs. Of the 79 mutations identified, 10 mutations were unique to virus or replicon RNA isolated from cells treated with either RBV or 2CMC.

Overall, this study has expanded understanding surrounding the discovery of a novel, persistently-infecting DENV-2 strain, v601-4B$_{T66A}$, however the precise mechanisms enabling establishment of a persistent infection *in vitro* remain elusive. Further experiments to advance the current understanding of this persistently-infecting DENV-2 strain and its effect on the host cholesterol biosynthesis and type I IFN pathways are required, and potential investigation routes based on the work carried out during this study are explored in more detail in Section 3.6. In the future, investigation into the mechanism that enabled persistent infection to initiate and be maintained should remain a priority, as well as studying the altered function of the NS4B$_{T66A}$ mutation compared to wild-type. This may involve considering alternative pathways to those focused on during this study that may be differentially affected by wild-type and persistent infection. Previous work using the same v601-4B$_{T66A}$ strain has suggested that the unfolded protein response (UPR) may play a role, and this could also justify further investigation (Ismail, 2015). Additionally, the discovery of a DENV-2 strain that causes persistent infection could have potential implications in the context of natural infections. Since flaviviruses are known to cause persistent infections it should not be unreasonable to anticipate that DENV could also be capable of this. In the future, *in vivo* experiments using v601-4B$_{T66A}$ may be warranted to determine whether the persistently-infecting phenotype can also be observed using animal models, and whether this could have potential ramifications in the wider context of natural infections.

Abbreviations

2CMC	2'C-methylcytidine
4-HPR	4-hydroxyphenylretinamide
Ab	antibody
ACTB	actin β
ADE	antibody-dependent enhancement
Ala	alanine
ANOVA	analysis of variance
AP-1	activating protein 1
Asp	aspartic acid
ATPase	adenosine triphosphatase
BHK	baby hamster kidney
BLASTn	Nucleotide Basic Local Alignment Search Tool
BME	β-Mercaptoethanol
BSL3	biological safety level 3
bp	base pairs
C	capsid
cDNA	complementary deoxyribonucleic acid
c-GAS	cyclic GMP-AMP synthase
CM	convoluted membrane
CO_2	carbon dioxide
CPE	cytopathic effect
DAPI	4',6-diamidino-2-phenylindole
DAVID	Database for Annotation, Visualisation and Integrated Discovery
DC	dendritic cell
DC-SIGN	dendritic cell-specific intercellular adhesion molecular-3-grabbing non-integrin
DENV	Dengue virus
DF	dengue fever
DHF	dengue haemorrhagic fever
DMEM	Dulbecco's Modified Eagle's Medium
DMSO	dimethyl sulfoxide
DNA	deoxyribonucleic acid
DNase	deoxyribonuclease
dsRNA	double-stranded RNA
DSS	dengue shock syndrome
dNTP	deoxynucleotide
E	envelope
EDTA	ethylenediaminetetraacetic acid
eGFP	enhanced green fluorescent protein
ER	endoplasmic reticulum
FASN	fatty acid synthase
FBS	foetal bovine serum
g	grams
GAPDH	glyceraldehyde-3-phosphate dehydrogenase
GFP	green fluorescent protein
h	hours
HCV	hepatitis C virus
His	histidine
HMGCR	3-hydroxy-3-methylglutaryl-CoA reductase
HMGCS1	3-hydroxy-3-methylglutaryl-CoA synthase 1
hpi	hours post-infection
IDI1	isopentenyl-diphosphate delta isomerase 1
IFA	immunofluorescence assay
IFITM	interferon-inducible transmembrane proteins
IFN	interferon
IFNAR	type I interferon receptor
IFNα	interferon alpha
IFNα-	interferon-α negative
IFNα+	interferon-α positive

IgG	immunoglobulin G
IL	interleukin
INSIG1	insulin-induced gene 1
IRF9	interferon regulatory factor 9
ISG	interferon-stimulated gene
ISGF3	interferon-stimulated gene factor 3
ISRE	interferon-stimulated response element
JAK1	Janus kinase 1
JEV	Japanese encephalitis virus
kDa	kilodaltons
l	litres
LD	lipid droplet
Leu	leucine
M	membrane
mAb	monoclonal antibody
MDA5	melanoma differentiation-associated gene 5
MDCK	Madin-Darby canine kidney
Met	methionine
mg	milligrams
min	minutes
ml	millilitres
MOI	multiplicity of infection
MPA	mycophenolic acid
MR	mannose receptor
MSMO1	methylsterol monooxygenase 1
MTase	methyltransferase domain
MVD	mevalonate (diphospho) decarboxylase
MVE	Murray Valley encephalitis
NCR	non-coding region
NFκB	nuclear factor kappa-light chain-enhancer of activated B cells
ng	nanograms
NGC	New Guinea strain
NK	natural killer
NS	non-structural
NS1	non-structural protein 1
NS2A	non-structural protein 2A
NS2B	non-structural protein 2B
NS3	non-structural protein 3
NS4A	non-structural protein 4A
NS4B	non-structural protein 4B
NS5	non-structural protein 5
NTC	no-template control
NTPase	nucleotide triphosphatase
ORF	open reading frame
PAC	puromycin N-acetyltransferase
PAMP	pathogen-associated molecular patterns
PBS	phosphate-buffered saline
PCR	polymerase chain reaction
PFA	paraformaldehyde
PKR	dsRNA-dependent kinase protein
pmol	picomoles
prM/M	pre-membrane/membrane
PRR	pathogen recognition receptor
pSTAT1	phosphorylated signal transducer and activator of transcription 1
pSTAT2	phosphorylated signal transducer and activator of transcription 2
qPCR	quantitative real-time polymerase chain reaction
RBV	ribavirin
RC	replication complex
RdRp	RNA-dependent RNA polymerase
RIG-1	retinoic-acid-inducible gene 1

RNA	ribonucleic acid
RNase	ribonuclease
RTPase	RNA triphosphatase
RT	reverse transcription
RT-PCR	reverse-transcriptase polymerase chain reaction
SQLE	squalene epoxidase
sec	seconds
ssRNA	single-stranded RNA
STAT1	signal transducer and activator of transcription 1
STAT2	signal transducer and activator of transcription 2
STING	stimulator of interferon genes
STRING	Search Tool for the Retrieval of Interacting Genes/Proteins
TBE	tris/borate/ethylenediaminetetraacetic acid
TBEV	tick-borne encephalitis virus
TGN	trans-Golgi network
Thr	threonine
TLR	toll-like receptor
TNF	tumour necrosis factor
Tyk2	tyrosine kinase 2
U	units
UBR4	ubiquitin ligase E3 recognin 4
UTR	untranslated region
v/v	volume per volume percent
V	volts
V-ATPase	vacuolar ATPase
Val	valine
VLDL	very low-density lipoprotein
VP	vesicle packet
w/v	weight per volume percent
WHO	World Health Organisation
WNV	West Nile virus
WT	wild-type
x *g*	times gravity
ΔΔCt	double-delta cycle threshold
α	alpha
β	beta
μg	micrograms
μl	microlitres
μM	micromolar

Cell lines

HEK293	human embryonic kidney 293
H-v601-Per1	HEK293T cells persistently-infected with v601-4B$_{T66A}$; cell line 1
H-v601-Per2	HEK293T cells persistently-infected with v601-4B$_{T66A}$; cell line 2
H-v601	HEK293T cells infected with v601
H-Rep	HEK293T cells containing pRepDV-GP2A replicons
H-Rep-4B$_{T66A}$	HEK293T cells containing pRepDV-GP2A-NS4B$_{T66A}$ replicons

Bibliography

Adams, B., Holmes, E. C., Zhang, C., Mammen, M. P., Nimmannitya, S., Kalayanarooj, S., and Boots, M. (2006). 'Cross-protective immunity can account for the alternating epidemic pattern of dengue virus serotypes circulating in Bangkok'. *Proceedings of the National Academy of Sciences*, 103(38), 14234–14239.

Aguirre, S., Luthra, P., Sanchez-Aparicio, M. T., Maestre, A. M., Patel, J., Lamothe, F., Fredericks, A. C., Tripathi, S., Zhu, T., Pintado-Silva, J., Webb, L. G., Bernal-Rubio, D., Solovyov, A., Greenbaum, B., Simon, V., Basler, C. F., Mulder, L. C. F., García-Sastre, A., and Fernandez-Sesma, A. (2017). 'Dengue virus NS2B protein targets cGAS for degradation and prevents mitochondrial DNA sensing during infection'. *Nature Microbiology*, Nature Publishing Group, 2(March), 1–11.

Aguirre, S., Maestre, A. M., Pagni, S., Patel, J. R., Savage, T., Gutman, D., Maringer, K., Bernal-Rubio, D., Shabman, R. S., Simon, V., Rodriguez-Madoz, J. R., Mulder, L. C. F., Barber, G. N., and Fernandez-Sesma, A. (2012). 'DENV Inhibits Type I IFN Production in Infected Cells by Cleaving Human STING'. *PLoS Pathogens*, 8(10).

de Alwis, R., Smith, S. A., Olivarez, N. P., Messer, W. B., Huynh, J. P., Wahala, W. M. P. B., White, L. J., Diamond, M. S., Baric, R. S., Crowe, J. E., and de Silva, A. M. (2012). 'Identification of human neutralizing antibodies that bind to complex epitopes on dengue virions'. *Proceedings of the National Academy of Sciences*, 109(19), 7439–7444.

Anders, K. L., Nguyet, N. M., Chau, N. V. V., Hung, N. T., Thuy, T. T., Lien, L. B., Farrar, J., Wills, B., Hien, T. T., and Simmons, C. R. (2011). 'Epidemiological factors associated with dengue shock syndrome and mortality in hospitalized dengue patients in Ho Chi Minh City, Vietnam'. *American Journal of Tropical Medicine and Hygiene*, 84(1), 127–134.

Apte-Sengupta, S., Sirohi, D., and Kuhn, R. J. (2014). 'Coupling of Replication and Assembly in Flaviviruses'. *Current Opinions in Virology*, 0, 134–142.

Ashour, J., Laurent-Rolle, M., Shi, P.-Y., and Garcia-Sastre, A. (2009). 'NS5 of Dengue Virus Mediates STAT2 Binding and Degradation'. *Journal of Virology*, 83(11), 5408–5418.

Avirutnan, P., Fuchs, A., Hauhart, R. E., Somnuke, P., Youn, S., Diamond, M. S., and Atkinson, J. P. (2010). 'Antagonism of the complement component C4 by flavivirus nonstructural protein NS1'. *The Journal of Experimental Medicine*, 207(4), 793–806.

Avirutnan, P., Hauhart, R. E., Somnuke, P., Blom, A. M., Diamond, M. S., and Atkinson, J. P. (2011). 'Binding of Flavivirus Nonstructural Protein NS1 to C4b Binding Protein Modulates Complement Activation'. *The Journal of Immunology*, 187(1), 424–433.

Baril, M., Racine, M.-E., Penin, F., and Lamarre, D. (2009). 'MAVS Dimer Is a Crucial Signaling Component of Innate Immunity and the Target of Hepatitis C Virus NS3/4A Protease'. *Journal of Virology*, 83(3), 1299–1311.

Barniol, J., Gaczkowski, R., Barbato, E. V., da Cunha, R. V., Salgado, D., Martínez, E., Segarra, C. S., Pleites Sandoval, E. B., Mishra, A., Laksono, I. S., Lum, L. C. S., Martínez, J. G., Núnez, A., Balsameda, A., Allende, I., Ramírez, G., Dimaano, E., Thomacheck, K., Akbar, N. A., Ooi, E. E., Villegas, E., Hien, T. T., Farrar, J., Horstick, O., Kroeger, A., and Jaenisch, T. (2011). 'Usefulness and applicability of the revised dengue case classification by disease: Multi-centre study in 18 countries'. *BMC Infectious Diseases*, 11, 1–12.

Barton, G. M. (2007). 'Viral recognition by Toll-like receptors'. *Seminars in Immunology*, 19(1), 33–40.

Barzon, L., Pacenti, M., Franchin, E., Lavezzo, E., Trevisan, M., Sgarabotto, D., and Palù, G. (2016). 'Infection dynamics in a traveller with persistent shedding of Zika virus RNA in semen for six months after returning from Haiti to Italy, January 2016'. *Eurosurveillance*, 21(32), 1–4.

Beatty, P. R., Puerta-Guardo, H., Killingbeck, S. S., Glasner, D. R., Hopkins, K., and Harris, E. (2015). 'Dengue virus NS1 triggers endothelial permeability and vascular leak that is prevented by NS1 vaccination'. *Science Translational Medicine*, 7(304).

Beltramello, M., Williams, K. L., Simmons, C. P., MacAgno, A., Simonelli, L., Quyen, N. T. H., Sukupolvi-Petty, S., Navarro-Sanchez, E., Young, P. R., De Silva, A. M., Rey, F. A., Varani, L., Whitehead, S. S., Diamond, M. S., Harris, E., Lanzavecchia, A., and Sallusto, F. (2010). 'The human immune response to dengue virus is dominated by highly cross-reactive antibodies endowed with neutralizing and enhancing activity'. *Cell Host and Microbe*, 8(3), 271–283.

Bhatt, S., Gething, P., Brady, O., Messina, J., Farlow, A., and Moyes, C. (2013). 'The global distribution and burden of dengue'. *Nature*, 496(7446), 504–507.

Blanc, M., Hsieh, W. Y., Robertson, K. A., Watterson, S., Shui, G., Lacaze, P., Khondoker, M., Dickinson, P., Sing, G., Rodríguez-Martín, S., Phelan, P., Forster, T., Strobl, B., Müller, M., Riemersma, R., Osborne, T., Wenk, M. R., Angulo, A., and Ghazal, P. (2011). 'Host defense against viral infection involves interferon mediated down-regulation of sterol biosynthesis'. *PLoS Biology*, 9(3).

Blaszczyk, K., Nowicka, H., Kostyrko, K., Antonczyk, A., Wesoly, J., and Bluyssen, H. A. R. (2016). 'The unique role of STAT2 in constitutive and IFN-induced transcription and antiviral responses'. *Cytokine and Growth Factor Reviews*, Elsevier Ltd, 29, 71–81.

Blaszczyk, K., Olejnik, A., Nowicka, H., Ozgyin, L., Chen, Y.-L., Chmielewski, S., Kostyrko, K., Wesoly, J., Balint, B. L., Lee, C.-K., and Bluyssen, H. A. R. (2015). 'STAT2/IRF9 directs a prolonged ISGF3-like transcriptional response and antiviral activity in the absence of STAT1'. *Biochemical Journal*, 466(3), 511–524.

Boutté, Y., Men, S., and Grebe, M. (2011). 'Fluorescent in situ visualization of sterols in Arabidopsis roots'. *Nature Protocols*, 6(4), 446–456.

Brady, O. J., Gething, P. W., Bhatt, S., Messina, J. P., Brownstein, J. S., Hoen, A. G., Moyes, C. L., Farlow, A. W., Scott, T. W., and Hay, S. I. (2012). 'Refining the Global Spatial Limits of Dengue Virus Transmission by Evidence-Based Consensus'. *PLoS Neglected Tropical Diseases*, 6(8).

Brass, A., Huang, I.-C., Benita, Y., John, S., Krishnan, M., Feeley, E., Ryan, B., Weyer, J., Weyden, L., Fikrig, E., Adams, D., Xavier, R., Farzan, M., and Elledge, S. (2009). 'The IFITM proteins mediate cellular resistance to influenza A H1N1 virus, West Nile virus, and dengue virus.' *Cell*, 139(7), 1243–1254.

Breiman, A., Grandvaux, N., Lin, R., Ottone, C., Akira, S., Yoneyama, M., Fujita, T., Hiscott, J., and Meurs, E. F. (2005). 'Inhibition of RIG-I-Dependent Signaling to the Interferon Pathway during Hepatitis C Virus Expression and Restoration of Signaling by IKK '. *Journal of Virology*, 79(7), 3969–3978.

Burke, D. S., Nisalak, A., Johnson, D. E., and Scott, R. M. (1988). 'A Prospective Study of Dengue Infections in Bangkok'. *The American Journal of Tropical Medicine and Hygiene*, 38(1), 172–180.

Burrell, C. J., Howard, C. R., and Murphy, F. A. (2017). 'Flaviviruses'. *Fenner and White's Medical Virology*, 493–518.

Cambi, A., De Lange, F., Van Maarseveen, N. M., Nijhuis, M., Joosten, B., Van Dijk, E. M. H. P., De Bakker, B. I., Fransen, J. A. M., Bovee-Geurts, P. H. M., Van Leeuwen, F. N., Van Hulst, N. F., and Figdor, C. G. (2004). 'Microdomains of the C-type lectin DC-SIGN are portals for virus entry into dendritic cells'. *Journal of Cell Biology*, 164(1), 145–155.

Carocci, M., Hinshaw, S. M., Rodgers, M. A., Villareal, V. A., Burri, D. J., Pilankatt, R., Maharaj, N. P., Gack, M. U., Stavale, E. J., Warfield, K. L., and Yanga, P. L. (2015). 'The bioactive lipid 4-hydroxyphenyl retinamide inhibits flavivirus replication'. *Antimicrobial Agents and Chemotherapy*, 59(1), 85–95.

Carro, A. C., and Damonte, E. B. (2013). 'Requirement of cholesterol in the viral envelope for dengue virus infection'. *Virus Research*, Elsevier B.V., 174(1–2), 78–87.

Castillo Ramirez, J. A., and Urcuqui-Inchima, S. (2015). 'Dengue Virus Control of Type I IFN Responses: A History of Manipulation and Control'. *Journal of Interferon & Cytokine Research*, 35(6), 421–430.

Chang, D. C., Hoang, L. T., Mohamed Naim, A. N., Dong, H., Schreiber, M. J., Hibberd, M. L., Tan, M. J. A., and Shi, P. Y. (2016). 'Evasion of early innate immune response by 2′-O-methylation of dengue genomic RNA'. *Virology*, Elsevier, 499, 259–266.

Chatel-Chaix, L., Fischl, W., Scaturro, P., Cortese, M., Kallis, S., Bartenschlager, M., Fischer, B., and Bartenschlager, R. (2015). 'A Combined Genetic-Proteomic Approach Identifies Residues within Dengue Virus NS4B Critical for Interaction with NS3 and Viral Replication'. *Journal of Virology*, 89(14), 7170–7186.

Chen, R., and Vasilakis, N. (2011). 'Dengue-Quo tu et quo vadis?' *Viruses*, 3(9), 1562–1608.

Chen, S. T., Lin, Y. L., Huang, M. T., Wu, M. F., Cheng, S. C., Lei, H. Y., Lee, C. K., Chiou, T. W., Wong, C. H., and Hsieh, S. L. (2008). 'CLEC5A is critical for dengue-virus-induced lethal disease'. *Nature*, 453(7195), 672–676.

Chen, W. J., Chen, S. L., and Fang, A. H. (1994). 'Phenotypic characteristics of dengue 2 virus persistently infected in a C6/36 clone of aedes albopictus cells'. *Intervirology*, 37(1), 25–30.

Chen, Y., Maguire, T., Hileman, R. E., Fromm, J. R., Esko, J. D., Linhardt, R. J., and Marks, R. M. (1997). 'Dengue virus infectivity depends on evelope protein binding to target cell heparan sulfate'. *Nature medicine*.

van Cleef, K. W. R., Overheul, G. J., Thomassen, M. C., Kaptein, S. J. F., Davidson, A. D., Jacobs, M., Neyts, J., van Kuppeveld, F. J. M., and van Rij, R. P. (2013). 'Identification of a new dengue virus inhibitor that targets the viral NS4B protein and restricts genomic RNA replication'. *Antiviral Research*, Elsevier B.V., 99(2), 165–171.

Clum, S., Ebner, K., and Padmanabhan, R. (1997). 'Cotranslational Membrane Insertion of the Serine Proteinase Precursor NS2B-NS3 (Pro) of Dengue Virus …'. *Journal of Biological Chemistry*, 272(49), 30715–30723.

Clyde, K., Kyle, J. L., and Harris, E. (2006). 'Recent Advances in Deciphering Viral and Host Determinants of Dengue Virus Replication and Pathogenesis'. *Journal of Virology*, 80(23), 11418–11431.

Coffey, L. L., Mertens, E., Brehin, A. C., Fernandez-Garcia, M. D., Amara, A., Després, P., and Sakuntabhai, A. (2009). 'Human genetic determinants of dengue virus susceptibility'. *Microbes and Infection*, 11(2), 143–156.

Crill, W. D., Hughes, H. R., Delorey, M. J., and Chang, G.-J. J. (2009). 'Humoral Immune Responses of Dengue Fever Patients Using Epitope-Specific Serotype-2 Virus-Like Particle Antigens'. *PLoS ONE*, 4(4), e4991.

Crill, W. D., and Roehrig, J. T. (2001). 'Monoclonal Antibodies That Bind to Domain III of Dengue Virus E Glycoprotein Are the Most Efficient Blockers of Virus Adsorption to Vero Cells'. *Journal of Virology*, 75(16), 7769–7773.

Cruz-Oliveira, C., Freire, J. M., Conceição, T. M., Higa, L. M., Castanho, M. A. R. B., and Da Poian, A. T. (2015). 'Receptors and routes of dengue virus entry into the host cells'. *FEMS Microbiology Reviews*, 39(2), 155–170.

Dalrymple, N. a, Cimica, V., and Mackow, E. R. (2015). 'Dengue Virus NS Proteins Inhibit RIG-I / MAVS Signaling by Blocking TBK1 / IRF3 Phosphorylation : Dengue Virus Serotype 1 NS4A Is a Unique Interferon-Regulating Virulence Determinant.' *mBio*, 6(3), 1–12.

Dejnirattisai, W., Jumnainsong, A., Onsirisakul, N., Fitton, P., Vasanawathana, S., Limpitikul, W., Puttikhunt, C., Edwards, C., Duangchinda, T., Supasa, S., Chawansuntati, K., Malasit, P., Mongkolsapaya, J., Screaton, G., and Idps, C. (2010). 'Cross-Reacting Antibodies Enhance Dengue Virus Infection in Humans'. *Science*, 328(May), 745–748.

Diamond, M. S., Zachariah, M., and Harris, E. (2002). 'Mycophenolic acid inhibits dengue virus infection by preventing replication of viral RNA'. *Virology*, 304(2), 211–221.

Dionicio, C. L., Peña, F., Constantino-Jonapa, L. A., Vazquez, C., Yocupicio-Monroy, M., Rosales, R., Zambrano, J. L., Ruiz, M. C., del Angel, R. M., and Ludert, J. E. (2018). 'Dengue virus induced changes in Ca2+homeostasis in human hepatic cells that favor the viral replicative cycle'. *Virus Research*, Elsevier, 245(November 2017), 17–28.

Duan, X., Lu, X., Li, J., and Liu, Y. (2008). 'Novel binding between pre-membrane protein and vacuolar ATPase is required for efficient dengue virus secretion'. *Biochemical and Biophysical Research Communications*, 373(2), 319–324.

Echebli, N., Tchitchek, N., Dupuy, S., Bruel, T., Passaes, P. B., Bosquet, N., Grand, R. Le, and Bourgeois, C. (2017). 'Stage-specific ISG expression reveals functional convergence

of type I and II IFNs in SIV infection'.
Falgout, B., Miller, R. H., and Lai, C.-J. (1993). 'Deletion Analysis of Dengue Virus Type 4 Nonstructural Protein NS2B: Identification of a Domain Required for NS2B-NS3 Protease Activity'. *Journal of Virology*, 67(4), 2034–2042.
Falgout, B., Pethel, M., Zhang, Y.-M., and Lai, C.-J. (1991). 'Both Nonstructural Proteins Ns2B and Ns3 Are Required for the Proteolytic Processing of Dengue Virus Nonstructural Proteins'. *Journal of Virology*, 65(5), 2467–2475.
Fink, J., Gu, F., Ling, L., Tolfvenstam, T., Olfat, F., Chin, K. C., Aw, P., George, J., Kuznetsov, V. A., Schreiber, M., Vasudevan, S. G., and Hibberd, M. L. (2007). 'Host gene expression profiling of dengue virus infection in cell lines and patients'. *PLoS Neglected Tropical Diseases*, 1(2).
Fischl, W., and Bartenschlager, R. (2011). 'Exploitation of cellular pathways by Dengue virus'. *Current Opinion in Microbiology*, Elsevier Ltd, 14(4), 470–475.
Fraser, J. E., Watanabe, S., Wang, C., Chan, W. K. K., Maher, B., Lopez-Denman, A., Hick, C., Wagstaff, K. M., Mackenzie, J. M., Sexton, P. M., Vasudevan, S. G., and Jans, D. A. (2014). 'A nuclear transport inhibitor that modulates the unfolded protein response and provides in vivo protection against lethal dengue virus infection'. *Journal of Infectious Diseases*, 210(11), 1780–1791.
Freire, J. M., Veiga, A. S. alom., de la Torre, B. G., Santos, N. C., Andreu, D., Da Poian, A. T., and Castanho, M. A. R. B. (2013). 'Peptides as models for the structure and function of viral capsid proteins: Insights on dengue virus capsid'. *Biopolymers*, 100(4), 325–336.
Fried, J. R., Gibbons, R. V., Kalayanarooj, S., Thomas, S. J., Srikiatkhachorn, A., Yoon, I. K., Jarman, R. G., Green, S., Rothman, A. L., and Cummings, D. A. T. (2010). 'Serotype-specific differences in the risk of dengue hemorrhagic fever: An analysis of data collected in Bangkok, Thailand from 1994 to 2006'. *PLoS Neglected Tropical Diseases*, 4(3), 1–6.
Gebhard, L. G., Filomatori, C. V., and Gamarnik, A. V. (2011). 'Functional RNA elements in the dengue virus genome'. *Viruses*, 3(9), 1739–1756.
Gebhard, L. G., Kaufman, S. B., and Gamarnik, A. V. (2012). 'Novel ATP-independent RNA annealing activity of the dengue virus NS3 helicase'. *PLoS ONE*, 7(4), 27–29.
Goldstein, J. L., and Brown, M. S. (1990). 'Regulation of the mevalonate pathway.' *Nature*, 343(6257), 425–430.
Gong, Y., Lee, J. N., Lee, P. C. W., Goldstein, J. L., Brown, M. S., and Ye, J. (2006). 'Sterol-regulated ubiquitination and degradation of Insig-1 creates a convergent mechanism for feedback control of cholesterol synthesis and uptake'. *Cell Metabolism*, 3(1), 15–24.
Gritsun, T. S., Nuttall, P. A., and Gould, E. A. (2003). *Advances in Virus Research Volume 61*. *Advances in Virus Research*, Elsevier Inc.
Gualano, R. C., Pryor, M. J., Cauchi, M. R., Wright, P. J., and Davidson, A. D. (1998). 'Identification of a major determinant of mouse neurovirulence of dengue virus type 2 using stably cloned genomic-length cDNA'. *Journal of General Virology*, 79(3), 437–446.
Gubler, D. J. (2007). 'The Continuing Spread of West Nile Virus in the Western Hemisphere'. *Clinical Infectious Diseases*, 45(8), 1039–1046.
Gullberg, R. C., Steel, J. J., Pujari, V., Rovnak, J., Crick, D. C., and Perera, R. (2018). 'Stearoly-CoA desaturase 1 differentiates early and advanced dengue virus infections and determines virus particle infectivity'. *PLoS Pathogens*, 14(8), e1007261.
Harrington, L. C., Fleisher, A., Ruiz-Moreno, D., Vermeylen, F., Wa, C. V., Poulson, R. L., Edman, J. D., Clark, J. M., Jones, J. W., Kitthawee, S., and Scott, T. W. (2014). 'Heterogeneous Feeding Patterns of the Dengue Vector, Aedes aegypti, on Individual Human Hosts in Rural Thailand'. *PLoS Neglected Tropical Diseases*, 8(8).
Harris, E., Guzman, M. G., and Harris, E. (2015). 'Dengue'. *Lancet*, 385(9966), 453–465.
Harrison, S. C. (2015). 'Viral membrane fusion'. *Virology*, 479–480, 498–507.
He, Z., Zhu, X., Wen, W., Yuan, J., Hu, Y., Chen, J., An, S., Dong, X., Lin, C., Yu, J., Wu, J., Yang, Y., Cai, J., Li, J., and Li, M. (2016). 'Dengue Virus Subverts Host Innate Immunity by Targeting Adaptor Protein MAVS'. *Journal of Virology*, 90(16), 7219–7230.
Heaton, N. S., Perera, R., Berger, K. L., Khadka, S., LaCount, D. J., Kuhn, R. J., and Randall, G. (2010). 'Dengue virus nonstructural protein 3 redistributes fatty acid synthase to sites

of viral replication and increases cellular fatty acid synthesis'. *Proceedings of the National Academy of Sciences*, 107(40), 17345–17350.
Heaton, N. S., and Randall, G. (2010). 'Dengue virus-induced autophagy regulates lipid metabolism'. *Cell Host and Microbe*, Elsevier Inc., 8(5), 422–432.
Heaton, N. S., and Randall, G. (2011). 'Multifaceted roles for lipids in viral infection'. *Trends in Microbiology*, Elsevier Ltd, 19(7), 368–375.
Heinz, F., Stiasny, K., and Allison, S. (2004). 'The entry machinery of flaviviruses.' *Archives of Virology. Supplementum*, 18, 133–137.
Helbig, K. J., Carr, J. M., Calvert, J. K., Wati, S., Clarke, J. N., Eyre, N. S., Narayana, S. K., Fiches, G. N., McCartney, E. M., and Beard, M. R. (2013). 'Viperin Is Induced following Dengue Virus Type-2 (DENV-2) Infection and Has Anti-viral Actions Requiring the C-terminal End of Viperin'. *PLoS Neglected Tropical Diseases*, 7(4).
Ho, L.-J., Hung, L.-F., Weng, C.-Y., Wu, W.-L., Chou, P., Lin, Y.-L., Chang, D.-M., Tai, T.-Y., and Lai, J.-H. (2005). 'Dengue Virus Type 2 Antagonizes IFN-α but Not IFN-γ Antiviral Effect via Down-Regulating Tyk2-STAT Signaling in the Human Dendritic Cell'. *The Journal of Immunology*, 174(12), 8163–8172.
Holmes, E. C. (1998). 'Molecular epidemiology and evolution of emerging infectious diseases.' *British Medical Bulletin*, 54(3), 533–543.
Holmes, E. C., and Burch, S. S. (2000). 'The causes and consequences of genetic variation in dengue virus'. *Trends in Microbiology*, 8(2), 74–77.
Holmes, E. C., and Twiddy, S. S. (2003). 'The origin, emergence and evolutionary genetics of dengue virus'. *Infection, Genetics and Evolution*, 3(1), 19–28.
Horton, J. D., Shah, N. A., Warrington, J. A., Anderson, N. N., Park, S. W., Brown, M. S., and Goldstein, J. L. (2003). 'Combined analysis of oligonucleotide microarray data from transgenic and knockout mice identifies direct SREBP target genes'. *Proceedings of the National Academy of Sciences*, 100(21), 12027–12032.
Hsu, Y. C., Chen, N. C., Chen, P. C., Wang, C. C., Cheng, W. C., and Wu, H. N. (2012). 'Identification of a small-molecule inhibitor of dengue virus using a replicon system'. *Archives of Virology*, 157(4), 681–688.
van den Hurk, A. F., Ritchie, S. A., and Mackenzie, J. S. (2009). 'Ecology and Geographical Expansion of Japanese Encephalitis Virus'. *Annual Review of Entomology*, 54(1), 17–35.
Igarashi, A. (1979). 'Characteristics of Aedes albopictus cells persistently infected with dengue viruses [16]'. *Nature*.
Ismail, R. (2015). 'Elucidation of the mechanism of action of a mutation in the dengue virus NS4B protein that confers a persistent phenotype in cell culture Rosmani Ismail'. University of Bristol.
Issur, M., Geiss, B. J., Bougie, I., Picard-Jean, F., Despins, S., Mayette, J., Hobdey, S. E., and Bisaillon, M. (2009). 'The flavivirus NS5 protein is a true RNA guanylyltransferase that catalyzes a two-step reaction to form the RNA cap structure'. *RNA*, 15, 2340–2350.
Ivashkiv, L. B., and Donlin, L. T. (2015). 'Regulation of type I interferon responses'. *Nature Reviews Immunology*, 14(1), 36–49.
Jessie, K., Fong, M. Y., Devi, S., Lam, S. K., and Wong, K. T. (2004). 'Localization of Dengue Virus in Naturally Infected Human Tissues, by Immunohistochemistry and In Situ Hybridization'. *The Journal of Infectious Diseases*, 189(8), 1411–1418.
Jiang, D., Weidner, J. M., Qing, M., Pan, X.-B., Guo, H., Xu, C., Zhang, X., Birk, A., Chang, J., Shi, P.-Y., Block, T. M., and Guo, J.-T. (2010). 'Identification of Five Interferon-Induced Cellular Proteins That Inhibit West Nile Virus and Dengue Virus Infections'. *Journal of Virology*, 84(16), 8332–8341.
Jones, C. T., Ma, L., Burgner, J. W., Groesch, T. D., Post, C. B., and Kuhn, R. J. (2003). 'Flavivirus capsid is a dimeric alpha-helical protein.' *Journal of Virology*, 77(12), 7143–9.
Juárez-Martínez, A. B., Vega-Almeida, T. O., Salas-Benito, M., García-Espitia, M., De Nova-Ocampo, M., del Ángel, R. M., and Salas-Benito, J. S. (2013). 'Detection and sequencing of defective viral genomes in C6/36 cells persistently infected with dengue virus 2'. *Archives of Virology*, 158(3), 583–599.
Katzelnick, L. C., Gresh, L., Halloran, M. E., Mercado, J. C., Kuan, G., Gordon, A., Balmaseda,

A., and Harris, E. (2017). 'Antibody-dependent enhancement of severe dengue disease in humans'. *Science*, 358, 929–932.
Kielian, M. (2006). 'Class II virus membrane fusion proteins'. *Virology*, 344(1), 38–47.
Kraemer, M. U. G., Sinka, M. E., Duda, K. A., Mylne, A. Q. N., Shearer, F. M., Barker, C. M., Moore, C. G., Carvalho, R. G., Coelho, G. E., Van Bortel, W., Hendrickx, G., Schaffner, F., Elyazar, I. R., Teng, H. J., Brady, O. J., Messina, J. P., Pigott, D. M., Scott, T. W., Smith, D. L., William Wint, G. R., Golding, N., and Hay, S. I. (2015). 'The global distribution of the arbovirus vectors Aedes aegypti and Ae. Albopictus'. *eLife*, 4, e08347.
Krishnan, M. N., Sukumaran, B., Pal, U., Agaisse, H., Murray, J. L., Hodge, T. W., and Fikrig, E. (2007). 'Rab 5 Is Required for the Cellular Entry of Dengue and West Nile Viruses'. *Journal of Virology*, 81(9), 4881–4885.
Kuhn, R. J., Zhang, W., Rossmann, M. G., Pletnev, S. V., Corver, J., Lenches, E., Jones, C. T., Mukhopadhyay, S., Chipman, P. R., Strauss, E. G., Baker, T. S., and Strauss, J. H. (2002). 'Structure of dengue virus: Implications for flavivirus organization, maturation, and fusion'. *Cell*, 108(5), 717–725.
Kurane, I., Kontny, U., Janus, J., and Ennis, F. A. (1990). 'Dengue-2 virus infection of human mononuclear cell lines and establishment of persistent infections'. *Archives of Virology*, 110(1–2), 91–101.
Large, M. K., Kittlesen, D. J., and Hahn, Y. S. (1999). 'Suppression of host immune response by the core protein of hepatitis C virus: possible implications for hepatitis C virus persistence'. *J Immunol*, 162(2), 931–938.
Lee, J. C., Tseng, C. K., Wu, Y. H., Kaushik-Basu, N., Lin, C. K., Chen, W. C., and Wu, H. N. (2015). 'Characterization of the activity of 2′-C-methylcytidine against dengue virus replication'. *Antiviral Research*, Elsevier B.V., 116, 1–9.
León-Juárez, M., Martínez-Castillo, M., Shrivastava, G., García-Cordero, J., Villegas-Sepulveda, N., Mondragón-Castelán, M., Mondragón-Flores, R., and Cedillo-Barrón, L. (2016). 'Recombinant Dengue virus protein NS2B alters membrane permeability in different membrane models'. *Virology Journal*, Virology Journal, 13(1), 1–11.
Leung, J. Y., Pijlman, G. P., Kondratieva, N., Hyde, J., Mackenzie, J. M., and Khromykh, A. A. (2008). 'Role of Nonstructural Protein NS2A in Flavivirus Assembly'. *Journal of Virology*, 82(10), 4731–4741.
Li, H., Clum, S., You, S., Ebner, K. E., and Padmanabhan, R. (1999). 'The serine protease and RNA-stimulated nucleoside triphosphatase and RNA helicase functional domains of dengue virus type 2 NS3 converge within a region of 20 amino acids.' *Journal of Virology*, 73(4), 3108–16.
Li, L., Hu, S. T., Wang, S. H., Lee, H. H., Wang, Y. T., and Ping, Y. H. (2010). 'Positive transcription elongation factor b (P-TEFb) contributes to dengue virus-stimulated induction of interleukin-8 (IL-8)'. *Cellular Microbiology*, 12(11), 1589–1603.
Liew, K. J. L., and Chow, V. T. K. (2006). 'Microarray and real-time RT-PCR analyses of a novel set of differentially expressed human genes in ECV304 endothelial-like cells infected with dengue virus type 2'. *Journal of Virological Methods*, 131(1), 47–57.
Lim, S. P., Koh, J. H. K., Seh, C. C., Liew, C. W., Davidson, A. D., Chua, L. S., Chandrasekaran, R., Cornvik, T. C., Shi, P. Y., and Lescar, J. (2013). 'A crystal structure of the dengue virus non-structural protein 5 (NS5) polymerase delineates interdomain amino acid residues that enhance its thermostability and de novo initiation activities'. *Journal of Biological Chemistry*, 288(43), 31105–31114.
Limjindaporn, T., Netsawang, J., Noisakran, S., Thiemmeca, S., Wongwiwat, W., Sudsaward, S., Avirutnan, P., Puttikhunt, C., Kasinrerk, W., Sriburi, R., Sittisombut, N., Yenchitsomanus, P. thai, and Malasit, P. (2007). 'Sensitization to Fas-mediated apoptosis by dengue virus capsid protein'. *Biochemical and Biophysical Research Communications*, 362(2), 334–339.
Lin, J., Lin, S., Chen, W., Yen, Y., Lai, C., Tao, M., Lin, Y., Miaw, S., and Wu-Hsieh, B. A. (2014). 'Dengue Viral Protease Interaction with NF-κB Inhibitor α/β Results in Endothelial Cell Apoptosis and Hemorrhage Development'. *The Journal of Immunology*, 193(3), 1258–1267.

Lindenbach, B. D., and Rice, C. M. (1999). 'Genetic Interaction of Flavivirus Nonstructural Proteins NS1 and NS4A as a Determinant of Replicase Function'. *Journal of Virology*, 73(6), 4611–4621.
Lindenbach, B. D., and Rice, C. M. (2007). 'Flaviviridae: The Viruses and Their Replication'. *Fields Virology*, 1101–1151.
Lindenbach, B. D., Thiel, H.-J., and Rice, C. M. (2007). 'Flaviviridae: The Viruses and Their Replication'. *Fields Virology*, Philadelphia, 1101–1152.
Liu, S., Cai, X., Wu, J., Cong, Q., Chen, X., Li, T., Du, F., Ren, J., Wu, Y. T., Grishin, N. V., and Chen, Z. J. (2015). 'Phosphorylation of innate immune adaptor proteins MAVS, STING, and TRIF induces IRF3 activation'. *Science*, 347(6227), 1–17.
Liu, W. J., Chen, H. B., and Khromykh, A. A. (2003). 'Molecular and Functional Analyses of Kunjin Virus Infectious cDNA Clones Demonstrate the Essential Roles for NS2A in Virus Assembly and for a Nonconservative Residue in NS3 in RNA Replication'. *Journal of Virology*, 77(14), 7804–7813.
Livak, K. J., and Schmittgen, T. D. (2001). 'Analysis of Relative Gene Expression Data Using Real-Time Quantitative PCR and the 2−ΔΔCT Method'. *Methods*, 25(4), 402–408.
Loo, Y.-M., Fornek, J., Crochet, N., Bajwa, G., Perwitasari, O., Martinez-Sobrido, L., Akira, S., Gill, M. A., Garcia-Sastre, A., Katze, M. G., and Gale, M. (2008). 'Distinct RIG-I and MDA5 Signaling by RNA Viruses in Innate Immunity'. *Journal of Virology*, 82(1), 335–345.
Loo, Y.-M., and Gale, M. (2011). 'Immune Signaling by RIG-I-like Receptors'. *Immunity*, Elsevier Inc., 34(5), 680–692.
Lulli, D., Carbone, M. L., and Pastore, S. (2016). 'Epidermal growth factor receptor inhibitors trigger a type I interferon response in human skin'. *Oncotarget*, 7(30), 47777–47793.
Mackenzie, J. M., Jones, M. K., and Young, P. R. (1996). 'Immunolocalization of the dengue virus nonstructural glycoprotein NS1 suggests a role in viral RNA replication.' *Virology*, 220(1), 232–240.
Mackenzie, J. M., Khromykh, A. A., Jones, M. K., and Westaway, E. G. (1998). 'Subcellular localization and some biochemical properties of the flavivirus Kunjin nonstructural proteins NS2A and NS4A'. *Virology*, 245(2), 203–215.
Mackenzie, J. S., Gubler, D. J., and Petersen, L. R. (2004). 'Emerging flaviviruses: The spread and resurgence of japanese encephalitis, west nile and dengue viruses'. *Nature Medicine*, 10(12), S98–S109.
Martina, B. E. E., Koraka, P., and Osterhaus, A. D. M. E. (2009). 'Dengue virus pathogenesis: An integrated view'. *Clinical Microbiology Reviews*, 22(4), 564–581.
Massé, N., Davidson, A., Ferron, F., Alvarez, K., Jacobs, M., Romette, J. L., Canard, B., and Guillemot, J. C. (2010). 'Dengue virus replicons: Production of an interserotypic chimera and cell lines from different species, and establishment of a cell-based fluorescent assay to screen inhibitors, validated by the evaluation of ribavirin's activity'. *Antiviral Research*, 86(3), 296–305.
Maxfield, F. R., and Wüstner, D. (2012). 'Analysis of Cholesterol Trafficking with Fluorescent Probes'. *Methods in Cell Biology*, 108(1), 367–393.
Maxwell, K. N., Soccio, R. E., Duncan, E. M., Sehayek, E., and Breslow, J. L. (2003). 'Novel putative SREBP and LXR target genes identified by microarray analysis in liver of cholesterol-fed mice'. *Journal of Lipid Research*, 44(11), 2109–2119.
Mazein, A., Watterson, S., Hsieh, W. Y., Griffiths, W. J., and Ghazal, P. (2013). 'A comprehensive machine-readable view of the mammalian cholesterol biosynthesis pathway'. *Biochemical Pharmacology*, Elsevier Inc., 86(1), 56–66.
Mazzon, M., Jones, M., Davidson, A., Chain, B., and Jacobs, M. (2009). 'Dengue Virus NS5 Inhibits Interferon-α Signaling by Blocking Signal Transducer and Activator of Transcription 2 Phosphorylation'. *The Journal of Infectious Diseases*, 200(8), 1261–1270.
McLean, J. E., Wudzinska, A., Datan, E., Quaglino, D., and Zakeri, Z. (2011). 'Flavivirus NS4A-induced autophagy protects cells against death and enhances virus replication'. *Journal of Biological Chemistry*, 286(25), 22147–22159.
Medin, C. L., Fitzgerald, K. A., Alan, L., and Rothman, A. L. (2005). 'Dengue Virus Nonstructural Protein NS5 Induces Interleukin-8 Transcription and Secretion'. *Journal of*

Virology, 79(17), 11053–11061.
van Meerloo, J., and Cloos, J. (2011). 'Cell sensitivity assays: The MTT assay'. *Methods in Molecular Biology*, 731, 237–245.
Messina, J. P., Kraemer, M. U. G., Brady, O. J., Pigott, D. M., Shearer, F. M., Weiss, D. J., Golding, N., Ruktanonchai, C. W., Gething, P. W., Cohn, E., Brownstein, J. S., Khan, K., Tatem, A. J., Jaenisch, T., Murray, C. J. L., Marinho, F., Scott, T. W., and Hay, S. I. (2016). 'Mapping global environmental suitability for Zika virus'. *eLife*, 5, 1–19.
Miller, J. L., deWet, B. J. M., Martinez-Pomares, L., Radcliffe, C. M., Dwek, R. A., Rudd, P. M., and Gordon, S. (2008). 'The Mannose Receptor Mediates Dengue Virus Infection of Macrophages'. *PLoS Pathogens*, 4(2), e17.
Miller, S., Kastner, S., Krijnse-Locker, J., Bühler, S., and Bartenschlager, R. (2007). 'The non-structural protein 4A of dengue virus is an integral membrane protein inducing membrane alterations in a 2K-regulated manner'. *Journal of Biological Chemistry*, 282(12), 8873–8882.
Miller, S., Sparacio, S., and Bartenschlager, R. (2006). 'Subcellular localization and membrane topology of the dengue virus type 2 non-structural protein 4B'. *Journal of Biological Chemistry*, 281(13), 8854–8863.
Mlera, L., Melik, W., and Bloom, M. E. (2014). 'The role of viral persistence in flavivirus biology'. *Pathogens and Disease*, 71(2), 137–163.
Modhiran, N., Watterson, D., Blumenthal, A., Baxter, A. G., Young, P. R., and Stacey, K. J. (2017). 'Dengue virus NS1 protein activates immune cells via TLR4 but not TLR2 or TLR6'. *Immunology and Cell Biology*, Nature Publishing Group, 95(5), 491–495.
Modhiran, N., Watterson, D., Muller, D. A., Panetta, A. K., Sester, D. P., Liu, L., Hume, D. A., Stacey, K. J., and Young, P. R. (2015). 'Dengue virus NS1 protein activates cells via Toll-like receptor 4 and disrupts endothelial cell monolayer integrity'. *Science Translational Medicine*, 7(304), 304ra142-304ra142.
Modis, Y., Ogata, S., Clements, D., and Harrison, S. C. (2003). 'A ligand-binding pocket in the dengue virus envelope glycoprotein'. *PNAS*, 100(12), 6986–6991.
Moerman-Herzog, A., and Nakagawa, M. (2015). 'Early defensive mechanisms against human papillomavirus infection'. *Clinical and Vaccine Immunology*, 22(8), 850–857.
Mongkolsapaya, J., Dejnirattisai, W., Xu, X. N., Vasanawathana, S., Tangthawornchaikul, N., Chairunsri, A., Sawasdivorn, S., Duangchinda, T., Dong, T., Rowland-Jones, S., Yenchitsomanus, P. T., McMichael, A., Malasit, P., and Screaton, G. (2003). 'Original antigenic sin and apoptosis in the pathogenesis of dengue hemorrhagic fever'. *Nature Medicine*, 9(7), 921–927.
Mongkolsapaya, J., Duangchinda, T., Dejnirattisai, W., Vasanawathana, S., Avirutnan, P., Jairungsri, A., Khemnu, N., Tangthawornchaikul, N., Chotiyarnwong, P., Sae-Jang, K., Koch, M., Jones, Y., McMichael, A., Xu, X., Malasit, P., and Screaton, G. (2006). 'T Cell Responses in Dengue Hemorrhagic Fever: Are Cross-Reactive T Cells Suboptimal?' *The Journal of Immunology*, 176(6), 3821–3829.
Morrison, J., Aguirre, S., and Fernandez-Sesma, A. (2012). 'Innate immunity evasion by dengue virus'. *Viruses*, 4(3), 397–413.
Muller, D. A., and Young, P. R. (2013). 'The flavivirus NS1 protein: Molecular and structural biology, immunology, role inpathogenesis and application asadiagnostic biomarker.' *Antiviral Research*, Elsevier B.V., 98(2), 192–208.
Muñoz-Jordan, J. L., Laurent-rolle, M., Martínez-sobrido, L., Ashok, M., Ian, W., and Mun, J. L. (2005). 'Inhibition of Alpha / Beta Interferon Signaling by the NS4B Protein of Flaviviruses Inhibition of Alpha / Beta Interferon Signaling by the NS4B Protein of Flaviviruses'. *Journal of Virology*, 79(13), 8004–8013.
Muñoz-Jordan, J. L., Sanchez-Burgos, G. G., Laurent-Rolle, M., and Garcia-Sastre, A. (2003). 'Inhibition of interferon signaling by dengue virus'. *Proceedings of the National Academy of Sciences*, 100(24), 14333–14338.
Murray, K., Walker, C., Herrington, E., Lewis, J. A., McCormick, J., Beasley, D. W. C., Tesh, R. B., and Fisher-Hoch, S. (2010). 'Persistent Infection with West Nile Virus Years after Initial Infection'. *The Journal of Infectious Diseases*, 201(1), 2–4.

Mustafa, M. S., Rasotgi, V., Jain, S., and Gupta, V. (2015). 'Discovery of fifth serotype of dengue virus (DENV-5): A new public health dilemma in dengue control'. *Medical Journal Armed Forces India*, 71(1), 67–70.

Nakao, S., Lai, C.-J., and Young, N. S. (1989). 'Dengue Virus, A Flavivirus, Propagates in Human Bone Marrow Progenitors and Hematopoietic Cell Lines'. *Blood*, 74(4), 1235–1240.

Nasirudeen, A. M. A., Wong, H. H., Thien, P., Xu, S., Lam, K. P., and Liu, D. X. (2011). 'RIG-i, MDA5 and TLR3 synergistically play an important role in restriction of dengue virus infection'. *PLoS Neglected Tropical Diseases*, 5(1).

Ndenga, B. A., Mutuku, F. M., Ngugi, H. N., Mbakaya, J. O., Aswani, P., Musunzaji, P. S., Vulule, J., Mukoko, D., Kitron, U., and LaBeaud, A. D. (2017). 'Characteristics of Aedes aegypti adult mosquitoes in rural and urban areas of western and coastal Kenya'. *PLoS ONE*, 12(12), 1–14.

Nemésio, H., and Villalaín, J. (2014). 'Membrane interacting regions of dengue virus NS2A protein'. *Journal of Physical Chemistry B*, 118(34), 10142–10155.

Netsawang, J., Noisakran, S., Puttikhunt, C., Kasinrerk, W., Wongwiwat, W., Malasit, P., Yenchitsomanus, P. thai, and Limjindaporn, T. (2010). 'Nuclear localization of dengue virus capsid protein is required for DAXX interaction and apoptosis'. *Virus Research*, 147(2), 275–283.

Ng, C. Y., Gu, F., Phong, W. Y., Chen, Y. L., Lim, S. P., Davidson, A., and Vasudevan, S. G. (2007). 'Construction and characterization of a stable subgenomic dengue virus type 2 replicon system for antiviral compound and siRNA testing'. *Antiviral Research*, 76(3), 222–231.

Odorizzi, P. M., and Wherry, E. J. (2013). 'An Interferon Paradox'. *Science*, 340(6129), 155–156.

Overby, A. K., Popov, V. L., Niedrig, M., and Weber, F. (2010). 'Tick-Borne Encephalitis Virus Delays Interferon Induction and Hides Its Double-Stranded RNA in Intracellular Membrane Vesicles'. *Journal of Virology*, 84(17), 8470–8483.

Paupy, C., Delatte, H., Bagny, L., Corbel, V., and Fontenille, D. (2009). 'Aedes albopictus, an arbovirus vector: From the darkness to the light'. *Microbes and Infection*, 11(14–15), 1177–1185.

Peña, J., and Harris, E. (2012). 'Early dengue virus protein synthesis induces extensive rearrangement of the endoplasmic reticulum independent of the UPR and SREBP-2 pathway'. *PLoS ONE*, 7(6), 1–15.

Perera, R., and Kuhn, J. (2008). 'Stuctural Proteomics of Dengue Virus'. *Current Opinion in Microbiology*, 11(4), 369–377.

Pessoa, R., Patriota, J. V., De Lourdes De Souza, M., Felix, A. C., Mamede, N., and Sanabani, S. S. (2016). 'Investigation into an outbreak of dengue-like illness in pernambuco, Brazil, revealed a cocirculation of Zika, Chikungunya, and dengue virus type 1'. *Medicine (United States)*, 95(12), 1–9.

Poidinger, M., Coelen, R. J., and Mackenzie, J. S. (1991). 'Persistent infection of Vero cells by the flavivirus Murray Valley encephalits virus'. *Journal of General Virology*, 72(3), 573–578.

Ponlawat, A., and Harrington, L. C. (2005). 'Blood Feeding Patterns of_Aedes aegypti_and_Aedes albopictus_in Thailand'. *Journal of Medical Entomology*, 42(5), 844–849.

Pryor, M. J., Carr, J. M., Hocking, H., Davidson, A. D., Li, P., and Wright, P. J. (2001). 'Replication of dengue virus type 2 in human monocyte-derived macrophages: Comparisons of isolates and recombinant viruses with substitutions at amino acid 390 in the envelope glycoprotein'. *American Journal of Tropical Medicine and Hygiene*, 65(5), 427–434.

Radhakrishnan, A., Sun, L. P., Kwon, H. J., Brown, M. S., and Goldstein, J. L. (2004). 'Direct binding of cholesterol to the purified membrane region of SCAP: Mechanism for a sterol-sensing domain'. *Molecular Cell*, 15(2), 259–268.

Ravi, V., Desai, a S., Shenoy, P. K., Satishchandra, P., Chandramuki, a, and Gourie-Devi,

M. (1993). ‘Persistence of Japanese encephalitis virus in the human nervous system.’ *Journal of medical virology*, 40(4), 326–9.
Rehermann, B. (2009). ‘Science in medicine Hepatitis C virus versus innate and adaptive immune responses : a tale of coevolution and coexistence’. *Science in medicine*, 119(7), 1745–1754.
Reich, N. G., Shrestha, S., King, A. A., Rohani, P., Lessler, J., Kalayanarooj, S., Yoon, I.-K., Gibbons, R. V., Burke, D. S., and Cummings, D. A. T. (2013). ‘Interactions between serotypes of dengue highlight epidemiological impact of cross-immunity’. *Journal of The Royal Society Interface*, 10(86), 20130414–20130414.
Rodenhuis-Zybert, I. A., Wilschut, J., and Smit, J. M. (2010). ‘Dengue virus life cycle: Viral and host factors modulating infectivity’. *Cellular and Molecular Life Sciences*, 67(16), 2773–2786.
Rothman, A. L. (2011). ‘Immunity to dengue virus: A tale of original antigenic sin and tropical cytokine storms’. *Nature Reviews Immunology*, Nature Publishing Group, 11(8), 532–543.
Rothwell, C., LeBreton, A., Young Ng, C., Lim, J. Y. H., Liu, W., Vasudevan, S., Labow, M., Gu, F., and Gaither, L. A. (2009). ‘Cholesterol biosynthesis modulation regulates dengue viral replication’. *Virology*, Elsevier Inc., 389(1–2), 8–19.
Sahili, A. El, and Lescar, J. (2017). ‘Dengue virus non-structural protein 5’. *Viruses*, 9(4), 1–20.
Saka, H. A., and Valdivia, R. (2012). ‘Emerging Roles for Lipid Droplets in Immunity and Host-Pathogen Interactions’. *Annual Review of Cell and Developmental Biology*, 28(1), 411–437.
Salas-Benito, J. S., and De Nova-Ocampo, M. (2015). ‘Viral interference and persistence in mosquito-borne flaviviruses’. *Journal of Immunology Research*, 2015.
Samsa, M. M., Mondotte, J. A., Iglesias, N. G., Assunção-Miranda, I., Barbosa-Lima, G., Da Poian, A. T., Bozza, P. T., and Gamarnik, A. V. (2009). ‘Dengue virus capsid protein usurps lipid droplets for viral particle formation’. *PLoS Pathogens*, 5(10).
Sánchez-Vargas, I., Scott, J. C., Poole-Smith, B. K., Franz, A. W. E., Barbosa-Solomieu, V., Wilusz, J., Olson, K. E., and Blair, C. D. (2009). ‘Dengue virus type 2 infections of Aedes aegypti are modulated by the mosquito’s RNA interference pathway’. *PLoS Pathogens*, 5(2).
Scaturro, P., Cortese, M., Chatel-Chaix, L., Fischl, W., and Bartenschlager, R. (2015). ‘Dengue Virus Non-structural Protein 1 Modulates Infectious Particle Production via Interaction with the Structural Proteins’. *PLoS Pathogens*, 11(11), 1–32.
Van Der Schaar, H. M., Rust, M. J., Chen, Van Der Ende-Metselaar, H., Wilschut, J., Zhuang, X., and Smit, J. M. (2008). ‘Dissecting the cell entry pathway of dengue virus by single-particle tracking in living cells’. *PLoS Pathogens*, 4(12).
Schneider, W. M., Chevillotte, M. D., and Rice, C. M. (2014). ‘Interferon-Stimulated Genes: A Complex Web of Host Defenses’. *Annual Review of Immunology*, 32, 513–545.
Screaton, G., Mongkolsapaya, J., Yacoub, S., and Roberts, C. (2015). ‘New insights into the immunopathology and control of dengue virus infection’. *Nature Reviews Immunology*, Nature Publishing Group, 15(12), 745–759.
Sessions, O. M., Tan, Y., Goh, K. C., Liu, Y., Tan, P., Rozen, S., and Ooi, E. E. (2013). ‘Host Cell Transcriptome Profile during Wild-Type and Attenuated Dengue Virus Infection’. *PLoS Neglected Tropical Diseases*, 7(3), 1–12.
Sharp, T. M., Tomashek, K. M., Read, J. S., Margolis, H. S., and Waterman, S. H. (2017). ‘A New Look at an Old Disease: Recent Insights into the Global Epidemiology of Dengue’. *Current Epidemiology Reports*, 4(1), 11–21.
Sharpe, L. J., and Brown, A. J. (2013). ‘Controlling cholesterol synthesis beyond 3-hydroxy-3-methylglutaryl-CoA reductase (HMGCR)’. *Journal of Biological Chemistry*, 288(26), 18707–18715.
Shresta, S., Kyle, J. L., Snider, H. M., Basavapatna, M., Beatty, P. R., and Harris, E. (2004). ‘Interferon-dependent immunity is essential for resistance to primary dengue virus infection in mice, whereas T- and B-cell-dependent immunity are less critical.’ *Journal of*

virology, 78(6), 2701–10.
Shrivastava, S., Tiwari, D., Diwan, A., Lalwani, S., Modak, M., Mishra, A., and Arankalle, V. A. (2018). 'Co-circulation of all the four dengue virus serotypes and detection of a novel clade of DENV-4 (genotype I) virus in Pune, India,during 2016 season.' *PLoS ONE*, 13(2), e0192672.
Simmonds, P., Becher, P., Bukh, J., Gould, E. A., Meyers, G., Monath, T., Muerhoff, S., Pletnev, A., Rico-Hesse, R., Smith, D. B., and Stapleton, J. T. (2017). 'ICTV virus taxonomy profile: Flaviviridae'. *Journal of General Virology*, 98(1), 2–3.
Sonn, C. H., Yu, Y.-B., Hong, Y.-J., Shim, Y.-J., Bluestone, J. a, Min, B.-H., and Lee, K.-M. (2010). 'Clusterin synergizes with IL-2 for the expansion and IFN-γ production of natural killer cells.' *Journal of leukocyte biology*, 88(5), 955–963.
Soto-Acosta, R., Bautista-Carbajal, P., Cervantes-Salazar, M., Angel-Ambrocio, A. H., and Del Angel, R. M. (2017). 'DENV up-regulates the HMG-CoA reductase activity through the impairment of AMPK phosphorylation: A potential antiviral target'. *PLoS Pathogens*, 13(4).
Soto-Acosta, R., Mosso, C., Cervantes-Salazar, M., Puerta-Guardo, H., Medina, F., Favari, L., Ludert, J. E., and Del Angel, R. M. (2013). 'The increase in cholesterol levels at early stages after dengue virus infection correlates with an augment in LDL particle uptake and HMG-CoA reductase activity'. *Virology*, Elsevier, 442(2), 132–147.
Sprokholt, J., Helgers, L. C., and Geijtenbeek, T. B. H. (2018). 'Innate immune receptors drive dengue virus immune activation and disease'. *Future Virology*, 13(4).
Staples, J. E., Breiman, R. F., and Powers, A. M. (2009). 'Chikungunya Fever: An Epidemiological Review of a Re-Emerging Infectious Disease'. *Clinical Infectious Diseases*, 49(6), 942–948.
Suzuki, Y., Chin, W. X., Han, Q., Ichiyama, K., Lee, C. H., Eyo, Z. W., Ebina, H., Takahashi, H., Takahashi, C., Tan, B. H., Hishiki, T., Ohba, K., Matsuyama, T., Koyanagi, Y., Tan, Y. J., Sawasaki, T., Chu, J. J. H., Vasudevan, S. G., Sano, K., and Yamamoto, N. (2016). *Characterization of RyDEN (C19orf66) as an Interferon-Stimulated Cellular Inhibitor against Dengue Virus Replication*. *PLoS Pathogens*.
Tabor, D. E., Kim, J. B., Spiegelman, B. M., and Edwards, P. a. (1999). 'Identification of conserved cis elements and transcription factors required for sterol regulated transcription of stearoyl CoA desaturase 1 and 2'. *Journal of Biological Chemistry*, 274(29), 20603–20610.
Takhampunya, R., Ubol, S., Houng, H. S., Cameron, C. E., and Padmanabhan, R. (2006). 'Inhibition of dengue virus replication by mycophenolic acid and ribavirin'. *Journal of General Virology*, 87(7), 1947–1952.
Tassaneetrithep, B., Burgess, T. H., Granelli-Piperno, A., Trumpfheller, C., Finke, J., Sun, W., Eller, M. A., Pattanapanyasat, K., Sarasombath, S., Birx, D. L., Steinman, R. M., Schlesinger, S., and Marovich, M. A. (2003). 'DC-SIGN (CD209) Mediates Dengue Virus Infection of Human Dendritic Cells'. *The Journal of Experimental Medicine*, 197(7), 823–829.
Taylor-Robinson, A. W. (2016). 'A Putative Fifth Serotype of Dengue - Potential Implications for Diagnosis, Therapy and Vaccine Design'. *International Journal of Clinical & Medical Microbiology Open Access*, 1(101), 1–2.
Taylor, S., Wakem, M., Dijkman, G., Alsarraj, M., and Nguyen, M. (2010). 'A practical approach to RT-qPCR-Publishing data that conform to the MIQE guidelines'. *Methods*, Elsevier Inc., 50(4), S1–S5.
Teijaro, J. R. (2016). 'Type I interferons in viral control and immune regulation'. *Current Opinions in Virology*, 16, 31–40.
Teijaro, J. R., Ng, C., Lee, A. M., Sullivan, B. M., Sheehan, K. C. F., Welch, M., Schreiber, R. D., De La Torre, J. C., and Oldstone, M. B. A. (2013). 'Persistent LCMV infection is controlled by blockade of type I interferon signaling'. *Science*, 340(6129), 207–211.
Teo, C. S. H., and Chu, J. J. H. (2014). 'Cellular Vimentin Regulates Construction of Dengue Virus Replication Complexes through Interaction with NS4A Protein'. *Journal of Virology*, 88(4), 1897–1913.

Torres, S., Hernández, J. C., Giraldo, D., Arboleda, M., Rojas, M., Smit, J. M., and Urcuqui-Inchima, S. (2013). 'Differential Expression of Toll-like Receptors in Dendritic Cells of Patients with Dengue during Early and Late Acute Phases of the Disease'. *PLoS Neglected Tropical Diseases*, 7(2).

Trapnell, C., Roberts, A., Goff, L., Pertea, G., Kim, D., Kelley, D. R., Pimentel, H., Salzberg, S. L., Rinn, J. L., and Pachter, L. (2012). 'Differential gene and transcript expression analysis of RNA-seq experiments with TopHat and Cufflinks'. *Nature Protocols*, Nature Publishing Group, 7(3), 562–578.

Ubol, S., Masrinoul, P., Chaijaruwanich, J., Kalayanarooj, S., Charoensirisuthikul, T., and Kasisith, J. (2008). 'Differences in Global Gene Expression in Peripheral Blood Mononuclear Cells Indicate a Significant Role of the Innate Responses in Progression of Dengue Fever but Not Dengue Hemorrhagic Fever'. *The Journal of Infectious Diseases*, 197(10), 1459–1467.

Umareddy, I., Chao, A., Sampath, A., Gu, F., and Vasudevan, S. G. (2006). 'Dengue virus NS4B interacts with NS3 and dissociates it from single-stranded RNA'. *Journal of General Virology*, 87(9), 2605–2614.

Vaughn, D. W., Green, S., Kalayanarooj, S., Innis, B. L., Nimmannitya, S., Suntayakorn, S., Endy, T. P., Raengsakulrach, B., Rothman, a L., Ennis, F. a, and Nisalak, a. (2000). 'Dengue viremia titer, antibody response pattern, and virus serotype correlate with disease severity.' *The Journal of infectious diseases*, 181(1), 2–9.

Volpon, L., and Lancelin, J. M. (2000). 'Solution NMR structures of the polyene macrolide antibiotic filipin III'. *FEBS Letters*, 478(1–2), 137–140.

Waggoner, J. J., Gresh, L., Vargas, M. J., Ballesteros, G., Tellez, Y., Soda, K. J., Sahoo, M. K., Nuñez, A., Balmaseda, A., Harris, E., and Pinsky, B. A. (2016). 'Viremia and Clinical Presentation in Nicaraguan Patients Infected With Zika Virus, Chikungunya Virus, and Dengue Virus'. *Clinical Infectious Diseases*, 63(12), 1584–1590.

Wang, C. C., Huang, Z. S., Chiang, P. L., Chen, C. T., and Wu, H. N. (2009a). 'Analysis of the nucleoside triphosphatase, RNA triphosphatase, and unwinding activities of the helicase domain of dengue virus NS3 protein'. *FEBS Letters*, Federation of European Biochemical Societies, 583(4), 691–696.

Wang, Z., Gerstein, M., and Snyder, M. (2009b). 'RNA-Seq: a revolutionary tool for transcriptomics'. *Nature Review Genetics*, 10(1), 57–63.

Watterson, D., Modhiran, N., and Young, P. R. (2016). 'The many faces of the flavivirus NS1 protein offer a multitude of options for inhibitor design'. *Antiviral Research*, Elsevier B.V, 130, 7–18.

Welsch, S., Miller, S., Romero-Brey, I., Merz, A., Bleck, C. K. E., Walther, P., Fuller, S. D., Antony, C., Krijnse-Locker, J., and Bartenschlager, R. (2009). 'Composition and Three-Dimensional Architecture of the Dengue Virus Replication and Assembly Sites'. *Cell Host and Microbe*, 5(4), 365–375.

Whitehorn, J., and Simmons, C. P. (2011). 'The pathogenesis of dengue'. *Vaccine*, 29(42), 7221–7228.

Wieland, S., Makowska, Z., Campana, B., Calabrese, D., Dill, M. T., Chung, J., Chisari, F. V., and Heim, M. H. (2014). 'Simultaneous detection of hepatitis C virus and interferon stimulated gene expression in infected human liver'. *Hepatology*, 59(6), 2121–2130.

World Health Organisation. (2017). 'Dengue and severe dengue'. *WHO website*.

Xagorari, A., and Chlichlia, K. (2008). 'Toll-Like Receptors and Viruses: Induction of Innate Antiviral Immune Responses'. *The Open Microbiology Journal*, 2(1), 49–59.

Xie, X., Gayen, S., Kang, C., Yuan, Z., and Shib, P.-Y. (2013). 'Membrane Topology and Function of Dengue Virus NS2A Protein'. *Journal of Virology*, 87(8), 4609–4622.

Xie, X., Wang, Q.-Y., Xu, H. Y., Qing, M., Kramer, L., Yuan, Z., and Shi, P.-Y. (2011). 'Inhibition of Dengue Virus by Targeting Viral NS4B Protein'. *Journal of Virology*, 85(21), 11183–11195.

Xie, X., Zou, J., Puttikhunt, C., Yuan, Z., and Shi, P.-Y. (2015a). 'Two Distinct Sets of NS2A Molecules Are Responsible for Dengue Virus RNA Synthesis and Virion Assembly'. *Journal of Virology*, 89(2), 1298–1313.

Xie, X., Zou, J., Wang, Q. Y., and Shi, P. Y. (2015b). 'Targeting dengue virus NS4B protein for drug discovery'. *Antiviral Research*, Elsevier B.V., 118, 39–45.

Yabe, D., Brown, M. S., and Goldstein, J. L. (2002). 'Insig-2, a second endoplasmic reticulum protein that binds SCAP and blocks export of sterol regulatory element-binding proteins.' *Proceedings of the National Academy of Sciences of the United States of America*, 99(20), 12753–8.

Ye, J., and DeBose-Boyd, R. A. (2011). 'Regulation of Cholesterol and Fatty Acid Synthesis'. *Cold Spring Harbor Perspectives in Biology*, 3(7), 1–14.

Young, P. R., Hilditch, P. A., Bletchly, C., and Halloran, W. (2000). 'An antigen capture enzyme-linked immunosorbent assay reveals high levels of the dengue virus protein NS1 in the sera of infected patients'. *Journal of Clinical Microbiology*, 38(3), 1053–1057.

Yu, C.-Y., Chang, T. H., Liang, J. J., Chiang, R. L., Lee, Y. L., Liao, C. L., and Lin, Y. L. (2012). 'Dengue virus targets the adaptor protein MITA to subvert host innate immunity'. *PLoS Pathogens*, 8(6).

Yu, I. M., Zhang, W., Holdaway, H. A., Li, L., Kostyuchenko, V. A., Chipman, P. R., Kuhn, R. J., Rossmann, M. G., and Chen, J. (2008). 'Structure of the immature dengue virus at low pH primes proteolytic maturation.' *Science*, 319(5871), 1834–1837.

Yung, C.-F., Lee, K.-S., Thein, T.-L., Tan, L.-K., Gan, V. C., Wong, J. G. X., Lye, D. C., Ng, L.-C., and Leo, Y.-S. (2015). 'Dengue Serotype-Specific Differences in Clinical Manifestation, Laboratory Parameters and Risk of Severe Disease in Adults, Singapore'. *The American Journal of Tropical Medicine and Hygiene*, 92(5), 999–1005.

Zaitseva, E., Yang, S. T., Melikov, K., Pourmal, S., and Chernomordik, L. V. (2010). 'Dengue virus ensures its fusion in late endosomes using compartment-specific lipids'. *PLoS Pathogens*, 6(10).

Zhang, Y., Corver, J., Chipman, P. R., Zhang, W., Pletnev, S. V, Sedlak, D., Baker, T. S., Strauss, J. H., Kuhn, R. J., and Rossmann, M. G. (2003). 'Structures of immature flavivirus particles'. *The EMBO Journal*, 22(11).

Zhang, Y., Zhang, W., Ogata, S., Clements, D., Strauss, J. H., Baker, T. S., Kuhn, R. J., and Rossmann, M. G. (2004). 'Conformational changes of the flavivirus E glycoprotein'. *Structure*, 12(9), 1607–1618.

Zhao, Y., Soh, T. S., Lim, S. P., Chung, K. Y., Swaminathan, K., Vasudevan, S. G., Shi, P.-Y., Lescar, J., and Luo, D. (2015a). 'Molecular basis for specific viral RNA recognition and 2′-O-ribose methylation by the dengue virus nonstructural protein 5 (NS5)'. *Proceedings of the National Academy of Sciences*, 112(48), 14834–14839.

Zhao, Y., Soh, T. S., Zheng, J., Chan, K. W. K., Phoo, W. W., Lee, C. C., Tay, M. Y. F., Swaminathan, K., Cornvik, T. C., Lim, S. P., Shi, P. Y., Lescar, J., Vasudevan, S. G., and Luo, D. (2015b). 'A Crystal Structure of the Dengue Virus NS5 Protein Reveals a Novel Inter-domain Interface Essential for Protein Flexibility and Virus Replication'. *PLoS Pathogens*, 11(3), 1–27.

Zheng, Z., Wang, L., and Pan, J. (2017). 'Interferon-stimulated gene 20-kDa protein (ISG20) in infection and disease: Review and outlook'. *Intractable and Rare Diseases Research*, 6(1), 35–40.

Zou, J., Lee, L. T., Wang, Q. Y., Xie, X., Lu, S., Yau, Y. H., Yuan, Z., Geifman Shochat, S., Kang, C., Lescar, J., and Shi, P.-Y. (2015a). 'Mapping the Interactions between the NS4B and NS3 Proteins of Dengue Virus'. *Journal of Virology*, 89(7), 3471–3483.

Zou, J., Xie, X., Wang, Q.-Y., Dong, H., Lee, M. Y., Kang, C., Yuan, Z., and Shi, P.-Y. (2015b). 'Characterization of Dengue Virus NS4A and NS4B Protein Interaction'. *Journal of Virology*, 89(7), 3455–3470.

Zybert, I. A., van der Ende-Metselaar, H., Wilschut, J., and Smit, J. M. (2008). 'Functional importance of dengue virus maturation: Infectious properties of immature virions'. *Journal of General Virology*, 89(12), 3047–3051.

Supplementary material.

Supplementary Table 1: Genes downregulated in H-v601-Per1 and H-v601-Per2 cells, and upregulated in H-v601 cells, relative to mock. Pairwise comparisons between the transcriptome of HEK293 (Mock), H-v601-Per1, H-v601-Per2, and H-v601 cells was performed. All genes that were differentially expressed by at least two-fold in at least one pairwise comparison were identified, and from these, 164 genes that were downregulated in H-v601-Per1 and H-v601-Per2, and upregulated in H-v601, relative to mock, were further identified. "Expression value" indicates the value reads derived from the transcriptomics sequencing, indicating level of gene expression; "Log_2 fold change" indicates the fold difference in gene expression from Sample A vs. Sample B.

Gene	Expression value						Log_2 fold change				
	Mock	H-v601-Per1	H-v601-Per2	H-v601	H-Rep	H-Rep-4B$_{T66A}$	Mock vs. H-v601	Mock vs. H-v601-Per1	Mock vs. H-v601-Per2	H-v601-Per1 vs. H-v601	H-v601-Per2 vs. H-v601
ALDH1A2	27.4431	22.5445	15.6866	39.0591	46.1925	29.9937	0.509216	-0.283669	-0.806913	0.792885	1.31613
ARL17A	0.686765	0.383318	0.582039	0.922575	0.770011	0.568848	0.42585	-0.841275	-0.238699	1.26712	0.664549
ARMCX4	0.431108	0.108809	0.373924	0.791748	0.005192	0.007628	0.87699	-1.98625	-0.205306	2.86324	1.0823
BMPER	0.530769	0.390212	0.278734	0.811001	0.241092	0.169452	0.61162	-0.443826	-0.929193	1.05545	1.54081
C8orf34	1.21281	0.761691	0.821389	1.80656	0.515554	0.458926	0.574889	-0.671075	-0.562215	1.24596	1.1371
CCNG2	6.00136	4.43303	4.62964	9.33893	5.36773	4.61509	0.637968	-0.436996	-0.37439	1.07496	1.01236
CETN3	38.8415	27.8694	35.9782	63.8936	42.5858	27.6015	0.718074	-0.478916	-0.110474	1.19699	0.828547
COL2A1	6.9222	3.42476	3.78209	7.63417	0.023382	0.024413	0.141241	-1.01523	-0.872047	1.15647	1.01329
CSTF3	74.147	47.9646	64.7698	104.472	65.1272	61.4391	0.494652	-0.628419	-0.195068	1.12307	0.68972
DFNB59	1.47376	0.847432	0.843055	2.02295	0.637803	0.61347	0.45696	-0.79833	-0.805801	1.25529	1.26276
DMC1	12.4989	10.3501	12.345	24.2723	11.7505	9.28562	0.957508	-0.272151	-0.017876	1.22966	0.975384
EYA1	2.44403	1.64507	1.42063	3.24436	3.81804	4.44176	0.408673	-0.571113	-0.782734	0.979786	1.19141
FABP5	7.62246	5.01068	6.14778	11.0871	13.9931	16.9905	0.540547	-0.605251	-0.31019	1.1458	0.850738
FAM150A	4.9985	2.31651	3.67517	9.05442	0.22936	0.556731	0.857128	-1.10954	-0.443684	1.96667	1.30081
FAM173B	6.97858	4.62885	5.11443	9.29097	5.16271	4.18649	0.412895	-0.59228	-0.448359	1.00518	0.861254
FAM3C	5.3898	3.42242	4.22822	7.08404	7.29714	6.32945	0.394342	-0.655213	-0.350181	1.04955	0.744522
FLVCR1-AS1	2.43812	2.28869	2.05627	4.77429	2.43523	1.71498	0.969516	-0.0912492	-0.245739	1.06077	1.21525
FOXB1	1.73221	0.96462	0.846749	2.09142	0.820184	1.22152	0.271869	-0.844581	-1.03261	1.11645	1.30448
GATA6-AS1	1.24874	0.780959	1.18482	1.8609	0.282028	0.428935	0.575525	-0.677155	-0.075808	1.25268	0.651334
GBE1	6.55615	3.42676	5.26767	9.1508	7.01548	6.45016	0.481049	-0.936006	-0.315686	1.41705	0.796734

Gene	Expression value						Log_2 fold change				
	Mock	H-v601-Per1	H-v601-Per2	H-v601	H-Rep	H-Rep-4B$_{T66A}$	Mock vs. H-v601	Mock vs. H-v601-Per1	Mock vs. H-v601-Per2	H-v601-Per1 vs. H-v601	H-v601-Per2 vs. H-v601
GJA1	22.1063	14.6298	17.7361	33.5795	39.612	29.9324	0.603123	-0.595549	-0.317768	1.19867	0.920892
GMFG	0.346512	0.147561	0.110066	0.607606	0.158576	0.191808	0.810229	-1.23159	-1.65454	2.04182	2.46477
GTF2A1	10.6052	7.51198	8.7086	16.2423	13.9298	9.8482	0.614992	-0.497501	-0.284254	1.11249	0.899245
GTF2H4	1.4484	1.13232	1.37359	2.32886	2.16322	1.81838	0.685166	-0.355175	-0.076504	1.04034	0.76167
H2AFZ	618.555	385.015	472.095	844.442	606.288	519.284	0.449097	-0.683987	-0.389827	1.13308	0.838923
HIST1H4I	0.592023	0.100401	0.199704	1.00721	0	0.555206	0.766645	-2.55988	-1.56779	3.32652	2.33443
HMGB1	57.3536	32.1961	41.3367	65.2439	56.1397	54.5732	0.185958	-0.832996	-0.472461	1.01895	0.65842
HMGCR	30.7668	19.0921	22.3969	41.4481	27.8005	26.4677	0.42993	-0.688397	-0.458078	1.11833	0.888008
HMGCS1	24.5027	11.0513	13.0036	36.7127	14.823	14.5208	0.583339	-1.14873	-0.914031	1.73207	1.49737
HNRNPA2B1	590.892	412.159	464.393	820.913	541.469	524.864	0.474334	-0.519694	-0.347548	0.994028	0.821883
HNRNPCL1	5.03041	4.24043	3.97049	9.27558	6.59825	6.32511	0.88276	-0.246465	-0.34136	1.12923	1.22412
HSP90B1	2825.7	1654.71	2471.85	7603.09	1223.86	1909.14	1.42798	-0.772029	-0.193019	2.20001	1.621
HSPA13	27.4569	26.3277	27.1017	62.6303	22.2519	17.7736	1.18969	-0.0605838	-0.018786	1.25028	1.20848
HSPD1	381.731	239.858	302.359	493.222	380.765	349.682	0.369682	-0.670375	-0.336295	1.04006	0.705976
HSPE1	156.336	95.111	114.676	206.312	147.153	151.811	0.400183	-0.716963	-0.447087	1.11715	0.847269
IDH1-AS1	2.72612	2.53265	2.31519	5.06143	1.52871	1.85464	0.892695	-0.106202	-0.235718	0.998897	1.12841
IDI1	49.4392	23.5415	30.9303	75.2657	33.1623	30.0975	0.606337	-1.07045	-0.676635	1.67678	1.28297
INSIG1	25.0952	12.5145	21.4595	43.1922	17.4371	14.0131	0.783357	-1.00381	-0.225798	1.78717	1.00916
IPO9-AS1	2.3561	2.19342	1.49937	3.04056	1.35623	1.57112	0.367937	-0.103217	-0.652042	0.471154	1.01998
ITGA8	1.46305	1.03773	1.05337	2.23719	1.29107	1.31371	0.612712	-0.495547	-0.473969	1.10826	1.08668
KIAA0101	42.4231	30.9669	32.959	64.3964	63.5105	57.1765	0.60213	-0.454124	-0.364178	1.05625	0.966308
LDLR	6.83483	3.57882	5.25353	7.50273	6.81145	5.04638	0.13451	-0.933421	-0.37962	1.06793	0.51413
LHB	0.921149	0.471416	0.5728	1.1223	0.79295	2.10258	0.28495	-0.966435	-0.685404	1.25138	0.970354
LINC00853	0.559103	0.405312	0.472307	0.810621	0.481821	0.434236	0.535914	-0.46408	-0.243389	0.999993	0.779303
LINC01351	1.5215	0.871104	0.940887	2.35184	1.03375	0.609878	0.628294	-0.804579	-0.693403	1.43287	1.3217
LOC100129216	3.95055	1.4746	2.84912	4.14529	5.31726	3.88718	0.0694188	-1.42173	-0.471536	1.49115	0.540955

Gene	Expression value						Log_2 fold change				
	Mock	H-v601-Per1	H-v601-Per2	H-v601	H-Rep	H-Rep-4B$_{T66A}$	Mock vs. H-v601	Mock vs. H-v601-Per1	Mock vs. H-v601-Per2	H-v601-Per1 vs. H-v601	H-v601-Per2 vs. H-v601
LOC101928812	1.458	0.988651	0.839633	2.2336	1.12156	0.858216	0.615382	-0.560457	-0.796158	1.17584	1.41154
LOC113230	2.10162	1.24044	0.924326	3.66502	0.473133	0.453538	0.802319	-0.760656	-1.18503	1.56298	1.98735
LOC650368	0.414999	0.161971	0.391356	0.783751	17.1521	17.119	0.917289	-1.35737	-0.084623	2.27466	1.00191
LOC731157	0.718552	0.560046	0.244996	0.969733	0.132509	0.711741	0.432495	-0.359547	-1.55234	0.792042	1.98483
LRP2	1.85517	0.946884	1.342	2.46823	0.294904	0.340945	0.411928	-0.970291	-0.467162	1.38222	0.879091
LUM	0.510362	0.28636	0.347368	1.32412	0.543278	0.196073	1.37544	-0.83369	-0.555056	2.20913	1.9305
MAD2L1	96.5252	65.7332	81.6432	154.734	105.142	82.195	0.680809	-0.554283	-0.241573	1.23509	0.922382
MANEA-AS1	0.789227	0.733018	0.763346	1.54225	0.534944	0.532869	0.966524	-0.106591	-0.048101	1.07311	1.01463
MDH1B	0.474595	0.415011	0.455175	0.829073	0.400692	0.55979	0.804801	-0.193549	-0.060278	0.99835	0.86508
MID1IP1-AS1	5.34565	2.67761	3.25419	5.62244	3.01085	2.87812	0.0728317	-0.997419	-0.716064	1.07025	0.788896
MIR1304	290.109	237.786	82.2472	396.035	236.994	322.491	0.449035	-0.286929	-1.81856	0.735964	2.26759
MIR1470	175.949	0	150.14	205.691	0	0	0.225322	#NAME?	-0.228849	inf	0.45417
MIR17	24.9535	13.8565	16.7025	28.361	11.8281	10.4282	0.184668	-0.848682	-0.57918	1.03335	0.763848
MIR221	76.2047	60.7734	70.6965	173.262	141.814	102.131	1.185	-0.32644	-0.10824	1.51144	1.29324
MIR3064	6110.53	4316.78	4611.04	10857.8	4375.36	5024.4	0.829364	-0.501343	-0.406207	1.33071	1.23557
MIR320A	26.7998	22.9944	0	62.6601	0	29.8894	1.22532	-0.22094	#NAME?	1.44626	inf
MIR3607	66.1326	0	0	166.185	0	36.3395	1.32936	#NAME?	#NAME?	inf	inf
MIR3614	78.2105	18.4441	20.1974	96.9441	13.7551	135.188	0.309792	-2.08421	-1.95319	2.394	2.26298
MIR3662	39.9439	0	0	51.8246	0	38.6094	0.375661	#NAME?	#NAME?	inf	inf
MIR3916	138.928	84.9389	47.0895	284.689	231.435	217.732	1.03505	-0.709844	-1.56087	1.74489	2.59591
MIR4517	590.363	335.48	139.019	689.01	368.363	359.084	0.222922	-0.815376	-2.08632	1.0383	2.30924
MIR5001	238.806	225.343	186.679	374.16	124.121	165.773	0.647813	-0.0837194	-0.355285	0.731533	1.0031
MIR5008	13.8109	0	0	19.0745	0	0	0.465836	#NAME?	#NAME?	inf	inf
MIR5047	2285.43	1140.05	1478.01	3532.48	2136.4	1916.04	0.628218	-1.00337	-0.628807	1.63159	1.25702
MIR564	289.12	137.126	251.426	444.423	94.788	240.711	0.620266	-1.07617	-0.201533	1.69643	0.821799
MIR641	132.324	95.2592	83.8138	230.889	62.1591	68.524	0.803121	-0.474146	-0.658816	1.27727	1.46194

Gene	Expression value						Log_2 fold change				
	Mock	H-v601-Per1	H-v601-Per2	H-v601	H-Rep	H-Rep-4B$_{T66A}$	Mock vs. H-v601	Mock vs. H-v601-Per1	Mock vs. H-v601-Per2	H-v601-Per1 vs. H-v601	H-v601-Per2 vs. H-v601
MIR6727	322.833	285.111	91.8261	1178.05	612.899	990.645	1.86754	-0.179263	-1.81381	2.0468	3.68135
MIR6764	175.949	150.966	0	205.691	0	0	0.225322	-0.22094	#NAME?	0.446261	inf
MIR6875	223.548	0	46.9927	257.519	101.556	161.356	0.204092	#NAME?	-2.25008	inf	2.45417
MIR7107	30.5086	26.1884	0	35.6583	0	0	0.225021	-0.220289	#NAME?	0.445309	inf
MIRLET7D	39.8537	0	0	101.633	75.0928	58.3851	1.35059	#NAME?	#NAME?	inf	inf
MSMO1	20.8557	10.7809	15.0143	30.3344	21.1019	17.5169	0.540515	-0.951965	-0.4741	1.49248	1.01461
MST1	1.38095	1.28696	0.749804	1.78692	0.669021	0.899452	0.371817	-0.101687	-0.881074	0.473504	1.25289
MZT1	53.2331	37.7417	39.434	99.8712	36.8131	28.1183	0.907745	-0.496163	-0.432885	1.40391	1.34063
N4BP2	4.3699	3.38795	3.49763	8.00689	2.92165	2.84634	0.873642	-0.367187	-0.321224	1.24083	1.19487
NUDCD2	40.5315	32.0306	40.1945	76.5897	38.3446	38.3195	0.918105	-0.339593	-0.012046	1.2577	0.930152
NUDT12	10.7347	8.22739	9.32255	16.4008	10.659	7.26533	0.611489	-0.38377	-0.20348	0.995259	0.814969
OR7E12P	0.252558	0.134445	0.115566	0.609711	10.6133	8.87469	1.27151	-0.909604	-1.12789	2.18111	2.3994
OSTN	3.26416	3.18425	2.34603	8.60667	1.45803	2.61806	1.39874	-0.0357595	-0.476491	1.4345	1.87523
PCYT1B	0.97227	0.628306	0.618774	1.31804	0.617351	0.362699	0.438961	-0.62989	-0.651945	1.06885	1.09091
PDHA1	41.3083	24.7734	39.5157	51.052	63.944	62.2375	0.305535	-0.73764	-0.064005	1.04317	0.36954
PGK1	210.976	142.552	180.242	310.859	114.77	104.379	0.559182	-0.565589	-0.227145	1.12477	0.786327
PIGA	9.21179	6.02201	7.6554	11.9709	6.91295	5.896	0.377973	-0.613237	-0.267003	0.99121	0.644976
PSAT1	165.464	143.782	161.241	315.385	96.963	81.1707	0.930599	-0.202632	-0.037297	1.13323	0.967896
PTPRCAP	0.446622	0.192189	0.330711	0.580051	0.573185	0.533204	0.377125	-1.21653	-0.433484	1.59366	0.810609
PUF60	2.9728	1.8277	1.93865	3.81279	2.29507	2.63868	0.359026	-0.701797	-0.61677	1.06082	0.975796
RAB40A	0.688402	0.561089	0.465167	1.04227	1.77531	0.923188	0.598404	-0.295022	-0.565501	0.893426	1.1639
RASL10B	0.701822	0.005591	0.01112	0.726967	0.037093	0.083631	0.0507839	-6.97197	-5.97988	7.02275	6.03066
RGS4	0.725831	0.386541	0.557353	0.791211	1.72379	1.56354	0.12443	-0.909013	-0.381042	1.03344	0.505472
RIPPLY2	7.06164	6.68791	5.63934	11.4222	0.934267	0.873719	0.693768	-0.0784475	-0.324477	0.772215	1.01824
RND2	3.92679	1.99985	3.31935	5.20836	2.10177	2.33269	0.407481	-0.973459	-0.242447	1.38094	0.649928
RNF139-AS1	2.51265	1.42332	0.636691	2.9527	1.18655	2.60626	0.232825	-0.819952	-1.98054	1.05278	2.21337

Gene	Expression value						Log_2 fold change				
	Mock	H-v601-Per1	H-v601-Per2	H-v601	H-Rep	H-Rep-4B$_{T66A}$	Mock vs. H-v601	Mock vs. H-v601-Per1	Mock vs. H-v601-Per2	H-v601-Per1 vs. H-v601	H-v601-Per2 vs. H-v601
RNF175	0.39961	0	0	1.03575	0.027464	0	1.37401	#NAME?	#NAME?	inf	inf
RNU4ATAC	17.5103	12.2151	8.91219	17.771	6.42007	16.5181	0.0213177	-0.519542	-0.974356	0.54086	0.995674
RNVU1-15	23.7721	15.6894	18.9443	39.989	7.79398	14.9101	0.750334	-0.599477	-0.32751	1.34981	1.07784
RPS18	0.579594	0.444927	0.442495	1.33463	0.748395	0.401897	1.20332	-0.381472	-0.389381	1.58479	1.5927
RPS29	448.813	175.023	256.459	521.998	417.543	445.172	0.217929	-1.35857	-0.807384	1.5765	1.02531
RSL24D1	58.9394	49.319	57.303	99.5207	64.5141	57.3207	0.755763	-0.257091	-0.040623	1.01285	0.796387
SCARNA20	3.4814	2.98706	2.97073	8.13977	0	7.76548	1.22532	-0.22094	-0.228849	1.44626	1.45417
SCARNA23	24.5762	24.398	8.91219	28.111	19.5395	15.531	0.193871	-0.0104967	-1.46341	0.204368	1.65728
SCARNA27	221.71	88.8814	141.327	228.95	212.654	127.128	0.0463645	-1.31872	-0.64963	1.36508	0.695994
SCD	148.447	91.0446	124.855	182.58	121.066	102.575	0.298576	-0.705304	-0.249691	1.00388	0.548267
SCML1	49.818	30.4456	44.7481	68.9251	30.5107	26.6447	0.468362	-0.710434	-0.154842	1.1788	0.623204
SCOC	55.0798	37.9976	45.6366	84.2861	58.4098	39.7	0.613771	-0.535615	-0.271332	1.14939	0.885103
SEC61G	222.502	199.751	217.184	514.023	225.485	214.82	1.20802	-0.155616	-0.034897	1.36363	1.24291
SEMA3C	4.26482	3.77488	2.28938	4.8151	2.99782	2.75164	0.175082	-0.176052	-0.897526	0.351134	1.07261
SHISA2	5.09843	3.13003	4.09327	7.10392	4.1841	3.45748	0.478562	-0.703877	-0.3168	1.18244	0.795362
SMIM14	3.01285	2.99224	2.84355	5.6819	1.45993	1.46921	0.915245	-0.0099013	-0.083433	0.925146	0.998678
SMS	26.2116	14.8745	23.9956	32.7871	39.6827	34.3452	0.322928	-0.817358	-0.127432	1.14029	0.450359
SNORA14B	174.57	111.673	99.6689	215.327	83.6392	93.2114	0.30272	-0.644528	-0.808594	0.947248	1.11131
SNORA15	6.35935	5.45636	5.48761	16.4188	5.86367	14.1849	1.3684	-0.22094	-0.2127	1.58934	1.5811
SNORA18	269.915	215.999	257.033	464.759	403.486	325.325	0.783976	-0.321479	-0.070552	1.10546	0.854528
SNORA29	65.5205	27.327	48.7197	75.4078	63.7769	38.0815	0.202769	-1.26162	-0.42744	1.46439	0.630209
SNORA58	3.99138	2.04267	2.37008	7.08306	3.6904	2.21264	0.827483	-0.966435	-0.751951	1.79392	1.57943
SNORA76C	239.136	47.0662	113.899	396.996	224.35	220.828	0.731295	-2.34506	-1.07008	3.07636	1.80137
SNORD105	22.3591	0	0	30.8773	0	0	0.465682	#NAME?	#NAME?	inf	inf
SNORD110	1001.67	635.914	518.271	1170.96	813.948	1282.59	0.225293	-0.6555	-0.950624	0.880792	1.17592
SNORD12	169.788	43.5691	115.431	289.556	188.657	243.172	0.770108	-1.96236	-0.556701	2.73246	1.32681

Gene	Expression value						Log_2 fold change				
	Mock	H-v601-Per1	H-v601-Per2	H-v601	H-Rep	H-Rep-4B$_{T66A}$	Mock vs. H-v601	Mock vs. H-v601-Per1	Mock vs. H-v601-Per2	H-v601-Per1 vs. H-v601	H-v601-Per2 vs. H-v601
SNORD126	21.8465	9.37946	0	27.8522	20.14	12.1921	0.350389	-1.21983	#NAME?	1.57021	inf
SNORD12B	92.494	32.1207	78.1571	138.319	154.353	135.504	0.580573	-1.52585	-0.242982	2.10643	0.823555
SNORD14C	265.06	66.0717	225.014	454.713	492.757	278.685	0.778635	-2.00422	-0.236305	2.78285	1.01494
SNORD16	335.351	188.88	311.755	450.431	467.967	358.222	0.425636	-0.828203	-0.105259	1.25384	0.530895
SNORD19B	524.163	404.784	482.763	1059.5	622.472	750.783	1.0153	-0.372864	-0.118702	1.38817	1.134
SNORD22	578.31	391.041	498.057	905.209	878.876	757.589	0.646408	-0.564524	-0.215534	1.21093	0.861941
SNORD28	1610.31	1014.39	1442.96	2360.33	2184.44	1881.24	0.551644	-0.666726	-0.158316	1.21837	0.70996
SNORD31	712.362	473.826	673.193	1240.58	1176.53	703.89	0.800327	-0.588254	-0.081590	1.38858	0.881917
SNORD42A	411.436	233.033	347.882	1038.93	762.177	302.908	1.33635	-0.820133	-0.242069	2.15649	1.57842
SNORD45C	455.723	149.707	238.093	704.53	263.009	593.686	0.628504	-1.60602	-0.936633	2.23452	1.56514
SNORD49A	964.667	677.814	869.776	1478.12	1226.72	527.051	0.61566	-0.509143	-0.149387	1.1248	0.765048
SNORD50B	361.505	51.4414	102.32	471.395	451.868	443.13	0.382923	-2.81301	-1.82092	3.19594	2.20385
SNORD53	40.2613	0	34.3556	149.74	74.2462	280.832	1.89499	#NAME?	-0.228849	inf	2.12384
SNORD65	966.92	874.549	562.812	2409.49	2083.3	997.348	1.31726	-0.144858	-0.780744	1.46211	2.098
SNORD67	67.3058	34.9167	45.5595	82.5355	49.7835	29.9135	0.294285	-0.946811	-0.562978	1.2411	0.857263
SNORD69	603.657	361.728	446.778	867.726	282.218	924.429	0.523509	-0.738823	-0.43417	1.26233	0.95768
SNORD72	30.478	0	0	42.0937	56.2047	0	0.465836	#NAME?	#NAME?	inf	inf
SNORD80	7284.71	4270.02	6288.28	11964.1	8484.51	5978.29	0.715772	-0.77063	-0.212208	1.4864	0.92798
SNORD96A	4635.73	2295.82	3240.26	5980.47	3179.16	2649.36	0.367462	-1.01379	-0.516687	1.38125	0.884149
SNORD98	525.351	224.283	519.631	1434.69	496.068	97.5646	1.44938	-1.22796	-0.015792	2.67734	1.46518
SNRPE	54.467	40.7081	41.5217	85.1558	61.2189	54.7783	0.644723	-0.420066	-0.391515	1.06479	1.03624
SNRPG	57.5128	39.6245	51.8299	83.4139	50.9643	61.2796	0.536403	-0.537493	-0.150099	1.0739	0.686503
SPAG8	0.556813	0.230565	0.384067	0.625074	0.429475	0.470186	0.166835	-1.27202	-0.535835	1.43885	0.70267
SPARC	4.45521	0.950907	1.96659	8.36797	12.7683	3.40761	0.909386	-2.22812	-1.1798	3.1375	2.08918
SPC25	0.307792	0.21935	0.290679	0.608486	0.188579	0.404005	0.98327	-0.488719	-0.082525	1.47199	1.0658
SQLE	54.6982	34.4122	43.9604	74.4243	45.4986	38.8255	0.44428	-0.668576	-0.31529	1.11286	0.75957

Gene	Expression value						Log_2 fold change				
	Mock	H-v601-Per1	H-v601-Per2	H-v601	H-Rep	H-Rep-4B$_{T66A}$	Mock vs. H-v601	Mock vs. H-v601-Per1	Mock vs. H-v601-Per2	H-v601-Per1 vs. H-v601	H-v601-Per2 vs. H-v601
ST3GAL6-AS1	0.460003	0.327822	0.316097	0.846371	0.428436	0.647632	0.879648	-0.488731	-0.541276	1.36838	1.42092
STARD4	8.11822	6.60576	6.6147	15.6302	6.80337	5.97456	0.9451	-0.297439	-0.295489	1.24254	1.24059
SULF1	3.2881	2.67036	2.80594	6.33437	6.94355	4.58935	0.945948	-0.300217	-0.228769	1.24617	1.17472
SULT1C4	2.02076	1.87774	1.94568	4.09329	0.178666	0.175046	1.01836	-0.105904	-0.054628	1.12426	1.07299
SYTL5	1.2429	1.23732	0.749094	1.90221	1.66049	1.63246	0.613973	-0.0064890	-0.730487	0.620462	1.34446
TFAM	23.3559	13.0286	18.8172	36.2233	44.572	45.0728	0.633129	-0.84211	-0.311741	1.47524	0.944869
TIMM17A	107.348	79.7757	77.0385	153.268	109.736	99.2525	0.513763	-0.428276	-0.478646	0.942039	0.992409
TMEM100	2.26495	1.39666	1.49263	4.77166	4.04012	1.92958	1.07501	-0.6975	-0.601618	1.77251	1.67663
TMSB4X	12.1564	9.25037	7.97571	23.1644	1.97314	3.67559	0.930193	-0.394132	-0.608029	1.32432	1.53822
TNFRSF10D	4.79517	2.43374	4.24356	5.43668	13.8757	13.5736	0.181143	-0.978408	-0.176309	1.15955	0.357452
TXNDC17	23.5686	16.7314	21.165	33.7328	22.8833	19.9296	0.517285	-0.494307	-0.155183	1.01159	0.672468
UBAC2-AS1	2.16774	1.41739	1.96355	2.82924	0.860653	0.707231	0.384222	-0.612959	-0.142726	0.997181	0.526947
ULBP1	1.24548	1.11871	0.774033	2.51809	0.992301	0.992666	1.01562	-0.15487	-0.686241	1.17049	1.70186
ZNF534	2.20946	1.7244	1.96618	3.69092	2.63516	3.42806	0.740284	-0.3576	-0.1683	1.09788	0.908584

Supplementary Table 2: Genes upregulated by at least 2-fold in H-v601-Per1 and H-v601-Per2 cells and downregulated in H-v601 cells, relative to mock. Pairwise comparisons between the gene expression levels of HEK293 (Mock), H-v601-Per1, H-v601-Per2 and H-v601 cells are shown. 673 genes that were both upregulated by at least 2-fold in H-v601-Per1 or H-v601-Per2 and downregulated by at least 2-fold in H-v601 cells were identified. "Expression value" indicates the value reads derived from the transcriptomics sequencing, indicating level of gene expression; "Log_2 fold change" indicates the fold difference in gene expression from Sample A vs. Sample B.

Gene	Expression value						Log_2 fold change				
	Mock	H-v601-Per1	H-v601-Per2	H-v601	H-Rep	H-Rep-4B$_{T66A}$	Mock vs. H-v601	Mock vs. H-v601-Per1	Mock vs. H-v601-Per2	H-v601-Per1 vs. H-v601	H-v601-Per2 vs. H-v601
ABCA1	0.388976	0.667666	0.778933	0.594448	0.501492	0.327372	0.611869	0.779445	1.00182	-0.16758	-0.38995
ABHD12B	1.59302	1.7189	1.87688	0.887118	1.77792	1.17446	-0.84457	0.109719	0.236568	-0.95429	-1.08114
ABLIM3	0.61981	1.23979	1.18146	0.462535	0.934001	1.2406	-0.42226	1.0002	0.93067	-1.42246	-1.35293
ACE	0.896309	1.36371	1.44573	0.667904	0.373676	0.683436	-0.42436	0.605465	0.689727	-1.02982	-1.11408
ACHE	2.18938	4.11218	2.49927	1.27835	0.577382	0.793506	-0.77624	0.909382	0.190986	-1.68562	-0.96723
ACTA2	2.21046	11.2412	4.8437	2.30426	4.78405	6.20859	0.059958	2.34638	1.13177	-2.28642	-1.07181
ACTL6B	0.193022	0.731714	0.588122	0.132588	0.196571	0.268348	-0.54182	1.92252	1.60735	-2.46433	-2.14917
ACVRL1	0.226039	0.581854	0.397841	0.139345	0.283179	0.219066	-0.69791	1.36409	0.815622	-2.06199	-1.51353
ADAMTS10	1.0478	2.11185	1.54659	0.912266	1.46528	1.68267	-0.19984	1.01114	0.561722	-1.21098	-0.76157
ADAMTS7	0.839739	1.1444	0.845135	0.542801	0.752679	0.55646	-0.62952	0.44658	0.009241	-1.0761	-0.63876
ADAMTSL5	0.636974	1.00036	0.744841	0.436186	0.723032	0.696839	-0.54629	0.651214	0.225699	-1.19751	-0.77199
ADPRHL1	2.11476	2.98354	2.92563	1.33347	1.40944	2.01782	-0.66531	0.496531	0.468252	-1.16184	-1.13356
AGPAT1	2.15119	2.43551	2.72746	1.28618	1.74898	1.89158	-0.74204	0.179086	0.34242	-0.92113	-1.08446
ALG1L9P	0.249564	0.520788	0.563749	0.204869	0.726413	0.430592	-0.28471	1.06129	1.17565	-1.34599	-1.46035
ALOXE3	0.470368	0.706565	0.855301	0.370851	0.524974	0.834387	-0.34295	0.587033	0.862643	-0.92998	-1.20559
AMDHD1	0.395953	1.08524	0.868128	0.502509	0.170593	0.27715	0.343821	1.45461	1.13258	-1.11079	-0.78876
ANKRD1	0.166076	3.41484	0.900942	0.257283	0.434185	0.778339	0.631509	4.3619	2.43959	-3.73039	-1.80808
ANKRD24	0.400621	0.889076	0.608301	0.388895	0.231328	0.408264	-0.04286	1.15007	0.602547	-1.19293	-0.64541
ANKRD31	0.263243	0.73079	0.629234	0.406084	0.176513	0.131475	0.625382	1.47306	1.2572	-0.84768	-0.63182
ANO9	0.007294	0.895018	0.397932	0.008527	0.014036	0.079417	0.225322	6.93908	5.76969	-6.71376	-5.54437
AP2A2	0.574906	0.662475	0.648914	0.333056	0.513891	0.536454	-0.78756	0.20454	0.174701	-0.9921	-0.96226
AP3B2	0.987194	2.30729	1.62904	0.627635	0.28099	0.735414	-0.65341	1.22479	0.72262	-1.8782	-1.37603

Gene	Expression value						Log$_2$ fold change				
	Mock	H-v601-Per1	H-v601-Per2	H-v601	H-Rep	H-Rep-4B$_{T66A}$	Mock vs. H-v601	Mock vs. H-v601-Per1	Mock vs. H-v601-Per2	H-v601-Per1 vs. H-v601	H-v601-Per2 vs. H-v601
AQP1	0.761035	0.787806	0.893197	0.44873	0.590085	0.544674	-0.76212	0.049877	0.231015	-0.81199	-0.99313
AR	0.156334	0.655635	1.05688	0.217105	4.6602	5.06171	0.473758	2.06826	2.75711	-1.5945	-2.28335
ARC	0.47948	1.27131	0.974281	0.323663	0.562431	1.47389	-0.56698	1.40677	1.02287	-1.97375	-1.58984
ARL14	0.054446	0.557679	0.168485	0.066837	0	0.163059	0.295839	3.35655	1.62973	-3.06071	-1.33389
ARL17A	0.587828	1.09864	1.34858	0.819286	0.943519	1.01659	0.478972	0.902254	1.19797	-0.42328	-0.719
ASGR1	0.66853	1.51198	0.702262	0.659871	0.909705	0.48374	-0.01881	1.17738	0.071018	-1.19618	-0.08983
ATAD3C	0.172624	0.893212	3.39836	0.094021	0.148728	0.121213	-0.87658	2.37137	4.29913	-3.24794	-5.17571
ATG9B	0.249037	0.578239	0.462332	0.238655	0.389946	0.692092	-0.06143	1.21531	0.892569	-1.27674	-0.954
ATOH8	0.274938	0.588412	0.492871	0.177782	0.424547	0.676818	-0.629	1.09772	0.842104	-1.72672	-1.4711
ATP1A1-AS1	1.54992	3.87146	3.21313	3.08516	3.6273	3.90461	0.993147	1.32068	1.05178	-0.32754	-0.05864
ATP1B2	4.02038	5.10192	5.3004	2.05292	3.79682	3.89194	-0.96965	0.343708	0.398769	-1.31336	-1.36842
ATP2A3	1.4457	1.48388	1.80854	0.849379	1.73405	2.41334	-0.76729	0.037603	0.323056	-0.80489	-1.09035
AURKC	0.346425	0.90963	0.825475	0.468403	0.608267	0.666768	0.435204	1.39274	1.25268	-0.95753	-0.81748
B3GAT1	1.24708	1.34809	1.43026	0.551378	0.821883	1.05061	-1.17744	0.112369	0.197722	-1.28981	-1.37516
BATF2	0.477129	0.861415	0.925849	0.383833	0.853625	0.807475	-0.3139	0.852329	0.956397	-1.16623	-1.2703
BCL3	1.38805	2.7427	2.26996	0.778128	1.79161	2.08487	-0.83498	0.982541	0.709612	-1.81752	-1.54459
BCYRN1	0	1.78237	1.77007	0.809493	1.33248	1.25658	inf	inf	inf	-1.1387	-1.12872
BDNF	0.190216	0.577617	0.453518	0.166341	0.107321	0.097082	-0.1935	1.60248	1.25352	-1.79597	-1.44702
BIK	0.393191	0.660228	0.798251	0.541608	1.52848	1.62921	0.462021	0.747734	1.02161	-0.28571	-0.55959
BOK	0.642932	0.7516	0.91076	0.349968	0.364457	0.438364	-0.87744	0.2253	0.502406	-1.10274	-1.37985
BRD4	37.4638	45.5346	42.4898	20.4867	42.9675	46.7056	-0.87081	0.281465	0.181619	-1.15228	-1.05243
BRSK1	3.33569	8.24774	5.89823	3.47611	6.91499	9.43808	0.059487	1.30601	0.822296	-1.24653	-0.76281
BSPRY	0.770282	1.4387	1.60315	0.810044	0.225126	0.542778	0.072615	0.901304	1.05745	-0.82869	-0.98484
BST2	0.771222	6.80426	9.21115	0.553639	1.17092	1.61115	-0.4782	3.14122	3.57816	-3.61942	-4.05636
C10orf10	0.771225	1.8976	1.58358	0.804173	1.15047	1.56432	0.060354	1.29895	1.03797	-1.23859	-0.97761
C10orf82	0.499001	0.571381	0.735607	0.217468	1.0854	1.08742	-1.19824	0.19541	0.559894	-1.39365	-1.75813

Gene	Expression value						Log$_2$ fold change				
	Mock	H-v601-Per1	H-v601-Per2	H-v601	H-Rep	H-Rep-4B$_{T66A}$	Mock vs. H-v601	Mock vs. H-v601-Per1	Mock vs. H-v601-Per2	H-v601-Per1 vs. H-v601	H-v601-Per2 vs. H-v601
C14orf23	0.760342	1.56206	1.1891	1.12386	3.98595	3.80171	0.563745	1.03873	0.645154	-0.47499	-0.08141
C19orf38	0.443487	0.9365	0.694059	0.591719	0.291199	0.442292	0.416023	1.07839	0.646169	-0.66237	-0.23015
C19orf66	0.550679	0.582955	0.629879	0.289461	0.180657	0.12941	-0.92784	0.082173	0.193864	-1.01002	-1.12171
C1QL1	5.05988	5.97589	5.18665	2.68166	3.52166	3.49268	-0.91598	0.240051	0.035701	-1.15603	-0.95168
C1QTNF1	1.27064	1.80233	1.64407	0.796523	1.13406	1.42608	-0.67377	0.504309	0.371715	-1.17808	-1.04548
C1RL	0.200078	0.340657	0.560659	0.133625	0.210788	0.238245	-0.58237	0.767755	1.48656	-1.35012	-2.06893
C2CD4A	0.084869	2.30631	1.17817	0.125185	0.044823	0.098971	0.560748	4.7642	3.79516	-4.20345	-3.23442
C6orf163	1.18038	1.28043	1.47848	0.647385	1.52076	1.92255	-0.86656	0.117371	0.324861	-0.98393	-1.19142
C7orf13	0.801421	1.43326	1.03503	0.584777	1.22191	1.26587	-0.45467	0.83867	0.369041	-1.29334	-0.82372
C7orf61	0.4419	0.626916	0.581149	0.209586	0.324086	0.383873	-1.07618	0.504552	0.39519	-1.58073	-1.47137
C8orf37-AS1	0.294131	1.39709	1.39605	0.483207	0	0.266883	0.716181	2.24789	2.24682	-1.53171	-1.53063
C8orf49	0.580177	0.682395	0.752857	0.212399	0.440977	0.57932	-1.44972	0.234114	0.375882	-1.68383	-1.8256
C9orf172	0.45368	0.548677	0.541876	0.274794	0.272086	0.777324	-0.72332	0.274281	0.256287	-0.9976	-0.97961
C9orf9	10.5851	11.4383	11.7949	5.88336	8.04507	7.78912	-0.84732	0.111843	0.156129	-0.95916	-1.00345
CABP1	1.57468	2.35464	1.99074	1.0749	0.663421	1.35958	-0.55085	0.580449	0.33825	-1.1313	-0.8891
CACNG6	0.528269	0.883671	0.888744	0.364485	0.115218	0.111157	-0.53541	0.742237	0.750494	-1.27765	-1.28591
CACNG8	2.02659	18.2891	2.15667	1.75242	2.61796	2.96622	-0.2097	3.17386	0.089752	-3.38357	-0.29945
CARD6	0.322362	0.938679	0.597225	0.537097	1.1841	0.84326	0.7365	1.54195	0.889594	-0.80545	-0.15309
CASP10	0.318222	0.808676	0.857354	0.677702	2.94915	3.84385	1.09062	1.34553	1.42986	-0.25491	-0.33924
CATSPER3	0.642969	1.06966	0.75662	0.34528	0.380078	0.532893	-0.89698	0.734333	0.23482	-1.63131	-1.1318
CCDC101	16.7026	19.3916	17.4238	9.51024	13.9994	18.3981	-0.81252	0.215357	0.060985	-1.02788	-0.8735
CCDC11	0.32703	0.789061	0.533309	0.363126	0.181381	0.525431	0.15105	1.27071	0.705551	-1.11966	-0.5545
CCDC159	0.933131	2.07732	1.99114	1.76143	1.03641	0.759176	0.916595	1.15457	1.09344	-0.23798	-0.17685
CCDC160	0.466243	1.05591	1.10695	0.869544	0.73746	0.662834	0.899177	1.17934	1.24744	-0.28016	-0.34827
CCDC62	0.584437	0.599027	0.666947	0.317817	0.561837	0.265153	-0.87885	0.035575	0.190525	-0.91443	-1.06937
CCDC65	1.65635	1.95014	1.90165	0.797177	2.27885	1.94543	-1.05503	0.235574	0.199252	-1.29061	-1.25428

Gene	Expression value						Log$_2$ fold change				
	Mock	H-v601-Per1	H-v601-Per2	H-v601	H-Rep	H-Rep-4B$_{T66A}$	Mock vs. H-v601	Mock vs. H-v601-Per1	Mock vs. H-v601-Per2	H-v601-Per1 vs. H-v601	H-v601-Per2 vs. H-v601
CCDC88B	0.454703	0.719027	0.542419	0.314299	0.766803	0.915932	-0.53279	0.661119	0.254481	-1.19391	-0.78727
CCKBR	0.435771	0.565324	0.880968	0.354616	0.659069	0.430043	-0.29731	0.375508	1.01552	-0.67282	-1.31283
CCL20	0.030603	1.27104	0.104579	0.035777	0	0.089667	0.225322	5.37618	1.77283	-5.15085	-1.54751
CCL27	0.080461	0.903263	0.823309	0.675496	0.909632	0.358946	3.06959	3.48879	3.35507	-0.4192	-0.28549
CCT6P3	1.03874	2.44344	1.69352	1.45919	0.95253	1.01904	0.490327	1.23407	0.705184	-0.74375	-0.21486
CD160	0.863877	0.998249	1.24676	0.448025	0.659422	0.612669	-0.94725	0.208573	0.52929	-1.15582	-1.47654
CD70	1.90711	4.84683	2.43555	2.00852	1.10143	1.56426	0.074745	1.34565	0.352855	-1.27091	-0.27811
CDA	0.625331	1.49078	1.14359	0.581213	2.41207	1.7933	-0.10555	1.25337	0.870882	-1.35892	-0.97643
CDH24	4.38285	5.53448	5.08597	2.78514	4.61271	5.29558	-0.65412	0.336578	0.214653	-0.9907	-0.86877
CDH3	0.550394	0.829009	0.734033	0.370093	0.736928	0.864708	-0.57258	0.590923	0.415379	-1.1635	-0.98796
CDHR1	2.72267	3.22871	3.61979	1.4827	1.62288	1.49827	-0.8768	0.245933	0.410883	-1.12273	-1.28768
CDIPT-AS1	1.95948	3.25084	2.24859	1.12276	1.36059	1.01906	-0.80342	0.730344	0.198555	-1.53376	-1.00197
CDKN1A	8.30769	26.3493	13.9835	9.9376	21.8498	23.5571	0.25845	1.66525	0.751208	-1.4068	-0.49276
CDKN2B	2.32284	4.65837	3.42033	2.35045	3.47982	3.23589	0.017046	1.00393	0.558242	-0.98689	-0.5412
CDR1	10.0709	10.759	10.9552	3.84499	22.482	31.0257	-1.38914	0.095358	0.121425	-1.4845	-1.51057
CDYL2	0.388237	1.55983	0.891225	0.267042	0.400698	0.317312	-0.53987	2.00638	1.19885	-2.54625	-1.73872
CEACAM19	1.60108	2.61088	3.32497	0.994781	1.62008	1.8459	-0.6866	0.705486	1.05429	-1.39208	-1.74089
CEL	0.441197	0.696588	0.494692	0.257107	0.401604	0.518137	-0.77905	0.658881	0.165105	-1.43793	-0.94416
CELF3	0.215114	0.614293	0.443046	0.186658	0.291708	0.318441	-0.2047	1.51383	1.04235	-1.71853	-1.24706
CERS6-AS1	0.891588	1.73218	2.78708	0	1.46166	0.817902	#NAME?	0.958141	1.6443	#NAME?	#NAME?
CGA	0.106823	0.585622	0.151659	0.049177	0.06852	0.129235	-1.11917	2.45475	0.505607	-3.57392	-1.62478
CGB7	0.028815	0.67376	0.319435	0.033686	0.164036	0.53053	0.225322	4.54734	3.47063	-4.32202	-3.24531
CHD5	0.620143	1.09422	0.776022	0.376874	0.441601	0.987424	-0.71852	0.819224	0.323497	-1.53774	-1.04201
CHRM3	0.586787	1.2879	0.836495	0.577601	0.161062	0.136959	-0.02276	1.13411	0.511521	-1.15688	-0.53428
CHRNB4	0.509023	0.590274	0.537809	0.279881	0.755763	0.696365	-0.86292	0.213652	0.079361	-1.07657	-0.94228
CIDECP	9.24243	19.8751	14.6607	9.50205	7.44642	11.0706	0.039967	1.10462	0.665613	-1.06465	-0.62565

Gene	Expression value						Log$_2$ fold change				
	Mock	H-v601-Per1	H-v601-Per2	H-v601	H-Rep	H-Rep-4B$_{T66A}$	Mock vs. H-v601	Mock vs. H-v601-Per1	Mock vs. H-v601-Per2	H-v601-Per1 vs. H-v601	H-v601-Per2 vs. H-v601
CLCF1	0.49885	0.81813	0.916536	0.376176	0.550764	0.582934	-0.4072	0.713724	0.877585	-1.12092	-1.28478
CLIC2	0.441859	0.795064	0.693451	0.367484	0.279788	0.288255	-0.26591	0.847484	0.650208	-1.11339	-0.91611
CLSTN2	0.398733	0.854161	0.610486	0.264632	0.212041	0.106909	-0.59143	1.09908	0.614535	-1.69052	-1.20597
CLU	2.78729	6.07669	3.64296	1.96644	6.67783	8.14954	-0.50328	1.12442	0.386244	-1.6277	-0.88952
CNN2	25.2867	30.9207	30.107	13.2573	26.6713	26.1587	-0.93159	0.290195	0.251724	-1.22178	-1.18331
CNTFR	8.03669	10.5708	8.42722	2.95249	4.56912	6.25931	-1.44467	0.395412	0.068455	-1.84008	-1.51313
COL12A1	0.23182	1.31233	1.32183	0.267944	0.038734	0.246957	0.208929	2.50106	2.51146	-2.29213	-2.30254
COL23A1	0.667856	0.943415	1.01625	0.38086	0.195053	0.619066	-0.81028	0.498356	0.605646	-1.30863	-1.41592
COL9A2	0.417938	0.658158	0.562502	0.319127	0.519099	0.348783	-0.38916	0.655146	0.428571	-1.0443	-0.81773
COMP	1.13895	1.59152	1.52845	0.774454	1.1222	0.881676	-0.55645	0.482704	0.424364	-1.03916	-0.98082
COPZ2	0.301225	0.402973	0.554134	0.195775	0.206362	0.158758	-0.62164	0.419843	0.879393	-1.04149	-1.50104
CPNE4	0.011812	0.548816	0.247763	0.02288	0.14386	0.133179	0.953771	5.53796	4.39061	-4.58419	-3.43683
CRABP2	30.5169	50.5193	64.2499	40.7327	8.29283	14.4832	0.416576	0.727224	1.07408	-0.31065	-0.65751
CREB3L1	1.83257	3.60319	3.03972	1.29443	2.75947	3.09045	-0.50156	0.975403	0.730065	-1.47696	-1.23162
CREBRF	1.56738	3.78393	2.47089	1.95773	1.95457	2.51846	0.320825	1.27153	0.656678	-0.9507	-0.33585
CRIP2	3.09235	6.44789	5.13269	2.33646	1.6701	2.93698	-0.40438	1.06012	0.731011	-1.4645	-1.13539
CRTAC1	0.411463	0.560106	0.587669	0.284914	0.273642	0.335881	-0.53024	0.444937	0.514242	-0.97517	-1.04448
CRTC1	3.34143	3.91859	3.8303	1.66855	3.43685	4.69864	-1.00187	0.229868	0.196991	-1.23174	-1.19886
CSAG3	0.832028	3.44518	2.14203	0.979938	0	0.12489	0.236057	2.04987	1.36427	-1.81382	-1.12821
CSF1	2.96186	5.14342	3.87909	2.16858	4.71816	5.68245	-0.44976	0.796221	0.389211	-1.24598	-0.83897
CSRNP1	2.73807	5.85895	4.27383	3.07744	2.45146	3.36974	0.168571	1.09748	0.642368	-0.92891	-0.4738
CTB-178M22.2	0.377634	0.744985	0.79292	0.500785	0.81552	0.821826	0.407203	0.980223	1.07019	-0.57302	-0.66298
CTSZ	4.11099	7.23539	7.29028	1.83842	0.202478	0.176168	-1.16102	0.815585	0.82649	-1.9766	-1.98751
CUZD1	1.57304	4.25248	2.48424	1.51606	1.77833	2.8649	-0.05324	1.43475	0.659244	-1.48798	-0.71248
CXCL1	0.183452	1.34395	0.498924	0.253091	0.077679	0.242286	0.464255	2.87301	1.44342	-2.40875	-0.97916
CXCL10	0	28.3439	12.2077	0.366124	0.109581	3.24027	inf	inf	inf	-6.27456	-5.05932

Gene	Expression value						Log_2 fold change				
	Mock	H-v601-Per1	H-v601-Per2	H-v601	H-Rep	H-Rep-$4B_{T66A}$	Mock vs. H-v601	Mock vs. H-v601-Per1	Mock vs. H-v601-Per2	H-v601-Per1 vs. H-v601	H-v601-Per2 vs. H-v601
CXCL11	0	4.33757	1.5576	0.071123	0.025716	0.305514	inf	inf	inf	-5.93042	-4.45286
CXCL16	3.52964	5.9659	4.18858	2.72581	1.21604	0.038589	-0.37284	0.757219	0.246941	-1.13006	-0.61978
CXCL8	0.012979	0.964232	0.221309	0.030345	0.023934	0.06158	1.22532	6.21515	4.09183	-4.98983	-2.86651
CYP1A1	0.630972	1.87063	1.29165	1.17027	0.478881	0.932771	0.891191	1.56788	1.03357	-0.67669	-0.14238
CYP4X1	0.236606	0.694947	0.41642	0.25383	0.445467	0.36741	0.101375	1.55441	0.815549	-1.45304	-0.71417
DDB2	8.76418	27.1183	19.4065	12.9478	16.6062	24.0843	0.563018	1.62957	1.14685	-1.06656	-0.58383
DDN	1.6837	2.11105	1.70718	0.831007	1.84669	0.764117	-1.0187	0.326326	0.019979	-1.34503	-1.03868
DDR2	3.25166	7.0399	6.72676	4.20976	14.538	17.0635	0.37256	1.11438	1.04873	-0.74182	-0.67617
DDX11-AS1	0.612856	0.830394	0.963473	0.470217	0.159877	0.38967	-0.38222	0.438247	0.652695	-0.82047	-1.03492
DDX58	1.25651	18.7631	9.06119	1.85958	1.51919	3.29363	0.56555	3.9004	2.85028	-3.33485	-2.28473
DDX60	0.508905	3.36884	1.44019	0.547093	0.474032	0.564124	0.104389	2.72678	1.50079	-2.62239	-1.3964
DENND1C	0.667248	0.838965	0.847886	0.349409	1.67861	1.34639	-0.93331	0.330386	0.345646	-1.26369	-1.27895
DENND6B	0.960026	2.07738	1.42832	0.778834	0.496692	1.01977	-0.30176	1.11362	0.573171	-1.41538	-0.87493
DHRS2	1.08018	10.3003	9.00445	1.77044	9.12038	24.202	0.712837	3.25334	3.05936	-2.5405	-2.34653
DHRS4L1	0.761742	1.48177	1.00691	0.737144	0.53195	0.704347	-0.04736	0.959943	0.402559	-1.0073	-0.44992
DHX58	0.105525	1.9657	1.04001	0.109051	0.198252	0.480382	0.047418	4.21939	3.30094	-4.17198	-3.25352
DISP2	0.74564	1.29918	0.976569	0.539393	0.519296	0.733048	-0.46714	0.801055	0.389244	-1.2682	-0.85639
DLG4	2.38077	4.97692	4.45634	2.29151	4.62529	4.62967	-0.05513	1.06382	0.904427	-1.11895	-0.95956
DLGAP1-AS1	0.274505	0.845708	0.378758	0.222979	0.188057	0.296352	-0.29992	1.62332	0.464441	-1.92325	-0.76437
DMRTA1	0.093684	0.788215	0.467057	0.142082	0.176455	0.206073	0.600844	3.07271	2.31772	-2.47186	-1.71687
DNAH17	0.189399	0.708397	0.32657	0.20893	0.153695	0.226961	0.141592	1.90313	0.785965	-1.76154	-0.64437
DNM1	14.2315	17.9134	20.1997	9.86789	17.2313	24.587	-0.52828	0.33195	0.50524	-0.86023	-1.03352
DPYD	0.10388	0.330584	0.919373	0.159057	0.311158	0.479177	0.614626	1.67009	3.14573	-1.05547	-2.5311
DPYSL3	1.1568	1.24006	3.81711	0.560754	1.48117	9.32358	-1.04469	0.100278	1.72235	-1.14497	-2.76704
DRAM1	0.758737	1.38401	0.860507	0.661549	1.97983	1.75655	-0.19775	0.867186	0.181588	-1.06494	-0.37934
DRICH1	0.682269	0.6851	0.924007	0.326758	0.537271	0.701876	-1.06212	0.005973	0.437562	-1.06809	-1.49968

Gene	Expression value						Log$_2$ fold change				
	Mock	H-v601-Per1	H-v601-Per2	H-v601	H-Rep	H-Rep-4B$_{T66A}$	Mock vs. H-v601	Mock vs. H-v601-Per1	Mock vs. H-v601-Per2	H-v601-Per1 vs. H-v601	H-v601-Per2 vs. H-v601
DTX2	1.78481	2.49373	2.21561	0.756582	1.54166	2.21533	-1.2382	0.482532	0.311933	-1.72074	-1.55014
DTX2P1-UPK3BP1-PMS2P11	0.454143	0.699685	0.735679	0.307103	0.331059	0.462625	-0.56442	0.623558	0.69593	-1.18798	-1.26035
DTX3	1.69327	4.92188	1.86662	1.23833	0.993943	0.410409	-0.45141	1.5394	0.140618	-1.99081	-0.59203
DUSP2	2.81752	4.37406	3.8237	1.38514	0.15082	0.115623	-1.0244	0.634547	0.440542	-1.65894	-1.46494
DUSP23	0.655095	0.816601	1.17303	0.223704	0	0.045161	-1.55012	0.317927	0.840461	-1.86804	-2.39058
EEF1A2	77.9157	135.718	84.278	54.753	22.142	38.3176	-0.50898	0.80063	0.113242	-1.30961	-0.62222
EFCAB14-AS1	0.54739	0.859257	0.892339	0.434534	0.948321	0.797014	-0.3331	0.650521	0.705024	-0.98362	-1.03812
EFNA2	2.3782	2.9144	2.57806	1.32986	1.66439	2.01442	-0.83859	0.293329	0.116415	-1.13192	-0.95501
EGFL7	24.2793	25.3655	29.3049	14.1993	26.0892	31.1986	-0.77391	0.063139	0.271414	-0.83705	-1.04532
EGR1	0.925038	2.70073	1.6876	0.802768	1.67927	2.13979	-0.20453	1.54576	0.867385	-1.75029	-1.07192
EGR2	0.285205	0.506634	0.603606	0.130608	0.381157	0.303296	-1.12675	0.828944	1.08161	-1.9557	-2.20836
EHD2	1.48639	1.74818	1.54213	0.772936	0.957582	0.263893	-0.94339	0.234041	0.053114	-1.17743	-0.99651
ELFN1	1.01913	1.18373	1.08853	0.395529	0.30597	0.420424	-1.36549	0.215995	0.09504	-1.58148	-1.46052
ELFN2	1.35726	1.63249	1.62424	0.663173	0.981422	1.19966	-1.03324	0.266376	0.259071	-1.29961	-1.29231
EMID1	3.96233	4.91335	4.38215	2.41931	2.79956	2.90553	-0.71176	0.310356	0.145288	-1.02211	-0.85705
EMP3	10.5101	22.1732	16.0955	11.8259	16.7023	10.4488	0.170173	1.07705	0.614887	-0.90687	-0.44471
EPB41L4A-AS2	0.491955	0.772917	0.680839	0.341264	0.560736	0.661917	-0.52764	0.651787	0.468787	-1.17943	-0.99643
ERBB4	0.447991	1.02844	1.02153	0.463482	0.034581	0.099199	0.049043	1.19892	1.18919	-1.14988	-1.14014
ETV4	0.475753	0.886341	1.09212	0.675113	0.286846	0.547152	0.504918	0.89765	1.19884	-0.39273	-0.69393
ETV7	0	0.965892	0.66149	0.07901	0.325127	0.805574	inf	inf	inf	-3.61175	-3.06561
EVA1C	0.421043	0.765186	0.482315	0.257514	0.498948	0.428096	-0.70932	0.861843	0.196007	-1.57116	-0.90533
FAAH	0.994515	1.88009	1.72134	0.7433	0.969756	1.02474	-0.42005	0.918736	0.791469	-1.33878	-1.21152
FAM131C	2.36105	2.9103	2.58286	0.763287	1.76859	2.70619	-1.62913	0.301738	0.129543	-1.93087	-1.75867
FAM133A	0.308383	0.354932	0.585806	0.276865	0.200308	0.323066	-0.15554	0.202819	0.925699	-0.35836	-1.08124
FAM228B	2.24448	2.98745	2.44098	1.49545	1.8303	1.8439	-0.5858	0.412531	0.121078	-0.99833	-0.70688

Gene	Expression value						Log_2 fold change				
	Mock	H-v601-Per1	H-v601-Per2	H-v601	H-Rep	H-Rep-4B$_{T66A}$	Mock vs. H-v601	Mock vs. H-v601-Per1	Mock vs. H-v601-Per2	H-v601-Per1 vs. H-v601	H-v601-Per2 vs. H-v601
FAM49A	0.438179	0.619591	0.613164	0.15889	0.22415	0.493058	-1.4635	0.499796	0.484754	-1.96329	-1.94825
FAM86HP	1.05975	1.33425	1.31057	0.639845	0.837384	1.49423	-0.72793	0.332309	0.306473	-1.06024	-1.0344
FAXDC2	0.633775	2.43368	1.93157	0.73303	2.8154	2.74654	0.2099	1.9411	1.60773	-1.7312	-1.39783
FBLL1	0.344856	1.13692	0.855162	0.402347	0.170086	0.175059	0.222446	1.72106	1.3102	-1.49862	-1.08776
FBXO2	1.01561	1.75055	1.70358	0.76225	1.31806	1.13696	-0.41401	0.785466	0.746224	-1.19948	-1.16023
FCHO1	2.03712	2.73932	2.59836	1.2852	2.99043	3.04273	-0.66454	0.427287	0.351071	-1.09183	-1.01561
FGF13	0.538425	3.08473	1.00353	0.346291	0.273277	2.52139	-0.63676	2.51833	0.898271	-3.15509	-1.53503
FGF17	0.693997	1.13577	0.766754	0.469682	0.501715	0.512567	-0.56325	0.710668	0.143835	-1.27391	-0.70708
FGF21	0	0.719958	0.487523	0.224896	0	0.239527	inf	inf	inf	-1.67866	-1.11621
FGFBP1	0.272097	0.624135	0.446113	0.394602	1.11664	1.05719	0.536275	1.19774	0.713286	-0.66146	-0.17701
FHL3	11.998	14.6358	13.4706	7.275	11.6585	12.3973	-0.72177	0.286709	0.167019	-1.00848	-0.88879
FIBCD1	0.364464	0.407617	0.563761	0.24784	0.140384	0.224749	-0.55637	0.161436	0.629305	-0.7178	-1.18567
FILIP1L	0.24178	0.648118	0.567015	0.302042	0.835091	0.68198	0.321052	1.42256	1.22969	-1.10151	-0.90864
FLJ22184	1.23671	1.62423	1.39654	0.701901	0.456238	0.406616	-0.81717	0.393242	0.175349	-1.21041	-0.99252
FOSL1	0.444647	0.976308	0.578217	0.172494	0.70951	0.479182	-1.36612	1.13467	0.378948	-2.50079	-1.74506
FOXA3	0.374312	1.14809	1.0323	0.58448	0.457667	0.721872	0.642914	1.61692	1.46356	-0.974	-0.82064
FRMD3	0.710377	1.22484	1.06438	0.533923	0.633057	0.996429	-0.41195	0.785934	0.583363	-1.19789	-0.99532
FUT1	0.034026	0.961976	0.414823	0.338034	0.082317	0.121088	3.31247	4.82131	3.6078	-1.50883	-0.29533
FXYD1	0.222291	0.742803	0.375798	0.064486	0.73871	0.461978	-1.7854	1.74053	0.757507	-3.52593	-2.54291
FXYD5	40.4384	46.544	40.5019	18.3795	85.3227	83.0206	-1.13763	0.20287	0.002266	-1.3405	-1.13989
GAB3	0.263213	0.640586	0.398237	0.226255	0.446689	0.232361	-0.21828	1.28316	0.597398	-1.50144	-0.81568
GABRA3	2.99314	4.10035	3.61476	1.35228	0.02784	0.027395	-1.14627	0.454086	0.272238	-1.60035	-1.4185
GABRE	0.180587	1.0766	0.585552	0.08006	0.493843	0.68445	-1.17354	2.57572	1.6971	-3.74926	-2.87064
GADD45B	5.29408	8.85917	6.83349	3.19068	4.46576	6.74098	-0.73052	0.742792	0.368244	-1.47331	-1.09876
GAL3ST1	0.521396	0.531125	0.627409	0.313045	0.471456	0.61492	-0.73601	0.026671	0.267026	-0.76268	-1.00303
GALNT14	1.51718	2.82374	2.38808	0.89009	1.38732	2.79088	-0.76937	0.896216	0.654459	-1.66558	-1.42383

Gene	Expression value						Log$_2$ fold change				
	Mock	H-v601-Per1	H-v601-Per2	H-v601	H-Rep	H-Rep-4B$_{T66A}$	Mock vs. H-v601	Mock vs. H-v601-Per1	Mock vs. H-v601-Per2	H-v601-Per1 vs. H-v601	H-v601-Per2 vs. H-v601
GALNT5	0.241392	0.564504	0.533201	0.406683	0.470168	0.281331	0.752528	1.22561	1.1433	-0.47308	-0.39078
GBP1P1	0.360467	0.81013	0.580436	0.452177	0.570176	0.949912	0.32702	1.16829	0.687268	-0.84127	-0.36025
GDF15	0.256	5.58996	1.75125	0.527909	1.36903	1.99498	1.04415	4.44862	2.77417	-3.40448	-1.73002
GFY	0.175342	0.293474	0.57645	0.13004	0.302467	0.633075	-0.43121	0.743064	1.71703	-1.17428	-2.14824
GHRL	0.467661	1.2915	0.793108	0.529308	2.10923	1.02102	0.178645	1.46551	0.762055	-1.28687	-0.58341
GIPC3	4.22597	6.18436	7.53451	2.91673	2.60615	1.55172	-0.53493	0.549341	0.834232	-1.08427	-1.36916
GNGT1	1.29299	2.76881	1.80188	1.76687	0.858146	0.23705	0.45048	1.09855	0.478792	-0.64807	-0.02831
GPNMB	0.210511	0.601713	0.348422	0.264688	0.191067	0.220567	0.330401	1.51518	0.726941	-1.18478	-0.39654
GPR146	0.518407	0.968837	0.887202	0.449227	0.801615	1.09386	-0.20664	0.90217	0.775179	-1.10881	-0.98182
GPR153	3.84692	4.51711	4.41739	2.15449	3.73926	4.38303	-0.83636	0.231697	0.19949	-1.06806	-1.03585
GPR3	0.772544	0.954042	0.773721	0.472525	0.868517	0.99315	-0.70923	0.304436	0.002197	-1.01366	-0.71142
GPR50	0.844394	2.63759	2.42264	0.447983	0.897989	1.3175	-0.91447	1.64323	1.52059	-2.5577	-2.43506
GPSM1	29.8243	35.4746	31.6895	16.6912	28.3144	33.8298	-0.8374	0.250301	0.087518	-1.0877	-0.92492
GRHL3	0.235648	0.784348	0.376881	0.154088	0.319009	0.505154	-0.61288	1.73486	0.677477	-2.34774	-1.29036
GRIK4	0.487219	1.07926	0.936658	0.4019	0.533146	0.682738	-0.27773	1.14739	0.942952	-1.42513	-1.22069
GRIK5	0.672017	0.985971	0.997559	0.417878	0.597801	0.678579	-0.68542	0.553047	0.569904	-1.23846	-1.25532
GRINA	80.68	89.4839	85.6119	37.0204	80.2789	92.0943	-1.12389	0.149416	0.0856	-1.27331	-1.20949
GSTO2	2.61929	4.15307	3.52459	2.0875	4.09462	6.92842	-0.3274	0.665003	0.42828	-0.9924	-0.75568
GTF2H2	0.417151	0.658691	0.475033	0.211956	0.548716	0.363933	-0.97681	0.659032	0.187457	-1.63584	-1.16426
GUCA1B	0.839316	1.43637	1.55078	0.582155	1.34958	0.939554	-0.52781	0.775145	0.885709	-1.30296	-1.41352
HCFC1-AS1	0.336662	0.555239	0.884082	0.241848	0.322013	0.602277	-0.4772	0.721807	1.39288	-1.19901	-1.87008
HERC5	9.78521	37.775	20.9894	9.42677	12.3198	11.3586	-0.05384	1.94876	1.10098	-2.0026	-1.15482
HES7	1.10221	1.98223	2.2803	1.84182	0.178261	0.605831	0.74073	0.846724	1.04882	-0.10599	-0.30809
HIC1	0.916235	1.18228	1.39149	0.481594	0.564947	0.675813	-0.9279	0.367779	0.602841	-1.29568	-1.53074
HIGD1B	0.683002	1.56296	0.842984	0.381026	1.25527	2.06931	-0.842	1.19432	0.303616	-2.03632	-1.14562
HIST1H1D	0.550948	0.658804	0.694791	0.140846	1.50179	2.21111	-1.96779	0.257932	0.334662	-2.22573	-2.30246

Gene	Expression value						Log$_2$ fold change				
	Mock	H-v601-Per1	H-v601-Per2	H-v601	H-Rep	H-Rep-4B$_{T66A}$	Mock vs. H-v601	Mock vs. H-v601-Per1	Mock vs. H-v601-Per2	H-v601-Per1 vs. H-v601	H-v601-Per2 vs. H-v601
HIST1H2AC	2.63969	6.41723	3.39992	1.94231	0.977072	2.62969	-0.4426	1.28158	0.365134	-1.72418	-0.80773
HIST1H2AD	0.251558	1.14707	0.648199	0.137918	0.361973	0.583118	-0.86708	2.189	1.36554	-3.05608	-2.23263
HIST1H2AI	0.81265	1.02993	1.37783	0.288875	0.559711	0.830634	-1.49219	0.34184	0.761695	-1.83403	-2.25389
HIST1H2AK	1.22603	1.98527	1.62096	0.953732	0.713545	0.944652	-0.36234	0.695344	0.402857	-1.05768	-0.7652
HIST1H2BD	5.28137	9.39957	7.04179	3.48782	2.44717	3.11551	-0.59859	0.831683	0.415031	-1.43027	-1.01362
HIST1H2BJ	4.53044	7.11791	5.57523	3.21204	2.76755	3.69694	-0.49616	0.651805	0.299381	-1.14797	-0.79554
HIST1H2BN	1.04497	2.50068	2.50664	1.01338	0.305875	1.1538	-0.04428	1.25886	1.26229	-1.30314	-1.30657
HIST1H3B	0.65824	1.2002	1.17668	0.440116	0.279638	1.1757	-0.58073	0.866588	0.838039	-1.44732	-1.41877
HIST1H3E	0.99011	1.89426	1.28695	0.457165	0.992434	1.76909	-1.11487	0.935976	0.378291	-2.05085	-1.49317
HIST1H4C	12.0847	22.8754	17.0104	1.76698	17.896	20.0735	-2.77382	0.920617	0.49324	-3.69444	-3.26706
HIST1H4H	0.692639	2.26405	1.65738	1.05664	1.48477	1.21222	0.609315	1.70873	1.25873	-1.09941	-0.64942
HIST2H2BE	1.1211	2.64543	1.52978	0.786422	0.44099	0.943914	-0.51154	1.23859	0.448409	-1.75013	-0.95995
HMOX1	57.5826	65.8089	59.2149	32.7096	29.5322	33.9519	-0.81592	0.192649	0.040327	-1.00857	-0.85624
HPCA	0.278401	0.814804	0.372979	0.127443	0.24707	0.242025	-1.12731	1.54929	0.421933	-2.6766	-1.54924
HPX	0.207559	0.563519	0.479756	0.261122	0.208044	0.216436	0.331203	1.44094	1.20878	-1.10974	-0.87758
HSD17B14	2.65746	5.57738	5.62679	2.87151	2.06845	2.23652	0.111761	1.06954	1.08227	-0.95778	-0.97051
HSPA6	0.047986	4.39407	0.997828	0.054957	0.014676	0.126517	0.195691	6.51681	4.37811	-6.32112	-4.18242
HSPB1	54.5839	82.5207	54.7107	35.6973	44.7406	10.8955	-0.61266	0.596282	0.00335	-1.20894	-0.61601
HSPB8	0.371605	3.75786	1.95774	0.998141	0.723672	0.833193	1.42547	3.33807	2.39735	-1.9126	-0.97188
HSPG2	1.81237	1.84596	1.99975	0.918625	2.37807	2.34621	-0.98033	0.026491	0.141945	-1.00682	-1.12227
HTR1D	0.732913	1.23599	0.990576	0.582243	0.253515	0.242853	-0.33202	0.75395	0.434625	-1.08597	-0.76665
HTR2C	0.17196	0.473776	0.682643	0.152518	0.205606	0.189262	-0.17309	1.46214	1.98906	-1.63522	-2.16215
HVCN1	0.359006	0.754928	0.727428	0.589402	0.099323	0.148371	0.715244	1.07233	1.0188	-0.35709	-0.30355
ICAM1	0.278806	1.22383	0.676758	0.0592	0.256751	0.388852	-2.23559	2.13407	1.27938	-4.36966	-3.51497
IDUA	1.29454	1.67045	1.51292	0.743641	1.15253	1.31701	-0.79976	0.367803	0.224906	-1.16756	-1.02466
IFI44	0	11.8179	3.58959	0.097924	0.509033	1.20929	inf	inf	inf	-6.9151	-5.19601

Gene	Expression value						Log$_2$ fold change				
	Mock	H-v601-Per1	H-v601-Per2	H-v601	H-Rep	H-Rep-4B$_{T66A}$	Mock vs. H-v601	Mock vs. H-v601-Per1	Mock vs. H-v601-Per2	H-v601-Per1 vs. H-v601	H-v601-Per2 vs. H-v601
IFI44L	0.273997	0.759502	0.81717	0.239876	0.644125	0.686612	-0.19187	1.47089	1.57648	-1.66276	-1.76834
IFI6	7.61894	19.5333	18.062	6.92534	12.5982	15.6811	-0.13771	1.35827	1.24529	-1.49598	-1.383
IFIH1	0.814504	21.0274	9.41731	1.23807	0.632006	1.60279	0.6041	4.6902	3.53132	-4.0861	-2.92722
IFIT1	1.00993	70.7712	32.0998	2.55953	2.64825	12.0786	1.34163	6.13084	4.99024	-4.78921	-3.64862
IFIT2	0.101339	81.6938	34.9401	1.4184	1.03569	14.1405	3.807	9.65489	8.42955	-5.84789	-4.62255
IFIT3	0.264017	80.337	31.1563	0.80443	0.883057	9.12587	1.60734	8.24929	6.88275	-6.64195	-5.27542
IFITM1	10.0568	14.7331	19.3776	6.34603	10.8528	10.0989	-0.66425	0.550889	0.946215	-1.21514	-1.61046
IFITM2	22.3026	34.1612	34.1453	10.7379	13.3013	10.8413	-1.0545	0.615149	0.614477	-1.66965	-1.66898
IFITM3	7.37645	19.4612	17.6457	4.10294	3.72201	3.61185	-0.84627	1.3996	1.25832	-2.24587	-2.10459
IFNB1	0.061254	19.935	4.20515	0.973042	0.115415	0.389048	3.98963	8.34629	6.10122	-4.35666	-2.11158
IGF2	1.50479	2.29717	2.1009	0.448355	0.58823	1.36703	-1.74685	0.61029	0.481439	-2.35714	-2.22829
IGFBP3	0.751658	1.33238	0.841011	0.421892	0.077128	0.071053	-0.8332	0.825854	0.162049	-1.65906	-0.99525
IGFBP4	4.06197	4.20684	4.49456	2.22292	1.84799	2.3571	-0.86973	0.050559	0.145999	-0.92028	-1.01572
IGFBP6	0.514302	1.5665	1.39448	0.85568	1.60899	1.18053	0.734457	1.60685	1.43904	-0.8724	-0.70458
IGFBP7	3.04212	4.10313	3.47171	1.45538	0.522328	0.818017	-1.06368	0.431649	0.190572	-1.49533	-1.25425
IGLL3P	0.502363	0.798452	0.91624	0.421823	1.33289	1.33279	-0.25209	0.668477	0.866997	-0.92057	-1.11909
IGSF1	0.180705	1.25047	1.26148	0.21735	1.12492	1.54727	0.266383	2.79076	2.80341	-2.52438	-2.53702
IGSF21	0.56645	1.25873	1.25914	0.373552	0.27829	0.631331	-0.60064	1.15195	1.15241	-1.75259	-1.75305
IKZF1	1.11321	1.36764	1.21654	0.451449	0.325898	0.389071	-1.30209	0.296957	0.128052	-1.59905	-1.43015
IL32	0.189866	9.85416	4.22578	0.060644	0.509106	1.95309	-1.64654	5.69768	4.47617	-7.34422	-6.12271
INHBE	0.246096	4.66225	2.46905	1.14214	0.261621	0.340889	2.21444	4.24373	3.32666	-2.02929	-1.11222
INPP5D	0.042257	1.32558	0.484673	0.093475	0.93821	1.36785	1.14538	4.97128	3.51974	-3.8259	-2.37436
INSC	0.245033	1.18081	0.80922	0.761841	0.123971	0.116932	1.63651	2.26873	1.72356	-0.63222	-0.08704
IQSEC2	5.77452	6.71848	6.29106	2.95208	5.83291	6.5306	-0.96797	0.218434	0.123601	-1.1864	-1.09157
ISG15	4.11058	203.473	72.8468	5.55473	5.31367	22.0228	0.434376	5.62935	4.14745	-5.19498	-3.71308
ISG20	0.470101	4.53632	1.58966	0.522967	0.340613	0.896555	0.153751	3.27048	1.75767	-3.11673	-1.60392

Gene	Expression value						Log$_2$ fold change				
	Mock	H-v601-Per1	H-v601-Per2	H-v601	H-Rep	H-Rep-4B$_{T66A}$	Mock vs. H-v601	Mock vs. H-v601-Per1	Mock vs. H-v601-Per2	H-v601-Per1 vs. H-v601	H-v601-Per2 vs. H-v601
JAM2	1.56402	3.36518	2.82712	1.53584	0.970892	1.27886	-0.02623	1.10542	0.854074	-1.13166	-0.88031
JUNB	8.68312	14.7472	10.999	5.67203	6.91467	9.54178	-0.61435	0.764156	0.34109	-1.3785	-0.95544
JUP	18.3302	28.7571	22.3234	13.8683	17.5967	18.8256	-0.40243	0.649699	0.284334	-1.05212	-0.68676
KCNB1	0.309917	0.692326	0.392662	0.344433	0.113461	0.257958	0.152341	1.15957	0.341405	-1.00723	-0.18907
KCND3	0.660028	0.929257	0.664756	0.264731	0.122026	0.188975	-1.318	0.49355	0.010297	-1.81155	-1.3283
KCNH2	2.36829	3.70535	2.44232	1.54552	0.511454	1.02804	-0.61575	0.645764	0.044407	-1.26151	-0.66016
KCNH3	0.345034	0.765149	0.618906	0.396014	0.693504	0.859886	0.198813	1.149	0.842981	-0.95019	-0.64417
KCNJ4	4.29918	4.97448	4.34141	2.49638	1.75136	2.00787	-0.78422	0.210485	0.014102	-0.99471	-0.79833
KCNN1	1.36405	1.85839	1.56308	0.928293	4.75874	6.55931	-0.55524	0.446159	0.196499	-1.0014	-0.75174
KCNN2	0.297813	0.623746	0.525709	0.15681	0.554612	0.471964	-0.92539	1.06655	0.819859	-1.99194	-1.74525
KCNN4	0.038558	0.818986	0.301789	0.011186	0.307649	0.336429	-1.78533	4.40873	2.96843	-6.19406	-4.75377
KCNS3	0.685919	0.750132	1.05954	0.364455	0.634406	0.638234	-0.9123	0.129105	0.627323	-1.0414	-1.53962
KCNV1	0	0.392635	0.609487	0.02659	0	0.046895	inf	inf	inf	-3.88424	-4.51865
KCTD8	0.049413	0.202962	0.716079	0.071922	0.045769	0.044396	0.541547	2.03826	3.85717	-1.49672	-3.31562
KLF2	1.04809	1.66023	1.20595	0.446947	1.89817	1.28493	-1.22958	0.663623	0.202413	-1.89321	-1.432
KLF4	1.66115	3.65211	2.73793	1.51636	1.53916	1.9323	-0.13157	1.13655	0.720908	-1.26812	-0.85248
KRBA2	0.334696	0.715557	0.396256	0.274032	0.661189	0.444841	-0.28851	1.09622	0.243584	-1.38472	-0.53209
KRT17	0.028861	1.36144	0.315167	0.04987	0.213203	0.62307	0.789054	5.55986	3.44892	-4.77081	-2.65987
KRT75	0.030725	1.58305	0.302546	0.014006	0.077248	0.372288	-1.13331	5.68716	3.29968	-6.82047	-4.43299
KRTAP21-2	0	3.3216	1.37524	0.754282	0.594925	0.945234	inf	inf	inf	-2.1387	-0.86651
L1CAM	0.246139	0.639772	0.446173	0.196344	0.315635	0.524373	-0.32609	1.37808	0.858128	-1.70417	-1.18422
L3MBTL4	0.295921	0.65766	0.412341	0.383057	0.022164	0	0.372345	1.15213	0.478623	-0.77978	-0.10628
LAMB2P1	0.454898	1.19446	1.00426	0.417378	0.612426	0.51786	-0.12419	1.39274	1.14252	-1.51693	-1.2667
LAMB3	0.056671	0.642536	0.242769	0.018887	0.097022	0.129869	-1.58521	3.5031	2.0989	-5.08831	-3.68411
LAMC3	1.07057	1.84614	1.59171	0.778337	1.51731	0.606594	-0.45991	0.786137	0.572195	-1.24605	-1.03211
LAMP3	0.294653	0.550267	0.312211	0.167628	0.565671	0.592734	-0.81375	0.901118	0.083505	-1.71487	-0.89726

Gene	Expression value						Log$_2$ fold change				
	Mock	H-v601-Per1	H-v601-Per2	H-v601	H-Rep	H-Rep-4B$_{T66A}$	Mock vs. H-v601	Mock vs. H-v601-Per1	Mock vs. H-v601-Per2	H-v601-Per1 vs. H-v601	H-v601-Per2 vs. H-v601
LCN15	0.777266	1.67493	1.48701	0.459896	0.193116	0.482348	-0.7571	1.10762	0.935938	-1.86472	-1.69304
LGALS1	5.59735	21.6096	9.80216	5.65326	11.2356	13.7016	0.014337	1.94886	0.808355	-1.93452	-0.79402
LGALS3BP	8.69439	19.9932	17.8915	1.89494	81.1998	69.7693	-2.19793	1.20135	1.04111	-3.39928	-3.23904
LIF	0.488434	3.16906	1.30207	0.583777	0.485112	0.886772	0.257254	2.69782	1.41457	-2.44056	-1.15732
LIMS2	1.15491	1.52216	1.1639	0.484967	0.23937	0.455535	-1.25182	0.398346	0.011193	-1.65016	-1.26301
LINC00515	0.23746	0.560418	0.539758	0.513026	1.19948	0.718195	1.11135	1.23882	1.18463	-0.12747	-0.07328
LINC00599	0.282306	0.39928	0.580237	0.303883	0.135631	0.076012	0.106256	0.50014	1.03938	-0.39388	-0.93313
LINC00652	0.418665	0.588811	0.527556	0.226805	1.09045	1.31628	-0.88434	0.492009	0.333527	-1.37635	-1.21787
LINC00663	0.326579	0.685335	0.429172	0.413652	0.697762	0.424006	0.340985	1.06938	0.394123	-0.72839	-0.05314
LINC00950	0.210648	0.58982	0.523711	0.300614	0.346135	0.376388	0.51308	1.48544	1.31394	-0.97237	-0.80086
LINC01234	2.28986	2.8805	2.59166	1.44777	13.3152	13.6095	-0.66143	0.33106	0.178615	-0.99249	-0.84004
LINC01252	0.345778	0.693215	0.536343	0.391101	0.053166	0.09645	0.177692	1.00346	0.633309	-0.82576	-0.45562
LINC01341	0.298643	0.46384	0.56025	0.270278	0.394295	0.434746	-0.14398	0.635205	0.907649	-0.77918	-1.05163
LINGO3	0.378156	0.622816	0.534322	0.164449	0.038929	0.036712	-1.20134	0.719826	0.49873	-1.92116	-1.70007
LIPE	1.04655	1.1859	1.47212	0.476657	2.27971	2.3071	-1.13461	0.180341	0.492261	-1.31495	-1.62687
LMCD1	1.01437	2.10472	1.2027	1.14103	0.811906	1.03672	0.169752	1.05304	0.245695	-0.88329	-0.07594
LMO3	0.765738	0.95778	1.24152	0.367268	0.043043	0.171931	-1.06002	0.322843	0.697187	-1.38286	-1.75721
LMOD1	2.44644	6.07747	4.20947	2.94264	2.7049	2.90569	0.266428	1.31279	0.782956	-1.04636	-0.51653
LMTK3	0.941077	1.01106	1.23956	0.553156	1.0723	1.56294	-0.76663	0.103479	0.397438	-0.87011	-1.16406
LOC100129148	0.401655	5.88846	2.97272	2.01341	1.98097	4.62243	2.32561	3.87386	2.88776	-1.54825	-0.56215
LOC100130691	0.282976	0.624471	0.414949	0.315368	0.244214	0.241862	0.156357	1.14195	0.552254	-0.9856	-0.3959
LOC100132057	0.567639	1.75203	1.19224	0.656062	0.290202	0.872182	0.208859	1.62599	1.07063	-1.41713	-0.86177
LOC100134368	0.792251	1.3198	1.11688	0.486084	1.19519	0.8949	-0.70475	0.736295	0.495442	-1.44105	-1.20019
LOC100240734	0.205566	0.422181	0.693532	0.396604	0.25025	0.492517	0.948099	1.03826	1.75436	-0.09016	-0.80627
LOC100268168	0.472845	1.11662	0.776622	0.580022	0.494456	0.382646	0.294741	1.2397	0.715845	-0.94496	-0.4211
LOC100289495	0.324122	0.755278	0.537797	0.440408	0.299005	0.322937	0.442302	1.22047	0.730523	-0.77817	-0.28822

Gene	Expression value						Log$_2$ fold change				
	Mock	H-v601-Per1	H-v601-Per2	H-v601	H-Rep	H-Rep-4B$_{T66A}$	Mock vs. H-v601	Mock vs. H-v601-Per1	Mock vs. H-v601-Per2	H-v601-Per1 vs. H-v601	H-v601-Per2 vs. H-v601
LOC100506082	3.14776	4.29741	3.3998	1.17027	1.51644	1.0469	-1.42749	0.449144	0.111127	-1.87663	-1.53861
LOC100506119	0.130543	0.610169	0.32874	0.261005	0.068397	0.048055	0.999547	2.22468	1.33242	-1.22513	-0.33287
LOC100507250	0.812373	1.37853	1.86167	1.07775	0.841938	0.664791	0.407815	0.762915	1.19639	-0.3551	-0.78857
LOC100652999	0.439931	0.661056	0.50022	0.117789	0.100086	0.233595	-1.90108	0.587495	0.185287	-2.48857	-2.08636
LOC101927217	0.19719	0.934275	0.625811	0.488787	0.090241	0.27288	1.30962	2.24426	1.66614	-0.93464	-0.35652
LOC101927571	0.135278	0.84172	0.921983	0	0.260318	0.150873	#NAME?	2.63741	2.76881	#NAME?	#NAME?
LOC101928470	1.90578	2.25035	2.69134	1.33	3.10811	1.94954	-0.51896	0.239763	0.497943	-0.75872	-1.0169
LOC101928837	0.69948	1.01275	2.86859	0.920614	0	0.427818	0.396314	0.53392	2.03599	-0.13761	-1.63968
LOC101928943	0.089309	0.684771	0.279512	0.227816	0.336557	0.238012	1.351	2.93875	1.64604	-1.58775	-0.29504
LOC101929221	0.291502	0.453227	0.636718	0.179442	0.327999	0	-0.69999	0.636726	1.12715	-1.33671	-1.82714
LOC101929715	0.753794	1.4444	1.68915	1.12039	0.983619	0.429037	0.571758	0.938229	1.16406	-0.36647	-0.5923
LOC102723439	0.189778	0.55536	0.800866	0.392805	0.472019	1.005	1.0495	1.54911	2.07725	-0.49961	-1.02775
LOC102724467	0.24423	1.21728	0.737416	0.433801	0.066576	0.125566	0.828791	2.31735	1.59424	-1.48856	-0.76545
LOC283070	2.6831	3.03938	2.99834	1.34478	2.18856	2.47633	-0.99653	0.179874	0.16026	-1.17641	-1.15679
LOC283352	0.479208	2.40437	0.673851	0	4.67657	4.29388	#NAME?	2.32693	0.491777	#NAME?	#NAME?
LOC283693	0.258813	0.710052	0.435608	0.347408	0.257815	0.435647	0.424718	1.45601	0.751119	-1.03129	-0.3264
LOC284837	0.366338	0.797736	0.736914	0.301529	0.791355	1.0677	-0.28088	1.12274	1.00832	-1.40362	-1.2892
LOC285074	1.02151	2.06144	1.97082	1.43157	2.15336	2.60901	0.486892	1.01295	0.948092	-0.52606	-0.4612
LOC441204	0.592693	0.657017	0.628256	0.329287	0.025175	0.095224	-0.84794	0.148645	0.084067	-0.99659	-0.93201
LOC441454	0.534543	0.820292	1.17022	0.513516	0.60116	0.551898	-0.0579	0.617831	1.13041	-0.67573	-1.1883
LOC642236	0.611967	0.920621	0.804328	0.374814	0.043236	0.065831	-0.70728	0.589153	0.39433	-1.29643	-1.10161
LOC643201	0.086773	0.665232	0.540324	0.198497	0.359569	0.983212	1.19381	2.93855	2.63852	-1.74474	-1.44471
LOC653160	0.631249	0.838586	0.848352	0.388657	0.7462	0.604136	-0.69971	0.40975	0.426455	-1.10946	-1.12616
LOC90246	1.86082	2.16088	2.24788	1.11307	1.03483	1.64304	-0.74139	0.215687	0.272633	-0.95708	-1.01402
LPPR3	4.35429	6.12316	6.26336	2.97535	1.27591	2.06097	-0.54938	0.49184	0.524499	-1.04122	-1.07388
LRFN3	5.07529	5.33001	5.61695	2.56724	6.22317	7.18701	-0.98328	0.070645	0.146295	-1.05392	-1.12957

Gene	Expression value						Log$_2$ fold change				
	Mock	H-v601-Per1	H-v601-Per2	H-v601	H-Rep	H-Rep-4B$_{T66A}$	Mock vs. H-v601	Mock vs. H-v601-Per1	Mock vs. H-v601-Per2	H-v601-Per1 vs. H-v601	H-v601-Per2 vs. H-v601
LRP4-AS1	0.246442	0.597578	0.81211	0.31418	0.555932	0.76571	0.350342	1.27788	1.72043	-0.92754	-1.37008
LRRC23	1.68895	3.40676	3.15044	2.67743	3.02868	2.23419	0.664719	1.01227	0.899423	-0.34755	-0.2347
LRRC4B	3.94702	4.95657	4.78783	2.04076	4.92506	5.41409	-0.95165	0.328581	0.278609	-1.28023	-1.23026
LRRC75A	2.28295	2.45531	2.74321	1.26735	1.92999	2.18023	-0.84909	0.105002	0.264963	-0.95409	-1.11405
LTBP2	0.51987	0.714114	0.723815	0.357505	0.457223	0.513126	-0.54019	0.458004	0.477469	-0.99819	-1.01766
LTBP3	7.81477	11.6228	9.03715	5.42754	5.63404	7.55806	-0.52591	0.572682	0.209665	-1.09859	-0.73557
LTC4S	0.295716	0.583561	0.681412	0.321832	0.161901	0.275933	0.122095	0.980669	1.20431	-0.85857	-1.08222
LXN	3.19036	4.17008	6.15521	2.54652	4.28149	4.0134	-0.32519	0.386357	0.94809	-0.71155	-1.27328
MAFA	1.55242	2.12935	2.15049	0.892376	1.21492	1.87885	-0.79879	0.455896	0.470147	-1.25469	-1.26894
MAGEB2	3.50442	8.25718	8.44491	2.73311	0	0.175757	-0.35863	1.23647	1.26891	-1.59511	-1.62754
MAGEC2	0.28523	0.782904	0.40827	0.247484	0.041014	0.158002	-0.20479	1.45671	0.517398	-1.6615	-0.72219
MAL2	0.279073	1.48604	3.13766	0.067312	0.112343	0.23612	-2.05171	2.41276	3.49097	-4.46447	-5.54268
MALAT1	46.4638	61.1971	61.7245	13.1531	61.4474	49.0718	-1.82071	0.397355	0.409736	-2.21807	-2.23045
MAMLD1	4.49642	5.19384	5.23767	2.37782	4.043	4.4656	-0.91914	0.208026	0.220151	-1.12716	-1.13929
MAMSTR	2.33385	2.55989	2.81196	1.36909	2.14474	2.08302	-0.7695	0.133369	0.268863	-0.90287	-1.03836
MATN1-AS1	0.618157	1.38926	1.06914	0.948549	0.651577	0.962595	0.617749	1.16827	0.790409	-0.55052	-0.17266
MBD6	15.9762	17.2934	16.5162	8.27748	21.7385	23.5946	-0.94866	0.114302	0.047961	-1.06296	-0.99662
MCF2L-AS1	0.703738	1.02835	1.03006	0.498423	0.270993	0.50879	-0.49767	0.547221	0.549622	-1.04489	-1.04729
MEIS3	4.25249	5.08834	5.78512	2.42473	2.05818	3.19596	-0.81048	0.258887	0.444038	-1.06937	-1.25452
MGAT5B	1.87838	2.14794	1.98622	1.0668	0.662635	1.31007	-0.8162	0.193461	0.080538	-1.00966	-0.89673
MGLL	1.70695	1.79381	1.82752	0.802469	1.44683	1.31641	-1.08891	0.071599	0.098466	-1.16051	-1.18737
MIR1256	4.99166	8.91033	8.47719	0	0	0	#NAME?	0.835959	0.764066	#NAME?	#NAME?
MIR1287	0.285128	21.6727	0.571235	0.404878	0.513678	0.273079	0.505879	6.24813	1.00248	-5.74225	-0.4966
MIR1302-8	0	6.35603	12.6153	5.11559	0	0	inf	inf	inf	-0.31323	-1.3022
MIR3665	0	27.0801	7.71208	4.5862	14.2848	0	inf	inf	inf	-2.56186	-0.74982
MIR3934	23.55	95.6119	66.2438	50.3813	44.8742	22.7752	1.09716	2.02146	1.49206	-0.9243	-0.3949

Gene	Expression value						Log_2 fold change				
	Mock	H-v601-Per1	H-v601-Per2	H-v601	H-Rep	H-Rep-4B$_{T66A}$	Mock vs. H-v601	Mock vs. H-v601-Per1	Mock vs. H-v601-Per2	H-v601-Per1 vs. H-v601	H-v601-Per2 vs. H-v601
MIR3936	0	42.9893	47.114	28.6267	0	12.5379	inf	inf	inf	-0.58661	-0.71879
MIR5193	0.271312	0.605378	0.491503	0.425469	0.484346	0.630292	0.649103	1.15788	0.857248	-0.50878	-0.20815
MIR548AN	75.5667	90.0779	257.557	34.7888	189.845	73.8029	-1.11913	0.253423	1.76907	-1.37255	-2.8882
MIR568	0.243943	10.8751	0.334766	0.244912	0.098893	0.08891	0.005721	5.47835	0.456611	-5.47262	-0.45089
MIR590	47.8669	116.893	193.728	86.4751	272.686	183.681	0.853258	1.2881	2.01694	-0.43484	-1.16368
MIR593	0	36.5859	26.6899	12.2059	0	0	inf	inf	inf	-1.58371	-1.12871
MIR6073	4.62067	27.4786	37.2945	1.30552	1.23726	1.08238	-1.82348	2.57213	3.01279	-4.39561	-4.83627
MIR612	21.1916	37.338	53.3414	0	20.0918	0	#NAME?	0.817155	1.33176	#NAME?	#NAME?
MIR6126	36.2359	61.273	45.6377	20.8712	34.3554	32.3983	-0.79591	0.757831	0.332805	-1.55374	-1.12871
MIR6132	7.18274	25.1688	24.4889	18.3169	27.0654	8.01186	1.35057	1.80903	1.76952	-0.45846	-0.41895
MIR621	77.2644	233.494	152.828	18.4981	148.867	159.422	-2.06243	1.59551	0.984038	-3.65793	-3.04646
MIR6513	0.991132	1.83736	1.18427	0.900387	234.162	1.93146	-0.13853	0.890486	0.256846	-1.02902	-0.39538
MIR6516	76.7335	92.8544	303.033	78.5102	46.9105	244.901	0.033023	0.275113	1.98155	-0.24209	-1.94853
MIR659	72.8647	95.9575	81.5146	0	138.195	21.7864	#NAME?	0.397177	0.16184	#NAME?	#NAME?
MIR6716	5.97363	6.35341	32.6852	4.52306	6.88478	6.3156	-0.40131	0.088922	2.45196	-0.49023	-2.85327
MIR6717	16.0656	16.2969	102.756	12.2194	111.303	16.0606	-0.3948	0.020622	2.67717	-0.41543	-3.07197
MIR6821	0	120.605	399.473	109.55	262.973	156.769	inf	inf	inf	-0.1387	-1.86651
MIR6835	241.064	318.934	410.963	0	0	134.427	#NAME?	0.403843	0.769592	#NAME?	#NAME?
MIR6872	0.980954	1.65868	113.525	0.986441	203.735	1.31074	0.008047	0.757778	6.85461	-0.74973	-6.84656
MIR7109	17.6281	109.523	200.36	16.1099	12.2572	132.672	-0.12993	2.63528	3.50665	-2.76521	-3.63658
MIR7113	0	623.889	803.913	601.278	907.434	0	inf	inf	inf	-0.05326	-0.41901
MIR7-3HG	0	0.545811	0.147349	0.047698	0.456893	0.16386	inf	inf	inf	-3.51641	-1.62724
MR1	0.846335	1.71822	1.22994	0.9888	1.38399	1.06003	0.224449	1.02162	0.53929	-0.79717	-0.31484
MRVI1-AS1	0	0.700087	0.416057	0.375334	0.175168	0.294451	inf	inf	inf	-0.89936	-0.14861
MTNR1A	0.522094	1.06686	0.663048	0.466357	0.821684	0.316736	-0.16287	1.03099	0.344805	-1.19386	-0.50768
MYOD1	0.554078	0.601817	0.600871	0.180911	0.022426	0.110339	-1.61481	0.119237	0.116966	-1.73405	-1.73178

Gene	Expression value						Log$_2$ fold change				
	Mock	H-v601-Per1	H-v601-Per2	H-v601	H-Rep	H-Rep-4B$_{T66A}$	Mock vs. H-v601	Mock vs. H-v601-Per1	Mock vs. H-v601-Per2	H-v601-Per1 vs. H-v601	H-v601-Per2 vs. H-v601
MYRIP	0.433538	0.972519	0.880981	0.317534	0.08452	0.0239	-0.44925	1.16557	1.02295	-1.61482	-1.4722
NACAD	0.461511	0.504475	0.590277	0.293464	0.357187	0.428324	-0.65318	0.12842	0.355028	-0.7816	-1.00821
NDUFA4L2	0.400713	1.00231	0.641498	0.551381	0.225402	0.375953	0.46048	1.32268	0.678878	-0.8622	-0.2184
NELL1	0.305085	0.916783	1.02994	0.362704	0.672508	0.50899	0.249583	1.58737	1.75528	-1.33779	-1.5057
NEURL1	0.603447	0.749009	0.819643	0.340916	0.875089	0.972246	-0.82381	0.311755	0.441769	-1.13557	-1.26558
NFIC	9.89553	10.9148	10.0485	3.2709	13.0206	14.7832	-1.59709	0.141432	0.022137	-1.73852	-1.61922
NFIX	11.4692	11.7567	11.7552	5.30169	15.2177	16.7362	-1.11324	0.035728	0.03554	-1.14897	-1.14878
NFKB2	7.79734	17.8928	12.6907	8.12523	8.5826	8.90137	0.059427	1.19833	0.702713	-1.1389	-0.64329
NFKBIA	12.4153	42.7488	21.8306	12.8923	11.9847	17.7671	0.054392	1.78377	0.814237	-1.72938	-0.75985
NGFR	0.360648	1.21557	0.862155	0.186617	0.252574	0.40068	-0.95051	1.75297	1.25735	-2.70348	-2.20787
NHLH1	0.467923	0.557861	0.486437	0.230305	0.55053	0.522923	-1.02273	0.253634	0.055983	-1.27636	-1.07871
NLRC5	0.313689	0.726757	0.662116	0.235592	0.742	0.790054	-0.41304	1.21214	1.07775	-1.62518	-1.49079
NMNAT2	1.58457	4.11432	2.60742	1.64158	0.558667	0.745857	0.051001	1.37657	0.718534	-1.32556	-0.66753
NOTCH3	10.591	11.5532	11.7238	5.90239	6.22225	6.21539	-0.84347	0.12545	0.146603	-0.96892	-0.99008
NOTUM	0.292346	0.524591	0.602251	0.421616	0.164506	0.201237	0.528252	0.843514	1.04269	-0.31526	-0.51444
NOV	0.115232	1.25656	0.761787	0.111411	0.18377	0.629603	-0.04865	3.44687	2.72484	-3.49552	-2.77349
NOVA2	3.3214	4.15385	3.65101	1.65801	2.0998	3.42284	-1.00234	0.322656	0.136503	-1.325	-1.13884
NOXA1	3.51956	7.02591	5.21088	3.23736	2.50932	2.83964	-0.12058	0.997291	0.566133	-1.11787	-0.68671
NPAS1	9.73561	11.5986	14.3904	6.68174	19.3651	19.8238	-0.54305	0.252612	0.56376	-0.79566	-1.10681
NPIPA1	0.635516	0.881171	0.665103	0.412596	0.533965	0.914016	-0.6232	0.471493	0.065648	-1.09469	-0.68885
NPM2	1.06717	1.09616	1.16768	0.517546	0.691717	0.792744	-1.04403	0.038666	0.129857	-1.0827	-1.17389
NR1D1	2.04873	2.69349	2.48402	1.30911	3.21752	4.0497	-0.64615	0.394747	0.277949	-1.04089	-0.9241
NRG2	1.8421	2.37828	2.13654	1.15788	1.98131	2.51207	-0.66987	0.368563	0.213921	-1.03844	-0.8838
NRXN2	0.988128	1.68496	1.28251	0.589651	0.806027	1.4821	-0.74484	0.769942	0.376204	-1.51478	-1.12104
NT5C1A	1.10787	1.92525	2.40797	1.27222	2.16901	2.29991	0.19956	0.797253	1.12002	-0.59769	-0.92047
NTNG2	0.401145	0.912564	0.793583	0.347042	0.347366	0.435113	-0.20902	1.1858	0.984256	-1.39481	-1.19327

Gene	Expression value						Log$_2$ fold change				
	Mock	H-v601-Per1	H-v601-Per2	H-v601	H-Rep	H-Rep-4B$_{T66A}$	Mock vs. H-v601	Mock vs. H-v601-Per1	Mock vs. H-v601-Per2	H-v601-Per1 vs. H-v601	H-v601-Per2 vs. H-v601
NUAK2	0.682384	1.40497	0.737593	0.536789	0.521342	0.80186	-0.34623	1.04188	0.112241	-1.38811	-0.45847
NUCB1-AS1	0.367382	0.790213	0.913215	0.312953	0.515862	0.263752	-0.23134	1.10496	1.31367	-1.3363	-1.54501
NUPR1	2.38119	25.1262	14.1212	2.8981	1.52597	2.39785	0.283426	3.39944	2.5681	-3.11601	-2.28468
NWD2	0.126617	0.461082	0.657441	0.208929	0.045963	0.08188	0.722543	1.86455	2.37639	-1.14201	-1.65385
NXPH4	10.3131	10.4368	12.0646	4.514	8.43872	9.57697	-1.192	0.01721	0.22631	-1.20921	-1.41831
NYAP1	0.285082	0.631664	0.422711	0.381691	0.732728	0.579276	0.421028	1.14778	0.568294	-0.72675	-0.14727
NYNRIN	5.24593	7.04532	5.9901	3.29343	5.1256	4.21963	-0.67161	0.425466	0.191381	-1.09707	-0.86299
OASL	0.039196	57.6914	25.7607	0.555126	0.592468	6.96536	3.82404	10.5234	9.36025	-6.6994	-5.53621
ODF3L2	0.647105	0.813046	0.723129	0.119773	0.343636	0.533965	-2.4337	0.329336	0.160253	-2.76304	-2.59396
OLFM2	8.93817	11.0271	11.1903	4.45488	7.0559	9.19644	-1.00459	0.302998	0.3242	-1.30759	-1.32879
OLFML2A	0.546393	0.989687	1.04696	0.33219	0.871199	0.912615	-0.71793	0.857032	0.938202	-1.57496	-1.65613
ONECUT1	0.738273	0.923932	0.786655	0.316909	0.40274	0.52361	-1.22009	0.323633	0.091577	-1.54372	-1.31166
OPRD1	0.738721	1.02133	0.846105	0.425871	0.071633	0.067553	-0.79461	0.467352	0.195809	-1.26196	-0.99042
OPTN	4.98782	12.2371	8.10134	6.78972	9.06259	6.87395	0.444942	1.29479	0.699752	-0.84984	-0.25481
OR2B6	0.559766	0.853142	0.629865	0.417926	0.198933	0.239491	-0.42158	0.607962	0.170219	-1.02954	-0.5918
ORAI3	2.38081	4.14931	3.26409	2.07215	2.45563	2.70332	-0.20033	0.801416	0.455227	-1.00174	-0.65555
OSBP2	4.65743	6.0044	4.79054	2.85052	3.36619	4.79215	-0.70831	0.366485	0.040653	-1.07479	-0.74896
OSBPL7	1.38264	3.20568	3.05954	1.45367	2.9006	2.84335	0.072268	1.2132	1.14589	-1.14093	-1.07362
OSGIN1	0.566757	1.03606	0.640843	0.389912	0.511973	0.585693	-0.53958	0.870304	0.177239	-1.40989	-0.71682
OSR1	0.47741	1.03376	0.559791	0.436062	0	0.020919	-0.1307	1.11459	0.229659	-1.24529	-0.36035
OVGP1	3.55463	7.17723	5.35996	2.06501	7.71818	9.77217	-0.78355	1.01373	0.592521	-1.79728	-1.37607
P4HA2-AS1	0.738056	1.81925	1.68245	1.27234	1.34862	1.57008	0.78568	1.30154	1.18876	-0.51586	-0.40308
PACS1	10.6753	13.1348	11.4982	5.65922	13.7904	13.1336	-0.9156	0.299121	0.107131	-1.21472	-1.02273
PALM	8.79135	9.56743	10.3509	4.97422	10.9645	11.4409	-0.82161	0.122047	0.235606	-0.94366	-1.05722
PARD6G-AS1	0.505945	0.605688	0.548376	0.225168	0.923998	0.685944	-1.16798	0.259594	0.116185	-1.42757	-1.28416
PARK2	0.627976	1.09588	0.691492	0.355824	0.116117	0.171855	-0.81955	0.803307	0.139004	-1.62285	-0.95855

Gene	Expression value						Log_2 fold change				
	Mock	H-v601-Per1	H-v601-Per2	H-v601	H-Rep	H-Rep-4B$_{T66A}$	Mock vs. H-v601	Mock vs. H-v601-Per1	Mock vs. H-v601-Per2	H-v601-Per1 vs. H-v601	H-v601-Per2 vs. H-v601
PCOLCE-AS1	0.185611	0.537474	0.582191	0.430682	0.177779	0.358357	1.21434	1.53391	1.64921	-0.31957	-0.43487
PDGFB	0.351329	0.860811	0.617758	0.419478	0.188846	0.224995	0.255771	1.29287	0.814216	-1.0371	-0.55845
PDGFD	0.094032	0.280785	0.548922	0.038388	0.028954	0.134999	-1.29248	1.57824	2.54538	-2.87072	-3.83786
PHLDA3	10.3332	20.913	12.2995	8.74107	19.1311	23.8652	-0.24141	1.01711	0.25131	-1.25851	-0.49272
PIANP	2.86477	3.55994	2.98849	1.78858	2.70622	3.74878	-0.67961	0.313432	0.060997	-0.99304	-0.74061
PIGZ	0.480355	0.765045	0.543681	0.373205	0.498502	0.580223	-0.36413	0.671443	0.178661	-1.03558	-0.54279
PILRA	0.869572	1.03073	1.24657	0.546626	0.557911	0.730485	-0.66975	0.245293	0.519585	-0.91504	-1.18934
PIP5KL1	0.369367	0.762441	0.976886	0.566741	0.754533	0.596515	0.617635	1.04557	1.40314	-0.42794	-0.7855
PITX3	1.16393	1.58142	1.57004	0.736017	1.50523	1.77498	-0.66119	0.442225	0.4318	-1.10341	-1.09299
PLA2G4C	0.249328	2.41811	1.05294	0.316544	0.16035	0.56646	0.344362	3.27777	2.07831	-2.93341	-1.73394
PLEKHA4	0.783856	2.17601	1.60742	0.619387	2.21701	1.90578	-0.33975	1.47303	1.03609	-1.81278	-1.37584
PLK3	1.65072	2.92464	2.28197	1.34149	2.31319	2.7719	-0.29926	0.825162	0.467184	-1.12442	-0.76644
PML	9.58754	12.8318	10.733	5.8715	9.55294	11.3267	-0.70743	0.420491	0.162825	-1.12792	-0.87026
PNCK	0.648564	1.77836	1.70829	0.628018	0.14156	0.323647	-0.04644	1.45523	1.39724	-1.50167	-1.44368
POLR2J4	1.39837	1.91541	1.58407	0.833973	1.37216	1.34672	-0.74567	0.453909	0.17989	-1.19958	-0.92556
PPAPDC1A	1.77953	1.99818	1.87857	0.826739	0.979641	1.2261	-1.10599	0.167192	0.078141	-1.27319	-1.18413
PPP1R15A	10.8062	48.955	24.6706	19.9789	14.525	18.8929	0.886614	2.17959	1.19093	-1.29298	-0.30432
PPP1R1A	1.88254	2.74104	2.98414	1.21662	1.05412	0.93239	-0.62981	0.54204	0.664632	-1.17185	-1.29444
PPP1R1C	0.519624	0.95646	1.15909	0.470533	0.601583	0.676894	-0.14317	0.880237	1.15745	-1.02341	-1.30063
PRC1-AS1	0.531662	0.881807	0.600932	0.160211	0.612063	0.402894	-1.73054	0.729955	0.176693	-2.46049	-1.90723
PRKCB	1.21652	4.54628	2.96462	1.30584	5.02642	8.25666	0.102221	1.90193	1.28509	-1.79971	-1.18287
PRKCG	0.510918	0.817665	0.579134	0.30019	0.472788	0.682511	-0.76722	0.678419	0.180806	-1.44563	-0.94802
PRPH	0.905419	1.35805	1.37611	0.331321	0.760505	0.594955	-1.45036	0.584883	0.603938	-2.03524	-2.05429
PRR24	5.60269	7.84665	5.95677	3.56934	5.6944	6.96194	-0.65046	0.485958	0.088412	-1.13642	-0.73887
PRR35	0.91095	1.38836	1.03051	0.300267	0.773644	0.671399	-1.60112	0.607941	0.17791	-2.20907	-1.77903
PRRT4	4.77119	5.74216	4.99367	2.42966	5.92394	5.81004	-0.9736	0.267245	0.065753	-1.24084	-1.03935

Gene	Expression value						Log$_2$ fold change				
	Mock	H-v601-Per1	H-v601-Per2	H-v601	H-Rep	H-Rep-4B$_{T66A}$	Mock vs. H-v601	Mock vs. H-v601-Per1	Mock vs. H-v601-Per2	H-v601-Per1 vs. H-v601	H-v601-Per2 vs. H-v601
PSPN	0.072931	0.380706	0.745723	0.271245	0.549671	0.295025	1.89499	2.38407	3.35403	-0.48908	-1.45905
PTCH2	0.701453	0.813541	0.789918	0.353557	0.609249	0.797817	-0.9884	0.21387	0.171358	-1.20227	-1.15976
PTGES	0.932843	1.90805	2.01359	0.6264	0.81208	1.12501	-0.57455	1.03239	1.11006	-1.60694	-1.68461
PTN	0.058583	0.422105	0.694227	0.016996	0.027976	0.042596	-1.78533	2.84905	3.56685	-4.63438	-5.35218
PVT1	3.07975	11.0299	7.06362	3.13623	4.56267	7.35351	0.02622	1.84054	1.19759	-1.81432	-1.17138
RAB38	1.89375	2.62875	3.83355	1.35469	0.087052	0.045445	-0.48329	0.473131	1.01743	-0.95642	-1.50072
RAB3IL1	4.87606	5.89743	4.89103	2.889	4.21968	5.11469	-0.75514	0.274371	0.004421	-1.02952	-0.75957
RAB6C-AS1	0.654489	0.847174	0.735684	0.416004	0.34412	0.371373	-0.65377	0.372289	0.168717	-1.02606	-0.82249
RAET1G	0.32639	0.651522	0.404511	0.205613	0.915436	0.686539	-0.66667	0.997217	0.309582	-1.66389	-0.97625
RAI2	1.18453	1.23669	1.33937	0.626962	0.760591	1.0617	-0.91786	0.06218	0.17724	-0.98004	-1.0951
RAP1GAP	4.12242	4.90912	4.24905	2.25237	3.32992	5.31611	-0.87205	0.251971	0.043647	-1.12402	-0.91569
RASD2	0.958727	1.34898	1.09141	0.625987	0.604397	0.924268	-0.61499	0.492673	0.187005	-1.10766	-0.80199
RASGEF1C	1.87861	2.80303	2.37697	0.971221	1.21422	1.27812	-0.95179	0.577325	0.339463	-1.52912	-1.29125
RBFOX3	2.02006	2.25192	2.75877	1.10343	2.24665	3.83617	-0.87241	0.156757	0.449626	-1.02916	-1.32203
RCAN3AS	0.146032	0.612879	0.678417	0.243114	0	0.193022	0.735342	2.06931	2.21588	-1.33397	-1.48054
RELB	0.975605	4.21438	2.50122	0.664736	1.33123	1.78122	-0.55352	2.11095	1.35826	-2.66447	-1.91178
RENBP	1.94963	5.62144	4.18161	2.38203	0.352583	0.572862	0.288993	1.52774	1.10086	-1.23875	-0.81186
RGS9	0.418809	0.799461	0.515832	0.31017	0.379349	0.598173	-0.43323	0.932736	0.300611	-1.36597	-0.73384
RHEBL1	0.624798	3.78373	1.80928	1.04877	0.90536	0.793238	0.747238	2.59835	1.53396	-1.85111	-0.78672
RIMS2	0.419479	0.927816	0.785977	0.724361	0.175288	0.2146	0.78811	1.14524	0.905887	-0.35713	-0.11778
RIN3	3.8432	4.36414	4.23838	1.94228	1.05525	1.09886	-0.98456	0.18339	0.141206	-1.16795	-1.12576
RND1	2.09238	4.6197	3.47834	2.52058	1.85813	2.35319	0.268611	1.14266	0.733256	-0.87404	-0.46465
RNF208	13.188	16.5325	13.1922	4.76799	1.3633	2.43166	-1.46777	0.326084	0.000464	-1.79385	-1.46823
RNU11	9.0816	21.0074	20.4299	0	11.5366	12.126	#NAME?	1.20988	1.16966	#NAME?	#NAME?
RNU12	4.14543	9.05637	5.22853	0	3.9303	0	#NAME?	1.12741	0.334884	#NAME?	#NAME?
RNU5B-1	0	9.54438	9.10979	6.24018	30.8153	9.68661	inf	inf	inf	-0.61306	-0.54583

Gene	Expression value						Log$_2$ fold change				
	Mock	H-v601-Per1	H-v601-Per2	H-v601	H-Rep	H-Rep-4B$_{T66A}$	Mock vs. H-v601	Mock vs. H-v601-Per1	Mock vs. H-v601-Per2	H-v601-Per1 vs. H-v601	H-v601-Per2 vs. H-v601
RNU86	7400.23	10139.1	12597.3	5860.48	3631.98	6934.03	-0.33655	0.454284	0.767471	-0.79084	-1.10402
ROCK1P1	0.286893	0.822292	0.405084	0.372708	0.277773	0.218183	0.377534	1.51914	0.497712	-1.14161	-0.12018
ROPN1L	0.397448	0.96626	0.578765	0.198433	0.673002	1.10367	-1.00212	1.28164	0.542211	-2.28376	-1.54433
RPA4	0.26384	0.614447	0.37163	0.364576	0.331045	0.535337	0.466558	1.21963	0.494205	-0.75307	-0.02765
RSAD2	0	1.43093	0.522221	0.015019	0.022194	0.304928	inf	inf	inf	-6.57403	-5.11981
RTDR1	0.581744	0.70722	0.601917	0.211341	0.318944	0.391781	-1.46081	0.281776	0.049181	-1.74259	-1.50999
RTN4RL1	2.02096	2.08226	2.42333	1.12736	1.27868	1.24528	-0.8421	0.04311	0.261945	-0.88521	-1.10404
RTN4RL2	6.79515	9.14033	7.58316	4.22223	4.25452	5.89769	-0.6865	0.427742	0.158295	-1.11424	-0.84479
RUNDC3A	0.613086	1.15246	1.20582	0.531863	0.513194	0.94772	-0.20504	0.91056	0.97585	-1.1156	-1.18089
RUNX1T1	1.6191	1.66921	2.67017	0.970463	1.63618	2.25799	-0.73845	0.043971	0.721739	-0.78242	-1.46019
RXRG	1.04811	1.63044	1.28395	0.741759	1.97441	1.9028	-0.49877	0.637471	0.292799	-1.13624	-0.79156
RYR2	0.234351	0.869736	0.480971	0.287192	0.615531	1.26552	0.293344	1.89191	1.03728	-1.59856	-0.74394
S100P	0.321975	0.555206	0.596654	0.162293	0	0.301952	-0.98835	0.786075	0.889945	-1.77443	-1.8783
SAMD9	0.738929	1.8174	1.45121	0.518334	2.03987	1.90229	-0.51155	1.29837	0.973752	-1.80992	-1.48531
SCARNA14	2.82907	10.117	7.23183	7.21456	5.44402	0	1.35059	1.83839	1.35403	-0.4878	-0.00345
SCARNA2	1.45283	1.48885	2.07365	0.526849	3.10034	4.08743	-1.4634	0.035333	0.513306	-1.49874	-1.97671
SCARNA4	14.5744	28.2424	24.4834	4.1973	6.90904	17.0352	-1.79591	0.954424	0.748363	-2.75033	-2.54427
SCARNA9	8.93381	11.7347	10.8551	4.22767	17.3991	19.3794	-1.07941	0.393438	0.281025	-1.47285	-1.36044
SCG3	0.354178	0.661553	0.761081	0.263258	0.267071	0.864759	-0.428	0.901383	1.10358	-1.32938	-1.53157
SCN3B	0.790131	1.70367	1.31259	0.578594	0.344272	0.666239	-0.44954	1.10848	0.732257	-1.55802	-1.1818
SDSL	1.68965	4.57491	2.4785	1.84618	2.53996	2.67464	0.12782	1.43702	0.552739	-1.3092	-0.42492
SECTM1	0.833914	2.02211	1.34193	0.706288	0.143575	0.215854	-0.23964	1.27789	0.686339	-1.51753	-0.92598
SELENBP1	9.95076	20.0553	13.059	12.2395	26.9279	27.756	0.298669	1.0111	0.39217	-0.71244	-0.0935
SEPSECS-AS1	0.322148	0.730004	0.362311	0.296024	0.284757	0.148338	-0.12201	1.18018	0.169506	-1.30219	-0.29152
SEZ6L2	7.42721	8.42927	7.99355	2.99922	10.926	12.5308	-1.30824	0.182587	0.106016	-1.49082	-1.41425
SFRP4	0.070775	0.569018	0.305775	0.115879	0.027078	0.31414	0.711309	3.00717	2.11116	-2.29586	-1.39985

Gene	Expression value						Log$_2$ fold change				
	Mock	H-v601-Per1	H-v601-Per2	H-v601	H-Rep	H-Rep-4B$_{T66A}$	Mock vs. H-v601	Mock vs. H-v601-Per1	Mock vs. H-v601-Per2	H-v601-Per1 vs. H-v601	H-v601-Per2 vs. H-v601
SHANK1	0.22312	0.568006	0.495077	0.266212	0.40005	0.394419	0.254753	1.34808	1.14983	-1.09333	-0.89508
SHC2	3.82076	10.5221	5.91119	4.79734	0.680069	1.74774	0.328374	1.4615	0.629587	-1.13312	-0.30121
SHD	0.206793	0.554455	0.350032	0.318553	0.313464	0.176526	0.623346	1.42288	0.759301	-0.79954	-0.13596
SHISA4	0.569565	2.0162	1.5029	0.691177	1.93631	2.38337	0.279193	1.8237	1.39982	-1.54451	-1.12063
SHISA8	3.54256	3.59721	3.98033	1.76836	1.45011	1.83816	-1.00238	0.022086	0.168093	-1.02447	-1.17048
SLC17A7	0.909397	1.2696	1.44318	0.565316	0.844145	1.10547	-0.68585	0.481397	0.666272	-1.16725	-1.35212
SLC22A4	0.786464	0.953144	0.853862	0.428235	0.552342	0.875017	-0.87698	0.277312	0.118622	-1.15429	-0.9956
SLC38A3	3.87354	5.02718	5.24248	2.47646	3.93165	5.46892	-0.64537	0.376099	0.4366	-1.02147	-1.08197
SLC6A16	0.619871	0.792346	0.918456	0.362591	1.12761	1.35082	-0.77362	0.354164	0.567243	-1.12779	-1.34087
SLC7A5P1	5.1319	9.86393	10.6259	7.98095	6.14758	11.2634	0.637068	0.942669	1.05002	-0.3056	-0.41295
SLC7A7	0.381218	0.670646	0.495125	0.267062	0.451581	0.46159	-0.51345	0.814934	0.377175	-1.32838	-0.89062
SLC8A2	0.453946	0.664982	0.656224	0.221066	0.327255	0.601764	-1.03804	0.550796	0.531669	-1.58884	-1.56971
SLC9A9	0.756686	2.3277	1.64449	1.35467	1.15957	1.03618	0.840169	1.62114	1.11987	-0.78097	-0.27971
SLCO3A1	1.15704	1.57582	1.51307	0.408828	0.462418	1.10901	-1.50087	0.445661	0.387042	-1.94653	-1.88791
SLFN5	1.13191	2.63615	1.99213	1.6196	0.870874	0.790516	0.516879	1.21967	0.815548	-0.70279	-0.29867
SMARCD3	28.8204	32.598	29.4986	16.2223	25.2075	33.8897	-0.82911	0.177689	0.033556	-1.0068	-0.86267
SNAP25	0.052965	1.05423	1.02338	0.026855	0.261745	0.323273	-0.97987	4.31501	4.27216	-5.29488	-5.25203
SNCG	0.665064	1.9192	1.01453	0.559025	0.954144	1.21472	-0.25058	1.52894	0.609246	-1.77952	-0.85983
SND1-IT1	0.367338	0.550267	0.561217	0.061274	0.348738	0.36562	-2.58375	0.583025	0.61145	-3.16678	-3.1952
SNORA68	38.6275	61.8524	40.6521	4.39151	72.4043	81.6235	-3.13684	0.679202	0.073704	-3.81604	-3.21054
SNORA74A	2.78519	7.28283	4.73797	0.817406	9.05249	7.64458	-1.76865	1.38673	0.766496	-3.15538	-2.53515
SNORA75	14.2292	22.05	14.4741	9.92185	15.8782	30.3755	-0.52017	0.631924	0.024617	-1.1521	-0.54479
SNORD14E	122.861	265.921	155.852	42.1018	112.418	101.987	-1.54507	1.11397	0.343152	-2.65904	-1.88823
SNORD15A	6.28778	12.5882	10.8077	8.68417	30.9209	15.4984	0.465836	1.00145	0.781439	-0.53562	-0.3156
SNORD3A	3.17065	16.6152	7.57918	2.77982	3.02082	9.93098	-0.18979	2.38965	1.25726	-2.57944	-1.44705
SNORD51	198.361	234.139	502.1	153.081	120.74	191.835	-0.37383	0.239235	1.33985	-0.61306	-1.71368

Gene	Expression value						Log$_2$ fold change				
	Mock	H-v601-Per1	H-v601-Per2	H-v601	H-Rep	H-Rep-4B$_{T66A}$	Mock vs. H-v601	Mock vs. H-v601-Per1	Mock vs. H-v601-Per2	H-v601-Per1 vs. H-v601	H-v601-Per2 vs. H-v601
SNORD6	119.909	205.765	357.679	140.178	0	66.8662	0.225322	0.77906	1.57672	-0.55374	-1.3514
SNORD95	954.619	1777.09	2317.09	1414.03	1023.5	3183.1	0.56682	0.896522	1.27932	-0.3297	-0.7125
SORCS2	0.292358	0.573116	0.437166	0.180863	0.285233	0.323512	-0.69284	0.971091	0.580446	-1.66393	-1.27328
SP110	0.419241	1.24456	0.862391	0.260142	0.446017	0.502349	-0.68848	1.56979	1.04056	-2.25827	-1.72905
SPATA18	1.29478	2.58221	1.93024	1.57535	1.92094	1.60824	0.282973	0.995904	0.57608	-0.71293	-0.29311
SPTBN4	1.00363	1.70618	1.36723	0.676372	1.09577	1.24298	-0.56934	0.765538	0.446026	-1.33488	-1.01537
SQRDL	0.268853	0.846041	0.713575	0.466755	0.301796	0.517987	0.795847	1.65391	1.40825	-0.85806	-0.6124
SRRM3	1.51332	2.72701	2.33557	1.19025	2.11935	2.6156	-0.34645	0.849606	0.626064	-1.19606	-0.97251
SRRM5	0.776296	1.12566	0.862118	0.539765	0.703512	0.896603	-0.52428	0.536091	0.151278	-1.06037	-0.67556
ST6GALNAC2	0.321336	0.620737	0.63758	0.238494	0.624481	0.300266	-0.43013	0.949898	0.988523	-1.38003	-1.41865
STAC	0.10245	0.371922	0.763313	0.009979	0.124568	0.052452	-3.3599	1.86008	2.89735	-5.21998	-6.25725
STAP2	0.570336	1.01562	1.2081	0.536978	0.95446	1.23479	-0.08695	0.832479	1.08286	-0.91943	-1.16981
STC1	0.134177	0.433214	0.944537	0.255879	0.67068	0.701056	0.931319	1.69094	2.81547	-0.75962	-1.88415
STRA6	0.374028	0.828662	0.400347	0.384276	0.325153	0.276569	0.038996	1.14764	0.098106	-1.10864	-0.05911
STX1A	4.25688	7.96447	6.83033	3.3525	4.86283	6.54592	-0.34456	0.903781	0.682158	-1.24834	-1.02672
STXBP6	1.79445	3.41744	2.92926	1.03915	2.43059	4.66706	-0.78813	0.929377	0.706997	-1.71751	-1.49513
SULT2B1	0.591963	1.21824	1.10006	0.716987	0.51906	0.85699	0.276439	1.04121	0.894001	-0.76478	-0.61756
SUSD4	2.14346	3.74443	2.18142	1.77071	0.705185	0.716542	-0.27561	0.804804	0.025326	-1.08042	-0.30094
SYN1	0.738564	0.994125	0.774922	0.083718	0.628394	1.39991	-3.14111	0.428705	0.06933	-3.56981	-3.21044
SYNC	0.543529	0.652876	0.621461	0.304271	0.821024	0.462867	-0.837	0.264452	0.193308	-1.10145	-1.03031
SYNDIG1	0.957778	1.85093	2.11241	0.543634	0.206117	0.52056	-0.81706	0.950489	1.14112	-1.76754	-1.95818
SYNGR4	0.170271	0.661361	0.368308	0.094426	1.05537	0.817721	-0.85057	1.95761	1.11308	-2.80818	-1.96365
SYNM	2.18628	3.38045	2.37853	1.65654	0.202855	0.126803	-0.40031	0.628736	0.121591	-1.02904	-0.5219
SYNPO	0.597193	1.50873	0.997257	0.396025	0.665365	0.945023	-0.59261	1.33706	0.739767	-1.92967	-1.33237
SYT12	0.273435	0.669163	0.607507	0.118292	0.402909	0.434862	-1.20884	1.29116	1.15171	-2.5	-2.36054
SYT14	1.09867	1.5286	1.25505	0.535109	0.279787	0.442736	-1.03785	0.47645	0.191982	-1.5143	-1.22984

Gene	Expression value						Log$_2$ fold change				
	Mock	H-v601-Per1	H-v601-Per2	H-v601	H-Rep	H-Rep-4B$_{T66A}$	Mock vs. H-v601	Mock vs. H-v601-Per1	Mock vs. H-v601-Per2	H-v601-Per1 vs. H-v601	H-v601-Per2 vs. H-v601
SYT9	1.11115	1.5573	1.45038	0.495185	0.197653	0.560653	-1.16601	0.486989	0.38438	-1.653	-1.55039
SYTL2	0.608713	0.873426	0.630461	0.414832	0.402878	0.470909	-0.55324	0.520923	0.050644	-1.07416	-0.60388
TAPBPL	0.317929	0.892016	0.735201	0.141423	0.369345	0.339087	-1.16868	1.48837	1.20944	-2.65705	-2.37812
TBX19	0.659868	1.77286	1.2737	0.696886	0.986121	0.884971	0.078745	1.42583	0.948778	-1.34709	-0.87003
TBXA2R	0.863292	1.18736	1.06026	0.246914	2.1394	2.60853	-1.80584	0.459836	0.296495	-2.26568	-2.10234
TCEAL7	0.199956	0.756158	0.305096	0.28091	0.038251	0.249499	0.490426	1.919	0.60958	-1.42858	-0.11915
TEKT3	0.386249	0.749502	0.430874	0.351105	0.351944	0.256381	-0.13763	0.956401	0.157736	-1.09403	-0.29536
TENC1	0.67373	1.01706	0.891514	0.331751	0.505735	0.661063	-1.02207	0.594169	0.404087	-1.61624	-1.42616
TFAP2E	0.684869	0.782639	0.736893	0.341348	0.4679	0.434561	-1.00458	0.192518	0.105627	-1.1971	-1.11021
TFEB	3.35918	4.70039	3.95566	2.19484	2.0411	2.25954	-0.61399	0.48467	0.235809	-1.09866	-0.8498
TGFA	0.681193	0.891027	0.699816	0.436279	0.765374	0.786835	-0.64281	0.387405	0.038913	-1.03022	-0.68173
TGFB1	19.7849	20.1392	20.6872	9.72128	16.1904	18.7152	-1.02518	0.02561	0.064337	-1.05079	-1.08952
TGM2	1.1296	1.21362	1.20588	0.554168	1.0308	1.50388	-1.02741	0.103511	0.094276	-1.13092	-1.12169
TINCR	1.16088	1.47709	1.51805	0.69778	1.36284	1.77466	-0.73437	0.347542	0.386998	-1.08192	-1.12137
TJP3	0.250025	0.686983	0.519969	0.294894	0.254767	0.376099	0.238128	1.45821	1.05636	-1.22008	-0.81823
TLDC2	0.6036	0.814629	0.76393	0.378721	0.715271	0.817237	-0.67246	0.43255	0.339847	-1.10501	-1.0123
TLX3	1.05311	1.31315	1.10763	0.598987	0	0.115988	-0.81407	0.318366	0.072819	-1.13243	-0.88688
TMEM108	2.46512	2.98793	2.74532	1.49335	2.96753	3.43136	-0.7231	0.277492	0.155319	-1.0006	-0.87842
TMEM132E	1.8701	3.57358	3.80269	1.57362	0.696846	1.30953	-0.24902	0.934256	1.02391	-1.18328	-1.27293
TMEM173	2.17555	3.48386	2.46804	1.34334	1.38292	1.09339	-0.69556	0.679306	0.181987	-1.37486	-0.87755
TMEM178A	0.355795	0.851185	0.771323	0.547766	0.227811	0.114447	0.622513	1.25843	1.11629	-0.63591	-0.49378
TMEM200A	0.321893	0.67154	0.424363	0.325195	0.069436	0.112813	0.014724	1.06089	0.398718	-1.04617	-0.38399
TMEM91	2.32755	3.27487	2.3777	1.45745	2.11029	3.133	-0.67536	0.492622	0.030753	-1.16799	-0.70612
TMPRSS9	0.344911	0.567595	0.381685	0.176922	0.698148	0.565145	-0.96312	0.718635	0.146155	-1.68175	-1.10927
TNC	0.207923	1.36339	0.866368	0.243394	1.57812	1.34578	0.227242	2.71307	2.05893	-2.48583	-1.83169
TNFAIP3	1.81701	5.36603	3.1747	1.395	2.38385	2.94879	-0.38131	1.56229	0.805052	-1.94359	-1.18636

Gene	Expression value						Log$_2$ fold change				
	Mock	H-v601-Per1	H-v601-Per2	H-v601	H-Rep	H-Rep-4B$_{T66A}$	Mock vs. H-v601	Mock vs. H-v601-Per1	Mock vs. H-v601-Per2	H-v601-Per1 vs. H-v601	H-v601-Per2 vs. H-v601
TNFRSF9	0.030688	0.961427	0.258151	0.035043	0.006476	0.052611	0.191461	4.96943	3.07246	-4.77796	-2.881
TOX3	0.135114	0.639577	1.08693	0.069521	0.256955	0.388591	-0.95866	2.24294	3.00801	-3.20161	-3.96668
TP53INP1	1.26724	3.17256	2.05626	1.87447	3.6578	2.70494	0.564794	1.32396	0.698334	-0.75916	-0.13354
TP53TG5	0.240229	0.559274	0.642909	0.354233	0.423878	0.667749	0.560287	1.21915	1.4202	-0.65886	-0.85992
TPTEP1	0.417843	1.68399	0.920718	0.3208	0.091731	0.05767	-0.38129	2.01085	1.1398	-2.39214	-1.52109
TRIM58	1.53726	2.55974	1.73011	0.948982	1.81413	2.28761	-0.69591	0.735641	0.170505	-1.43155	-0.86641
TSPAN11	0.619793	0.917112	0.685033	0.430422	0.131195	0.121798	-0.52604	0.565313	0.144387	-1.09135	-0.67042
TTC21A	0.609635	1.06315	1.17653	0.586688	0.918097	0.757455	-0.05535	0.802329	0.948522	-0.85768	-1.00388
UAP1L1	11.1263	16.6617	13.5961	7.89349	6.36341	8.45268	-0.49524	0.582562	0.289213	-1.0778	-0.78445
UBE2L6	5.54932	13.6653	7.84131	4.17926	8.06634	7.2096	-0.40906	1.30014	0.498785	-1.7092	-0.90785
UBE2QL1	0.78759	1.13625	0.849185	0.468189	0.181389	0.422108	-0.75035	0.528758	0.108635	-1.27911	-0.85899
UCN	3.11531	3.72786	3.63317	1.70189	4.22505	4.27192	-0.87224	0.258973	0.221853	-1.13121	-1.09409
UNC5A	1.60761	1.91175	1.67006	0.855272	0.567908	0.701067	-0.91047	0.249969	0.054983	-1.16044	-0.96545
UNC5B-AS1	0.265097	0.726233	0.674649	0.275635	0.419492	0.64409	0.056242	1.45391	1.34762	-1.39767	-1.29138
UTF1	1.18028	2.03497	1.91491	0.493042	0.354012	0.333845	-1.25935	0.785884	0.698146	-2.04523	-1.95749
VLDLR-AS1	0.09298	0.67718	0.39382	0.184219	0.05968	0.060837	0.986436	2.86455	2.08255	-1.87812	-1.09611
VPREB3	1.03447	2.52975	1.08935	0.439989	0.872995	0.970141	-1.23336	1.2901	0.074574	-2.52346	-1.30793
VSNL1	0.065544	0.221257	0.682049	0.067816	0.310496	0.357832	0.049165	1.7552	3.37935	-1.70603	-3.33018
VSTM2B	0.208464	0.309703	0.575201	0.121521	0.036079	0.034024	-0.77859	0.571085	1.46427	-1.34968	-2.24286
VSTM2L	2.42129	3.26696	2.47503	1.30069	1.01704	1.72392	-0.8965	0.432176	0.03167	-1.32867	-0.92817
VWA5A	0.153463	0.536321	0.633557	0.32042	0.539304	0.6427	1.06207	1.80521	2.04559	-0.74314	-0.98351
WDR31	0.596396	2.00721	1.67381	0.986228	0.671168	0.788182	0.725651	1.75085	1.48879	-1.0252	-0.76314
WDR63	1.24833	2.29766	1.67086	0.874447	1.32414	1.36233	-0.51355	0.880172	0.4206	-1.39372	-0.93415
WIPF3	2.85652	3.24097	3.29039	1.3815	2.67321	2.1657	-1.04802	0.182165	0.203999	-1.23019	-1.25202
YPEL3	4.30294	11.137	9.68341	4.31799	11.9679	10.8623	0.005035	1.37196	1.17019	-1.36693	-1.16516
ZC3H3	5.63746	6.36651	5.80086	2.62791	6.12882	7.87729	-1.10113	0.175457	0.041221	-1.27659	-1.14235

Gene	Expression value						Log$_2$ fold change				
	Mock	H-v601-Per1	H-v601-Per2	H-v601	H-Rep	H-Rep-4B$_{T66A}$	Mock vs. H-v601	Mock vs. H-v601-Per1	Mock vs. H-v601-Per2	H-v601-Per1 vs. H-v601	H-v601-Per2 vs. H-v601
ZFHX2	1.51916	2.10114	1.69743	0.97399	1.25102	1.72984	-0.64129	0.467898	0.160075	-1.10919	-0.80137
ZFP2	0.536066	0.876031	0.633863	0.394076	0.730983	0.572895	-0.44394	0.708572	0.24176	-1.15251	-0.6857
ZFP36	1.78164	4.89857	4.47172	1.10054	1.46311	1.89861	-0.695	1.45915	1.32762	-2.15415	-2.02262
ZNF205-AS1	0.475826	0.643664	0.761039	0.340234	0.468543	0.303906	-0.48391	0.435873	0.677537	-0.91978	-1.16144
ZNF233	0.50026	0.758265	0.635561	0.162584	0.984583	0.915689	-1.62149	0.600025	0.345354	-2.22152	-1.96685
ZNF296	7.12544	7.85218	7.99829	3.01654	6.55648	9.02722	-1.24009	0.140113	0.166711	-1.3802	-1.4068
ZNF385A	8.93348	12.1163	10.3131	3.48818	9.61181	12.8125	-1.35675	0.439655	0.207185	-1.7964	-1.56393
ZNF385C	0.361664	1.1169	1.02354	0.264854	0.588524	0.753147	-0.44946	1.62677	1.50085	-2.07623	-1.95031
ZNF423	1.85471	2.09609	2.24289	1.06038	0.830492	1.17006	-0.80662	0.176505	0.274161	-0.98313	-1.08078
ZNF426	1.1529	2.18995	2.55379	0.885176	7.05667	7.92575	-0.38123	0.925633	1.14737	-1.30686	-1.5286
ZNF429	1.65906	2.94861	2.46272	1.29941	2.9778	3.60804	-0.35252	0.829663	0.569885	-1.18218	-0.9224
ZNF433	0.724617	1.51557	1.18453	0.392099	2.40761	2.23029	-0.886	1.06457	0.709023	-1.95057	-1.59503
ZNF441	0.676212	1.40405	1.38144	0.678512	2.96443	3.9004	0.004899	1.05405	1.03062	-1.04915	-1.02572
ZNF442	0.261478	0.686198	0.57653	0.456506	0.676434	0.958259	0.803941	1.39193	1.1407	-0.58799	-0.33676
ZNF462	2.14899	3.29356	4.11779	0.973547	5.82719	6.26891	-1.14234	0.615988	0.938211	-1.75833	-2.08055
ZNF467	1.84751	4.90592	3.51259	1.48747	1.82777	2.947	-0.31273	1.40894	0.92695	-1.72167	-1.23968
ZNF502	0.073155	0.249917	0.553845	0	1.78022	2.49183	#NAME?	1.77241	2.92045	#NAME?	#NAME?
ZNF582-AS1	1.52429	3.76176	2.98343	1.96655	2.16762	2.7681	0.367532	1.30327	0.968832	-0.93574	-0.6013
ZNF585A	5.90977	12.0408	9.32334	7.9956	11.8907	11.8103	0.436105	1.02676	0.657745	-0.59065	-0.22164
ZNF628	2.34507	2.68328	2.46951	1.27289	2.48312	3.11118	-0.88153	0.194365	0.07459	-1.07589	-0.95612
ZNF785	0.91208	1.19481	1.1985	0.58365	0.606253	0.861547	-0.64406	0.389543	0.393997	-1.0336	-1.03805
ZNF793	0.227752	0.354717	0.62425	0.152341	2.0533	3.13245	-0.58017	0.639202	1.45466	-1.21937	-2.03482
ZNF91	1.8502	2.86759	3.75439	1.16228	4.45974	5.04043	-0.67072	0.632156	1.0209	-1.30288	-1.69162
ZNFX1	4.90971	8.26963	5.80172	4.07475	4.97952	6.09443	-0.26893	0.752184	0.240842	-1.02111	-0.50977
ZP3	1.15503	1.74722	1.72578	0.683949	0.504347	0.489152	-0.75597	0.597133	0.579325	-1.3531	-1.33529
ZSCAN18	1.9744	5.8128	4.11182	2.68337	3.9301	7.57307	0.442629	1.55782	1.05836	-1.11519	-0.61573

Gene	Expression value						Log_2 fold change				
	Mock	H-v601-Per1	H-v601-Per2	H-v601	H-Rep	H-Rep-$4B_{T66A}$	Mock vs. H-v601	Mock vs. H-v601-Per1	Mock vs. H-v601-Per2	H-v601-Per1 vs. H-v601	H-v601-Per2 vs. H-v601
ZSWIM4	1.56366	2.40235	2.04788	1.05534	1.13634	1.45048	-0.56721	0.619523	0.389207	-1.18674	-0.95642
ZYX	55.5033	63.9702	56.665	31.4093	62.06	67.5325	-0.82138	0.204826	0.029883	-1.02621	-0.85127